

PROCEEDINGS OF THE AUSTRALIAN PHYSIOLOGICAL AND PHARMACOLOGICAL SOCIETY



PROCEEDINGS OF THE AUSTRALIAN PHYSIOLOGICAL AND PHARMACOLOGICAL SOCIETY

Volume 33

August 2003



Correspondence

Correspondence concerning literary and technical aspects of the journal should be addressed to the Editor. Correspondence concerning subscriptions to the journal should be addressed to the Treasurer and that involving all other Society business should be addressed to the National Secretary.

**AUSTRALIAN AUSTRALIAN PHYSIOLOGICAL AND PHARMACOLOGICAL
SOCIETY INC.**

President: P.W. Gage (2000-)
Department of Physiology,
JCSMR, ANU
Canberra 2601

National Secretary: D.A. Saint (2002-)
Molecular and Biomedical Sciences
University of Adelaide
Adelaide SA 5005

Treasurer: C.B. Neylon (2002-)
Department of Anatomy & Cell Biology
University of Melbourne
VIC 3010

Editor: D.F. Davey (2002-)
D'Entrecasteaux
378 Manuka Road
Kettering,
Tasmania 7155

Elected Members of Council(Year of retirement in parentheses)

A. Allen	(2003)	University of Melbourne
D. Laver	(2003)	University of Newcastle
M. Roberts	(2003)	University of Adelaide
D. Robertson	(2004)	University of Western Australia
D.J. Adams	(2005)	University of Queensland
L. Delbridge	(2005)	University of Melbourne

Co-opted Members of Council

D. Tracey	(2003)	University of NSW (FASTS rep)
S. Malpas	(2003)	University of Auckland (PSNZ Secretary)
M. Day	(2003)	University of Sydney (Local Secretary)

© 2003 Australian Physiological and Pharmacological Society

**PROCEEDINGS OF THE AUSTRALIAN
PHYSIOLOGICAL AND
PHARMACOLOGICAL SOCIETY**

Volume 33

August 2003

CONTENTS

APPS/PSNZ Sydney 2003 Meeting - Abstracts

Symposium 1: Stretch-induced muscle damage in sport and disease

- Popping sarcomere hypothesis explains stretch induced muscle damage*
D.L. Morgan and U. Proske 1P
- Training with eccentric exercise to prevent hamstring strains*
U. Proske, P. Percival and D.L. Morgan..... 2P
- Stretch-activated channels in stretch-induced muscle damage - role in muscular dystrophy*
E.W. Yeung and D.G. Allen 3P
- Mechanisms of muscle damage in muscular dystrophy*
G.S. Lynch..... 4P
- The role of Dystrophin in muscle maintenance within the zebrafish embryo and the identification of zebrafish models of human muscular dystrophy*
P.D. Currie..... 5P

**Symposium 2: Potassium channels and endothelium-derived hyperpolarising factor:
Physiological and clinical roles**

- Endothelium-derived hyperpolarising factor and cell coupling: Factors and fiction?*
S.L. Sandow 6P
- Endothelial potassium channels in the regulation of vascular tone in health and in disease*
H.A. Coleman, M. Tare and H.C. Parkington 7P
- Changes in endothelium-derived hyperpolarising factor in ageing and hypertension:
response to chronic treatment with renin-angiotensin system blockers*
K. Goto, K. Fujii, Y. Kansui and M. Iida 8P
- Potassium channels in the cerebral circulation in health and vascular disease*
C.G. Sobey 9P

Free Communications 1: Skeletal Muscle

- Near-membrane cytosolic $[Ca^{2+}]$ levels and Ca^{2+} transients measured in myotubes grown from normal and dystrophic (mdx) mice using the Ca^{2+} indicator FFP-18*
A.J. Bakker, R. Han and M.D. Grounds..... 10P
- Elevated temperature effects on sarcoplasmic reticulum function in mammalian skeletal muscle fibres*
C. van der Poel and D.G. Stephenson 11P
- Effect of low ATP concentrations on action potential-induced Ca^{2+} release in mechanically-skinned EDL fibres of the rat*
T. Dutka and G.D. Lamb 12P
- Magnesium inhibition of skeletal RyRs modified by DIDS, ryanodine and ATP*
E.R. O'Neill, G.D. Lamb and D.R. Laver..... 13P
- Nitric oxide alters the rate and sensitivity of sarcoplasmic reticulum calcium uptake in ovine skeletal muscle*
J.J. Cottrell, R.D. Warner, F.R. Dunshea, M.B. McDonagh and R. Kuypers..... 14P
- Phosphorylation status of calsequestrin does not alter its ability to regulate native ryanodine receptors*
N.A. Beard, M.G. Casarotto, D.R. Laver and A.F. Dulhunty 15P

Free Communications 2: Ion channels and biophysics

- NO donors increase persistent sodium current in HEK293 cells transfected with the human cardiac Na^+ channel α -subunit*
W. Wu, F. Leves and P.W. Gage 16P
- Aphidicolin-induced stress pathway in pre-implantation embryos*
H.-S. Lee and M.L. Day 17P
- Distinct expression of intermediate-conductance calcium-activated potassium (IK) channels in intrinsic primary afferent neurons of the rat gastrointestinal tract*
C.B. Neylon, H.L. Robbins, B. Hunne, S.E. Moore and J.B. Furness..... 18P
- Inhibition of human large conductance calcium-activated potassium channels by a fungal toxin*
J.E. Dalziel, S.C. Finch and J. Dunlop..... 19P
- Estimations of relative anion-cation permeabilities deduced from reversal (dilution) potential measurements, as in glycine receptor channel studies, are essentially model independent*
P.H. Barry, A. Keramidas, A.J. Moorhouse and P.R. Schofield 20P

<i>Role of charged residues in coupling ligand binding and channel activation in the extracellular domain of the glycine receptor</i> N.L. Absalom, T.M. Lewis, W. Kaplan, K.D. Pierce and P.R. Schofield	21P
--	-----

APPS Lecture - David Allen

<i>Skeletal muscle function: the role of ionic changes in fatigue, damage and disease</i> D.G. Allen	22P
---	-----

Free Communications 3: Cardiac Muscle

<i>Tolerance of male and female rat papillary muscles to acute metabolic compromise</i> I.R. Wendt and B. Zoltkowski.....	23P
--	-----

<i>The rate of reactivation of the cardiac sodium hydrogen exchanger following inhibition with cyanide</i> J.M. Tipene and D.G. Allen	24P
--	-----

<i>Activity of the cardiac Na⁺-H⁺ exchanger during ischaemia</i> X.-H. Xiao and D.G. Allen	25P
---	-----

<i>The effect of polyunsaturated fatty acids on cardiac ryanodine and inositol triphosphate receptors</i> B. Honen, D. Saint and D.R. Laver.....	26P
---	-----

<i>ATP modulates intracellular Ca²⁺ and firing rate through a P2Y₁ purinoceptor in cane toad pacemaker cells</i> Y.K. Ju, W. Huang, L. Jiang, J. Barden and D.G. Allen	27P
---	-----

<i>Calcium loading properties of sarcoplasmic reticulum from rat ventricular myocardium</i> L.M. Gibson and D.G. Stephenson	28P
--	-----

Free Communications 4: Nervous system and special senses

<i>Temperature sensitivity of dopaminergic neurons in the Substantia Nigra pars compacta</i> K.K. Chung and J. Lipski.....	29P
---	-----

<i>The nature of non-linear interaction between P2 purinergic and α₁ adrenergic receptors in hypoglossal motoneurons is determined by the temporal pattern of receptor activation</i> R. Kanjhan, A. Jung, G.B. Miles, J. Lipski, G.D. Housley, M.C. Bellingham and G.D. Funk	30P
---	-----

<i>Glutamate alters the morphology of dendritic spines in motoneurons</i> A.J.C. McMorland, D.M. Robinson, C. Soeller, M.B. Cannell and G.D. Funk	31P
--	-----

<i>μ and δ opioid receptor mRNA and protein expression in the cerebellum of the foetal, neonatal, and adult rat</i> J.H. Miller, E.M. Mrkusich, B.M. Kivell and D.J. Day	32P
---	-----

<i>Upregulation of ecto-nucleoside triphosphate diphosphohydrolases 1 and 2 in noise-exposed rat cochlea</i> S.M. Vlajkovic, G.D. Housley, D.J.B. Munoz, S.C. Robson, J. Sevigny, C.J.H. Wang and P.R. Thorne.....	33P
<i>Quantifying local diffusion in the rat lens by two-photon flash photolysis</i> M.D. Jacobs, C. Soeller, M.B. Cannell and P.J. Donaldson.....	34P
1615 - Poster Communications 1	
<i>Motor unit discharge properties of respiratory muscles during quiet breathing</i> J.P. Saboisky, J.E. Butler and S.C. Gandevia.....	35P
<i>Block of the divalent anion channel in the SR of rabbit skeletal muscle by disulfonic stilbene derivatives</i> K. Bradley and D.R. Laver.....	36P
<i>Aberrant splicing of ryanodine receptor in myotonic dystrophy</i> T. Kimura, M.P. Tkahashi and S. Sakoda.....	37P
<i>Glutathione transferase mu-2 modulation of the activity of muscle sarcoplasmic reticulum</i> Y.A. Abdellatif, S. Watson, A.F. Dulhunty, P. Board and P.W. Gage.....	38P
<i>The effect of prolonged ischemia on the tonic stretch reflex of the tibialis anterior muscle and stiffness of the ankle joint</i> J.A. Burne and A.R.N.M.H. Haque.....	39P
<i>The effect of background contraction and prolonged ischemia on the tendon reflex</i> A.R.N.M.H. Haque and J.A. Burne.....	40P
<i>Acute incremental exercise, sprint exercise, as well as chronic intermittent hypoxia each decrease muscle Na⁺K⁺ATPase activity</i> R.J. Aughey, J.A. Hawley, C.J. Gore, A.G. Hahn, D.T. Martin, S.A. Clark, N.E. Townsend, T. Kinsman, M.J. Ashenden, K.E. Fallon, G.J. Slater, A.P. Garnham, C.M. Chow and M.J. McKenna.....	41P
<i>A simple method for determining regional visual acuity in humans</i> D.F. Davey and W. Burke.....	42P
<i>ATP acts as both a competitive antagonist and a positive allosteric modulator at recombinant NMDA receptors</i> A. Kloda, J.D. Clements, R. Lewis and D.J. Adams.....	43P
<i>Inhibitory synaptic transmission in mouse type A and B medial vestibular nucleus neurones in vitro</i> A.J. Camp, B.A. Graham, R.J. Callister and A.M. Brichta.....	44P

<i>Ryanodine receptor isoforms in the neonatal rat cochlea</i> R.T. Whitehead, M.B. Cannell and G.D. Housley	45P
<i>Localisation of P2X6 receptor protein expression in the adult rat cochlea</i> D. Greenwood, L.K. Yang, P.R. Thorne and G.D. Housley	46P
<i>GABA_A receptor subunit composition in cultured hippocampal neurons from newborn rats</i> N. Ozsarac, M.L. Tierney and P.W. Gage	47P
<i>Affinity purification of the skeletal muscle ryanodine receptor using a glutathione-S-transferase-FKBP12 fusion protein</i> P. Pouliquin, S. Pace and A.F. Dulhunty	48P
<i>The role of the Ether-à-go-go K⁺ channel in cellular proliferation in the mouse preimplantation embryo</i> S.L. Jones and M.L. Day	49P
<i>The Cys-loop's role in ligand-binding and channel-gating in the GABA_A receptor</i> V.A.L. Seymour, T. Luu, M.L. Tierney and P.W. Gage	50P
<i>Expression of calcium release channels in rat arteries</i> T.H. Grayson and C.E. Hill	51P
<i>Mineralocorticoid activates epithelial sodium channel via exocytosis in mouse renal collecting duct cells</i> Y. Hosoda, M. Pedler, H. Hu, A. Beesley, C. Bailey, A. Dinudom, J.E.J. Rasko and D.I. Cook	52P
Symposium 3: Role of neural angiotensin II in regulation of cardiovascular function	
<i>Angiotensin in the ventrolateral medulla</i> A.M. Allen	53P
<i>Brain angiotensin and body fluid homeostasis</i> M.J. McKinley, T. Alexiou, P. Sinnayah and M. Mathai	54P
<i>Superoxide mediates excitatory actions of angiotensin II in the rostral ventrolateral medulla during acute stress</i> D.N. Mayorov, G.A. Head and R. De Matteo	55P
<i>Modulation of neurohumoral effector gain as a novel mechanism for the long term regulation of blood pressure</i> G.A. Head and S.L. Burke	56P
<i>Role of angiotensin II in regulating long term levels of sympathetic activity</i> S.C. Malpas, C.J. Barrett, S.J. Guild, R. Ramchandra and D. Budgett.....	57P

Symposium 4: Regulation of ion transport

Regulation of the epithelial sodium channels

A. Dinudom..... 58P

Links between cell proliferation and K channel activity

M.L. Day 59P

Regulation of the glutamine transporter SN1 (SNAT3)

S. Bröer 60P

The familial intrahepatic cholestasis type 1 protein: a P-type ATPase influencing bile acid transporters

M.J. Harris and I.M. Arias 61P

Free Communications 5: Skeletal muscle

Variations in myosin expression along the length of orbital fibres in the rabbit extraocular muscle

C.A. Lucas and J.F.Y. Hoh 62P

Fibre types in rat laryngeal muscles and their transformations following denervation and reinnervation

H.S. Rhee, C.A. Lucas and J.F.Y. Hoh..... 63P

There is no difference in the net efficiency of fast- and slow-twitch mouse muscles

C.J. Barclay and C.L. Weber..... 64P

Treatment with the β_2 -agonists formoterol or salmeterol produce greater muscle hypertrophy in rats than fenoterol

J.G. Ryall, D.R. Plant and G.S. Lynch..... 65P

Ca^{2+} handling properties of mechanically skinned fibres from fast and slow muscles of adult and old rats following chronic fenoterol treatment

D.R. Plant, J.G. Ryall, P. Gregorevic and G.S. Lynch 66P

Free Communications 6: Ion channels and membrane transport

Involvement of a voltage-dependent calcium channel in signal transduction in the 2-cell embryo

Y. Li, M.L. Day and C. O'Neill 67P

Negative feedback inhibition of Ca^{2+} influx during P_{2Y2} receptor activation

H. Hu, M.M. Cummins, Y. Hosoda, P. Poronnik, M.L. Day and D.I. Cook..... 68P

Calcium release-activated calcium current in rat hepatocytes

G.Y. Rychkov, T. Litjens, M.L. Roberts and G.J. Barritt..... 69P

<i>Characterisation of chloride currents in the mouse pre-implantation embryo</i> I. Pons-Meneghetti, M.L. Day, D.I. Cook and M.H. Johnson	70P
<i>Clustering of recombinant GABA_A receptors alters channel properties</i> A.B. Everitt, M.L. Tierney and P.W. Gage.....	71P
Invited Lecture - Julian Paton	
<i>Signalling across the blood brain barrier: Implications for blood pressure control</i> J.F.R. Paton	72P
Poster Session 2	
<i>Effect of oscillating airway smooth muscle length on bronchoconstriction — the role of the airway wall</i> P.B. Noble, P.K. McFawn and H.W. Mitchell	73P
<i>Bronchial response to protease-activated receptor stimulation of airway luminal and adventitial surfaces</i> H.W. Mitchell, H.L. Goh, N. Asokanathan, R.S. Lan, G.A. Stewart and A. Sharma	74P
<i>Measurement of culture confluency and volume of human airway smooth muscle cells using quantitative phase microscopy</i> C.L. Curl, C.J. Bellair, T. Harris, B.E. Allman, A. Roberts, K.A. Nugent, P.J. Harris, A.G. Stewart and L.M.D. Delbridge	75P
<i>Increases in renal angiotensinogen mRNA levels following a mixed amino acid infusion in late gestation fetal sheep</i> A.C. Boyce, K.J. Gibson, J. Wu and E.R. Lumbers.....	76P
<i>Central program and ovarian feedback both influence LH secretion in flying-foxes</i> G.M. O'Brien and K.-A. Gray	77P
<i>The dorsomedial hypothalamic nucleus modulates the baroreceptor reflex</i> L.M. McDowall, S. Killinger and R.A.L. Dampney	78P
<i>Renal sympathoexcitatory response evoked from the dorsomedial hypothalamic nucleus is mediated by presympathetic vasomotor neurons in the rostral ventrolateral medulla</i> J. Horiuchi, S. Killinger, R.M. McAllen, A.M. Allen and R.A.L. Dampney	79P
<i>Blockade of angiotensin type 1 (AT1) receptors in the rostral ventrolateral medulla increases renal sympathetic activity and arterial pressure under hypoxic conditions</i> J. Sheriff, M.A.P. Fontes, S. Killinger and R.A.L. Dampney	80P
<i>Angiotensin II microinjections in the nucleus tractus solitarius has an inhibitory effect on the cardiac but not the non-cardiac sympathetic component of the baroreceptor reflex</i> P. Tan and R.A.L. Dampney.....	81P

<i>Angiotensin II via AT₁ receptors may mediate apoptosis in the cardiac conduction system of rats</i> U. Vongvatcharanon, S. Vongvatcharanon, N. Radenahmad, P. Kirirat, P. Intasaro, P. Sobhon and T. Parker	82P
<i>Effect of sinoaortic denervation on baroreflex sensitivity assessed with complex demodulation in the anaesthetised rat</i> Y.C. Tzeng, P.D. Larsen and D.C. Galletly	83P
<i>Change in baroreflex sensitivity during induction of anaesthesia with propofol</i> P.D. Larsen, Y.C. Tzeng and D.C. Galletly	84P
<i>Calbindin D-28K and parvalbumin calcium-binding proteins in SA and AV node of rat heart</i> S. Vongvatcharanon and U. Vongvatcharanon	85P
<i>Cardiac remodelling contributes to altered ventricular mechanics in hypertensive cardiomyopathy</i> A.P. Pope, B.H. Smaill and I.J. LeGrice	86P
<i>Autoperfused hindlimb as a physiologically relevant model to study skeletal muscle function and metabolism</i> A.J. Hoy, G.E. Peoples and P.L. McLennan	87P
<i>Vascular remodeling and changes in cellular coupling during vascular disease</i> N.M. Rummery, S.L. Sandow, T.D. Brackenbury and C.E. Hill.....	88P
<i>Initiation and coordination of vasomotion in rat cerebral arteries</i> R.E. Haddock, T.D. Brackenbury and C.E. Hill	89P
<i>Functional remodeling in response to prolonged agonist exposure or elevated pressure delays arteriolar relaxation</i> S.J. Potocnik, M.A. Hill, L.A. Martinez-Lemus and G.A. Meininger.....	90P
Free communications 7: Exercise physiology	
<i>Opposing effects of acute and chronic high intensity exercise on Na⁺K⁺ATPase activity in skeletal muscle</i> R.J. Aughey, K.T. Murphy, S.A. Clark, J. Christie, A.G. Hahn, C.J. Gore, A.P. Garnham, C.M. Chow, J.A. Hawley and M.J. McKenna.....	91P
<i>Acute intense exercise upregulates Na⁺,K⁺-ATPase isoform mRNA, but not protein expression in human skeletal muscle</i> K.T. Murphy, R.J. Snow, A.C. Petersen, R.M. Murphy, J. Mollica, J.S. Lee, A.P. Garnham, R.J. Aughey, J.A. Leppik, I. Medved, D. Cameron-Smith and M.J. McKenna.....	92P

<i>Increased Na⁺K⁺ATPase content is associated with improved potassium regulation during maximal exercise after sprint training in non-diabetics, but not in type 1 diabetes mellitus</i> A.R. Harmer, P.A. Ruell, M.J. McKenna, D.J. Chisholm, J.M. Thom, S.K. Hunter and J.R. Sutton	93P
<i>Effect of exercise on intracellular insulin signalling in human skeletal muscle</i> K.F. Howlett, K. Sakamoto, H. Yu, L.J. Goodyear and M. Hargreaves.....	94P
<i>Exercise and myocyte enhancer factor 2 regulation in human skeletal muscle</i> M. Hargreaves and S.L. McGee.....	95P
<i>Effect of exercise on Ca²⁺-sensitive protein kinases in human skeletal muscle</i> A.J. Rose, B. Michell, B.E. Kemp and M. Hargreaves	96P
<i>The effect of repeated bouts of level and downhill treadmill walking on plasma interleukin-6</i> N.C. Bevan, P.M. Bergin, T.J. Connor and S.A. Warmington	97P
<i>Determinants of muscle buffer capacity</i> D. Bishop and J. Edge.....	98P
Symposium 5: Hormonal, metabolic and neural control of the kidney	
<i>Activation of renal calcium and water excretion by novel activators of the calcium-sensing receptor</i> A.D. Conigrave and H. Lok	99P
<i>Molecular changes in proximal tubule function in diabetes mellitus</i> P. Poronnik and C.A. Pollock.....	100P
<i>Differential neural control of glomerular ultrafiltration</i> K.M. Denton, S.E. Luff, A. Shweta and W.P. Anderson.....	101P
<i>Neural control of renal medullary perfusion</i> R.G. Evans, G.A. Eppel, S.C. Malpas and K.M. Denton.....	102P
Symposium 6: Functional imaging	
<i>Gaining new insights into physiological function from biophotonics</i> M.B. Cannell	103P
<i>Biosensors for investigating neuronal Ca²⁺ signalling</i> D.A. Williams, M.L. Smart and C.A. Reid.....	104P
<i>New views of lens structure and function</i> P.J. Donaldson, A.C. Grey, B.R. Merriman-Smith, A.M.G. Sisley, C. Soeller, M.B. Cannell and M.D. Jacobs.....	105P

<i>Quantitative phase microscopy - a new way to interrogate the structure and function of unstained viable cells</i>	
C.L. Curl and L.M.D. Delbridge.....	106P
<i>High throughput imaging of extended tissue volumes</i>	
I.J. LeGrice, G. Sands, D. Hooks, D. Gerneke and B.H. Smaill.....	107P
Symposium 7: Active Learning	
<i>Active learning: If it works, why aren't we all doing it?</i>	
J.A. Michael	108P
<i>Promoting active learning with a Generic Skills Guide</i>	
M.I. Frommer	109P
<i>Where should we focus, teaching or learning?</i>	
M.L. Roberts	110P
Free communications 8: Skeletal muscle, microcirculation, and reproduction	
<i>Role of the calcineurin signal transduction pathway in muscle regeneration in dystrophic mdx mice</i>	
N. Stupka, D.R. Plant and G.S. Lynch.....	111P
<i>Muscle damage in mdx mice is reduced after treatment with streptomycin</i>	
N.P. Whitehead and D.G. Allen	112P
<i>Influence of lowered $[Na^+]_o$ on single and trains of action potentials in soleus muscle fibres of the mouse</i>	
S.P. Cairns and J.M. Renaud	113P
<i>The effect of reactive oxygen species on muscle fatigue at room temperature compared to body temperature</i>	
T.R. Moopanar and D.G. Allen.....	114P
<i>Nutritive and non-nutritive blood flow and oxygen consumption in active rat skeletal muscle</i>	
A.J. Hoy, G.E. Peoples and P.L. McLennan	115P
<i>Glutathione synthesis in whole human red blood cells</i>	
J.E. Raftos	116P
<i>Circadian gene expression in mouse uterus and liver</i>	
A.A. Lim, M.H. Johnson and M.L. Day	117P

Free communications 9: Fetal and renal physiology

- Effects of vitamin D insufficiency in the fetus and in early life on vascular reactivity in young adult rats*
H.C. Parkington, S.J. Emmett, R. Morley, C. Skordilis, H.A. Coleman and M. Tare 118P
- Possible role of the brain angiotensin system in programming and maintaining hypertension in sheep prenatally exposed to dexamethasone*
A. McAlinden, A. Jefferies, M. Cock, E. Wintour, C. May and M. Dodic..... 119P
- The effects of maternal renal dysfunction and a high salt diet on the renin angiotensin systems of the pregnant ewe and her fetus*
K.J. Gibson, A.C. Boyce, B.M. Karime, C.L. Thomson, J. Wu, Y.P. Zhou and E.R. Lumbers 120P
- The role of renal sympathetic nerve activity in the hypertension induced by chronic nitric oxide blockade*
R. Ramchandra, C.J. Barrett, S.J. Guild and S.C. Malpas 121P
- Baroreflexes play a major role in regulating the long-term level of sympathetic nerve activity*
S.J. Guild, C.J. Barrett, R. Ramchandra and S.C. Malpas 122P
- NO and α -adrenoceptor subtypes in regional renal vascular responses to renal nerve stimulation in rabbits*
G.A. Eppel, L.L. Lee, K.M. Denton, S.C. Malpas and R.G. Evans..... 123P
- Do nitric oxide and prostaglandins protect the renal medullary circulation from ischaemia during renal nerve stimulation?*
N.W. Rajapakse, G.A. Eppel, K.M. Denton, S.C. Malpas and R.G. Evans..... 124P
- ## **Symposium 8: Integrating cardiac function: From molecules to man**
- Ion channelopathies: What have they taught us about arrhythmias and anti-arrhythmic therapy?*
J.I. Vandenberg and T.J. Campbell..... 125P
- Cardiac hypertrophy: comparing models and counting genes*
L.M.D. Delbridge..... 126P
- Modelling and imaging cardiac function during excitation-contraction coupling*
C. Soeller and M.B. Cannell 127P
- Cardiac structure and electrical activation: models and measurement*
B.H. Smaill..... 128P

Symposium 9: Exocytosis and neurosecretion

Differential regulation of two modes of exocytosis by protein phosphatases

A.T.R. Sim 129P

Coupling G protein-coupled receptors to exocytosis

P.D. Marley 130P

PI-3 kinase type II C2 α is essential for ATP-dependent priming of neurosecretory granules prior to exocytosis

F.A. Meunier, G. Hammond, P.J. Parker, G. Schiavo, F.T. Cooke and J. Domin..... 131P

Pre- and postsynaptic factors controlling synaptic efficacy at central synapses

M.C. Bellingham and M.L. Kerr 132P

Popping sarcomere hypothesis explains stretch induced muscle damage

D.L. Morgan and U. Proske, Monash University, Clayton, Vic 3800, Australia. .SP

It has been known for over 100 years that active stretch of muscle, also known as eccentric or pliometric contraction, can lead to sore and stiff muscles, beginning the day after exercise and lasting up to a week. Mechanically eccentric contractions use muscles as brakes rather than motors, and occur in activities such as horse-riding, skiing and walking down hill. Histologically, such muscles show small areas of disrupted filament structure, confined to single fibres, and ranging in length from a single half sarcomere. Tension is also reduced more, and for longer, than after similar shortening contractions. Such exercise induces a rapid training effect, so that a second identical bout of exercise typically causes much reduced symptoms.

In 1990, it was suggested that the damage results from extremely non-uniform lengthening of sarcomeres, due to the instability of sarcomere lengths that results from the descending limb of the length-tension curve and the asymptote of the force-velocity curve (Morgan, 1990). Stretch of muscle beyond optimum length is concentrated in the sarcomere that has the lowest yield tension. This greater lengthening, on the descending limb of the length-tension curve, causes the isometric tension, and hence the yield point, to decrease. The asymptotic shape of the force velocity curve means that the sarcomere will be unable to support the existing tension at any velocity, and so will "pop", i.e. stretch rapidly and uncontrollably, limited only by passive viscosity and mass, until a length is reached where rising passive tension in that sarcomere increases to match the total tension being generated by the other un-lengthened sarcomeres. This will repeat with the next weakest sarcomere. The stretch then proceeds by popping sarcomeres in myofibrils, essentially one at a time in order from the weakest towards stronger. This explains why tension always rises during stretch, even beyond optimum length.

This hypothesis further postulated that the training effect consisted of growing extra sarcomeres in series to avoid stretch beyond optimum length. This was consistent with earlier observations that the number of sarcomeres in a fibre could change).

Since then, a number of results have supported this hypothesis. It has been shown in toad and rat muscle, that such stretch induced muscle damage is greater when the stretches are applied at longer length. It has been shown in rats and humans that training is accompanied by a shift in optimum length towards longer muscle lengths. In rats it has been confirmed that this is accompanied by an increase in the mean number of sarcomeres in the fibres of the muscle, and that the adaptation is ineffective if the stretches are moved to the same part of the length-tension curve rather than the same length.

Morgan, D.L. (1990) *Biophysical Journal*, **57**: 209-221.

Morgan, D.L. & Allen, D.G. (1999) *Journal of Applied Physiology*, **87**: 2007-2115.

Training with eccentric exercise to prevent hamstring strains

U. Proske¹, P. Percival² and D.L. Morgan², ¹*Department of Physiology, and* ²*Department of Electrical and Computer Systems Engineering, Monash University, Clayton, VIC 3800, Australia. .SP*

Eccentric exercise, where the contracting muscle is lengthened, is distinct from other forms of exercise because in someone unaccustomed to it, their muscles become stiff and sore next day. It is believed that the soreness is the result of microscopic damage to muscle fibres, leading to an inflammatory response and sensitisation of nociceptors. The soreness persists for about a week. A second period of eccentric exercise, a week after the first, is followed by much less soreness, the result of an adaptation process accompanying repair of the damage.

An indicator of muscle damage, present immediately after a period of eccentric exercise, is a shift of the muscle's length-tension relation in the direction of longer lengths (Jones *et al.*, 1997). It is believed that this is due to the presence of disrupted, non-functioning sarcomeres in series with still functional sarcomeres, and this produces an increase in whole-muscle series compliance. The shift reverses within 1–2 days. A second, sustained shift in the length-tension relation is apparent a week later. It persists for several weeks. This is the adaptation response of the muscle which is thought to involve the incorporation of additional sarcomeres into the repaired muscle fibres. As a result of this secondary shift, less of the muscle's working range lies on the descending limb of the length-tension relation, the region where disruption and damage is most likely to occur (Morgan, 1990).

Hamstring strains are the most important soft-tissue injury in the Australian Football League (AFL). There is evidence that hamstring strains occur while players are carrying out eccentric contractions during rapid knee extensions in sprinting and kicking a ball. We have recently proposed that the microscopic damage from eccentric contractions can, during repeated contractions, act as a point of weakness for development of a more major tear injury, involving many muscle fibres (Brockett *et al.*, 2001). The group at greatest risk of a hamstring strain are previously injured players. We have shown that optimum angles for torque in previously injured hamstrings were at shorter muscle lengths than for uninjured muscles, making them more susceptible to damage from eccentric exercise and therefore more prone to injury. This is because with a short optimum length more of the muscle's working range is on the descending limb of the length-tension curve, the potential region for damage. The reasons for the shorter optimum remain uncertain, but may include factors such as a player's natural predisposition, the development of scar tissue during healing and insufficient eccentric exercise during rehabilitation.

It is possible to provide protection against the damage from eccentric exercise by means of a controlled program of eccentric training. Such a program would be designed to keep all damage at the microscopic level, yet produce an adequate shift of the optimum angle, so that less of the muscle's working range included the descending limb of the length-tension relation. We are therefore proposing a strategy of regular testing of optimum angles together with a program of mild, targetted eccentric exercise as a means of reducing the incidence of hamstring strains, indeed, of strain injuries in all susceptible muscles.

Brockett, C.L., Morgan, D.L. & Proske, U. (2001) *Medicine and Science in Sports and Exercise*, 33:783-790.

Jones, C., Allen, T., Talbot, J., Morgan, D.L. & Proske, U. (1997) *European Journal of Applied Physiology and Occupational Physiology*, 76:21-31.

Morgan, D.L. (1990) *Biophysical Journal*, 57:209-221.

Stretch-activated channels in stretch-induced muscle damage - role in muscular dystrophy

E.W. Yeung¹ and D.G. Allen², ¹Department of Rehabilitation Sciences, Hong Kong Polytechnic University, Hong Kong, and ²Institute for Biomedical Research and Department of Physiology, University of Sydney, NSW 2006, Australia. .SP

Unaccustomed eccentric contractions result in damage to skeletal muscles which can last for up to one week. In normal individuals, this muscle damage represents a transient weakness and discomfort after unaccustomed exercise. However in muscular dystrophy repetitive damage cannot be adequately repaired and contributes to progressive weakness and muscle degeneration.

We have studied the causes of stretch-induced muscle damage in single mouse muscle fibres which were stretched by 40% of optimal length (L_0) during 10 maximal tetani (Balnave & Allen, 1995). As a consequence of eccentric contractions, the recognised features of damage included: (i) reduced maximal force; (ii) greater reduction of force at low stimulation frequencies; and (iii) a shift in L_0 to a longer muscle length, which is characteristic of sarcomere disorganisation. Isometric tetani or stretches of resting fibres produced none of these features.

The cause of the reduced force and muscle damage are not established but one theory is that tears in the muscle membrane allow influx of ions such as Na^+ and Ca^{2+} and the efflux of proteins such as creatine kinase. To investigate this mechanism we measured intracellular sodium concentration ($[\text{Na}^+]_i$) after both isometric or eccentric tetani. $[\text{Na}^+]_i$ was unaffected by isometric tetani but increased after eccentric contractions from the resting level of 7.2 ± 0.5 mM to 16.3 ± 1.6 mM over 1-2 min and the increase persisted for more than 30 min. There was no evidence of localised elevations of $[\text{Na}^+]_i$ which might result from membrane tears but, instead, the rise could be prevented by gadolinium (Gd^{3+}), a blocker of stretch-activated channels (Yeung *et al.*, 2003). These results suggest that a stretch-activated Na^+ permeable channel is opened following eccentric contractions and causes the increased $[\text{Na}^+]_i$. Since Gd^{3+} reduced Na^+ influx we tested whether it could prevent muscle damage as measured by the force production 10 min after eccentric contractions. When Gd^{3+} was applied over the period in which $[\text{Na}^+]_i$ rises (i.e. for the first 10 min after the eccentric contractions), it increased the force from 36 ± 5 to $49 \pm 4\%$.

Given that Gd^{3+} prevented Na^+ entry and minimised force reduction following eccentric contractions in wild-type fibres, we examined the same phenomena in *mdx* muscles. We establish that *mdx* fibres have a higher than normal resting $[\text{Na}^+]_i$ and show that single fibres from *mdx* muscle are more susceptible to eccentric damage. The rise in $[\text{Na}^+]_i$ following eccentric contraction was greater in *mdx* compared to wild-type mice. This rise in $[\text{Na}^+]_i$ could be reduced by Gd^{3+} and, as with wild-type fibres, the force after eccentric contractions was increased when Gd^{3+} was applied over the period in which $[\text{Na}^+]_i$ rose.

Stretch-activated channels are also permeable to Ca^{2+} , so they could provide a leak pathway for Ca^{2+} to enter the cell causing cellular damage. Investigations in Ca^{2+} handling as a result of activity of the stretch-sensitive channels after eccentric contractions should enhance our understanding of muscle damage in muscular dystrophy

Balnave, C.D. & Allen, D.G. (1995) *Journal of Physiology*, 488, 25-36.

Yeung, E.W., Ballard, H.J., Bourreau, J-P. & Allen, D.G. (2003) *Journal of Applied Physiology*, 94, 2475-2482.

Mechanisms of muscle damage in muscular dystrophy

G.S. Lynch, Department of Physiology, The University of Melbourne, Victoria 3010, Australia. SP
Muscular dystrophies are a group of neuromuscular disorders characterised by progressive and extensive muscle wasting and weakness. Patients with Duchenne muscular dystrophy (DMD) have mutations in the gene for the subsarcolemmal protein dystrophin. The muscles of the *mdx* mouse, an animal model for DMD, also lack dystrophin. Although *mdx* mice exhibit a relatively benign phenotype, the lack of dystrophin renders their limb muscles more susceptible to contraction-induced injury (Brooks 1998; DelloRusso *et al.*, 2002). Due to its role in linking the cytoskeleton to the extracellular matrix, dystrophin is postulated to have a mechanical function, namely the stabilisation of the muscle fibre membrane integrity in both quiescent and contracting muscles (Lynch *et al.*, 2000). Support for this hypothesis has been demonstrated by the sarcolemmal fragility of fibres from *mdx* mice which have a greater susceptibility to rupture following osmotic shock and active muscle lengthening, although the findings remain controversial (Brooks, 1998). In many cases, the severity of the contraction protocols used, make it difficult to discern genuine differences between the injury susceptibility of normal and dystrophin-deficient skeletal muscle.

More recently, contraction protocols have been devised that might more accurately test the hypothesis that dystrophin deficiency increases the likelihood of contraction-mediated damage. These protocols are important for testing whether muscles from transgenic *mdx* mice, expressing different truncated dystrophins are protected against damage caused by muscle activity. In fact, injection of adeno-associated viruses carrying micro-dystrophins into dystrophic muscles of immunocompetent *mdx* mice results in a significant reversal of the histopathological features of the disease, and protection from contraction injury, highlighting the clinical potential of these therapeutic approaches (Harper *et al.*, 2002).

It is generally accepted that damage to membranes in dystrophic muscle represents a component of the initial mechanism of injury that does not occur in normal muscles. Membrane disruption could allow influx of calcium that triggers the cellular pathways of destruction, leading to necrosis. However, the lack of dystrophin may not be the sole reason for the greater susceptibility of dystrophic muscles to contraction-mediated damage. Other studies have suggested that the appearance of significant numbers of abnormally branched fibres in dystrophic muscles might also contribute to the aetiology of damage. Branched fibres and their specific branching points may render them inherently weaker than non-branched fibres and this may help explain why regeneration ultimately fails (Schmalbruch, 1984).

Traditionally, it was thought that larger calibre fibres were more susceptible to contraction-mediated damage than small calibre muscle fibres, and that increasing the size of dystrophic muscle fibres following treatment with anabolic agents may actually increase injury susceptibility. Instead, recent work by Bogdanovich and colleagues (2002) suggests that making muscle fibres larger may ameliorate the symptoms of the disease, as advocated previously (Lynch, 2001). Although these results are encouraging from a clinical perspective, it is still possible that these hypertrophied dystrophic muscles remain vulnerable to extreme stress (Zammit & Partridge, 2002).

Bogdanovich, S., Krag, T.O.B., Barton, E.R., Morris, L.D., Whittemore, L-A., Ahima, R.S. & Khurana, T.S. (2002) *Nature* 420, 418-421.

Brooks, S.V. (1998) *Journal of Muscle Research and Cell Motility* 19, 179-187.

DelloRusso, C., Crawford, RW, Chamberlain, J.S. & Brooks, S.V. (2002) *Journal of Muscle Research and Cell Motility* 22, 467-475.

Harper, S.Q., Hauser, M.A., DelloRusso, C., Duan, D., Crawford, R.W., Phelps, S.F., Harper, H.A., Robinson, A.S., Engelhardt, J.F., Brooks, S.V. & Chamberlain, J.S. (2002) *Nature Medicine* 8, 253-261.

Lynch, G.S., Rafael, J.A., Chamberlain, J.S. & Faulkner, J.A. (2000) *American Journal of Physiology (Cell Physiology)* 279, C1290-C1294.

Lynch, G.S. (2001) *Expert Opinion on Therapeutic Patents* 11, 587-601.

Schmalbruch, H. (1984) *Neurology* 34, 60-65.

Zammit, P.S. & Partridge, T.A. (2002) *Nature Medicine* 8, 1355-1356.

Supported by research grants from the Muscular Dystrophy Association (USA)

The role of Dystrophin in muscle maintenance within the zebrafish embryo and the identification of zebrafish models of human muscular dystrophy

P.D. Currie, Victor Chang Cardiac Research Institute, 384 Victoria Street, Darlinghurst NSW 2010, Australia. (Introduced by David Allen) .SP

Large-scale mutagenic screens of the zebrafish genome have identified numerous mutations that disrupt differentiation and maintenance of skeletal muscle within the zebrafish embryo. Mutants possess phenotypes that range from a failure of myoblasts to elongate and fuse into a multinucleate muscle fibres to those that exhibit muscle degeneration reminiscent of human muscular dystrophies. Homozygous mutants of this latter class form myofibrils normally but are lost focally or globally, depending on the loci involved, during early larval life. Here we present data specifically on one member of the zebrafish dystrophic mutant class and reveal that its phenotype results from mutations within the zebrafish Dystrophin orthologue. We will present a detailed characterisation of the phenotype that arises as a consequence of the loss of Dystrophin expression within the embryonic and larval myotomes of zebrafish. This analysis points to the critical and novel roles that the Dystrophin and its associated-glycoprotein complex plays in the ontogeny of zebrafish muscle. We will compare and contrast the function of Dystrophin in teleost and mammalian muscle fibre biogenesis. This analysis represents the first identification of a zebrafish model of a human muscular dystrophy and we will discuss the possible application of zebrafish genetic methodologies to the study of the human dystrophic condition.

Endothelium-derived hyperpolarising factor and cell coupling: Factors and fiction?

S.L. Sandow, Division of Neuroscience, John Curtin School of Medical Research, ANU, Canberra, ACT 0200, Australia. SP

Together with nitric oxide and prostaglandins, endothelium-derived hyperpolarising factor (EDHF) is one of three vasodilatory factors produced by the arterial endothelium. The nature and mechanism of action of EDHF is the subject of intense current research interest. EDHF activity has been reported to be dependent on either the release of a diffusible substance from the endothelium or to the direct contact of endothelial cells and smooth muscle cells via gap junctions. Diffusible factors proposed as EDHFs include K^+ ions, H_2O_2 , epoxyeicosatrienoic acids, L-NAME insensitive nitric oxide, and C-type natriuretic peptide. Contact-mediated EDHF is dependent on myoendothelial gap junctions (MEGJs) that enable the passage of small molecules, and/or direct electrical coupling between the two cell layers. In the latter case, this coupling would result in an endothelial cell hyperpolarisation being directly transferred to the smooth muscle, for the subsequent generation of an arterial relaxation. This latter mechanism represents the simplest explanation of EDHF activity.

Interestingly, it has been shown that the nature and mechanism of action of EDHF can differ along and between vascular beds, and that it can also change during development and in ageing and disease. Furthermore, in the mesenteric vascular bed of the rat, EDHF has been described to be K^+ ions, H_2O_2 , L-NAME insensitive nitric oxide, CNP, as well as to be due to the direct electrical coupling of endothelial cells and smooth muscle cells. This variation is likely to be due to methodological differences between the laboratories in which such studies were made. Thus, the debate in the EDHF field is often clouded by such unfortunately inconsistent reports.

Studies from our laboratory have focused on the potential role of MEGJs in EDHF activity. We have found that the distribution and activity of MEGJs is correlated with the presence of EDHF within and between vascular beds, during development and in disease. In smaller distal mesenteric arteries of the rat, for example, MEGJs are more prevalent than in larger proximal vessels (Sandow & Hill, 2000), in line with the EDHF-mediated relaxation being more prominent in the smaller than in the larger vessels (Shimokawa *et al.*, 1996). In this vascular bed, EDHF-mediated hyperpolarisation and the transfer of endothelial cell hyperpolarisation are correlated with the presence of MEGJs (Sandow *et al.*, 2002). Furthermore, in the femoral artery of the rat the lack of MEGJs is correlated with the absence EDHF-mediated hyperpolarisation (Sandow *et al.*, 2002). In the lateral saphenous artery of the juvenile rat, MEGJs are prevalent and EDHF-mediated hyperpolarisation and relaxation present (Sandow *et al.*, 2003a). This is in contrast to the saphenous artery of the adult, where MEGJs were rare and EDHF absent (Sandow *et al.*, 2003a). The relationship between EDHF and MEGJs is somewhat more complicated in disease states, such as in hypertension. In a comparative study of the caudal artery of the hypertensive SHR and normotensive WKY rat, EDHF activity was maintained, in spite of an increase in the number of smooth muscle cell layers in the vessels from the hypertensive rat. This maintenance was found to be due to a concomitant increase in the incidence of MEGJs in the caudal artery of the SHR rat (Sandow *et al.*, 2003b).

These studies demonstrate that there is a consistent positive correlation between MEGJs and EDHF activity, both of which show a heterogeneous distribution within and between vascular beds, during development and in disease. Thus, these studies demonstrate that heterocellular coupling can account for EDHF activity. Further studies will enable the identification of potential new therapeutic targets for the regional control of vasodilator function, vascular tone and cardiovascular disease.

Sandow, S.L. & Hill, C.E. (2000) *Circulation Research*, 86, 341-346.

Sandow, S.L., Tare, M., Coleman, H.A., Hill, C.E. & Parkington, H.C. (2002) *Circulation Research*, 90, 1108-1113.

Sandow, S.L., Bramich, NJ, Bandi, HP, Rummery, N & Hill, C.E. (2003a) *Arteriosclerosis, Thrombosis, and Vascular Biology*, 23, 822-828.

Sandow S.L., Goto, K, Rummery, N & Hill, C.E. (2003b). FEPS Abstract. 3, 100.

Shimokawa, H., Yasutake, H., Fujii, K., Owada, M.K., Nakaike, R., Fukumoto, Y., Takayanagi, T., Nagao, T., Egashira, K., Fujishima, M. & Takeshita, A. (1996) *Journal of Cardiovascular Pharmacology*, 28, 703-711.

Endothelial potassium channels in the regulation of vascular tone in health and in disease

H.A. Coleman, M. Tare and H.C. Parkington, Department of Physiology, Monash University, Vic 3800, Australia. .SP

Ionic mechanisms underlying EDHF. The elusive nature of endothelium-derived hyperpolarising factor (EDHF) has hampered detailed study of the underlying ionic mechanisms. By cutting arterioles into electrically short lengths it is possible to record membrane currents using single electrode voltage-clamp when the smooth muscle and endothelial cells remain in their normal functional relationship. Membrane potential can also be recorded simultaneously with contractile activity in these preparations. With this approach it is thus possible to study endothelial-dependent ionic mechanisms irrespective of the processes involved and to relate the currents to contractile activity.

In the presence of nitric oxide and prostaglandin synthesis inhibitors, acetylcholine (ACh) evoked hyperpolarisation and relaxation of guinea-pig submucosal arterioles which were abolished by the K⁺ channel blockers charybdotoxin (ChTx) plus apamin. Under voltage-clamp, ACh evoked an outward current. ChTx reduced the amplitude, while apamin plus ChTx abolished the outward current. Subtraction of the currents revealed the ChTx- and apamin-sensitive currents and their separate current-voltage relationships. Both currents reversed near the expected K⁺ equilibrium potential, were weakly outwardly rectifying, and displayed little, if any, time or voltage-dependent gating. The components have the biophysical and pharmacological characteristics of the intermediate- and small-conductance calcium-activated K⁺ channels, IK_{Ca} and SK_{Ca}, respectively (Coleman *et al.*, 2001).

Myoendothelial electrical coupling. Electrotonic spread between endothelial and smooth muscle cells is an important consideration for EDHF. Smooth muscle specific responses recorded from dye-labelled endothelial cells were indistinguishable from those recorded from dye-labelled smooth muscle cells. In contrast, in rat femoral artery, in which the smooth muscle and endothelial layers are not coupled electrically, ACh evoked hyperpolarisation only in endothelial cells. This supports the idea that EDHF hyperpolarisation results from electrotonic spread from the endothelium to the smooth muscle (Coleman *et al.*, 2001; Sandow *et al.*, 2002).

EDHF *in vivo*. The functional significance of EDHF *in vivo* was addressed by the local infusion of ACh into the rat mesenteric vascular bed. With nitric oxide and prostaglandin synthesis blocked, ACh evoked increases in blood flow that were blocked with the local infusion of ChTx plus apamin. These results indicate that EDHF contributes to endothelium-dependent vasorelaxation *in vivo* (Parkington *et al.*, 2002).

EDHF in diabetes. Vasodilator dysfunction is a well established hallmark of diabetes. In arteries from diabetic rats and women, EDHF is diminished. This is not only associated with reduced EDHF hyperpolarisation in vascular smooth muscle, but is also associated with a reduced hyperpolarisation in the endothelial cells (Wigg *et al.*, 2001).

In conclusion, the most economical explanation for EDHF is that it arises from activation of IK_{Ca} and SK_{Ca} channels in endothelial cells. The resulting endothelial hyperpolarisation spreads via myoendothelial junctions to result in the EDHF-attributed hyperpolarisation in vascular smooth muscle cells. These processes contribute to endothelium-dependent vasodilation *in vivo* and their dysfunction contributes to the impairment of vascular regulation that occurs in diabetes.

Coleman, H.A., Tare, M. & Parkington, H.C. (2001). *Journal of Physiology*, 531(2), 359-373.

Parkington, H.C., Chow, J.-A.M., Evans, R.G., Coleman, H.A. & Tare, M. (2002). *Journal of Physiology*, 542, 929-937.

Sandow, S.L., Tare, M., Coleman, H.A., Hill, C.E. & Parkington, H.C. (2002). *Circulation Research*, 90, 1108-1113.

Wigg, S.J., Tare, M., Tonta, M.A., O'Brien, R.C., Meredith, I.T. & Parkington, H.C. (2001). *American Journal of Physiology*, 281, H232-H240.

Changes in endothelium-derived hyperpolarising factor in ageing and hypertension: response to chronic treatment with renin-angiotensin system blockers

K. Goto, K. Fujii, Y. Kansui and M. Iida, Department of Medicine and Clinical Science, Graduate School of Medical Sciences, Kyushu University, Maidashi 3-1-1, Higashi-ku, Fukuoka, 812-8582, Japan. (Introduced by Prof. Caryl Hill) .SP

Endothelial cells play an important role in the regulation of vascular tone through the release of relaxing factors such as nitric oxide, prostacyclin, and endothelium-derived hyperpolarising factor (EDHF). EDHF appears to be a dominant vasodilator in resistance arteries although its identity is still elusive. Several clinical and experimental studies have shown that endothelial function is impaired in ageing and hypertension, which may be associated with an increase in cardiovascular disease. In addition, several clinical studies have shown that blocking the renin-angiotensin system (RAS) improves endothelial function not only in hypertensive patients but also in normotensive patients with other cardiovascular diseases, such as chronic heart failure and/or myocardial infarction. The aim of the present study was to test whether or not EDHF-mediated hyperpolarisation and relaxation change in ageing and hypertension, and if so, whether or not chronic treatment with RAS blockers (an angiotensin-converting enzyme inhibitor enalapril and an angiotensin II receptor antagonist candesartan) improves such change. EDHF-mediated hyperpolarisation and relaxation were examined in mesenteric arteries obtained from 3-, 6-, 12-, and 24-month-old normotensive Wistar-Kyoto rats (WKY) and 12-month-old spontaneously hypertensive rats (SHR). Furthermore, both strains were treated for three months with either RAS blockers or a conventional therapy with hydralazine and hydrochlorothiazide from 9- to 12-month-old. The rats used were anaesthetised with ether and killed by decapitation. In arteries of WKY, EDHF-mediated hyperpolarisation and relaxation were impaired at the age of 12- and 24-months compared with 3- and 6-month-old rats, with the response tending to be further impaired in 24-month-old rats. Three months of treatment with RAS blockers but not with a conventional therapy with hydralazine and hydrochlorothiazide improved the age-related impairment of EDHF-mediated responses, despite a similar reduction in blood pressure in both treatments. In arteries of SHR, EDHF-mediated hyperpolarisation and relaxation were impaired at the age of 12-months compared with age-matched, 12-month-old WKY. In SHR, all antihypertensive treatments improved the impairment of EDHF-mediated responses; however, the improvement achieved by RAS blockers was greater than that with a conventional therapy with hydralazine and hydrochlorothiazide. These findings suggest that: (1) EDHF-mediated hyperpolarisation and relaxation decline with ageing and hypertension in rat mesenteric arteries; (2) chronic treatment with RAS blockers improves the age-related impairment of EDHF-mediated responses presumably through the blockade of RAS but not lowering the blood pressure alone; (3) antihypertensive treatment restores the impaired EDHF-mediated responses in hypertension; and (4) RAS blockers may be more efficacious in improving the endothelial dysfunction associated with hypertension.

Potassium channels in the cerebral circulation in health and vascular disease

C.G. Sobey, Department of Pharmacology, The University of Melbourne, Parkville, Victoria 3010, Australia. (Introduced by C.E. Hill) .SP

Vascular K⁺ channel function. Potassium ion (K⁺) channel activity is a major regulator of vascular smooth muscle cell membrane potential, and is therefore an important determinant of vascular tone. Several diverse endogenous vasodilator stimuli act at least in part via activation of vascular K⁺ channels. The function of several types of vascular K⁺ channels is altered during major cardiovascular diseases, such as hypertension, atherosclerosis, diabetes and subarachnoid haemorrhage (SAH). Vasoconstriction and compromised ability to dilate are likely consequences of defective K⁺ channel function in blood vessels during these disease states. Increased K⁺ channel function may help to compensate for excessive vascular tone. In recent years our laboratory has investigated the functional importance of K⁺ channels in the cerebral circulation in physiology and during SAH and chronic hypertension.

Reactive Oxygen Species (ROS) as openers of K⁺ channels. ROS are powerful cerebral vasodilators and mediators of responses to bradykinin and arachidonate. Both agents produce endothelium-dependent dilatation of cerebral arterioles that is indomethacin- and catalase-sensitive, indicating that cyclooxygenase-derived ROS mediate these responses. Dilatation of cerebral arterioles by bradykinin, arachidonate or exogenous hydrogen peroxide (H₂O₂) can be blocked using tetraethylammonium (TEA) or iberiotoxin, suggesting a key role for activation of large conductance calcium-activated K⁺ (BK_{Ca}) channels.

Extracellular K⁺. Raising extracellular K⁺ concentration from approx. 3-5 mM to ≤15 mM increases outward K⁺ current through inwardly rectifying K⁺ (K_{IR}) channels, causing vascular smooth muscle hyperpolarisation and relaxation. K⁺ is a particularly powerful dilator in the cerebral circulation, and its effect is selectively inhibited by barium ion (≤ 50 μM) indicating an involvement of K_{IR} channels. Our recent data indicate that K⁺ is a more potent vasodilator in cerebral arteries of females than males.

K⁺ channel function after SAH. After SAH, bleeding and clot formation occur around the ventral surface of the brain, including major arteries, often resulting in death or severe disability. Delayed spasm and impaired dilatation of the affected arteries are critical complications of SAH. These cerebral arteries are more depolarised than control vessels, possibly due to decreased activity of K⁺ channels in vascular muscle. Vasodilator drugs which produce hyperpolarisation, such as K⁺ channel openers, appear to be effective for dilating cerebral arteries after experimental SAH.

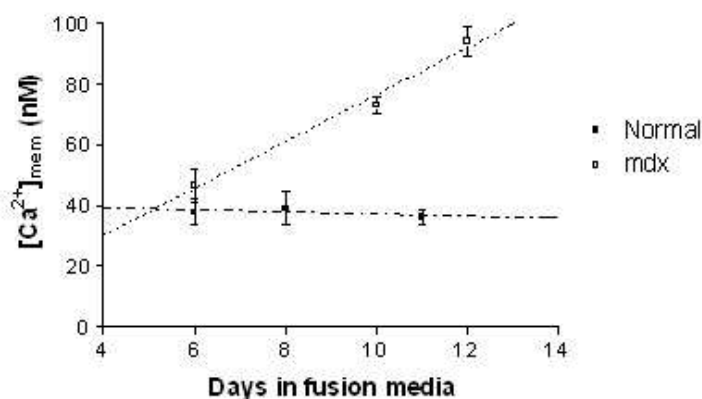
NADPH-oxidase, ROS and Hypertension. NADPH, a substrate for NADPH-oxidase, stimulates superoxide production in basilar arteries which is blocked by diphenyleneiodonium (DPI, a NADPH-oxidase inhibitor), and this production is >2-fold higher in SHR versus WKY rats. Cerebral artery mRNA expression of the NADPH-oxidase subunit, Nox4, is 4-fold higher in SHR. Application of NADPH to the basilar artery *in vivo* causes greater dilatation in SHR than WKY. DPI or inhibitors of superoxide dismutase (diethyldithiocarbamate, DETCA), H₂O₂ or BK_{Ca} channels attenuate NADPH-stimulated vasodilatation. Interestingly, bilateral carotid artery occlusion to increase flow in the basilar artery induces nitric oxide-independent vasodilatation that is inhibited by DPI. Thus, a novel mechanism for ROS-mediated vasodilatation appears to exist in the cerebral circulation in response to NADPH or increased flow, whereby NADPH-oxidase-derived superoxide is reduced by SOD to form H₂O₂. H₂O₂ then opens BK_{Ca} channels, leading to vasodilatation. Furthermore, cerebral NADPH-oxidase activity is augmented during chronic hypertension.

Near-membrane cytosolic $[Ca^{2+}]$ levels and Ca^{2+} transients measured in myotubes grown from normal and dystrophic (*mdx*) mice using the Ca^{2+} indicator FFP-18.

A.J. Bakker¹, R. Han¹ and M.D. Grounds², ¹School of Biomedical & Chemical Sciences and ²School of Anatomy & Human Biology, The University of Western Australia, Crawley, WA 6009, Australia.

Abnormal extracellular Ca^{2+} influx has been suggested to be involved in the process of muscle wasting in Duchenne muscular dystrophy. However, studies comparing the resting intracellular Ca^{2+} levels in normal and dystrophic muscle cells from patients with Duchenne muscular dystrophy and *mdx* mice have yielded contradictory findings (Gillis, 1996). Ca^{2+} indicators targeted to the inner sarcolemmal membrane have recently been reported to be more sensitive to sarcolemmal Ca^{2+} influx than standard cytosolic Ca^{2+} indicators such as fura-2 (Bruton *et al.*, 1999). In this study, we measured the resting Ca^{2+} levels and Ca^{2+} transients in myotubes grown from *mdx* and normal mice using the near-membrane Ca^{2+} indicator FFP-18.

Skeletal muscle satellite cells were isolated from the hind limbs of neonatal normal and *mdx* mice that had been killed by decapitation. Myotubes were grown on glass coverslips coated with collagen. The myotubes were loaded with the Ca^{2+} indicator by exposure to FFP-18-AM (3 μ M) and 0.0125% Pluronic F-127 for 45 min at room temperature (22-23°C). Ca^{2+} measurements were made with a Cairn spectrophotometer attached to a Nikon inverted microscope equipped for epifluorescence. The myotubes were stimulated by electrical field stimulation (EFS) via two small platinum wires (single 0.2 ms pulse).



Resting near membrane $[Ca^{2+}]$ ($[Ca^{2+}]_{mem}$) levels increased significantly during development in the *mdx* myotubes, (slope; 8.19 ± 1.47 , $p < 0.0001$). However, no change in $[Ca^{2+}]_{mem}$ was found in normal myotubes during development (slope; -0.40 ± 1.14 , $p = 0.73$). From the fitted lines, the $[Ca^{2+}]_{mem}$ in 12 days old *mdx* and normal myotubes was estimated at 93 and 36 nM respectively (Figure). Increasing the driving force for Ca^{2+} influx by raising extracellular Ca^{2+} to 18 mM, increased the steady state $[Ca^{2+}]_{mem}$ by 156.1 ± 14.2 % (to ~ 208 nM) ($n = 14$) in *mdx* myotubes, while in normal myotubes, the $[Ca^{2+}]_{mem}$ increased by only 28.8 ± 7.6 % (to ~ 49 nM) ($n = 6$), ($p = 0.007$, unpaired Student's *t*-test). The half-relaxation time of EFS-induced Ca^{2+} transients was significantly increased in *mdx* (314.5 ± 36.9 ms, $n = 8$) compared to normal myotubes (163.3 ± 28.4 ms, $n = 6$) ($p = 0.01$, unpaired *t*-test), which is consistent with previous studies using standard Ca^{2+} indicators.

The results of this study further support the hypothesis that increased Ca^{2+} influx results in raised intracellular levels in dystrophin-deficient skeletal muscle cells. The use of FFP-18 to measure steady state cytosolic Ca^{2+} in normal and *mdx* myotubes in the presence of raised extracellular Ca^{2+} could provide a more reliable method for detecting the altered Ca^{2+} homeostasis in dystrophic muscle cells.

Bruton J.D., Katz A. & Westerblad H. (1999) *Proceedings of the National Academy of Sciences USA*,

96, 3281-3286.

Gillis J.M. (1996) *Acta Physiologica Scandinavica*, **156**, 397-406.

Elevated temperature effects on sarcoplasmic reticulum function in mammalian skeletal muscle fibres

C. van der Poel and D.G. Stephenson, School of Zoology, Faculty of Science and Technology, La Trobe University, Victoria 3086, Australia. .SP

Superoxide (O₂⁻) has been shown to be produced by the muscle at elevated temperatures (40-46°C) and to cause marked reversible changes in contractile activation characteristics of mammalian skinned fibres (van der Poel & Stephenson, 2002). Here we examine the effect of similar temperature treatments on sarcoplasmic reticulum (SR) function in mammalian skeletal muscle. Long-Evans hooded rats were killed by an overdose of halothane in accordance with the procedure approved by La Trobe University Animal Ethics Committee. Extensor digitorum longus (EDL) muscles were dissected out and underwent temperature treatment at 40°C for either 5 or 30 min, 43°C for 30 min and 46°C for 5 min. Single muscle fibres were dissected from EDL muscles after exposure to elevated temperatures, mechanically skinned under paraffin oil and mounted on a force transducer. The endogenous SR Ca²⁺ content was then estimated by releasing all SR Ca²⁺ with 30mM caffeine and low Mg²⁺ (Release Solution), and measuring the area under the force response as an indicator of the amount of SR Ca²⁺ released. The fibre was then re-loaded with Ca²⁺ under standard conditions ([Ca²⁺] 200nM and pH 7.10) for either 30, 60 or 90sec and the SR Ca²⁺ was subsequently released in the Release solution. The relative area under the force responses was again used as the indicator of the relative amount of Ca²⁺ in the SR prior to the exposure to the Release solution. In order to determine the extent of Ca²⁺ leak out of the SR, the preparation was loaded with Ca²⁺ for 90 sec and then washed for either 30 or 90 sec in a leak solution (pCa = 8, 0.5mM EGTA). The remaining Ca²⁺ in the SR was then released in the Release solution and the ratio between the areas under the caffeine-induced responses after 90 and 30 sec exposure to leak solution was used to estimate the fraction of SR Ca²⁺ remaining after 60 sec in the leak solution (Macdonald & Stephenson, 2001). Results show that after exposure of the EDL muscle to 40°C for 5 or 30 min, 43°C for 30 min and 46°C for 5 min the endogenous amount of Ca²⁺ in the SR was greatly reduced. This was accompanied by a significant decrease in the rate and ability of the SR to load Ca²⁺ and by a large increase in the rate of SR Ca²⁺ leak, which could explain the decrease in both endogenous SR Ca²⁺ and the rate of SR Ca²⁺ loading. No significant recovery was observed in the parameters (0-3hrs after temperature treatment). Experiments using 20 µM TBQ (2,5-di(tert-butyl)-1,4-hydroquinone) to block the SR Ca²⁺ pump and Ruthenium Red (5 µM) to block the RyR/SR Ca²⁺ release channels indicated that the major route of the Ca²⁺ leak was through the SR Ca²⁺ pump. Pre-treatment of the muscles with the superoxide scavenger Tiron (20mM) markedly reduced the temperature-induced changes on the SR function suggesting that the observed temperature effects are influenced by O₂⁻ production. The results can explain the earlier observations on isolated muscle preparations exposed to temperatures greater than 35°C, when force production becomes markedly and irreversibly depressed (Lännergren & Westerblad, 1986). Lännergren, J. & Westerblad, H. (1986) *Journal of Physiology*, 390: 285-293. Macdonald, W. A. & Stephenson, D. G. (2001) *Journal of Physiology*, 532: 499-508. van der Poel, C. & Stephenson, D. G. (2002) *Journal of Physiology*, 544: 765-776.

Effect of low ATP concentrations on action potential-induced Ca²⁺ release in mechanically-skinned EDL fibres of the rat

T. Dutka and G. Lamb, Department of Zoology, La Trobe University, Victoria 3086, Australia. .SP

During vigorous and/or prolonged activity, the average [ATP] within the cytoplasm may decrease from ~7 mM to ~1 mM (Karatzferi *et al.*, 2001). It may decrease even lower in areas with high ATP utilisation and/or limited diffusion (e.g. triadic junction). Furthermore, ATP facilitates the opening of isolated Ca²⁺ release channels (RyRs) (Laver *et al.*, 2001), but it is currently unclear whether ATP is needed on the RyR for it to be activated by the voltage-sensor (VS) when the VS is activated in a potent and coordinated manner by an action potential (AP). By using adenosine (a competitive weak agonist for the ATP stimulatory site on the RyR) and examining force development of twitch and tetanic force responses, we sought to address whether ATP is crucial for normal AP-mediated Ca²⁺ release.

Male Long-Evans hooded rats were killed under deep anaesthesia (2% v:v halothane) and the extensor digitorum longus (EDL) muscles were excised. Single fibres were mechanically-skinned, connected to a force transducer and immersed in a standard K-HDTA solution (1mM free Mg²⁺; 8 mM total ATP; 10 mM creatine phosphate (CP) at pH 7.10, containing 50 µM EGTA, pCa 7.0). Individual fibres were then electrically stimulated (75 V cm⁻¹, 2 ms pulse) to produce either twitch or tetanic (50 Hz) force responses at control (8 mM ATP) or at low [ATP] (0.1-2 mM, where ATP was replaced with CP) with or without adenosine present (2 or 4 mM). In parallel experiments, the response of the contractile apparatus to [Ca²⁺] steps was examined by pre-equilibrating a fibre in a weakly Ca²⁺-buffered K-HDTA solution (100 µM EGTA) at pCa 7.0 at a given [ATP] and/or adenosine condition, and then rapidly activating it by plunging it into a heavily Ca²⁺-buffered solution (50 mM CaEGTA/EGTA, pCa 6.0 or 4.4) with the same [ATP] to produce either submaximal or maximal force. These fibres had been Triton X-100 treated so only the contractile apparatus was functional.

Compared to the bracketing control responses (8 mM ATP), the mean twitch peak amplitude was significantly (P<0.05) reduced under all low [ATP] conditions (to 71±4%, n=7; 66±3%, n=24; 56±3%, n=51 and 28±4%, n=8, in the presence of 2, 1, 0.5 and 0.1 mM ATP respectively). Peak tetanic force and the rate of tetanic force production was also reduced at low [ATP]. The slowing of the rise in tetanic force at ≤0.5 mM ATP was greater than that explicable by effects of low [ATP] on the rate of force development by the contractile apparatus. Therefore, it appears that the amount of AP-mediated Ca²⁺ release must have been reduced at ≤0.5 mM ATP. The reduction of twitch peak amplitude was exacerbated as the ratio of [adenosine]:[ATP] (mM:mM) was increased (2:8=96±2%, n=3; 2:2=67±4%, n=4; 2:1=41±4%, n=17; 4:1=36±3%, n=7, compared to the absence of adenosine). Since adenosine did not significantly hinder force development of the contractile apparatus, this finding indicates that adenosine competitively interfered with ATP binding to the RyR (Laver *et al.*, 2001), and hence caused reduced Ca²⁺ release. These experiments indicate that ATP must be bound to the stimulatory site on RyRs for the VS to trigger Ca²⁺ release in response to an AP, the normal *in vivo* stimulus.

Karatzferi, C., de Haan, A., Ferguson, R.A., van Mechelen, W. & Sargeant, A.J. (2001) *Pflügers Archiv*, 442: 467-474.

Laver, D.R., Lenz, G.K.E. & Lamb, G.D. (2001) *Journal of Physiology*, 537 (3): 763-778.

Magnesium inhibition of skeletal muscle ryanodine receptors modified by DIDS, ryanodine and ATP

E.R. O'Neill¹, G.D. Lamb² and D.R. Laver¹, ¹School of Biomedical Sciences, University of Newcastle, Australia and ²Department of Zoology, LaTrobe University, Australia. .SP

In skeletal muscle the activity of ryanodine receptor (RyR) calcium release channels in the sarcoplasmic reticulum is regulated by the dihydropyridine receptor (DHPR) voltage sensors in the t-tubule membrane. Ca²⁺, Mg²⁺ and ATP are potent intracellular regulators of RyRs. The effects of these substances on isolated RyRs are well characterised yet it is not clear how they regulate RyR opening under voltage-sensor control. RyRs are activated by μ M cytoplasmic Ca²⁺ and mM ATP while physiological [Mg²⁺] (~1 mM) in the cytoplasm fully inhibits them. It is proposed that during muscle contraction, DHPRs transiently relieve Mg²⁺ inhibition which then permits activation of RyRs by ATP (Lamb *et al.*, 1991).

Mg²⁺ is thought to inhibit RyRs by binding both to low affinity sites that show little specificity between divalent ions (I-sites) and to high affinity sites for Ca²⁺ (A-sites) thus preventing Ca²⁺ from activating the channel (Laver *et al.*, 1997). However, ATP is known to activate RyRs in the absence of cytoplasmic Ca²⁺ so it is not clear how Mg²⁺ at the A-sites affects channel opening under physiological conditions. Here we investigate the mechanism of Mg²⁺ inhibition in the presence of ATP and two drugs, 4,4'-diisothiocyano-stilbene-2,2'-disulfonic acid (DIDS) and ryanodine, which also activate RyRs in the absence of Ca²⁺.

RyRs were isolated from rabbit skeletal muscle and incorporated into lipid bilayers using standard techniques (O'Neill *et al.*, 2003). Skeletal muscle was removed from dead rabbits. Cytoplasmic solutions contained 250 mM Cs⁺ (230 mM CsCH₃O₃S and 20 mM CsCl) 10 mM TES at pH 7.4. Luminal solutions contained 50 mM Cs (30 mM CsCH₃O₃S and 20 mM CsCl), 10 mM TES, pH 7.4.

DIDS decreased I-site affinity for Mg²⁺ and Ca²⁺ by 10 fold and ryanodine abolished binding completely. Cytoplasmic Mg²⁺ inhibited RyRs via the Ca²⁺ activation site even in the absence of Ca²⁺ indicating that Mg²⁺ inhibition is not merely due to the prevention of Ca²⁺ binding. In the case of ryanodine modified RyRs, monovalent ions (Cs⁺) could also activate the channel. RyR activity in the virtual absence of Ca²⁺ (~1 nM) was not due to sensitisation of the channel to Ca²⁺ as previously thought (Du *et al.*, 2001; Masumiya *et al.*, 2001) but was due to Ca²⁺-independent channel opening by ryanodine. The apparent Mg²⁺ affinity at the A-site was decreased by cytoplasmic Cs⁺ and Ca²⁺ as well as by luminal Ca²⁺ in a way which suggests that cytoplasmic Mg²⁺, Cs⁺ and Ca²⁺ compete for a site near the cytoplasmic entrance. Ions at this site may progress to the A-site further into the pore. Binding of these ions at the A-site is in competition with luminal Ca²⁺ and leads to either activation (2 \times Cs⁺ or Ca²⁺) or inhibition (Mg²⁺) of RyRs.

Du, G.G., Guo, X, Khanna, V.K. & MacLennan, D.H. (2001) Ryanodine sensitizes the cardiac Ca²⁺ release channel (ryanodine receptor isoform 2) to Ca²⁺ activation and dissociates as the channel is closed by Ca²⁺ depletion. *Proceedings of the National Academy of Sciences of the United States of America*, 98: 13625-30.

Lamb, G.D. & D.G. Stephenson (1991). Effect of Mg²⁺ on the control of Ca²⁺ release in skeletal muscle fibres of the toad. *Journal of Physiology*, 434: 507-528.

Laver, D.R., T.M. Baynes & A.F. Dulhunty (1997). Magnesium inhibition of ryanodine-receptor calcium channels: evidence for two independent mechanisms. *Journal of Membrane Biology*, 156: 213-229.

Masumiya, H., Li, P., Zhang, L., & Chen, S.R. (2001) Ryanodine sensitizes the Ca²⁺ release channel (ryanodine receptor) to Ca²⁺ activation. *Journal of Biological Chemistry*, 276: 39727-35.

O'Neill E.R., Sakowska, M.M., & Laver D.R. (2003) Regulation of the calcium release channel from skeletal muscle by suramin and the disulphonate stilbene derivatives DIDS, DBDS, and DNDS.

Biophysical Journal, 84: 1-16,

Nitric oxide alters the rate and sensitivity of sarcoplasmic reticulum calcium uptake in ovine skeletal muscle

J.J. Cottrell¹, R.D. Warner¹, F.R. Dunshea¹, M.B. McDonagh¹ and R. Kuypers², ¹Department of Primary Industries, Research and Development Division, 600 Sneydes Rd, Werribee, 3030, Victoria, Australia and ²Food Science Australia, P.O. Box 3312, Tingalpa, 4173, Queensland, Australia. .SP

Calcium leakage from the sarcoplasmic reticulum (SR) to the cytosol can occur via reduced sarcoplasmic/ endoplasmic reticulum ATPase (SERCA) activity, increased efflux via the Ryanodine receptor (RyR) Ca⁺⁺ channel or SR membrane leakage. The aim of this experiment was to investigate if nitric oxide (NO) influences SR Ca⁺⁺ uptake and release from lamb carcasses after control (none), medium (300V, 14Hz) or high (700V, 14Hz) voltage electrical stimulation (ES) applied for 1 min approximately 5 min post-mortem. From 9 lambs, the SR was isolated from the *Longissimus thoracis et lumborum* (LTL) at the 13th thoracic vertebra approximately 10 min post-mortem. Isolated SR membranes were incubated for 30 min with the 100mM final concentration of the NO donors Diethylamine NONOate (NONO) or Sodium nitroprusside (SNP) at 25°C before assay of SR Ca⁺⁺ uptake, release and ATPase activity. Incubation with NONO increased the linear and maximal rates V_{max} of SR Ca⁺⁺ uptake (P<.05 and P<.01 respectively), without affecting the ATPase activity (P>.05). This resulted in an increased coupling ratio (P<.05) between V_{max} and ATPase for NONO, indicating greater efficiency of the SERCA pump. The calcium concentration for half maximal uptake ([Ca⁺⁺]_{0.5}) was also increased by NONO, indicating reduced sensitivity of Ca⁺⁺ induced Ca⁺⁺ uptake. Collectively, these data indicate that while NONO increases the rate of Ca⁺⁺ uptake, NO desensitised the SERCA to initiate Ca⁺⁺ uptake. No effect of SNP or ES was observed on SR Ca⁺⁺ uptake (P>0.05). Neither NONO nor SNP affected SR Ca⁺⁺ release via the RyR. However, ES resulted in increased SR Ca⁺⁺ efflux following thapsigargin-induced inhibition of the SR ATPase. Due to the low rates of release observed, this was most likely due to membrane damage or increased SR permeability, not opening of RyR. In conclusion, the NO donor NONO influenced the SERCA, reducing its Ca⁺⁺ sensitivity, but increasing its rate of uptake. Reduced sensitivity of Ca⁺⁺ induced Ca⁺⁺ uptake ([Ca⁺⁺]_{0.5}) may increase cytosolic Ca⁺⁺ concentrations due higher Ca⁺⁺ required to induce uptake, likely increasing cytosolic Ca⁺⁺ concentrations and activating Ca⁺⁺ dependent proteases.

Phosphorylation status of calsequestrin does not alter its ability to regulate native ryanodine receptors

N.A. Beard¹, M.G. Casarotto¹, D.R. Laver² and A.F. Dulhunty¹, ¹John Curtin School of Medical Research, Australian National University, Canberra, ACT, and ²School of Biomedical Science, Faculty of Health, University of Newcastle, NSW, Australia. .fp 10 S

Depolarisation of the sarcolemma triggers Ca²⁺ release through ryanodine receptor (RyR) calcium release channels in the sarcoplasmic reticulum (SR) of skeletal muscle. The protein responsible for calcium storage within the SR is calsequestrin (CSQ), which is located wholly within the SR lumen. CSQ is tethered to the RyR by two anchoring proteins, triadin and junctin, as well as probably forming a direct physical coupling with the channel itself.

Recent studies have shown that CSQ regulates RyRs via two mechanisms. The first (indirect) interaction is presumably mediated by triadin and junctin, resulting in RyR inhibition, whilst the second interaction is via a direct physical connection between CSQ and the RyR (Szegedi *et al.*, 1999; Herzog *et al.*, 2000; Beard *et al.*, 2000). This second interaction requires dephosphorylated CSQ to modify RyR activity. The role *in vivo* of CSQ phosphorylation is not clear, nor has a definitive phosphorylation mechanism been reported. It is unknown whether the interaction of CSQ with native RyRs (those containing RyR co-proteins, such as triadin and junctin) depends on CSQ dephosphorylation in the same manner as the direct interaction of CSQ with purified RyRs.

To study the effects of altering CSQ's phosphorylation status on its ability to regulate native RyR regulation, rabbit skeletal SR vesicles containing RyRs (isolated from back and leg muscle of New Zealand male rabbits killed by a captive bolt) were incorporated into artificial planar lipid bilayer membranes, which were formed across an aperture with a diameter of 150-200 µm in a delrin cup. The bilayer separates two chambers, *cis* (cytoplasmic) and *trans* (luminal). Solutions contained Ca²⁺ (1 mmol/l), CsCl₂ (20 mmol/l), caesium methane sulfonate (250/30 mmol/l; *cis/trans*) and TES (10 mmol/l). CSQ was purified according to Costello *et al.*, (1986). Phosphorylation status of CSQ was determined using ³¹P NMR, and CSQ was dephosphorylated according to the methods of Cala & Jones (1983).

In a single channel study, RyRs were exposed to 500 mM Cs⁺ to dissociate endogenous CSQ (recently shown to successfully dissociate CSQ from bilayer incorporated RyRs; Beard *et al.*, 2002). After subsequent perfusion of the *trans* chamber with 250 mM Cs⁺, 20-50 µg of either phosphorylated or dephosphorylated CSQ was added to the *trans* chamber. There was no significant difference between the regulation of the RyR by phosphorylated or dephosphorylated CSQ. Both forms of CSQ significantly inhibited RyR activity.

Unlike the phosphorylation-dependant regulation of purified RyRs by CSQ, altering the phosphorylation status of exogenous CSQ did not alter CSQs ability to inhibit native skeletal RyR activity. In combination with the results of Szegedi *et al.* (1999) and Herzog *et al.* (2000), these data illustrate that CSQ imposes two very different regulatory mechanisms on RyRs, and suggest that phosphorylation-dependant changes *in vivo* do not alter the triadin/junctin mediated regulation of RyRs and SR Ca²⁺ release by CSQ.

Beard, N.A., Sakowska, M.M., Dulhunty, A.F. & Laver, D.R. (2002) *Biophysical Journal*, 82(1):310-20.

Cala, S.E. & Jones, L.R. (1983) *Journal of Biological Chemistry*, 258:11932-11936.

Costello, B., Chadwick, C., Saito, A., Chu, A., Maurer, A. & Fleischer, S. (1986) *Journal of Cell Biology*, 103:741-753.

Herzog, A., Szegedi, C., Jona, I., Herberg, F.W. & Varsanyi, M. (2000) *FEBS Letters*, 472:73-77.

Szegedi, C., Sarkozi, S., Herzog, A., Jona, I. & Varsanyi, M. (1999) *Biochemical Journal*, 337:19-22.

NO donors increase persistent sodium current in HEK293 cells transfected with the human cardiac Na⁺ channel α -subunit

W. Wu, F. Leves and P.W. Gage, *Membrane Biology Program, John Curtin School of Medical Research, Australian National University, PO Box 334, Canberra, ACT 2601, Australia.* .SP

Voltage-gated Na⁺ channels play an essential role in excitable cells in which they transiently increase Na⁺ conductance in response to membrane depolarisation. However, many tissues have a component of Na⁺ current that is resistant to inactivation. This persistent Na⁺ current (I_{Nap}) plays an important role in generation of rhythmic oscillations in neurons. Pathological changes in these channels are associated with diseases such as ischaemia, cardiac arrhythmias and epilepsy. Nitric oxide (NO), the major endothelium-derived relaxing factor, reduces whole-cell Na⁺ current in isolated ventricular myocytes (Ahmed *et al.*, 2001) but increases I_{Nap} in rat neuronal and cardiac cells (Hammarstrom & Gage, 1999). NO is also a potential endogenous regulator of I_{Nap} under physiological and pathophysiological conditions (Ahern *et al.*, 2000). The target for NO on Na⁺ channels is not known.

We have tested the effects of NO on I_{Nap} in HEK 293 cells transiently transfected with the human cardiac Na⁺ channel α -subunit. Persistent Na⁺ channel activity in inside-out patches was increased ~10 fold after exposure to NO donors, s-nitroso-n-acetyl penicillamine (SNAP) and sodium-nitroprusside (SNP). Our results suggest that the effect of NO on I_{Nap} is caused by NO directly interacting with Na⁺ channel α -subunit, or with closely associated protein(s): Na⁺ channel β -subunits appear not to be necessary for this effect. The effect of NO on I_{Nap} was inhibited by the sodium channel blocker, lidocaine (50 μ M) and by the reducing agent dithiothreitol (DTT, 2 mM).

Ahern, G. P., Hsu, S. F., Klyachko, V. A. & Jackson, M. B. (2000) *Journal of Biological Chemistry*, **275**, 28810-28815.

Ahmed, G. U., Xu, Y., Hong Dong, P., Zhang, Z., Eiserich, J. & Chiamvimonvat, N. (2001) *Circulation Research*, **89**, 1005-1013.

Hammarstrom, A. K. M. & Gage, P. W. (1999) *Journal of Physiology*, **520**, 451-461.

Aphidicolin-induced stress pathway in pre-implantation embryos

H.-S. Lee and M.L. Day, Department of Physiology, University of Sydney, NSW 2006, Australia. .SP

The cell cycle is a ubiquitous and complex process that is essential for the proper growth and development of the pre-implantation embryo. There has been increasing evidence that correlates the cell cycle with the activity of ion channels, in particular potassium channels. In a previous study we have shown that aphidicolin-induced G1 cell cycle arrest of pre-implantation embryos results in the constitutive activation of a cell cycle-related potassium channel (Day *et al.*, 1998). The present study was aimed at identifying the various signalling pathways activated upon the administration of aphidicolin using flow cytometry and microarrays and from there, decipher the link between these pathways and potassium channel activity.

Results suggest that aphidicolin-induced cell cycle arrest was due to stimulation of the stress-activated kinase pathway (SAPK) that proceeds via p38MAP kinase. This provides a potential link between the mitogen-activated kinase (MAPK) pathways and the activity of the cell cycle-related potassium channels present in embryos.

Day, M.L., Johnson, M.H. & Cook, D.I. (1998) *EMBO Journal*, **17**: 1952-1960.

Distinct expression of intermediate-conductance calcium-activated potassium (IK) channels in intrinsic primary afferent neurons of the rat gastrointestinal tract

C.B. Neylon¹, H.L. Robbins¹, B. Hunne¹, S.E. Moore² and J.B. Furness¹, ¹Department of Anatomy & Cell Biology, and Centre for Neuroscience, University of Melbourne, Parkville, Victoria 3010, Australia. and ²Neurology and GI CEDD, GlaxoSmithKline, New Frontiers Science Park, Harlow CM19 5AW, U.K. .SP

Intrinsic primary afferent neurons (AH neurons) in the intrinsic ganglia of the small intestine have a broad action potential that is followed by early and late afterhyperpolarising potentials (AHP). Our laboratory has reported electrophysiological evidence consistent with intermediate-conductance calcium-activated potassium channels (IK channels) being responsible for the AHP in enteric primary afferent neurons (Vogalis *et al.*, 1992), however the molecular expression of IK channels has not been reported in these cells. This study was undertaken to investigate whether IK channels are expressed in the enteric nervous system and whether their expression corresponds to those cells known to express AHP currents.

To localise the IK channels, an antibody was generated in rabbits against the N-terminal 15 amino acids of the rat IK channel and immunohistochemistry performed on whole mount preparations of rat gastrointestinal tract. Evidence for specificity of the antibody was shown in Western blots where it was found to recognise a single band of 160kD in HEK 293 cells transfected with IK cDNA plasmid but not in cells transfected with vector alone or vector containing SK2 cDNA, or on blots probed with pre-immune serum.

IK channel immunoreactivity was found in specific nerve cell bodies throughout the gastrointestinal tract, from the esophagus to the rectum. The majority of immunoreactive neurons had Dogiel type II morphology and in the myenteric plexus of the ileum almost all immunoreactive neurons were of this shape. Intrinsic primary afferent neurons in the rat small intestine are Dogiel type II neurons that are immunoreactive for calretinin, and it was found that almost all the IK channel immunoreactive neurons were also calretinin immunoreactive. IK channel immunoreactivity also occurred in calretinin-immunoreactive, Dogiel type II neurons in the caecum. Within immunoreactive cells, the initial segments of the axons contained the highest density of sites, but not axon terminals. No immunoreactivity was found in surrounding muscle or glia.

Molecular evidence for IK expression was determined by RT-PCR analysis using oligonucleotide probes based on the rat IK sequence (Neylon *et al.*, 1990). RT-PCR cloning from a highly enriched myenteric ganglion extract revealed an mRNA sequence that was identical to the IK channel mRNA expressed in other cell types.

It is concluded that IK channels are expressed on specific neurons of the gastrointestinal tract. They are almost exclusively located on cell bodies and proximal parts of axons of intrinsic primary afferent neurons. From functional studies, these IK channels are predicted to control the excitability states of the enteric nervous system.

Neylon, C.B., Lang, R.J., Fu, Y., Bobik, A. & Reinhart, P.H. (1999) *Circulation Research*, 85, e33-e43.
Vogalis, F., Harvey, J.R. & Furness, J.B. (2002) *Journal of Physiology*, 538, 421-33.

Inhibition of human large conductance calcium-activated potassium channels by a fungal toxin

J.E. Dalziel¹, S.C. Finch² and J. Dunlop¹, ¹AgResearch Limited, Grasslands Research Centre, Private Bag 11008, Palmerston North, New Zealand and ²Ruakura Research Centre, Private Bag 3123, Hamilton, New Zealand. .SP

The aim of this research was to investigate possible receptor/ion channel sites of action of a fungal toxin (designated compound A) that produces ataxia, tremors, and hypersensitivity to external stimuli when injected into mice. Compound A is distinct among neurotoxins in that it has a long duration of action, producing tremors that can last for up to three days rather than only a few hours. It also inhibits electrically stimulated smooth muscle contraction, increases neurotransmitter release, and elevates blood pressure. These effects suggested the disruption of large conductance calcium-activated potassium (BK) channels, as they have important regulatory roles in smooth muscle contraction and in control of neurotransmitter release (Gribkoff *et al.*, 2001). We investigated this possibility using *hSlo* (α subunit) BK channels expressed in human embryonic kidney cells and patch-clamping. We discovered that compound A potently inhibits BK channel-activation at nanomolar concentrations in inside-out membrane patches. BK channel currents activated by depolarising voltage pulses in the presence of 10 μ M free calcium were inhibited by compound A in a concentration-dependent manner. 100 nM compound A completely inhibited outward potassium currents in less than one minute. The concentration that produced half maximal inhibition was approximately 3 nM, indicating a high apparent affinity for BK channels. This is the first time a molecular site of action has been determined for a compound of this structural class and identifies a novel BK channel blocker.

Gribkoff V.K., Starrett J.E., Jr. & Dworetzky S.I. (2001) *Neuroscientist*, 7:166-77.

Estimations of relative anion-cation permeabilities deduced from reversal (dilution) potential measurements, as in glycine receptor channel studies, are essentially model independent

P.H. Barry¹, A. Keramidas¹, A.J. Moorhouse¹ and P.R. Schofield², ¹School of Medical Sciences, University of New South Wales, NSW 2052 and ²Garvan Institute of Medical Research, Darlinghurst, NSW 2010, Australia. .SP

In a recently completed series of structure-function studies on human recombinant glycine receptor (GlyR) channels, expressed in HEK293 cells, we have shown that a single, double (SDM) and triple (STM) point mutations in the M2 region of the glycine receptor were able to each switch the GlyR selectivity from being anion- to cation-selective (Keramidas *et al.*, 2000, 2002; Moorhouse *et al.*, 2002). In order to relate ion selectivity to changes in electrostatic effects in the channel pore and in its minimum pore diameter, we needed both anion-cation permeability ratios and minimum pore diameters. The latter were determined by measuring cation-cation (or anion-anion) permeability ratios for a series of large test cations (anions) for the different cation-selective (anion-selective) mutant GlyRs. They were determined from bionic potentials, measuring the change in reversal potential, under whole cell patch clamp conditions, when the external solution cation (anion) was substituted by various larger cations (anions) for cation selective (anion-selective) mutant GlyRs. It has been shown that for such bionic measurements, the form of the membrane potential equation is essentially independent of the mathematical model underlying it, as discussed in Barry & Gage (1984).

However, concern has been expressed about the validity of using the Goldman-Hodgkin-Katz (GHK) equation (see Barry & Gage, 1984) for dilution potential measurements, given the inherent assumptions (a constant electrical field in the membrane and independence of ion fluxes) in its derivation. Experimentally, the anion-cation permeability ratios (P_{Cl}/P_{Na}) were determined from dilution potentials by measuring the change in reversal potential, when the external solution NaCl concentration was decreased to about 50% and then to about 25% and each shift in reversal potentials plotted against external NaCl activity. Experimentally, it was noted that the data did fit the GHK equation with the predicted straight line and constant permeability ratio. The GHK equation is:

$$\Delta V_{rev} = RT/F \ln [a_{Na}^o + (P_{Cl}/P_{Na})a_{Cl}^i] / [a_{Na}^i + (P_{Cl}/P_{Na})a_{Cl}^o]$$

where ΔV_{rev} is the shift in reversal potential, R, T and F have their usual significance and a_{Na} and a_{Cl} represent the activities of Na⁺ and Cl in the external (o) and internal (i) solutions respectively.

We then fitted the data to the Planck equation, derived by solving the Nernst-Planck flux equations, which has virtually opposite underlying assumptions (a non-constant electrical field and a macroscopic electroneutrality condition) to the GHK ones. The Planck equation is:

$$\Delta V_{rev} = (RT/F) (P_{Na} P_{Cl}) / (P_{Na} + P_{Cl}) \ln a_{NaCl}^o / a_{NaCl}^i$$

However, it produced very similar permeabilities to those of the GHK equation. For example, P_{Cl}/P_{Na} values using the GHK [Planck] equation for the SDM and STM cation-selective mutant GlyRs were 0.12 [0.14] and 0.27 [0.27] and P_{Cl}/P_{Na} for the anion-selective WT GlyR was 28.5 [26.2].

Hence, the anion-cation permeability ratios determined using the GHK or Planck equations are essentially independent of the limiting underlying assumptions of those equations.

Barry, P.H. & Gage, P.W. (1984) In: *Current Topics in Membranes and Transport*, 21, ed. Stein, W.E. pp. 1-51. Orlando: Academic Press.

Keramidas, A., Moorhouse, A.J., French, C.R., Schofield, P.R. & Barry, P.H. (2000) *Biophysical Journal*, 78, 247-259.

Keramidas, A., Moorhouse, A.J., Pierce, K.D., Schofield, P.R. & Barry P.H. (2002) *Journal of General Physiology*, 119, 393-410.

Moorhouse, A.J., Keramidas, A., Zaykin, A., Schofield, P.R. & Barry P.H. (2002) *Journal of General Physiology*, 119, 411-425.

Role of charged residues in coupling ligand binding and channel activation in the extracellular domain of the glycine receptor

N.L. Absalom¹, T.M. Lewis², W. Kaplan³, K.D. Pierce¹ and P.R. Schofield¹, ¹Neurobiology Research Program, Garvan Institute of Medical Research, 384 Victoria Street, Darlinghurst, NSW 2010, ²Department of Physiology and Pharmacology, School of Medicine, University of New South Wales, NSW 2052 and ³Peter Wills Bioinformatics Centre, Garvan Institute of Medical Research, 384 Victoria Street, Darlinghurst, NSW 2010, Australia. .SP

The glycine receptor is a member of the ligand gated ion channel receptor superfamily that mediates fast synaptic transmission in the brainstem and spinal cord. Following ligand binding, the receptor undergoes a conformational change that is conveyed to the transmembrane regions of the receptor resulting in the opening of the channel pore. Using the acetylcholine binding protein structure as a template, we modelled the extracellular domain of the glycine receptor α -1 subunit and identified the location of charged residues within loops 2 and 7 (the conserved Cys-loop). These loops have been postulated to interact with the M2-M3 linker region between the transmembrane domains 2 and 3 as part of the receptor activation mechanism. Charged residues were substituted with cysteine, resulting in a shift in the concentration-response curves to the right in each case. Covalent modification with 2-trimethylammonioethyl methanthiosulfonate was demonstrated only for K143C, which was more accessible in the open state than the closed state, and resulted in a shift in the EC₅₀ towards wild-type values. Charge reversal mutations (E53K, D57K and D148K) also impaired channel activation, as inferred from increases in EC₅₀ values and the conversion of taurine from an agonist to an antagonist in E53K and D57K. Thus, each of the residues E53, D57, K143 and D148 are implicated in channel gating. However, the double reverse charge mutations E53K:K276E, D57K:K276E and D148K:K276E did not restore glycine receptor function. These results indicate that loops 2 and 7 in the extracellular domain play an important role in the mechanism of activation of the glycine receptor.

Skeletal muscle function: the role of ionic changes in fatigue, damage and disease

D.G. Allen, Department of Physiology, University of Sydney (F13), NSW 2006, Australia. .SP

Repeated activity of skeletal muscle changes its properties in a variety of ways; muscles become weaker with intense use (fatigue), may feel sore and tender after excessive use, and can degenerate in many disease conditions. Early ionic changes are critical to the development of each of these conditions.

Central to this experimental approach has been the development of the single fibre preparation of mouse muscle. Individual cells can be dissected with intact tendons and stimulated to produce force. Fluorescent indicators can be micro-injected into the fibres and intracellular Ca^{2+} , Na^+ , pH, Mg^{2+} , ATP etc can all be measured from one cell whilst simultaneously monitoring the mechanical performance. Other substances can be injected into the cells (proteins, peptides, caged compounds, plasmids etc) and after activity the cell can be prepared for immunohistochemistry, light microscopy, electron microscopy etc.

In 1988 when we started this work, the dominant theory was that intracellular acidosis caused muscle fatigue. In contrast we found that single fibres could fatigue with little or no pH change (Westerblad & Allen, 1992) but failure of calcium release was found to be a major cause of fatigue (Westerblad & Allen, 1991). Currently we propose that precipitation of calcium and phosphate in the sarcoplasmic reticulum contributes to the failure of calcium release (Allen & Westerblad, 2001).

Muscles can be used to shorten and produce force or they can be used to decelerate loads (eccentric contractions). A day after intense eccentric exercise muscles are weak, sore and tender and this damage can take a week to recover. In this condition sarcomeres are disorganised and there are increases in resting Ca^{2+} and Na^+ (Balnave & Allen, 1995; Yeung *et al.*, 2003). Recently we discovered that the elevation of Na^+ occurs through a stretch-activated channel which can be blocked by either gadolinium or streptomycin. Preventing the rise of $[\text{Na}^+]_i$ with gadolinium also prevents part of the muscle weakness after eccentric contractions (Yeung *et al.*, 2003).

Duchenne muscular dystrophy is a lethal degenerative disease of muscles in which the protein dystrophin is absent. Dystrophic muscles are more susceptible to stretch-induced muscle damage and the stretch-activated channel seems to be one pathway for the increases in intracellular Ca^{2+} and Na^+ which are a feature of this disease. We have recently shown that blockers of the stretch-activated channel can minimize some of the short-term damage in muscles from the *mdx* mouse, which also lacks dystrophin (Yeung *et al.*, submitted). Currently we are testing whether blockers of the stretch-activated channels given systemically to *mdx* mouse can protect against some features of this disease.

Allen, D.G. & Westerblad, H. (2001). *Journal of Physiology* **536**, 657-665.

Balnave, C.D. & Allen, D.G. (1995). *Journal of Physiology* **488**, 25-36.

Westerblad, H. & Allen, D.G. (1991). *Journal of General Physiology* **98**, 615-635.

Westerblad, H. & Allen, D.G. (1992). *Journal of Physiology* **449**, 49-71.

Yeung, E.W., Ballard, H.J., Bourreau, J.P. & Allen, D.G. (2003). *Journal of Applied Physiology* **94**, 2475-2482.

Support from the NHMRC over many years is gratefully acknowledged.

Tolerance of male and female rat papillary muscles to acute metabolic compromise

I.R. Wendt and B. Zoltowski, Department of Physiology, Monash University, Victoria 3800, Australia.

.SP

The presence of functional oestrogen receptors within cardiac myocytes identifies the heart as a target organ for oestrogen, and raises the possibility that sex hormone effects on the heart may contribute to sex differences in the incidence of heart disease. We have previously reported that, under comparable conditions, the amplitude of the intracellular Ca^{2+} ($[\text{Ca}^{2+}]_i$) transient is larger in male as compared to female rat cardiac myocytes (Curl *et al.*, 2001). It has also been suggested that oestrogen can protect the heart against ischemia-reperfusion injury by limiting the associated increase in $[\text{Ca}^{2+}]_i$ (Zhai *et al.*, 2000). The aim of the present study was to determine whether there is a sex difference in the decline and recovery of function, and ability to maintain $[\text{Ca}^{2+}]_i$ homeostasis, in intact cardiac muscle subjected to acute metabolic compromise.

Left ventricular papillary muscles were dissected from the hearts of adult (300 – 350g) male and female Wistar rats that had been killed by chloroform overdose and decapitation. The muscles were mounted in a chamber located on the stage of an inverted fluorescence microscope to allow for simultaneous recording of force and tissue fluorescence. For monitoring of $[\text{Ca}^{2+}]_i$ the muscles were loaded with fura-2 by 3 hr incubation with fura-2/AM. Muscles were equilibrated in HEPES buffered physiological saline solution containing 2.5 mM Ca^{2+} , 10 mM glucose, and aerated with 100% O_2 . They were then subjected to 20 min of metabolic inhibition followed by 60 min of recovery. To achieve metabolic inhibition 2 mM NaCN was added to the PSS, and glucose and O_2 were omitted. The temperature was maintained at 30°C and the muscles were stimulated at 0.25 Hz throughout.

Following 20 min of metabolic inhibition developed force had declined to 10.8 ± 1.6 and 12.1 ± 1.8 % of the preceding steady-state control level in male ($n = 12$) and female ($n = 14$) papillary muscles respectively. In contrast, the amplitude of the Ca^{2+} transient only decreased to around 75% of the control amplitude in both sexes. Muscles from both sexes recovered with a similar time course, with developed force returning to approximately 90% of control by 60 min. There were also increases in passive force and diastolic $[\text{Ca}^{2+}]_i$ during metabolic inhibition, however, the increase in resting force was considerably less than might have been expected from the increase in diastolic $[\text{Ca}^{2+}]_i$. Overall, there were no significant differences between the sexes in either the decline in contractile force, increase in resting force, or changes in $[\text{Ca}^{2+}]_i$ during 20 min of metabolic inhibition.

Addition of 1×10^{-6} M 17β -oestradiol to the solutions resulted in a slight decrease (around 10%) in contractile force and amplitude of the Ca^{2+} transient in both male and female papillary muscles. The acute presence of oestradiol, however, had no significant effect on the changes in force or $[\text{Ca}^{2+}]_i$ that occurred during metabolic inhibition.

The results demonstrate that there are no apparent differences in the tolerance of isolated male and female rat papillary muscles to 20 min of metabolic inhibition. In addition, the acute presence of a high concentration of 17β -oestradiol did not provide any protection against the effects of metabolic inhibition in either sex. In muscles of both sexes there appeared to be some dissociation of force and $[\text{Ca}^{2+}]_i$ during metabolic inhibition.

Curl, C.L., Wendt, I.R. & Kotsanas, G. (2001) *Pflügers Archiv*, 441, 709-716.

Zhai, P., Eurell, T.E., Cooke, P.S., Lubahn, D.B. & Gross, D.R. (2000) *American Journal of Physiology*, 278, H1640-H1647.

The rate of reactivation of the cardiac sodium hydrogen exchanger following inhibition with cyanide

J.M. Tipene and D.G. Allen, Department of Physiology, University of Sydney (F13), NSW 2006, Australia. .SP

The cardiac sodium hydrogen exchanger (NHE1) has been implicated in ischaemia/reperfusion damage of the heart. Coupled activity of NHE1 and the sodium calcium exchanger (NCX) are thought to cause calcium overload which is responsible for the resulting the contractile dysfunction and tissue necrosis (Allen & Xiao, 2003).

It is believed that the NHE1 is inactivated by some aspect of metabolic inhibition that occurs during ischaemia and reactivated upon reperfusion (Lazdunski *et al.*, 1985; Park *et al.*, 1999). The time course of this reactivation has indirectly been shown to be very rapid. Park *et al.* (1999) demonstrated that $[Na^+]_i$ started to rise within 30 seconds of reperfusion and reached a peak after 5 minutes. In this study we directly examined the rate of proton flux (J_H ($mmol \cdot l^{-1} \cdot min^{-1}$)) via NHE1 in the acid-loaded ventricular myocytes.

Female SD rats (4-6 weeks) were anaesthetised with pentobarbitone. Single ventricular myocytes were isolated from the heart using a combination of enzymatic digestion and mechanical dispersion. Cells were loaded with the pH indicator carboxy- SNARF-1 and perfused with bicarbonate-free HEPES buffered solution, conditions under which NHE1 is the only acid-extruding mechanism. An isolated cell was then exposed to an NH_4Cl (20 mM) prepulse, and the rate of recovery from acidosis was measured (dpH_i/dt). After return of pH_i to the resting level (7.1) the cell was exposed for 10 minutes to a 2mM NaCN followed by a second NH_4Cl prepulse. The rate of recovery from acidosis was then assessed in the presence of NaCN and then upon its removal.

In control conditions J_H was 0.086 ± 0.022 mM/min (mean \pm SEM) when J_H values were calculated in the pH_i range 6.84 – 7.0. In the presence of 2mM NaCN, the J_H value decreased to 0.017 ± 0.005 ($P < 0.05$). This data shows that cyanide inhibits the exchanger. Within 30 s of removal of NaCN, the proton flux had increased to 0.0151 ± 0.019 but part of this apparent flux is caused by the metabolic changes associated with removal of cyanide. After the correction for the effects of the removal of NaCN the mean J_H value was 0.108 ± 0.022 whereas the control measured over the same pH range was 0.050 ± 0.017 which is significantly smaller. These data suggest that the NHE1 activity rapidly reactivates after removal of metabolic inhibition and may show a period of enhanced activity.

Allen, D.G. & Xiao, X-H. (2003) *Cardiovascular Research*, **57**, 934-941.

Lazdunski, M, Frelin, C., & Vigne P. (1985). *Journal of Molecular and Cellular Cardiology*, **17**, 1029-1042.

Park, C.O., Xiao, X.H., & Allen, D.G. (1999). *American Journal of Physiology*, **276**, H1581-H1590.

Activity of the cardiac Na⁺-H⁺ exchanger during ischaemia

X.-H. Xiao and D.G. Allen, *Department of Physiology F13, University of Sydney, NSW 2006, Australia.*
.SP

There is dispute about whether the cardiac Na⁺-H⁺ exchanger (NHE1) remains active during ischaemia (Allen & Xiao, 2003). The conclusion that the NHE1 was active during ischaemia is based on the large intracellular acidosis which would be expected to drive sodium entry on NHE1 and the fact that some NHE1 inhibitors, such as amiloride, reduce the rise of [Na⁺]_i during ischaemia (Murphy *et al.*, 1991). However, pH_i shows no recovery during ischaemia and NHE1 inhibitor do not change the pH_i during ischaemia, which suggested that the Na⁺-H⁺ exchanger was inhibited during ischaemia (Park *et al.*, 1999). We took advantage of a new potent and selective NHE1 inhibitor, zoniporide (Marala *et al.*, 2002) to reassess the activity of NHE1 during ischemia.

Rats were anaesthetised with pentobarbitone and hearts were isolated and stimulated at 5 Hz. Ischaemia was induced by turning perfusion off for 30 minutes. Intracellular sodium ([Na⁺]_i) was measured with sodium binding benzofuran isophthatale (SBFI).

In control hearts 30 minutes ischaemia increased [Na⁺]_i from 7.2 ± 0.2 mM to 17.3 ± 0.7 mM and reperfusion resulted in a large transient increase of [Na⁺]_i (peak 31 ± 2.3 mM (n=6)). In the presence of zoniporide (1 μM, n=5) present throughout ischaemia and reperfusion, ischaemia still caused a similar [Na⁺]_i rise to 16.2 ± 0.5 mM but the large transient increase of [Na⁺]_i on reperfusion was abolished (peak 13.8 ± 2.4 mM). With amiloride (100 μM, n=4) treatment, [Na⁺]_i was unchanged at the end of ischemia (6.7 ± 0.7 mM) and the increase of [Na⁺]_i on reperfusion was abolished (peak 7.4 ± 0.3 mM).

Both zoniporide and amiloride abolished the transient increase of [Na⁺]_i on reperfusion, which results from activity of NHE1. However they showed different effects during ischaemia: noly amiloride abolished the [Na⁺]_i rise during ischaemia. Amiloride derivatives reduce the persistent Na⁺ current (Chattou *et al.*, 2000). Furthermore, the rise of [Na⁺]_i during ischaemia is abolished by low concentrations of tetrodotoxin which inhibit the persistent Na⁺ current (Xiao & Allen, 1999). Thus we propose that the ability of amiloride to prevent the [Na⁺]_i rise during ischaemia arises from inhibition of the persistent Na⁺ current. Measurements of the effect of amiloride and zoniporide on persistent Na⁺ current are required to confirm this hypothesis.

Allen, D.G. & Xiao, X-H. (2003) *Cardiovascular Research*, 57, 934-941.

Murphy, E., Perlman, M., London R.E. & Steenbergen C. (1991) *Circulation Research*, 68, 1250-1258

Park C.O., Xiao X-H., Allen D.G.(1999) *American Journal of Physiology*, 276, H1581-90

Marala, R.B., Brown J.A., Kong J.X. *et al.* (2002) *European Journal of Pharmacology* 451, 37-41

Chattou S., Coulombe A., Diacono J., Le Grand B., John G. & Feuvray D. (2000) *Journal of Molecular and Cellular Cardiology* 32, 1181-1192.

Xiao, X-H. & Allen, D.G. (1999) *Circulation Research*, 85, 723-730

The effect of polyunsaturated fatty acids on cardiac ryanodine and inositol triphosphate receptors

B. Honen¹, D. Saint² and D.R. Laver¹, ¹Department of Human Physiology, School of Biomedical Science, The University of Newcastle, Callaghan, NSW 2308 and ²Department of Physiology, School of Molecular and Biomedical sciences, The University of Adelaide, Adelaide, SA 5005, Australia. .SP

It is well recognised that the consumption of fish correlates with a reduction in mortality due to cardiovascular disease (Burr *et al.*, 1989). Whole heart studies have identified that dietary fish oil confers protection from cardiac arrhythmias (McLennan, 1993). Many studies have shown that the acute application of the polyunsaturated fatty acids present in fish oil, docosahexaenoic acid (DHA) and eicosapentaenoic acid (EPA) to cardiac myocytes significantly reduce the amplitude of the various sarcolemmal ion currents responsible for the cardiac action potential (Xiao *et al.*, 1995; Xiao *et al.*, 1997; Bogdanov *et al.*, 1998). It is believed that this reduction in electrical excitability is the mechanism by which fish oil confers protection from cardiac arrhythmias. However some arrhythmias also arise from abnormal calcium handling by internal stores. Thus it has been suggested that the anti-arrhythmic effects of long chain polyunsaturated fatty acids (PUFAs) may be related to their ability to alter calcium handling in cardiac myocytes (Honen & Saint 2002, O'Neill *et al.*, 2002). Therefore we investigated the effects of EPA and DHA on the kinetics of the cardiac calcium release channels (*i.e.* the ryanodine receptor (RyR) and the inositol triphosphate receptor (IP₃R)).

RyRs and IP₃R isolated from sheep hearts and were incorporated into artificial bilayers formed from a solution of phosphatidylethanolamine and phosphatidylcholine dissolved in either n-decane or n-tetradecane using standard techniques (O'Neill *et al.*, 2003). Cytoplasmic solutions contained 250 mM Cs⁺ (230 mM CsCH₃O₃S, 20 mM CsCl), 10 mM TES at pH 7.4. Luminal solution contained 50 mM Cs⁺ (30 mM CsCH₃O₃S, 20 mM CsCl), 10 mM TES and 1 mM CaCl₂, pH 7.4.

Concentrations of EPA ranging between 10 and 50 μM, when applied to either the cytosolic or luminal side of the RyR, produced a dose dependent inhibition of RyR open probability with $K_I = 32$ μM and Hill coefficient, $n_I = 3.8$. This inhibition typically occurred within 30 seconds of application. Inhibition was independent of the n-alkane solvent and whether RyRs were activated by ATP or Ca²⁺. Like EPA, the cytosolic application of 50 μM DHA also resulted in a reduction in channel open probability.

Like with RyR, the open probability of the IP₃R fell upon the application of 50 μM EPA. IP₃R were identified by their activation by IP₃ and inhibition by 10 μM heparin, a reversible IP₃R blocker.

The results suggest that both EPA and DHA affect calcium handling by directly inhibiting RyRs at micromolar concentrations. The actions of both EPA and DHA may be mediated via the membrane or by binding to a hydrophobic site on the channel itself. This provides a potential avenue by which PUFAs confer protection from cardiac arrhythmias.

Bers, D.M., Bridge, J.H. & Spitzer, K.W. (1989) *Journal of Physiology*, 417: 537-553.

Bogdanov, K.Y., Spurgeon, H.A., Vinogradova, T.M. & Lakatta, E.G. (1998) *American Journal of Physiology*, 274:H571-579.

Honen, B.N. & Saint, D.A. (2002) *Journal of Nutritional Biochemistry*, 13:322-329.

McLennan, P.L. (1993) *American Journal of Clinical Nutrition*, 57:207-212.

O'Neill, S.C., Perez, M.R., Hammond, K.E., Sheader, E.A. & Negretti, N. (2002) *Journal of Physiology*, 538(1): 179-184.

O'Neill E.R., Sakowska, M.M., Laver D.R. (2003) *Biophysical Journal*, 84: 1-16.

Xiao, Y.F., Kang, J.X., Morgan, J.P. & Leaf, A. (1995) *Proceedings of the National Academy of Sciences of the United States of America*, 92(24):11000-11004.

Xiao, Y.F., Gomez, A.M., Morgan, J.P., Lederer, W.J. & Leaf, A. (1997) *Proceedings of the National Academy of Sciences of the United States of America*, 94(8):4182-4187.

ATP modulates intracellular Ca^{2+} and firing rate through a P2Y_1 purinoceptor in cane toad pacemaker cells

Y.K. Ju, W. Huang, L. Jiang, J. Barden and D.G. Allen, Departments of Physiology and Anatomy, University of Sydney F13, NSW 2006, Australia. .SP

Recent studies on cardiac pacemaker cells have demonstrated that interventions which affect intracellular Ca^{2+} concentration ($[\text{Ca}^{2+}]_i$) also influence firing rate (Zhou & Lipsius, 1993; Ju & Allen, 1998; Bogdanov *et al.*, 2001). To investigate the involvement of $[\text{Ca}^{2+}]_i$ in modulation of heart rate by ATP, we examined the effect of extracellular ATP (10-100 μM) on $[\text{Ca}^{2+}]_i$ and spontaneous firing rate in single pacemaker cells isolated from the sinus venosus of cane toads*. In spontaneously firing cells, ATP initially increased peak $[\text{Ca}^{2+}]_i$, diastolic $[\text{Ca}^{2+}]_i$, and the firing rate. These early effects were followed by a late phase in which the peak $[\text{Ca}^{2+}]_i$, diastolic $[\text{Ca}^{2+}]_i$ and the firing rate all declined. Previous studies suggested that positive phase was mediated by P2 purinoceptors, activated by ATP, while the negative phase was mediated by P1 purinoceptors, activated by adenosine (Burnstock & Meghji, 1981). To define the subtype of purinoceptors involved we used $\alpha\beta$ -methylene ATP, adenosine, and UTP (respectively $\text{P2X}_{1,3}$, P1 and $\text{P2Y}_{2,4,6}$ selective agonists). However, we found that these agonists caused no significant change in $[\text{Ca}^{2+}]_i$ and had little or no effect on firing rate. In contrast the P2Y_1 selective agonist 2-MesADP (1 μM) mimicked the biphasic effects of ATP and these effects were inhibited by the non-selective purinoceptor antagonist suramin and by the P2Y_1 selective antagonist MSR 2179.

Immunohistochemistry using an anti- P2Y_1 antibody demonstrated that P2Y_1 receptors were present on the cell surface. To establish the specificity of the antibody we performed Western blotting analysis on the protein extracts from toad tissues including sinus venosus and aorta as well as rat aorta as positive control. The immunoreaction with the P2Y_1 antibody resulted in a major band of apparent molecular weight of approximately 57 kDa in all three samples. Thus the P2Y_1 antibody recognized a similar molecular weight protein in both amphibian and mammalian tissues as reported by others (Moore *et al.*, 2000).

To investigate the nature of the biphasic response we studied the effect of ATP on Ca^{2+} store content. We found that the effects of ATP were related to the sarcoplasmic reticulum (SR) Ca^{2+} store. After depletion of the SR Ca^{2+} store with caffeine or ryanodine, ATP no longer had any effect on $[\text{Ca}^{2+}]_i$ or firing rate. Furthermore, the SR Ca^{2+} store content was decreased during the late phase of 2-MesADP application. The effect of ATP was coupled to phospholipase C (PLC) activity because the PLC inhibitor U-73122 eliminated the effect of ATP.

Our study shows that in toad pacemaker cells, the biphasic effects of ATP on pacemaker activity are mainly through P2Y_1 purinoceptors, which are able to modulate Ca^{2+} release from the SR Ca^{2+} store. We propose that inositol 1,4,5-triphosphate generated by PLC facilitates SR Ca^{2+} release causing the early increase in peak $[\text{Ca}^{2+}]_i$. The increased Ca^{2+} release partially depletes the SR Ca^{2+} store accounting for the subsequent decline in peak $[\text{Ca}^{2+}]_i$.

Bogdanov, K.Y., Vinogradova, T.M., & Lakatta, E.G. (2001) *Circulation Research* 88, 1254-1258.

Burnstock, G. & Meghji, P. (1981) *British Journal of Pharmacology* 73, 879-885.

Ju, Y-K & Allen, D.G. (1998) *Journal of Physiology* 508, 153-166.

Moore, D., Chambers, J., Waldvogel, H., Faull, R., & Emson, P. (2000) *Journal of Comparative Neurology* 421, 347-384.

Zhou, Z. & Lipsius, S.L. (1993) *Journal of Physiology* 466, 263-285.

Supported by NH&MRC

*The experiments were approved by the Animal Ethical Committee of University of Sydney.

Calcium loading properties of sarcoplasmic reticulum from rat ventricular myocardium

L.M. Gibson¹ and D.G. Stephenson², ¹Pharmacy Department, School of Health and Environment, Faculty of Regional Development, La Trobe University Bendigo, Victoria 3552 and ²School of Zoology, Faculty of Science and Technology, La Trobe University, Bundoora, Victoria 3083, Australia. .SP

There is a very large range of estimates for SR Ca²⁺ capacity of cardiac muscle in the literature, as reviewed by Bers (2001). For example estimates for ventricular myocardium SR Ca²⁺ capacity may vary by a factor of up to 6 times. In part this range may be attributed to the differences in the functional state of the SR. In this study we tried to emulate the conditions prevalent in “active” and “resting” cardiac muscle by exposing preparations to ATP containing solutions at different concentrations of EGTA and pCa during the skinning procedure. Such conditions are known to either facilitate a prolonged activation (0.1 mmol L⁻¹ EGTA_{Total}, pCa 7.1) or prevent any activation (10.0 mmol L⁻¹ EGTA_{Total}, pCa 9). Kabbara & Stephenson (1997) showed that when Ca²⁺ entry was facilitated during the skinning procedure the SR was loaded with more Ca²⁺ under the same loading conditions compared with skinning when Ca²⁺ entry was prevented. They regarded these responses as being reminiscent of those from “active” cardiac muscle compared with more quiescent or “resting” cardiac muscle.

Right ventricular muscle bundles were homogenised in either highly (10.0 mmol L⁻¹ EGTA_{Total}, pCa 9) or weakly (0.1 mmol L⁻¹ EGTA_{Total}, pCa 7.1) calcium buffered skinning solutions to mechanically render the sarcolemma “leaky”. The preparations were then subjected to a simple protocol developed to estimate the SR Ca²⁺ content. Briefly, the preparation was immersed into a solution of known [EGTA]_{Total} at a desired pCa for up to 10.0 minutes to allow the SR to equilibrate with calcium. Then the preparation was moved into an identical solution, which also contained 30 mmol L⁻¹ caffeine where a caffeine-induced force transient was recorded. This procedure was then repeated without reloading the SR with Ca²⁺. On second immersion into the caffeine containing solution, there was no SR Ca²⁺ release, and force only increased due to the higher sensitivity of the contractile apparatus for Ca²⁺ in the presence of caffeine. By overlaying the force responses we could subtract the myofibrillar force response component due to caffeine, which allowed measurement of the SR Ca²⁺ released which could then be converted to the amount of Ca²⁺ released by the fibre volume at the peak of the caffeine-induced force response.

The SR Ca²⁺ content estimated from the caffeine-induced force responses for preparations loaded at pCa 7.0, over a range of [EGTA]_{Total} (0.02 to 0.2 mmol L⁻¹) were on average 197 ± 35 (mean ± SEM, n=3) mmol Ca²⁺ L⁻¹ cytosol for preparations skinned under weakly buffered conditions for calcium, emulating “active” myocardium. When preparations were skinned in 10 mmol L⁻¹ EGTA_{Total} (pCa 9) however, this was reduced to 142 ± 2 (mean ± SEM, n=3) mmol Ca²⁺ L⁻¹ cytosol where the preparations were expected to behave more like “resting” muscle. Hence there appeared to be a shift towards higher calcium loading and release by the SR when the preparations have been skinned under conditions analogous to “active” cardiac muscle compared with conditions more like those of the “resting” cardiac muscle.

Bers, D.M. (2001) *E-C Coupling and Cardiac Contractile Force*, 2nd Ed. Kluwer Academic Publishers, Dordrecht, p 179.

Kabbara, A.A. & Stephenson, D.G. (1997) *American Journal of Physiology*,. 273, H1347-H1357.

Temperature sensitivity of dopaminergic neurons in the Substantia Nigra pars compacta

K.K. Chung and J. Lipski, Department of Physiology, University of Auckland, Private Bag 92019, Auckland 1020, New Zealand.

Certain neurons in the CNS display a high temperature sensitivity ($Q_{10} > 2.0$) with respect to their firing frequency, e.g. in the hypothalamus, where such neurons are known to play a role in thermoregulation. There are reports of other brain regions expressing similar sensitivity, however, the cellular mechanism and pathophysiological significance of temperature sensitivity in extrahypothalamic neurons remain unclear. We hypothesise that this is due in part to the expression of temperature-sensitive ion channels in cell membranes. This hypothesis is supported by the recent discovery of a family of channels known as TRP (Transient Receptor Potential) channels (Minke & Cook, 2002). One member of the family (TRPV3), which is expressed both in the CNS and at the periphery, is sensitive to temperature changes in the physiological range (around 37°) (Xu *et al.*, 2002). In addition, this cation channel is relatively selective for calcium ions (Xu *et al.*, 2002), which suggests it plays a role not only in the control of neuronal excitability but also of intracellular Ca^{2+} homeostasis.

The Substantia Nigra pars compacta (SNc) is a component of the basal ganglia important in motor control. Degeneration of this structure, associated with intracellular Ca^{2+} overload, leads to Parkinson's disease (Hirsch *et al.*, 1997). We have recently found that SNc neurons are temperature sensitive (Lipski *et al.*). The aim of the present study was to further characterise this sensitivity using a combination of whole-cell patch clamp recording and calcium imaging techniques and to explore what role, if any, TRP channels play in the temperature sensitivity of SNc neurons.

Transverse midbrain slices (250 μ m) containing the SNc were obtained from young, anaesthetised Wistar rats and kept in aCSF bubbled with 95% O_2 /5% CO_2 . SNc neurons were visualised with IR-DIC (E600FN microscope, Nikon) and identified using a combination of morphological and electrophysiological criteria. Cells were patched with glass pipettes (2.5-5 M Ω) filled with a solution containing (in mM): 145 K-gluconate, 10 HEPES, 0.75 EGTA, 2 Mg₂ATP, 0.3 Na₃GTP, 2 MgCl₂, 0.1 CaCl₂, and held at -60 mV under voltage clamp. In some experiments, the Ca^{2+} indicator fura-2 (0.25 mM) was loaded into the cell by diffusion from the pipette solution. The level of free intracellular Ca^{2+} was monitored using the ratiometric technique (340/380 nm). Slices were maintained at 34°C except when temperature ramps were performed.

Transient cooling (by 2, 5 or 10°C) or heating (2 or 5°C) of the slice resulted in an outward (cooling) or inward (heating) current and corresponding changes in cell membrane resistance. The responses were fully reversible on return to control temperature (34°C). Temperature ramps with variable slopes demonstrated slow current kinetics. There was no sign of current desensitisation when steady-state temperature was reached. Cooling of slices by 5°C in the presence of ruthenium red (100 μ M; a blocker of TRPV3 channel) produced a small reduction (22%; paired t-test $P < 0.005$, $n = 5$) of cooling-induced outward current. Ca^{2+} imaging experiments revealed temperature dependence of intracellular Ca^{2+} concentration consistent with the hypothesis that Ca^{2+} permeable channels are active at high temperatures and closed during cooling.

These experiments demonstrate a distinct pattern of electrophysiological and Ca^{2+} signal responses evoked by temperature changes in SNc neurons. Further studies are needed to confirm the involvement of TRP channels in temperature sensitivity and control of Ca^{2+} homeostasis in these neurons.

Supported by N.Z. Neurological Foundation.

Hirsch, E. C., Faucheux, B., Damier, P., Mouatt-Prigent, A. & Agid, Y. (1997) *Journal of Neural Transmission. Supplementum*, **50**, 79-88.

Lipski, J., Guatteo, E., Berretta, N., Bernardi, G. & Mercury, N. B. Unpublished observations.

Minke, B. & Cook, B. (2002) *Physiological Reviews*, **82**, 429-472.

Xu, H., Ramsey, I.S., Kotecha, S.A., Moran, M.M., Chong, J.A., Lawson, D., Ge, P., Lilly, J., Silos-Santiago, I., Xie, Y., DiStefano, P.S., Curtis, R. & Clapham, D.E. (2002) *Nature*, **418**, 181-186.

The nature of non-linear interaction between P2 purinergic and α_1 adrenergic receptors in hypoglossal motoneurons is determined by the temporal pattern of receptor activation

R. Kanjhan^{1,2}, A. Jung¹, G.B. Miles¹, J. Lipski¹, G.D. Housley¹, M.C. Bellingham² and G.D. Funk¹,

¹Department of Physiology, University of Auckland, Auckland, New Zealand and ²School of Biomedical Sciences, University of Queensland, St. Lucia, QLD 4072, Australia. .SP

Hypoglossal motoneurons (XII MNs) innervate the genioglossus muscle of the tongue and increase muscle tone during inspiration, thereby protecting airway patency. Their activity is constantly adjusted by a vast number of neuromodulatory systems to meet the changing demands placed on the respiratory system such as those accompanying changes in behaviour (suckling, vocalisation), environment (hypoxia) and arousal state (sleep-wake cycling). Reductions in XII MN activity and genioglossus muscle tone during sleep are believed to contribute to obstructive sleep apnea in adults and sudden infant death syndrome in newborns. Thus, there is considerable interest in understanding how modulatory systems alter the activity of XII MNs, particularly during sleep. Norepinephrine (NE) potentiates XII MN activity primarily through activation of α_1 adrenergic receptors and subsequent blockade of a resting K⁺ conductance. Reduced release of NE during sleep is believed to contribute to a reduction of XII MN activity, airway instability and apnea. Extracellular adenosine 5'-triphosphate (ATP) also potentiates inspiratory XII motor output through activation of P2 receptors. A likely source of ATP is via co-release with NE. The goal of this study was to explore how NE and ATP signaling systems interact to affect XII MN activity and inspiratory motor output. Phenylephrine (PE, α_1 adrenergic receptor agonist, 1-100 μ M) and ATP (0.1-10 mM) were applied alone and together (in the presence of 100 μ M theophylline), either simultaneously or sequentially, to the XII nucleus of medullary slice preparations that continue to generate a respiratory-related rhythm *in vitro* following isolation from anaesthetised neonatal rats.

Bath or local application (15-30s) of PE or ATP alone potentiated ipsilateral XII inspiratory nerve output (n=6), and activated inward currents in whole-cell voltage-clamped XII MNs (n=90). PE responses developed slowly and lasted for many minutes. ATP responses comprised a rapid-onset excitatory component, presumably mediated by P2X receptors. These fast, ATP-gated inward currents were further classified according to their desensitisation kinetics as fast-, slow- and non-desensitising. The excitatory phase was followed in some cases by a slow onset, inhibitory component which manifest as a decrease in burst amplitude or a small amplitude outward current, suggestive of a P2Y receptor mechanism. To assess interactions, we compared the magnitude of currents induced by PE and ATP alone and in combination. ATP, when applied prior to PE, attenuated the PE current to 62% of control (n=32; p<0.01), suggesting a negative interaction. Surprisingly, when PE was applied prior to ATP, a positive interaction was observed. In 45% of MNs (16 of 35), particularly those showing non-desensitising responses to ATP, PE caused up to a 3-fold potentiation of both the fast-inward and slow-outward components of the ATP current. That this did not simply reflect differences between MNs was demonstrated in 5 MNs (in 1 μ M TTX) where both positive and negative interactions were produced by switching the order of agonist application.

In summary, we have defined a novel mechanism where the nature of the non-linear interaction (positive vs. negative) between two neuromodulatory signaling cascades is determined by their temporal pattern of activation. While the underlying pathways remain to be determined, it is clear that such a mechanism will dramatically increase the dynamic range over which a given modulatory input can modify neuronal excitability.

Supported by the Marsden Fund, HRC of New Zealand, and Lotteries Health.

Glutamate alters the morphology of dendritic spines in motoneurons

A.J.C. McMorland¹, D.M. Robinson¹, C. Soeller¹, M.B. Cannell¹ and G.D. Funk², ¹Physiology, University of Auckland, New Zealand, and ²Physiology, University of Alberta, Canada. .fp 10 S

Dendrites are the primary receptive component of neurons. In motoneurons (MNs), for example, the dendritic tree comprises ~90% of the membrane surface area (Cullheim *et al.*, 1987), up to 60% of which is covered with presynaptic terminals (Örnung *et al.*, 1998). Dendrites therefore play a primary role in determining neuronal information processing. The first opportunity for dendritic signal processing is at the synapse. In a variety of neuron types, synapses occur on spines, specialised membrane projections where the effect of a synaptic input on the cell can be dynamically regulated by altering spine morphology. Spines have only rarely been reported on MNs. As an initial step toward understanding the functional significance of spines for MN function, we combined laser-scanning fluorescence microscopy, whole-cell recording and image processing techniques to characterise the density, distribution and dynamic morphology of dendritic spines in hypoglossal (XII) MNs from neonatal mice.

Medullary slice preparations (200 µm thick) were prepared from anaesthetised Swiss CD-1 mice (postnatal day 0-3) and XII MNs were labelled during whole-cell recording using pipettes filled with avidin-conjugated biocytin (Molecular Probes). For morphological experiments, tissue was fixed (4% paraformaldehyde), and recorded cells were visualised using Alexa 488-avidin conjugate (Molecular Probes) and imaged using confocal microscopy.

Dendritic segments displayed two distinct morphological patterns: (Type I) smooth, uniformly tapered segments with spines at low density (0.09 ± 0.01 spine.µm⁻¹, n = 3), or (Type II) periodically swollen segments that lacked spines. Spines also displayed a range of morphologies, including the classical mushroom-headed (pedunculated) form (site of synaptic inputs in other neurons) and those characterised by long filopodia but no head (proposed to be important for synaptogenesis; Cailliau Portera & Yuste, 2001).

We then tested the hypothesis that spine structure is not fixed but can be dynamically modulated in response to glutamate receptor activation. Moreover, based on observations in cultured cortical neurons (Hasbani *et al.*, 2001), we hypothesised that the Type II morphology results from retraction of spines and local swelling of dendrites at these sites in response to high concentrations of glutamate. XII MNs were labelled with Alexa Fluor 350 or 488 Hydrazide (Molecular Probes) under voltage-clamp conditions. Spines were identified and their morphologies recorded before, during and after bath-application of glutamate (125 - 500 µM for 5 - 10 minutes), using two-photon excitation microscopy. Glutamate application was associated with membrane depolarisation (from -59 ± 7 mV, to -5 ± 0.7 mV, n = 2), spine retraction and dendritic swelling, which transformed dendrites from Type I to Type II as defined in fixed preparations. These changes partially reversed upon glutamate wash-out. Membrane potential returned to -52 ± 2 mV and dendritic swelling was reduced.

These data confirm the presence at low density of dendritic spines on XII MNs, and establish that their morphology is not fixed but can be modified by glutamate receptor activation. Whether these changes in spine morphology represent a physiological mechanism important for synaptogenesis, for modulating synaptic strength (Hasbani *et al.*, 2001) or reflect the pathological consequence of glutamate-induced excitotoxicity remains to be determined.

Cailliau Portera, C. & Yuste, R. (2001). *Revista de Neurologia*, **33**, 1158-1166 (translated from Spanish).

Cullheim, S., Fleshman, J.W, Glenn, L.L. & Burke, R.E. (1987) *Journal of Comparative Neurology*, **255**, 68-81.

Hasbani, M.J., Schlieff, M.L., Fisher, D.A. & Goldberg, M.P. (2001) *Journal of Neuroscience*, **21**, 2393-2403.

Örnung, G, Ottersen, O.P., Cullheim, S. & Ulfhake, B. (1998) *Experimental Brain Research*, **118**, 517-532.

μ and δ opioid receptor mRNA and protein expression in the cerebellum of the foetal, neonatal, and adult rat

J.H. Miller, E.M. Mrkusich, B.M. Kivell and D.J. Day, School of Biological Sciences, Victoria University of Wellington, P.O. Box 600, Wellington, New Zealand. .SP

The three classical opioid receptors, μ , δ , and κ , are found in many regions of the rat brain where they act to modulate neurotransmission in the adult and regulate neurogenesis in the fetus and neonate. Based on radioligand binding and autoradiography, it is generally accepted that within the lobes of the rat cerebellum only δ opioid receptors are expressed. This is in contrast to the situation in humans and rabbits in which both μ and δ receptors are expressed in the cerebellum. Using frozen, paraformaldehyde-fixed cerebellar sections from foetal, neonatal, and adult Wistar rats, we investigated μ and δ opioid receptor protein distributions by immunohistochemistry, and opioid receptor mRNAs by fluorescent *in situ* hybridisation. Immunohistochemical staining using commercially available μ and δ antibodies followed standard procedures. For *in situ* hybridisation, riboprobes directly labeled with a fluorescent marker were used, thus, allowing comparative quantification of the message in brain tissue sections. cRNA probes complimentary to the 5' untranslated region of the mRNA were prepared. Targeting of this region rather than the coding region minimised cross hybridisation of cRNA probe between the closely related opioid receptor mRNAs that share significant regions of sequence similarity in their coding regions. Labeled cRNA probes were prepared from T7-tailed PCR products by *in vitro* transcription with T7 RNA polymerase and incorporation of Cy3-UTP or fluorescein-UTP into the reaction mixture. The results of this study showed that both μ and δ opioid receptor proteins and mRNAs were present in the adult and six day old neonatal rat cerebellum, specifically within Purkinje cells and in the granular layer. Expression of μ opioid receptor mRNA was also detected within cells of the molecular layer, but at lower levels than those seen within the Purkinje cells. Abundant expression of μ and δ opioid receptor mRNAs was also detected in the external germinal layer of the immature cerebellum of the foetal sixteen day post-conception rat, a finding that suggests a role for opioid receptors in neurogenesis of the developing cerebellum. Identification of both μ and δ opioid receptors within the developing cerebellum, and the known role of the cerebellum in coordinating multi-joint movements, supports the hypothesis that opioid receptors and their ligands affect development of coordinated movements in the neonate.

Upregulation of ecto-nucleoside triphosphate diphosphohydrolases 1 and 2 in noise-exposed rat cochlea

S.M. Vlajkovic¹, G.D. Housley¹, D.J.B. Munoz², S.C. Robson³, J. Sévigny⁴, C.J.H. Wang¹ and P.R. Thorne², ¹Department of Physiology, Faculty of Medical and Health Sciences, The University of Auckland, Auckland, New Zealand, ²Discipline of Audiology, Faculty of Medical and Health Sciences, The University of Auckland, Auckland, New Zealand, ³Department of Medicine, Beth Israel Deaconess Medical Center, Harvard Medical School, Boston, MA, USA and ⁴Centre de Recherche en Rhumatologie et Immunologie, CHUQ, Université Laval, Sainte-Foy, Québec, Canada. .SP

Extracellular ATP acting via P2 receptors in the inner ear initiates a variety of signalling pathways that may be involved in noise-induced cochlear injury (Thorne *et al.*, 2002). NTPDase1/CD39 and NTPDase2/CD39L1 are key elements for regulation of extracellular nucleotide concentrations and P2 receptor signalling in the cochlea (Vlajkovic *et al.*, 1999, 2002). This study characterised the effect of noise exposure on regulation of NTPDase1 and NTPDase2 expression in the cochlea using a combination of real-time RT-PCR, immunohistochemistry and functional studies. Adult Wistar rats were exposed to broad band noise at 90 dB and 110 dB sound pressure level (SPL) for 72 hours. Their auditory function was assessed by auditory brainstem response to clicks and pure tones. Exposure to 90 dB SPL induced a small and temporary change of auditory thresholds (temporary threshold shift), whilst exposure to 110 dB SPL induced a robust and permanent change of auditory thresholds (permanent threshold shift). NTPDase1 and NTPDase2 mRNA transcripts were upregulated in the cochlea exposed to 110 dB SPL, whilst mild noise (90 dB SPL) altered only NTPDase1 mRNA expression levels. Changes in NTPDase expression did not correlate with levels of circulating corticosterone, implying that the upregulation of NTPDase expression was not stress-related. Quantitative immunohistochemistry in the cochlea exposed to 110 dB SPL localised the increased NTPDase1 and NTPDase2 expression in the stria vascularis and upregulation of NTPDase2 in the intraganglionic spiral bundle. Whilst NTPDase1 was upregulated in the secretory tissues of the lateral wall, it was down-regulated in the cell bodies of the spiral ganglion neurones. Tissue distribution of NTPDases was not altered in the cochlea exposed to 90 dB SPL, implying a differential regulation of NTPDase expression in the cochlea in response to different noise levels. Functional studies revealed increased ectonucleotidase activity in the cochlea after exposure to 110 dB SPL, consistent with upregulation of NTPDases. These data indicate that the regulation of NTPDase1 and NTPDase2 expression in the cochlea is responsive to noise as a stimulus that also upregulates P2 receptor signalling pathways. The changes in NTPDase expression may reflect compensatory responses of cochlear tissues to limit ATP signalling during noise exposure and protect the cochlea from noise.

Thorne, P.R., Muñoz, D.J.B., Nikolic, P., Mander, L., Jagger, D., Greenwood, D., Vlajkovic, S.M., Housley, G.D. (2002) *Audiology & Neuro-Otology*, 7:180-184.

Vlajkovic, S.M., Housley, G.D., Greenwood, D., Thorne, P.R. (1999) *Molecular Brain Research*, 73:85-92.

Vlajkovic, S.M., Thorne, P.R., Sévigny, J., Robson, S.C., Housley, G.D. (2002) *Hearing Research*, 170:48-59.

Supported by the New Zealand Lottery Grants Board and Health Research Council of New Zealand. All studies were approved by the University of Auckland Animal Ethics Committee.

Quantifying local diffusion in the rat lens by two-photon flash photolysis

M.D. Jacobs, C. Soeller, M.B. Cannell and P.J. Donaldson, Department of Physiology, The University of Auckland, Private Bag 92019, Auckland, New Zealand 92019. .fp 10 S

The vertebrate ocular lens is an avascular organ composed of fibre-shaped cells that run from the anterior pole to the posterior pole of the lentoid mass. Often measuring several millimetres or more in diameter, the lens cannot rely on passive diffusion alone in order to maintain homeostasis and transparency. A model of lens micro-circulation has been proposed based upon external electrophysiological, and biochemical data (Donaldson *et al.*, 2001). However, few functional studies to date have focused on transport mechanisms at varying depths within the lens mass. As a transparent tissue composed of highly ordered and regularly-shaped cells, the lens is an ideal system for studying intra- and intercellular transport by optical methods. We have applied two-photon microscopy and image analysis to lenses loaded with a caged fluorescent dye, in order to quantify local diffusion within and between fibre cells at varying depths. We have compared these functional results with our previous structural studies (Jacobs *et al.*, 2001) to elucidate structure-function relationships of fibre cell transport.

Lenses were extracted from adult rats killed by CO₂ asphyxiation in accordance with protocols approved by The University of Auckland Animal Ethics Committee. Lenses were cut in half through the equator and placed in a perfusion chamber containing intracellular medium and 1mM fluorescein bis-(5-carboxymethoxy-2-nitrobenzyl) ether (CMNB-caged fluorescein). The chamber was mounted on the stage of a confocal microscope modified for two-photon excitation. The two-photon laser beam bypassed the scanning system of the microscope and was focused inside a selected fibre cell to uncage the fluorescein by two-photon flash photolysis. Movement of the fluorescein away from this point source, both within and between cells, was imaged in real-time using confocal optics in x-y and line-scan modes. Data were written to hard disk and quantitative analysis of dye movement was performed using custom-written software.

In the lens periphery the spread of the uncaged fluorescein was highly directional, corresponding to radial rows of fibre cells. Deeper in the lens (>300 µm) the cell-cell coupling was approximately isotropic around the cell targeted for photorelease. The directional cell-cell coupling observed at the periphery corresponded to the local expression pattern of gap junctions on opposite broad sides of the hexagonal fibre cells. The isotropic coupling deeper in the lens corresponded to the dispersal of gap junctions in older fibre cells. Quantitative image analysis allowed characterisation of the time courses of differential dye transfer between neighboring fibre cells in different regions of the lens. Cytosolic fluorescein diffusion coefficients were estimated by fitting diffusion equations and by comparison with numerical simulations. Taken together, our functional and structural data are consistent with a lens micro-circulation model in which gap junctions near the lens equator facilitate solute transport to the lens surface where appropriate ion channels and transporters are concentrated.

Donaldson, P., Kistler, J. & Mathias, R.T. (2001) *News in Physiological Sciences*, 16:118-123.

Jacobs, M.D., Soeller, C., Cannell, M.B. & Donaldson, P.J. (2001) *Cell Communication & Adhesion*, 8:349-353.

Support: The Marsden Fund of New Zealand, The University of Auckland Research Committee and The Wellcome Trust (UK).

Motor unit discharge properties of respiratory muscles during quiet breathing

J.P. Saboisky, J.E. Butler and S.C. Gandevia, Prince of Wales Medical Research Institute, Randwick, Sydney, NSW 2031, Australia. .SP

The diaphragm is considered the principal muscle of inspiration. However, many other muscles have an inspiratory action with different mechanical linkages to the rib cage. In this study we compared the discharge properties of single motor units in a range of “obligatory” human inspiratory muscles to quantify the distribution of inspiratory neural drive to each of the inspiratory motoneurone pools during quiet tidal breathing.

Studies were performed on 5 healthy volunteer subjects who sat comfortably in an upright chair while breathing through a mouth piece. We recorded single motor unit activity from five separate inspiratory muscles; diaphragm, scalenes, parasternal intercostals, dorsal external intercostals (third space) and dorsal external intercostals (fifth space), during normal quiet breathing (e.g. Gandevia *et al.*, 1999; De Troyer *et al.*, 2003). Electromyography recordings were made from 10 sites within each muscle using monopolar needle electrodes. Each of the muscles were studied on separate occasions. Before each measurement, the thicknesses of the musculature at the sites of intramuscular electrode insertion were assessed using ultrasonography (e.g. De Troyer *et al.*, 1997). Data were sampled and analysed through a commercially available spike-analysis system. Measurements were made of the onset and peak discharge properties of single motor units, and inspiratory flow and were averaged over three breaths.

In total, we recorded from 260 single motor units. The data (mean \pm SEM) are summarised in the Table below.

Muscles	Diaphragm	Scalenes	Parasternal intercostal	Dorsal external intercostal (3 rd Space)	Dorsal external intercostal (5 th Space)
No. of units	40	57	63	66	34
Onset time (ms)*	377 \pm 62	421 \pm 73	666 \pm 50	637 \pm 61	1119 \pm 129
Onset time %**	21.7 \pm 3.3	21.0 \pm 3.4	31.6 \pm 2.4	30.4 \pm 2.2	41.7 \pm 3.8
Onset frequency (Hz)	8.0 \pm 0.3	5.9 \pm 0.2	7.0 \pm 0.6	7.9 \pm 0.6	5.9 \pm 0.2
Frequency peak (Hz)	12.6 \pm 0.5	9.1 \pm 0.3	11.8 \pm 0.3	12.4 \pm 0.4	10.2 \pm 0.4

* defined as the time after onset of inspiratory flow.

** defined as onset time relative to total inspiratory time.

The results suggest that there is relatively early recruitment of the diaphragm and scalene muscles. The diaphragm and dorsal external intercostal muscles (third space) had the highest initial ($P<0.05$) and peak firing frequencies ($P<0.01$). The data describe for the first time the discharge properties of inspiratory motoneurons from a range of human inspiratory muscles during quiet breathing. It is likely that there is a non-uniform output from the different inspiratory motoneurone pools during quiet tidal breathing.

De Troyer, A., Leeper, J.B., McKenzie, D. K. & Gandevia, S.C. (1997) *American Journal of Respiratory Critical Care Medicine*, **155**, 1335-1340.

De Troyer, A., Gorman, R. B. & Gandevia, S. C. (2003) *Journal of Physiology*, **546**, 943-954.

Gandevia, S. C., Gorman, R. B., McKenzie, D. K. & De Troyer, A. (1999) *American Journal of Respiratory Critical Care Medicine*, **160**, 1598-1603.

Block of the divalent anion channel in the SR of rabbit skeletal muscle by disulfonic stilbene derivatives

K. Bradley and D.R. Laver, School of Biomedical Science, University of Newcastle, Australia. .SP

Previous studies have identified two types of anion channels in the sarcoplasmic reticulum (SR) of rabbit skeletal muscle (Kourie *et al.*, 1996). One of these anion channels has an appreciable anion conductance (saturating at 20pS for phosphate (P_i) and 60pS for SO_4^{2-}). It was proposed that these channels could be responsible for movement of phosphate across the SR membrane (Laver *et al.*, 2001). To further investigate this hypothesis we have searched for specific inhibitors of the divalent anion channel with the rationale that these inhibitors would prevent P_i transport across the SR.

SR vesicles containing the anion channels were isolated from rabbit skeletal muscle that was removed from dead rabbits. Transport of P_i across the SR vesicle membrane was inferred from the P_i assisted component of Ca^{2+} uptake by the SERCa pump. Ca^{2+} uptake was measured from the optical absorbance of antipyrylazo III (Dulhunty *et al.*, 1999). Ca^{2+} uptake experiments were carried out using solutions containing 100 mM KCl or KP_i , 4mM $MgCl_2$, 1mM ATP, 5 μ M ruthenium red, 0.5 mM antipyrylazo III, 5 mM TES (pH 7). Anion channels were incorporated into lipid bilayers using standard techniques (Laver *et al.*, 2001). Cytoplasmic solutions contained 260 mM Mg^{2+} (250 mM $MgSO_4$ and 10 mM $MgCl_2$), 1 mM $CaCl_2$, 10 mM TES at pH 7.4. Luminal solutions contained 60 mM Mg^{2+} (50 mM $MgSO_4$ and 10 mM $MgCl_2$), 10 mM TES, pH 7.4.

Lipid bilayer studies showed that the divalent anion channels were inhibited by the disulfonated stilbene derivatives, Diisothiocyanostilbene-2',2'-di-sulfonic acid (DIDS), 4,4'-dinitrostilbene-2,2'-disulfonic acid (DNDS), 4,4'-dibenzamidostilbene-2,2'-disulfonic acid (DBDS) and by suramin. Reversible block by these compounds inhibited these channels with high affinity from the cytoplasmic side (~0.1-1 μ M) and low affinity from the luminal side (0.1 - 1 mM). The voltage-dependent kinetics of drug binding and dissociation indicated that these compounds can dissociate from the channel to either side of the membrane (*i.e.* they are permeant blockers). DIDS also produces non-reversible inhibition of the channel.

Measurements of P_i facilitated calcium uptake by rabbit SR vesicles were used to assay the degree of P_i transport across the SR membrane. The presence of DBDS at concentrations sufficient to block the divalent anion channel in lipid bilayers (~1-10 μ M) had no effect on P_i transport. Thus it appears that while this channel conducts P_i , it is not the major pathway for P_i in the SR membrane.

Dulhunty, A.F., Laver, D.R., Gallant, E.M., Casarotto, M.G., Pace, S.M. & Curtis, S. (1999)

Biophysical Journal, **77**:189-203

Kourie, J.I., Laver, D.R., Junankar, P.R., Gage, P.W. & Dulhunty, A.F. (1996) *Biophysical Journal*,

70:202-221.

Laver, D.R., Lenz, G.K.E., Dulhunty, A.F. (2001) *Journal of Physiology*, **535**:715-728.

Aberrant splicing of ryanodine receptor in myotonic dystrophy

T. Kimura^{1,2}, M.P. Takahashi¹ and S. Sakoda¹, ¹*Clinical Neuroscience (Neurology), Graduate School of Medicine, Osaka University, Suita, Osaka, Japan.* and ²*Present Address: Muscle Research, John Curtin School of Medical Research, Australian National University, Canberra ACT, Australia.*
(Introduced by A.F. Dulhunty) .fp 10 S

It was reported that mRNAs for chloride channel (Mankodi *et al.*, 2002), cardiac troponin T, insulin receptor and myotubularin-related 1 were aberrantly spliced in muscles from myotonic dystrophy (DM). In all cases, the developmentally regulated splice switch that involves a choice between two or more alternative isoforms is skewed, resulting in preferential expression of the isoform that is usually expressed in immature or non-skeletal muscle tissues. We previously reported the induction of the mRNA of small-conductance Ca²⁺-activated K⁺ (SK3) channel that is usually expressed in immature fibers (Kimura *et al.*, 2000). Taken together, we postulate that there is a maturation-related abnormality in DM that explains the abnormal splicing and transcription. Based on this hypothesis, we investigated the splicing of two candidate mRNAs, which are developmentally regulated.

We used 28 muscle specimens; 10 from myotonic dystrophy type 1 (DM1), 5 from Amyotrophic Lateral Sclerosis, 5 from Polymyositis, 2 from limb-girdle muscular dystrophy and 6 from normal control. Myotubes cultured from 2 muscle specimens; 1 from DM1 and 1 from normal control, were also used. We examined splicing pattern of insulin receptor, ryanodine receptor of skeletal muscle type (RyR1) and β -tropomyosin, using RT-PCR. The total amount of RyR3 mRNA, which is expressed in immature muscles, was quantified. We also employed transgenic mice model of DM1, in which expanded CUG repeat expression in skeletal muscle leads to a DM-like phenotype, for the splicing pattern of RyR1.

We found a significant increase of an alternatively spliced isoform of RyR1 in DM1 patients. The alternative splicing results in the deletion of 5 amino acids at a modulatory region of the receptor and the isoform is normally expressed in undifferentiated muscles. The other splicing isoform of RyR1 was not significantly altered. The splicing of β -tropomyosin and the total amount of mRNA for RyR1 and RyR3 did not differ significantly. In mice, we found a significant increase of the same spliced isoform in long-repeat transgenic mice compared with short-repeat transgenic mice or wild type mice.

The same splicing pattern was found in DM1 patients and DM1 model mice, suggesting that expanded CUG repeat is sufficient for the abnormal splicing. The increase of an immature isoform of RyR1 supports our hypothesis of maturation-related abnormality in DM. Furthermore, RyR1 channel is a major calcium release pathway from sarcoplasmic reticulum and regulate contraction of skeletal muscle. It is possible that the aberrant isoform may be responsible for muscular degeneration of DM, although functional studies for this isoform are needed.

Kimura, T., Takahashi, M.P., Okuda, Y., Kaido, M., Fujimura, H., Yanagihara, T., & Sakoda, S. (2000) *Neuroscience Letters*, 295(3):93-6.

Mankodi, A., Takahashi, M.P., Jiang, H., Beck, C.L., Bowers, W.J., Moxley, R.T., Cannon, S.C., & Thornton, C.A. (2002) *Molecular Cell*, 10(1):35-44.

Glutathione transferase mu-2 modulation of the activity of muscle sarcoplasmic reticulum

Y.A. Abdellatif, S. Watson, A.F. Dulhunty, P. Board and P.W. Gage, Muscle Research Group, John Curtin School of Medical Research, Australian National University, Mills Road, Acton, Canberra, ACT 2601, Australia. .SP

Glutathione transferases (GST) are versatile enzymes with a wide range of activities ranging from conjugation of glutathione to toxic xenobiotics to maintaining protein disulfide bonds (Sheehan *et al.*, 2001).

Members of the GST family have been shown by our group to affect the activity of both skeletal and cardiac ryanodine receptors (RyR) (Dulhunty *et al.*, 2001). The present work focuses on glutathione transferase mu-2 (GST mu-2), one of the major GST isoforms in humans (Van Bladeren *et al.*, 2000).

The effects of GST mu-2 on skeletal and cardiac RyRs (isolated from New Zealand rabbit back and hind leg and pig heart respectively) were observed at the single channel level using planar lipid bilayers using symmetrical caesium methansulphonate as current carrier (250/250 mmol/l; *cis* (cytoplasmic)/*trans* (luminal)). CaCl₂ (100 µmol/l) was used to activate the channel on the cytoplasmic side at ± 40 millivolt of holding potentials. When GST mu-2 was added to the cytoplasmic side of the skeletal RyR, different effects were observed depending on the holding potential. At +40 millivolt there was a decline in the activity of the channel in a dose dependent manner. Up to approx 80% decrease in the relative mean current (mean current in presence of GST mu-2 compared to control) was observed with 16 µmol/l GST mu-2 (*n*=8). Further investigation revealed that the effect of GST was voltage dependent (14 out of 16 channels) as at -40 millivolt GST mu-2 significantly activated the channel showing about 3 fold increase in the relative mean current (*n*=8). In the presence of GST mu-2, cardiac ryanodine receptor showed a decrease in activity at -40 millivolt, the inhibition being more prominent at +40 millivolt. 2 µmol/l GST mu-2 led to approx 40% decrease in the relative mean current at -40 millivolt compared to approx 60% decrease at +40 millivolt (*n*=6).

The effect of GST mu-2 on calcium induced calcium release and calcium uptake was investigated in skeletal muscle sarcoplasmic reticulum using stopped-flow technique. 8 µmol/l GST mu-2 reduced the rate constant of calcium release by approx 40% (average of 50 traces in 6 experiments) while 10 µmol/l GST mu-2 increased calcium uptake rate constant by approx 13% (average of 40 traces in 6 experiments).

In conclusion (1) GST mu-2 inhibited skeletal RyR at + 40 millivolt while it activated it at 40 millivolt; indicating that GST mu-2 modulation of the skeletal RyR was voltage dependent; (2) GST mu-2 inhibited cardiac RyR, the inhibition being more prominent at positive voltage; (3) GST mu-2 inhibited calcium induced calcium release in skeletal sarcoplasmic reticulum; (4) GST mu-2 potentiated calcium uptake by the skeletal sarcoplasmic reticulum; (5) GST mu-2 effect on calcium release and uptake is potentially a product of the interaction with both the ryanodine receptor and the calcium pump.

Dulhunty, A., Watson, S., Board, P., & Gage, P. 2001. *Journal of Biological Chemistry* 276(5):3319-23.

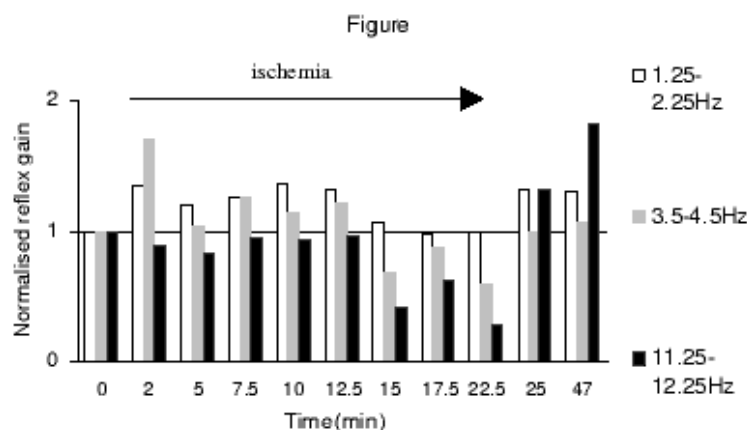
Sheehan, D., Meade, G., Foley, V.M., & Dowd, C.A. 2001 *Biochemical Journal* 360(Pt 1):1-16.

Van Bladeren, P.J. 2000 *Chemico-Biological Interactions*: 129: 6176.

The effect of prolonged ischemia on the tonic stretch reflex of the tibialis anterior muscle and stiffness of the ankle joint

J.A. Burne and A.R.N.M.H. Haque, School of Biomedical Science, University of Sydney, P0 Box 170, Lidcombe, NSW 2141, Australia. (Introduced by J.M. Lingard)

The aim of this study was to characterise the response of large and small muscle afferents to stretches over the low range of frequencies encountered during normal voluntary movement and to relate these changes to changes in joint stiffness. In 12 normal human volunteers, we elicited tonic stretch reflexes (TSR) in the contracting (10% of maximum voluntary contraction (MVC)) ankle dorsi-flexors using a complex 2min stretch sequence. The sequence contained frequencies spanning 0.1-14 Hz. The stretch was digitally generated and applied by a position-controlled servomotor before, during and after 24.5 min of ischemia produced by inflation of a cuff above the knee. The surface electromyography (EMG), joint angle and resistive torque records were analogue low-pass filtered (400 Hz) and digitised at 1000Hz. Reflex gain and coherence were computed by correlating the rectified and low-pass filtered EMG signals with the record of joint angle. (Matlab V6, Mathworks, USA).



The figure shows relative changes in TSR gain before (time=0), during (2-22.5min) and after (25-47min) ischemia for 3 representative frequency ranges. The gain of the reflex response to the lowest frequencies increased in early ischemia (at 2, 5, 7.5, 10 & 12.5 min) but not significantly (ANOVA, $P>0.05$) in comparison to control values (time=0). The gain of the middle frequency range increased significantly at 2 min of ischemia (ANOVA, $P=0.03$) and then declined during 15 - 22.5 min. The high frequency gain was most sensitive to ischemia. It tended to decline 2 min after cuff inflation and remained significantly decreased at 15 and 22.5 min (ANOVA, $P<0.05$, $P<0.01$) by about 70% of the control value. The high frequency gain showed significant recovery at 0.5 and 22.5 min after cuff deflation (ANOVA, $P=0.002$, $P=0.003$) compared with the last ischemic TSR value.

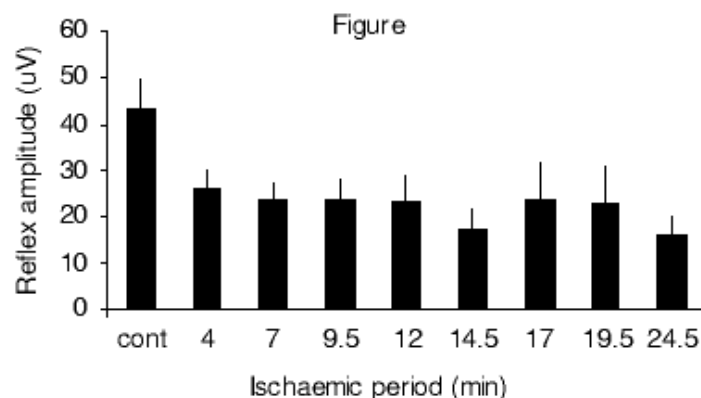
The resonant frequency (RF) of the ankle joint, calculated from the resistive torque data, increased in a linear manner with contraction of the ankle dorsi-flexors up to 20% of MVC (linear regression analysis, $P<0.00001$) (rest= $7.07+1.15$ Hz). The RF tended to decrease slightly during ischemia. However, the change was significant only at 2 min (ANOVA, $P=.04$) compared to the control value.

We conclude that both ischemia-sensitive and ischemia-resistant muscle afferents contribute to the stretch response and that they can be distinguished partly through their different stretch frequency responses. The evidence for an association between muscle reflex effects and effects on mechanical joint stiffness was not strong under the experimental conditions.

The effect of background contraction and prolonged ischemia on the tendon reflex

A.R.N.M.H. Haque and J.A. Burne, School of Biomedical Science, University of Sydney, PO Box 170, Lidcombe, NSW 2141, Australia. (Introduced by J.M. Lingard)

We studied the tendon reflex with the aim of characterising the contributing afferents on the basis of their sensitivity to ischemia. The experiment was done on 12 healthy human volunteers. The left foot was strapped to a foot plate controlled by a servo-motor that could detect force changes about the ankle. Tendon taps were applied to the Achilles tendon with a hammer that was hinged and fell under gravity to deliver a constant blow. A series of 10 responses was recorded at each background contraction of rest, 5%, 10%, 15%, 20% of maximum voluntary contraction (MVC) of the ankle plantar-flexor against the foot plate. Then ischemia was induced in the recorded lower limb by inflation of a blood pressure cuff on the left thigh. Taps were applied to the resting muscle during ischemia at the times shown in the figure and at 2.5 min intervals up to 32.5 min after cuff deflation. Even after our attempts to standardise the delivered taps, we found a large variance within each series of 10 and between subjects. This has been noted earlier (Toft *et al*, 1991). Coefficients of variations (CV) were high at all contraction levels but decreased for the taps applied at 15% and 20% of MVC. Despite the high CVs, the amplitude, when averaged over the series of 10, increased in a highly linear manner with the contraction level (linear regression, $P < 0.00001$). This result emulates the effect of contraction level on the tonic stretch reflex gain (Neilson & McCoughy, 1981) but has not been previously observed in tendon reflexes. The tendon reflex amplitude, after normalising for background contraction level, decreased significantly (ANOVA, $P < 0.000001$) after 4 min of ischemia to about 50% of the control value and remained depressed throughout the ischemic period. A transient recovery occurred after cuff deflation (ANOVA, $P = .00002$, data not shown in the figure) when compared with the last ischemic tap amplitude but the response remained depressed for the rest of the measured post ischemic period.



The data indicate that the tendon reflex is mediated by both ischemia-sensitive and ischemia-resistant fibres. The data from the accompanying abstract (Burne & Haque, 2003) suggest that fibres mediating high frequency stretches are more sensitive to ischemia than those mediating low frequencies. Given that taps constitute a broad-band stretch containing frequencies 0.1-100 Hz (data not shown), the high frequency component might be responsible for the quick depression and the low frequency component for the ischemia-resistant component.

Burne, J. & Haque, A. (2003) *Proceedings of Australian Physiological and Pharmacological Society*, **33**:39P.

Neilson, P. & McCoughy, J. (1981) *Journal of Neurology, Neurosurgery and Psychiatry*, **44**: 1007-1012.

Toft, E., Sinkjaer, T. & Rasmussen, A. (1991) *Acta Neurologica Scandinavica*, **84**: 311-315.

Acute incremental exercise, sprint exercise, as well as chronic intermittent hypoxia each decrease muscle Na⁺K⁺ATPase activity

R.J. Aughey¹, J.A. Hawley², C.J. Gore³, A.G. Hahn³, D.T. Martin³, S.A. Clark², N.E. Townsend³, T. Kinsman³, M.J. Ashenden³, K.E. Fallon³, G.J. Slater³, A.P. Garnham⁴, C.M. Chow⁵ and M.J. McKenna¹, ¹Centre for Rehabilitation, Exercise and Sports Science, Victoria University of Technology, Melbourne, ²RMIT University, Melbourne, ³Australian Institute of Sport, Canberra, ⁴Deakin University, Melbourne, and ⁵University of Sydney, NSW 2006, Australia. .sp -0.25c

The Na⁺K⁺ATPase enzyme is vital in maintaining skeletal muscle excitability. Athletes commonly use hypoxic exposure to improve athletic performance, favouring the live high, train low approach (LHTL). Paradoxically, muscle Na⁺K⁺ATPase content is reduced by chronic hypoxia (Fraser *et al.*, 2002), which would be expected to reduce muscle performance. Muscle maximal Na⁺K⁺ATPase activity is also decreased with fatiguing single-leg kicking exercise (Fraser *et al.*, 2002), although the effects of acute intense cycle exercise are unknown. We therefore investigated the effects of acute incremental and sprint exercise and of LHTL on muscle Na⁺K⁺ATPase activity and exercise performance.

Two studies were performed, where control subjects slept and trained in Canberra (altitude ~600m), whilst the LHTL groups slept in a hypoxic room (study 1, 3000m for 23-nights; study 2, 2650 m for 20-n), and trained at 600m. In study 1, 13 endurance athletes were assigned to either a control (CON, n=6) or LHTL group (n=7). In study 2, 21 endurance athletes were assigned to a control (CON2, n=7), 20 consecutive night LHTL (LHTL_c, n=7), or an intermittent 20 night LHTL (LHTL_i, 4 x [5-n LHTL then 2-n CON]) group. The lower simulated altitude and intermittent exposure in study 2 were used to reflect common athletic practice. A vastus lateralis muscle biopsy was taken at rest and immediately after incremental exercise prior to (Pre) & after (Post) 23-n of LHTL (study 1); and at rest and immediately after ~1-min sprint exercise prior to (Pre) and after (Post) 20-n LHTL (study 2.) The timecourse of adaptation was investigated in study 2 via an additional rest and post sprint exercise muscle biopsy taken after 5-n of LHTL. Muscle was analysed for maximal *in vitro* Na⁺K⁺ATPase (K⁺ stimulated, 3-O-MFPase) activity. Arterialised venous plasma [K⁺] was analysed during and following incremental (study 1) and sprint exercise (study 2).

Muscle 3-O-MFPase activity was depressed to a similar extent after both incremental (-12.4±0.8%, study 1, exercise effect, *P*<0.05) and sprint exercise (-12.3±0.5%, study 2, exercise effect, *P*<0.05). In study 1, the change in resting 3-O-MFPase activity (Pre - Post) was greater in LHTL (-2.9±1.1%, *P*<0.05) than CON (0.4±0.5%, NS). In study 2, resting muscle 3-O-MFPase was also reduced from Pre to Day 5 in both LHTL_c and LHTL_i groups (-2.1±0.4% and -2.3±0.2% respectively, *P*<0.05), but was unchanged in CON (0.3±0.9%, NS). Resting 3-O-MFPase activity (Day 5 - Post) was unchanged in LHTL_c and CON (-0.8±0.7% and 0.5±0.6 respectively, NS), but was reversed and increased in LHTL_i (3.5±1.2%). The Pre - Post change in resting 3-O-MFPase activity was lowered in LHTL_c (-2.9±0.7%, *P*<0.05), remained unchanged in CON (0.8±1.0%), but tended to increase in LHTL_i (1.1 ± 1.2%). Plasma [K⁺] rose with exercise and then declined post-exercise (*P*<0.05) in each study, but was unchanged by LHTL, LHTL_c and LHTL_i (data not shown).

In conclusion, markedly different exercise regimes each acutely depressed skeletal muscle maximal Na⁺K⁺ATPase activity, with no residual effect evident after 5d recovery. This effect was reproducible, suggesting an obligatory response to heavy exercise. LHTL at 3000m for 23-n, and at 2650m for 20-n each induced only a small reduction in resting Na⁺K⁺ATPase activity, which was reversed with inclusion of normoxic nightly exposure. In contrast to continuous hypoxic exposure, LHTL caused only a small depression in Na⁺K⁺ATPase activity. This was insufficient to adversely affect muscle performance or plasma K⁺ regulation, but may be energetically advantageous and might explain why exercise performance is not impaired with LHTL.

Fraser, S.F., Li, J.L., Carey, M.F., Wang, X.N., Sangkabutra, T., Sostaric, S., Selig, S.E., Kjeldsen, K.

& McKenna, M.J. (2002) *Journal of Applied Physiology*, 93, 1650-1659.
Green, H., Roy, B., Grant, S., Burnett, M., Tupling, R., Otto, C., Pipe, A. & McKenzie, D. (2000)
Journal of Applied Physiology, 88, 634-640.

This work was partially funded by an Australian Research Council SPIRT grant (C00002552).

A simple method for determining regional visual acuity in humans

D.F. Davey¹ and W. Burke^{1,2}, ¹Department of Physiology and ²Department of Anatomy & Histology, Institute for Biomedical Research, University of Sydney, NSW 2006, Australia. .SP

Diseases affecting the retina do not create a uniform lesion throughout the retina. It is therefore useful to be able to assess the functioning of small regions of the retina, both for diagnostic reasons and also to monitor the progress of the disease and treatment. The following method was devised specifically to monitor the development, progress and treatment of a condition known as 'macular hole' in which there is detachment of the retina at the fovea. For this reason the regions of retina studied were in the foveal region, but the method could be adapted to any other part of the retina.

Acuity in the vicinity of the fovea was determined at nine positions. Position 0 was centred on the fovea, positions 1-4 were in the outer fovea, positions 5-8 were in the parafovea. They were chosen in order to determine the spread of the macular hole, if it developed, and whether it developed symmetrically. The method of testing was as follows: the subject sat so that the eye being tested was at 57 cm from the screen of a cathode ray tube monitor (280 cm × 210 cm; 1 cm on the screen \equiv 1°), the other eye being covered. If the subject would normally wear corrective spectacles for that working distance, they were worn for the test. Except during a trial, the screen displayed only cross-bars. The subject focussed on the position on the screen corresponding to the point where the cross-bars would intersect. This procedure avoided having a fixation mark in the same place as a letter at position 0. When ready the subject pressed the space bar and a letter flashed on the screen in one of the nine positions. The identification of the letter by the subject was entered into the computer. The duration of the flash (100 ms), being less than the reaction time, prevented identification of the letter subsequent to an eye movement.

The letters used were the following: A, B, C, D, E, F, H, L, O, P, S, T, X, and Z, a set used in many Snellen charts. The font used was Helvetica Bold. The luminance of the letters was 3.1 cd/m² against a background luminance of 23.5 cd/m², the ambient luminance in the room being about 18 cd/m². The choices of letter and of position in which it was flashed were determined randomly. The GNU (Free Software Foundation) C-library *rand()* function was used to generate a pseudo-random selection from the 14 letters of the Snellen character set for each test flash. The same function was used to select the flash position from the nine test positions. The initial size of a letter was 60 point, occupying 1 cm on the screen, i.e. subtending 1°.

When a letter was identified correctly, the next time a letter was flashed in that position its size was reduced by a factor of $\sqrt{2}$. When a letter was identified incorrectly, the program kept the size unchanged in that position for a further nine trials. After ten trials at one position, if the percentage correct was 70% or less, the size was increased by a factor of $\sqrt{2}$ and ten trials applied with the new size. If the percentage correct was 80% or more, the size of letter was decreased by a factor of $\sqrt{2}$ and ten trials applied with the new size. The aim of this procedure was to determine a letter size that could be identified on 75% of trials. This size was obtained by linear interpolation between the sizes straddling the 75% correct value. This value was taken as a reasonable measure of the acuity at that position. Comparison of the values within the outer foveal and parafoveal permitted assessment of the symmetry of acuity, while comparisons over time using repeated tests allowed changes in acuity to be detected.

ATP acts as both a competitive antagonist and a positive allosteric modulator at recombinant NMDA receptors

A. Kloda¹, J.D. Clements², R. Lewis¹ and D.J. Adams¹, ¹*School of Biomedical Sciences, University of Queensland, Brisbane, QLD 4072* and ²*Synaptic Dynamics Lab, John Curtin School of Medical Research, Australian National University, Canberra ACT 0200, Australia.* .SP

ATP and glutamate are excitatory neurotransmitters in the CNS, and both modulate synaptic plasticity and LTP in hippocampal neurons (Wieraszko and Ehrlich, 1994). NMDA receptors are primarily responsible for the modulatory actions of glutamate, but the mechanisms underlying ATP's modulatory effects remain uncertain. In the present study, we investigated the effect of ATP on recombinant NR1a+2A and NR1a+2B NMDA receptors expressed in *Xenopus* oocytes. ATP inhibited currents evoked by low concentration of glutamate. ATP shifted the glutamate concentration-response curve to the right, suggesting a competitive interaction with the agonist binding site. It was a more potent inhibitor at NR1a+2A receptors than at NR1a+2B receptors. The inhibition was voltage-independent indicating that ATP acts outside the membrane electric field. Other nucleotides including ADP, GTP, CTP and UTP inhibited glutamate-evoked currents with different potencies indicating that the inhibition is dependent on the phosphate chain as well as the nucleotide ring structure. Surprisingly, ATP potentiated currents evoked by saturating concentrations of glutamate. At these concentrations, glutamate out-competes ATP at the agonist-binding site. Therefore the potentiation must be due to ATP binding at a separate site, where it acts as a positive allosteric modulator of channel gating. A simple model of the NMDA receptor was constructed, with ATP acting both as a competitive antagonist at the glutamate binding site and as a positive allosteric modulator at a distinct site. The model reproduced all of the main features of the data. Wieraszko, A and Ehrlich, Y.H. (1994)., *J. Neurochem.*63:1731-1738. This work was funded by ARC Postdoctoral Fellowship awarded to A.K. and ARC Large Grant (A00105778). J.D.C is funded by an ARC Senior Research Fellowship.

Inhibitory synaptic transmission in mouse type A and B medial vestibular nucleus neurones *in vitro*

A.J. Camp, B.A. Graham, R.J. Callister and A.M. Brichta, School of Biomedical Sciences, Faculty of Health, University of Newcastle, Callaghan, NSW 2308, Australia. .SP

The precise roles played by the neurotransmitters GABA and glycine in the maintenance of posture and balance are poorly understood. In the medial vestibular nucleus (MVN) fast inhibitory drive is known to be mediated by GABA_A receptors (GABA_AR) and indirect evidence suggests that glycine also plays a role. To directly assess the contribution of GABA_AR-mediated and glycine receptor (GlyR) mediated synaptic transmission we recorded miniature inhibitory synaptic currents (mIPSC) in the two major physiological classes (Type A and Type B) of MVN neurones. All experimental procedures were approved by the University of Newcastle Animal Care and Ethics Committee. Transverse brainstem slices (300 µm thick) were prepared from 21-28 day-old mice overdosed with Ketamine (100 mg/kg, i.p.). Whole-cell recordings (-70 mV holding potential) were made at room temperature (23°C) from infra-red visualised MVN neurones using patch electrodes with a CsCl-based internal solution. GABA_AR-mediated mIPSCs were isolated in TTX (1 µM), CNQX (10 µM), strychnine (1 µM) and were blocked by bicuculline (10 µM). GlyR-mediated mIPSCs were isolated in CNQX (10 µM), TTX (1 µM), bicuculline (10 µM) and were blocked by strychnine (1 µM). MVN neurones (24/29) received exclusively GABA_Aergic, exclusively glycinergic, or mixed mIPSCs (both types). Of the 24 MVN neurones displaying inhibitory events, 10 (42%) received purely GABA_Aergic inputs, 3 (12%) received purely glycinergic inputs, and 11 (46%) received Mixed mIPSCs. The rise times of GABA_A- and GlyR-mediated mIPSCs were similar for both types of mIPSC (0.7 ± 0.1 ms vs. 0.9 ± 0.5 ms), however the decay time constants for GABA_A-mediated events were significantly slower than those for GlyR-mediated events (9.6 ± 1.2 ms vs. 4.3 ± 0.9 ms). Having established that both GABA and glycine are involved in fast inhibitory synaptic transmission in MVN neurones, we next examined if inhibitory drive differed for Type A and Type B neurones. MVN neurones receiving mixed (GABA_Aergic and glycinergic) and exclusively glycinergic inputs had higher background discharge rates than those receiving exclusively GABA_Aergic inputs (24.1 ± 8.9 Hz n=4 and 9.4 ± 3.4 Hz n=2, respectively vs. 5.4 ± 1.0 Hz n=6). The type of inhibitory input was also correlated with the MVN neurone's physiological class. Using a combination of voltage- and current-clamp recording techniques, our initial results suggest that Type A neurones, which have a monophasic AHP, receive both glycinergic and mixed inhibitory inputs. Type B neurones, which have a biphasic AHP, receive only GABA_Aergic inhibitory inputs. These findings show that both GABA and glycine contribute to inhibitory synaptic processing in MVN neurones. Furthermore, inhibition mediated by GABA_ARs and GlyRs may differ in Type A and Type B MVN neurones.

Supported by Hunter Medical Research Institute (HMRI), and the Garnett Passe & Rodney Williams Memorial Foundation.

Ryanodine receptor isoforms in the neonatal rat cochlea

R.T. Whitehead, M.B. Cannell and G.D. Housley, Department of Physiology, Faculty of Medical Health Science, University of Auckland, Private Bag 92019, Auckland, New Zealand. .SP

Intracellular Ca^{2+} plays an essential role in many aspects of cochlear function. The ryanodine receptor (RyR) intracellular Ca^{2+} release channel has been implicated in the regulation of both auditory neurotransmission and sound transduction (Bobbin, 2002; Kennedy and Meech, 2002; Sridhar *et al.*, 1997). Nevertheless, there is a lack of data on the localisation of RyR mRNA and protein in the cochlea.

RyR isoform (RyR1, RyR2, RyR3) mRNAs were amplified from postnatal day 10 rat spiral ganglion neuron (SGN), organ of Corti, and whole cochlea cDNA using the reverse transcription-polymerase chain reaction (RT-PCR) with RyR isoform-specific primers. The identity of the cDNA PCR products was confirmed by sequencing. Ca^{2+} imaging of RyR-mediated Ca^{2+} store release was imaged using 300 μm neonatal rat cochlear slices loaded with 10 μM fluo 4-AM.

All three RyR isoform mRNA transcripts were detected in the whole rat cochlea and SGN cDNA. However, only RyR1 and RyR3 mRNA transcripts were detected in the organ of Corti. As previously reported, a primary antibody recognising both RyR1 and RyR2 revealed protein expression in the SGN cell bodies and organ of Corti in adult rat cochlea (Whitehead *et al.*, 2002). However, a RyR2-specific antibody showed staining only in the SGN cell bodies, thus the organ of Corti labelling probably reflects RyR1 expression. Functional expression of RyR in the neonatal rat cochlea was confirmed by increases in intracellular Ca^{2+} in the SGN cell bodies and the organ of Corti with bath superfusion of the RyR agonist caffeine (5mM).

This study confirms the expression of multiple RyR isoform mRNA transcripts in the neonatal rat cochlea, and the expression of functional RyR protein in the SGN and organ of Corti. Co-expression of all three RyR isoform mRNA transcripts in the SGN cell bodies suggests a complexity of RyR-mediated Ca^{2+} signalling associated with auditory neurotransmission. The detection of RyR1 and RyR3 mRNA and the immunolabelling for RyR1 in the organ of Corti suggests that both isoforms contribute to regulation of sound transduction.

Bobbin, R.P. (2002) *Hearing Research*, 174: 172-182.

Kennedy, H.J. & Meech, R.W. (2002) *Journal of Physiology*, 539: 15-23.

Sridhar, T.S, Brown, M.C. & Sewell, W.F. (1997) *Journal of Neuroscience*, 17: 428-37.

Whitehead, R.T., Cannell, M.B. & Housley, G.D. (2002) *Proceedings of the Physiological Society of New Zealand*, 21: 29.

Localisation of P2X6 receptor protein expression in the adult rat cochlea

D. Greenwood, L.K. Yang, P.R. Thorne and G.D. Housley, Department of Physiology, University of Auckland, Private Bag 92 019, Auckland 1009, New Zealand. .SP

The P2X6 receptor (P2X6R) is one of seven P2X receptors forming a homologous family of mammalian channel proteins (ATP-gated ion channels). P2X6R cDNA was first isolated from a superior cervical ganglion cDNA library (Collo *et al.*, 1996). mRNA expression of this subtype is highly distributed throughout the brain. There is extensive overlap in localisation of P2X6R mRNA with the other subunits, especially P2X4R and P2X2R, indicating potential for forming heteromeric P2X receptors (Collo *et al.*, 1996). Co expression of P2X6R with P2X2R (King *et al.*, 2000), or P2X4R (Le *et al.*, 1998) can produce modified channel phenotypes whereby the original P2X2R or P2X4R properties are altered, supporting the likely occurrence of P2X6R as a heteromer and extending the functional diversity of these receptors. In the mammalian cochlea extracellular ATP acting at P2X receptors has a major role in auditory function, including sound transduction and auditory neurotransmission. All seven P2XR subunit mRNAs are represented in the cochlea (Greenwood *et al.*, 1999). Previously, P2X6R expression has been localised to the spiral ganglion (Brandle *et al.*, 1999; Xiang *et al.*, 1999). In this study we used immunoperoxidase histochemistry and confocal immunofluorescence to investigate the sites of P2X6R protein expression in adult cochlea. Given the propensity for P2X6R to co localise with P2X2R (Collo *et al.*, 1996) and a recent report demonstrating an up-regulation of P2X2R protein expression in auditory hair cells and spiral ganglion neurones in response to noise (Wang *et al.*, 2003) we investigated whether P2X6R expression was also modified by noise exposure.

Adult Wistar rats were subjected to either ambient noise (control) or white noise at 110dB for 72 hours. Paraformaldehyde fixed cochleae were isolated. Floating 50 mm sections were labelled using a rabbit anti-rat antibody raised against an intracellular C-terminus peptide of the P2X6R coding sequence (Roche, Palo Alto). P2X6R immunoreactivity was detected using a Vectastain Elite ABC kit (Vector Laboratories) and visualised after incubation with the chromogenic substrate 3, 3-diaminobenzidine tetrahydrochloride (Vector Laboratories). A Cy3-conjugated anti-rabbit IgG goat antibody (Chemicon) was utilised as the secondary antibody in the immunofluorescence study. Specificity of the antibody was confirmed by (i) omission of the primary antibody and (ii) with a peptide block of the P2X6R epitope. Intensity of fluorescent P2X6R labelling was analysed using Image Pro Plus software (Adobe).

In this study, the spiral ganglion was confirmed as the principal site of P2X6R expression. Other notable structures showing P2X6R expression included supporting cells of the organ of Corti, and the stria vascularis. P2X6R protein expression was unchanged by noise exposure unlike P2X2R, a potential co-subunit. This finding suggests that P2X6R expression may contribute to heteromultimeric assembly with other P2XR in the cochlea. Possible phenotype modulation conferred by P2X6R may be diminished by noise-induced up-regulation of co-assembled P2XR.

Brandle, U., Zenner, H.P. & Ruppersberg, J.P. (1999) *Neuroscience Letters*, 273: 105-108.

Collo, G., North, R.A., Kawashima, E., Merlopich, E., Neidhart, A., Surprenant, A. & Buell, G. (1996) *Journal of Neuroscience*, 16: 2495-2507.

Greenwood D., Burrows M., Kanjhan R., Raybould N.P., Salih S.G. & Housley G.D. (1999) *Proceedings of the Physiological Society of NZ*, 18: 55p.

King, B.F., Townsend-Nicholson, A., Wildman, S.S, Thomas, T., Spyer, K.M. & Burnstock, G. (2000) *Journal of Neuroscience*, 20: 4871-4877.

Le, K.T., Babinski, K. & Seguela, P. (1998) *Journal of Neuroscience*, 18: 7152-7159.

Wang J.C.C., Raybould N.P., Lin L., Ryan A.F., Cannell M.B., Thorne P.R. and Housley G.D. (2003) *NeuroReport*, 14(6:) 817-23.

Xiang, Z., Bo, X. & Burnstock, G. (1999) *Hearing Research*, 128 190-196.

Studies approved by University of Auckland Animal Ethics Committee. Funded by: Health Research Council, Marsden Fund, Maurice and Phyllis Paykel Trust. I. Oglesby at Roche Palo Alto is thanked for supplying the P2X6 antisera

GABA_A receptor subunit composition in cultured hippocampal neurons from newborn rats

N. Ozsarac¹, M.L. Tierney² and P.W. Gage¹, ¹John Curtin School of Medical Research, Australian National University, PO Box 334, Canberra, ACT 2601 and ²School of Biochemistry & Molecular Biology, Faculty of Science, Australian National University, Canberra, ACT 2601, Australia. .fp 10 S

GABA_A receptors are the major inhibitory neurotransmitter receptors in the central nervous system. These heteromeric receptors are composed of five subunits and so far six, α -, three β -, three γ -, one δ -, one ϵ -, one π - and one θ - subunit have been identified in the mammalian nervous system. A number of pharmacologically important drugs such as benzodiazepines, barbiturates, anaesthetics and convulsants produce at least part of their clinically relevant effects by directly binding to GABA_A receptors. These drugs exert their effects by changing channel kinetics or channel conductance, or both. The generally reported conductance for synaptic GABA_A receptors is 25-30 pS. We have reported much higher conductances of up to 100 pS, and an increase in conductance in the presence of some of the above drugs, in cultured hippocampal neurons from newborn rats (Eghbali *et al.*, 1997). A possible reason for the discrepancy between our results and those of some others is that cultured neurons from newborn rats may have an unusual complement of subunits. Our aim is to identify the subunit composition of GABA_A receptors in these neurons by reverse transcriptase PCR (RT-PCR) in seven-day-old hippocampal cultures from newborn Wistar rats. In initial work, we are concentrating on the main subunits: α , β , γ and δ . Our preliminary results show an absence or a very low quantity of α -1 and 6, β -2, γ -2 and -3 in these cultured cells.

Eghbali, M., Curmi, J.P., Birnir, B. & Gage, P.W. (1997) *Nature*, 388:71-75.

Affinity purification of the skeletal muscle ryanodine receptor using a glutathione-S-transferase-FKBP12 fusion protein

P. Pouliquin, S. Pace and A.F. Dulhunty, Muscle Research Group, John Curtin School of Medical research, Australian National University, Mills Road, Acton, ACT 2601, Australia. .SP

Calcium is the most ubiquitous second messenger. In numerous cell types, the calcium release channel ryanodine receptor (RyR) plays a central role in calcium signalling. This channel is associated with a plethora of proteins in the cell, and constitutes the core of a supra-macromolecular complex which integrates cell signals and translates them into a calcium signal. In the heart and in the skeletal muscle, RyRs associated with their co-/accessory proteins are central to the excitation-contraction process which is still not fully understood at the molecular level. A better understanding of this critical step and, by extension, of the calcium signalling in many cell types requires better knowledge of the mechanisms which determine the ryanodine receptor function, *via* improved structure-function studies. The most precise studies of ryanodine receptor function are based on single channel recordings after incorporation of the RyR into planar lipid bilayers. Unfortunately, purity of the channel used in those experiments has not been adequate to determine RyR's intrinsic properties. Most studies have been done with microsomal vesicles enriched in RyR. The so called purified receptor contains significant contamination by several proteins. When RyR has been exogenously expressed in cells which don't express it endogenously, the extent of the channel's association with other proteins is not known. Determination of the channel's intrinsic properties and of the precise influence of its numerous co-/accessory proteins requires functional studies performed with pure RyR.

FKBP12 is a small protein which associates tightly with the RyR (Mackrill *et al.*, 2001). We have expressed a GST-FKBP12 fusion protein and used it to perform affinity purification of the RyR from rabbit skeletal muscle isolated after animals had been euthanased by captive bolt. The procedure has been described with few modifications (Mackrill *et al.*, 2001). Heavy sarcoplasmic vesicles were solubilised with 3-[(3-cholamidopropyl)-dimethylamino]-1-propanesulfonate in the presence of phosphatidylcholine. Non solubilised proteins were eliminated by ultracentrifugation; supernatant was then incubated with GST-FKBP12 fusion proteins immobilised on agarose beads. Unbound and unspecifically bound material was removed by successive washes. Purity of the purified ryanodine receptor and yield of the protein were estimated by silver nitrate staining of SDS-PAGE and colorimetric assay, respectively. Attempt to release RyR from the beads-fusion protein complex by the drug rapamycin failed. The ryanodine receptor-fusion protein complex was released from the beads by glutathione, and the excess of fusion protein eliminated by gel filtration. The RyR was purified virtually to homogeneity, the main usual contaminants (calsequestrin and Ca²⁺-ATPase) not being detected on silver nitrate. Yield of the purified RyR from the heavy sarcoplasmic vesicles was estimated close to 60%.

Intrinsic functional properties of the purified protein will be studied using single channel recordings and ³H-ryanodine binding assays. We are also expressing some RyR's co-/accessory proteins as fusion proteins with tags allowing their affinity purification. Addition of those purified co-/accessory proteins to the buffer bathing the purified channel should allow us to explore their regulatory effects on the receptor.

Mackrill, J.J., O'Driscoll, S., Lai, S.F.A., & McCarthy, T.V. (2001) *Biochemical and Biophysical Research Communications* **285**, 5257.

The role of the Ether-à-go-go K⁺ channel in cellular proliferation in the mouse preimplantation embryo

S.L. Jones and M.L. Day, Department of Physiology and Institute for Biomedical Research, University of Sydney, NSW 2006, Australia. .SP

The initiation of cell division is a complex process that is currently thought to depend on changes in membrane ion permeability, especially that resulting from K⁺ channel activity (Amigorena *et al.*, 1990; Wonderlin and Strobl, 1996). Furthermore, K⁺ channel expression and activity (Day *et al.*, 1993; Amigorena *et al.*, 1990) have also been found to be modulated during the cell cycle, which may suggest a novel, non-excitabile K⁺ channel function: the regulation of cell cycle progression. Ether-à-go-go (*eag*) is a voltage-activated K⁺ channel, thought to be involved in cell proliferation (Brüggemann *et al.*, 1997; Pardo *et al.*, 1998).

This study aims to examine the cell cycle dependent expression of *eag* in MCF-7 and trophoblast stem cell lines and determine the extent to which *eag* alters the membrane potential in a cell cycle dependent manner. The expression and potential change will also be examined during development of the mouse preimplantation embryo.

The effects of loss of *eag* expression on membrane potential and cell division will also be examined by specific downregulation of the gene using RNA interference. A plasmid vector will be employed to synthesise siRNA homologous to *eag* mRNA within the cells resulting in degradation of the *eag* mRNA transcript.

These methods may allow a greater understanding of the cell cycle regulated expression of *eag* and the impact of this on changes in membrane potential and the proliferative response.

Amigorena, S., Choquet, D., Teillaud, J., Korn, H. & Fridman, W.H. (1990) *The Journal of Immunology*, **144**: 2038-2045.

Wonderlin, W.F. & Strobl, J.S. (1996) *Journal of Membrane Biology*, **154**: 91-107.

Day, M.L., Pickering, S.J., Johnson, M.H. & Cook, D.I. (1993) *Nature*, **365**: 560-562.

Brüggemann, A., Stühmer, W. & Pardo, L.A. (1997) *Proceedings of the National Academy of Sciences of the USA*, **94**: 537-542.

Pardo, L.A., Brüggemann, A., Camacho, J. & Stühmer, W. (1998) *The Journal of Cell Biology*, **143**: (3) 767-775.

The Cys-loop's role in ligand-binding and channel-gating in the GABA_A receptor

V.A.L. Seymour¹, T. Luu¹, M.L. Tierney² and P.W. Gage¹, ¹Department of Molecular Biosciences, John Curtin School of Medical Research, Building 54 - ANU, Mills Rd, Acton ACT 0200 and ²Biochemistry and Molecular Biology, Faculty of Science, Building 41 - ANU, Linnaeus Way, Acton ACT 0200, Australia. .SP

The Cys-loop is conserved amongst members of the ligand-gated ion channel (LGIC) family. Within this loop there is a conserved motif referred to as the XPZD motif which sits at the bottom of the Cys-loop at positions 8 to 11 where the conserved cysteines are designated positions 1 and 15. The 4 residues that comprise the XPZD motif in the GABA_A receptor are either conserved throughout the LGIC family or the chemical nature of the residue is conserved. The recently solved crystal structure of an acetylcholine binding protein places the Cys-loop at the junction between the extracellular ligand-binding and transmembrane domains (Brejc *et al.*, 2001). We hypothesise that the Cys-loop may play a role in linking ligand-binding to channel-gating in the GABA_A receptor. To test this hypothesis we are mutating residues in the conserved XPZD motif within the Cys-loop of GABA_A receptor subunits and examining their ability to function as ion channels.

Mouse L929 cells were transfected with combinations of wild type (WT) ($\alpha 1\beta 1\gamma 2s$) and mutant GABA subunit cDNAs. When the invariant proline residue in the Cys-loop was replaced with alanine (P9'A) in the α or β subunit and co-expressed with the remaining WT subunits, the whole cell response to GABA was reduced. The reduced response could be caused by fewer receptors in the membrane as a result of lower expression, impaired assembly or defective trafficking of receptors or the reduction could be a result of changes in channel properties such as kinetics. To determine the cause of the reduced response, immunofluorescence and radioactive muscimol binding studies are being used to quantitate and compare the presence of mutant receptors in the membrane with the WT receptor and secondly, single channel currents are being recorded to examine if the reduced response is caused by changes in channel kinetics.

The response of GABA_A receptors to agonists can be potentiated by drugs such as diazepam, pentobarbitone and etomidate. The effects of these drugs were tested on GABA_A receptor mutants and compared with the effects on WT GABA_A receptors. Responses were generated with 1 μ M GABA followed by potentiation with 1 μ M diazepam, 100 μ M etomidate or 50 μ M pentobarbitone. The potentiated response to each drug was less than the WT response when proline was mutated to alanine at 9' in the Cys-loop in either α or β subunits.

The (P9'A) mutation in the Cys-loop of GABA_A subunits reduces the whole cell current in response to GABA and changes responses to various drugs. Further studies are being undertaken to test the role of the Cys-loop in these fundamental actions of the ion channel.

Brejc, K., van Dijk, W. J., Klaassen, R.V., Schuurmans, M., van Der Oost, J., Smit, A.B. & Sixma, T.K. (2001) *Nature*, **411**, 269-276.

Expression of calcium release channels in rat arteries

T.H. Grayson and C.E. Hill, Division of Neuroscience, John Curtin School of Medical Research, Australian National University, Canberra, ACT 0200, Australia.

Changes in intracellular calcium concentration, as a consequence of the regulated opening and closing of Ca^{2+} channels, controls many cellular responses. In arteries, Ca^{2+} released from intracellular stores in smooth muscle cells can cause vasoconstriction or vasodilation, depending on the signaling pathways and calcium sources that are involved (see Hill *et al.*, 2001). Similarly, in the endothelium Ca^{2+} released from IP₃-sensitive stores is associated with vasodilation but the contribution of other Ca^{2+} sources is unknown. Responses to Ca^{2+} fluxes are coordinated through the endothelium and smooth muscle via gap junctions composed of connexins (Cxs). Differential distribution of Ca^{2+} release channels and Cx subtypes may underlie the variability in responses observed between functionally distinct vessels. We used real-time PCR to examine the subtype-specific expression of mRNA for the inositol 1,4,5-trisphosphate receptor (IP₃R), ryanodine receptor (RyR), transient receptor potential channels (TrpC), and vascular Cx isoforms in thoracic aorta (ThA), mesenteric (MA) and basilar (BA) arteries removed from juvenile (14-17 day) and adult (9-13 week) Wistar rats that had been anaesthetised with ether and decapitated (Animal Experimentation Ethics Committee, ANU).

IP₃R1 was the most abundantly expressed IP₃R subtype in all arteries. Compared with the juvenile, the expression of IP₃R1 was increased in the adult ThA but not in other arteries, and the expression of IP₃R2 and IP₃R3 was reduced in the adult MA and BA.

RyR2 was the predominantly expressed RyR subtype in all arteries. RyR3 was detected at a low level in each artery except in the MA where it constituted 25% of RyR expression. Compared with the juvenile, RyR2 was more abundant in the adult ThA but there were no other significant changes with development. RyR1 was not detected in any artery.

TrpC1 was the predominant TrpC channel in all arteries and, compared with the juvenile, was more abundant in the adult ThA. TrpC3 was mainly expressed in the BA and MA, while TrpC4 was mainly expressed in the MA. TrpC6 expression was at a relatively low level in each artery and was much reduced in the adult. TrpC2, TrpC5 and TrpC7 were not detected in any artery. No other substantial changes were found during development.

The expression of vascular Cxs showed that $\text{Cx43} \gg \text{Cx37} > \text{Cx40} > \text{Cx45}$ in the ThA while $\text{Cx37} \gg \text{Cx40} \approx \text{Cx45} > \text{Cx43}$ in the MA and BA. Relative levels of Cx expression did not change substantially between the juvenile and adult, although Cx40 expression was significantly reduced in the adult BA and Cx43 was significantly increased in the adult ThA.

The pattern of expression for IP₃Rs was similar amongst the 3 arteries however there were differences between elastic (ThA) and resistance (BA, MA) arteries in the expression of TrpC3 and Cxs. Furthermore, MA was distinguished by the expression of TrpC4 and RyR3. Using subtype-specific antibodies we have recently shown that IP₃R1 was found in vascular smooth muscle and endothelium while IP₃R2 and IP₃R3 were almost exclusively restricted to the vascular endothelium (Grayson *et al.*, 2003). Future work will determine whether protein expression and distribution of the other Ca^{2+} channel subtypes varies in a similar manner.

Hill, C.E., Phillips, J.K. & Sandow, S.L. (2001) *Medical Research Reviews*, 21:1-60.

Grayson, T.H., Haddock, R.E., Murray, T.P., Wojcikiewicz, R.J.H. & Hill, C.E. (2003) *ANZMS 11th Symposium Abstracts*, Fraser Island, Queensland, Australia, 11-14 September.

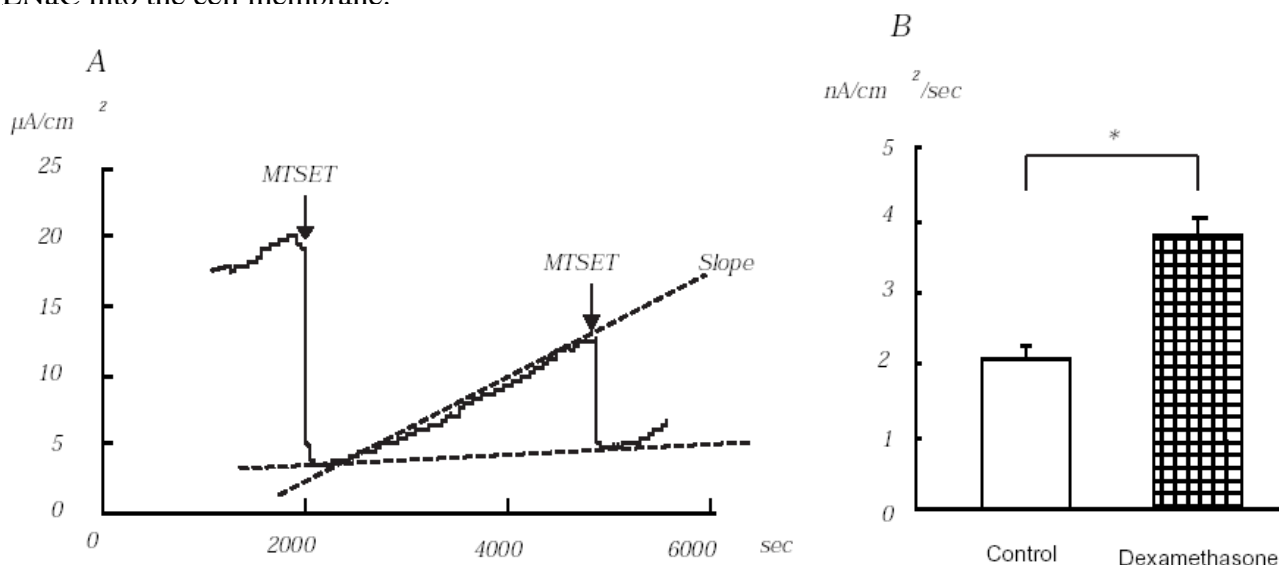
Mineralocorticoid activates epithelial sodium channel via exocytosis in mouse renal collecting duct cells

Y. Hosoda¹, M. Pedler², H. Hu¹, A. Beesley¹, C. Bailey², A. Dinudom¹, J.E.J. Rasko² and D.I. Cook¹,

¹Department of Physiology, University of Sydney, NSW 2006 and ²Centenary Institute of Cancer Medicine & Cell Biology, & Sydney Cancer Centre, Newtown, NSW 2042, Australia.

The epithelial sodium channel (ENaC) plays a critical role in regulating body sodium and fluid homeostasis. Activity of ENaC is regulated by hormones such as aldosterone and insulin. Aldosterone increases ENaC activity within 30 min and this early effect of the hormone is non-genomic. Although the mechanisms that underlie the early effect of aldosterone on ENaC activity are still unknown, it is believed that this effect may be mediated by increasing insertion of ENaC from a cytosolic pool into the cell membrane. To investigate this hypothesis, we used a retroviral expression system and Ussing chamber technique to study regulation of ENaC activity in the mouse collecting duct (M1) cell line. To investigate insertion of ENaC, a glycine codon in the amiloride-sensitive region of the γ ENaC gene was mutated to cysteine (G542C). A retrovirus expressing this gene was constructed and used to stably transfect M1 cells. The M1 cells that were transfected with G542C γ ENaC were selected using neomycin resistance and then cultured on Millicell-CM for 14-16 days until the transmembrane resistance was fully developed. The Ussing chamber method was used to measure equivalent short circuit current (I_{sc}) across the monolayer. The G542C mutation makes ENaC sensitive to [2-(trimethylammonium) ethyl] methanethiosulfonate bromide (MTSET). MTSET forms a disulfide bond with cysteine and inhibits ENaC activity irreversibly. Recovery rate of the MTSET-sensitive current was then used to measure the rate of insertion of active ENaC into the cell membrane.

One hour before each experiment, 100 nM dexamethasone was added to the culture medium. Application of MTSET to the apical side of the monolayers decreased I_{sc} from 13.0 ± 0.8 to $2.6 \pm 0.1 \mu\text{A}/\text{cm}^2$ (n=10). Dexamethasone significantly increased baseline MTSET-sensitive I_{sc} from $10.3 \pm 0.8 \mu\text{A}/\text{cm}^2$ (n=10) to $19.1 \pm 1.2 \mu\text{A}/\text{cm}^2$ (n=9, P<0.01). After the maximum inhibitory effect of MTSET was observed, the chamber was perfused with HEPES solution for 45 minutes and the slope of MTSET-sensitive I_{sc} was measured (A in Figure). The slope measured in the dexamethasone treated group ($3.8 \pm 0.2 \text{ nA}/\text{cm}^2/\text{s}$) was significantly higher than that of the control group ($2.1 \pm 0.1 \text{ nA}/\text{cm}^2/\text{s}$) (B in Figure, P<0.001). The second MTSET sensitive I_{sc} recovered to 50% of original MTSET sensitive I_{sc} in both control and dexamethasone groups. Our study, therefore, clearly indicates that the early effect of dexamethasone on Na⁺ transport in M1 cells is mediated by increasing insertion of ENaC into the cell membrane.



*Inhibition of equivalent short circuit current on M1 cells by MTSET. A: representative trace for change of equivalent short circuit current. MTSET was applied to the apical side only. B: the comparison of slopes between control (n = 10) and dexamethasone treated group (n = 9). * < 0.001.*

Angiotensin in the ventrolateral medulla

A.M. Allen, Howard Florey Institute, The University of Melbourne, Vic. 3010, Australia. .SP

The ventrolateral medulla contains groups of neurons that regulate autonomic functions such as respiration and cardiovascular control. This presentation will concentrate on two of these groups, the caudal and rostral ventrolateral medulla (CVLM and RVLM respectively). These nuclei contain catecholaminergic and non-catecholaminergic cells, which regulate sympathetic vasomotor nerve activity and neuroendocrine function. The CVLM contains a group of GABA-ergic interneurons that are involved in the sympathetic component of the baroreceptor reflex, and noradrenergic A1 neurons that project to the magnocellular neurosecretory neurons of the hypothalamus to modulate vasopressin release. The RVLM contains spinally-projecting neurons (some of which are adrenergic (C1 cells)) whose activity is essential for the tonic and reflex regulation of sympathetic vasomotor tone.

Angiotensin AT₁ receptors occur throughout the ventrolateral medulla in all mammals, including humans. In the human the AT₁ receptors are associated with the catecholaminergic neurons. Angiotensin II-like immunoreactivity also occurs in the region of the catecholaminergic neurons in the rat suggesting that neuronally released angiotensin might act in this region (see Allen *et al.*, 1992).

Microinjections of angiotensin into the ventrolateral medulla of anesthetized animals induce decreases in blood pressure and vasopressin release in the CVLM and increases in blood pressure from the RVLM. Studies *in vitro* support this observation with angiotensin II increasing the activity of presumed C1 RVLM neurons via activation of an AT₁ receptor (Li & Guyenet, 1995).

Microinjections of the selective AT₁ receptor antagonists into the RVLM of anesthetized animals have little effect under basal conditions. Interestingly these agents elicit a pressor response from the RVLM of conscious animals – the mechanism responsible for this is not yet elucidated (Fontes, *et al.*, 2000). However, there are some situations in which endogenous angiotensin does elicit an excitatory action in the RVLM. These include the sympathetic excitation following airjet stress (Mayorov & Head, 2003) or activation of the hypothalamic paraventricular nucleus (Tagawa & Dampney, 1999), and in several models of hypertension including the spontaneously hypertensive rat (Allen, 2001), the transgenic (mREN2) rat (Fontes, *et al.*, 2000) and the Dahl salt sensitive rat (Ito, *et al.*, 2003). Interestingly microinjection of an AT₁ receptor antagonist into the RVLM of the L-NAME-induced hypertensive rat does not affect blood pressure indicating that not all forms of hypertension involve activation of AT₁ receptors in the RVLM (Bergamaschi *et al.*, 2002).

Thus, via activation of AT₁ receptors, angiotensin acts as an excitatory neuromodulator in the ventrolateral medulla to regulate cardiovascular function. The physiological role of this angiotensinergic input is still being elucidated but the input to the RVLM is activated in several forms of hypertension, contributing to the sympathetic activation observed in some forms of this disease.

Allen, A.M., Paxinos, G., Song, K. & Mendelsohn F.A.O. (1992) *Handbook of Chemical Neuroanatomy*, Vol 11, Elsevier Science B.V. Amsterdam, 1-35.

Allen, A.M. (2001) *Journal of the Renin, Angiotensin, Aldosterone System*, 2, S120-S124.

Bergamaschi, C.T., Biancardi, V.C., Lopes, O.U. & Campos, R.R. (2002) *Brain Research*, 927, 195-199.

Fontes, M.A., Baltatu, O., Caligiorni, S., Campagnole-Santos, M.J., Ganten, D., Bader, M. & Santos, R.A. (2000) *Physiological Genomics*, 33: 643-652.

Ito, S., Hiratsuka, M., Komatsu, K., Tsukamoto, K., Kanmatsuse, K. & Sved, A.F. (2003) *Hypertension*, 41, 744-750.

Li, Y-W. & Guyenet, P.G. (1995) *American Journal of Physiology*, 268, R272-R277.

Mayorov, D.N. & Head, G.A. (2003) *Hypertension*, 41, 1168-1173.

Tagawa, T. & Dampney, R.A.L. (1999) *Hypertension*, 34, 1301-1307.

Brain angiotensin and body fluid homeostasis

M.J. McKinley, T. Alexiou, P. Sinnayah and M. Mathai, Howard Florey Institute of Experimental Physiology and Medicine, University of Melbourne, Victoria 3010, Australia. (Introduced by R.A.L. Dampney) .SP

The angiotensin AT1 receptor is expressed in many regions of the mammalian brain. High concentrations of AT1 receptors are found in the subfornical organ, organum vasculosum of the lamina terminalis (OVLT) and area postrema, regions of the brain that lack a blood-brain barrier. The endogenous ligand for these AT1 receptors is angiotensin II derived from the blood. Circulating angiotensin II is prevented from having access to the AT1 receptors in other of the brain regions such as the hypothalamic paraventricular nucleus, median preoptic nucleus, lateral parabrachial nucleus, nucleus of the solitary tract or ventrolateral medulla by the blood-brain barrier. It seems likely that the endogenous ligand for these AT1 receptors may be angiotensin synthesised within the brain. We have utilised pharmacological agents to investigate possible roles of brain angiotensin in body fluid homeostasis and cardiovascular control in sheep. Intracerebroventricular (ICV) administration of the AT1 receptor antagonist losartan in conscious sheep has been shown to block water drinking, vasopressin secretion, reduced renin secretion, reduced renal sympathetic nerve activity, and the pressor response to centrally administered hypertonic saline as well as to ICV angiotensin II, suggesting that an angiotensinergic pathway within the brain may have a role in osmoregulation. However, when we tested the effect of the same dose of ICV losartan on the water drinking response to systemic infusion of hypertonic saline which gradually increased plasma osmolality over 30 min, there was no inhibition of the water drinking response, which challenges the idea that a central angiotensinergic pathway mediates physiological osmoregulatory drinking. Moreover, we have recently observed in mice (Agt^{-/-} mice) in which the angiotensinogen gene had been deleted by gene targeting techniques, that they are able to respond to osmotic challenges (water deprivation for 24 hours or intraperitoneal injection of hypertonic saline) with appropriate increases in water intake. In rats, we observed that ICV administration of an 18-mer antisense oligonucleotide directed against part of the angiotensinogen gene in order to reduce angiotensinogen synthesis in the brain caused a large reduction in the water drinking response to ICV renin (administered 24 h later), suggesting that brain angiotensinogen levels had fallen. However, such antisense treatment did not reduce water drinking in response to systemically administered hypertonic saline or to water deprivation, also suggesting that brain angiotensinergic mechanisms are not mediating osmoregulatory thirst. Thus, our data in several species does not favour a major role for brain angiotensinergic mechanisms in osmoregulation.

Superoxide mediates excitatory actions of angiotensin II in the rostral ventrolateral medulla during acute stress

D.N. Mayorov, G.A. Head and R. De Matteo, Baker Heart Research Institute, PO Box 6492, St. Kilda Rd. Central, Melbourne, Victoria 8008, Australia. .SP

Reactive oxygen species (ROS) are thought to be important intracellular mediators of angiotensin II (AII) actions in the brain (Zimmerman *et al.*, 2002). We recently found that AII in the rostral ventrolateral medulla (RVLM) mediates the blood pressure (BP) response to emotional stress in rabbits (Mayorov & Head, 2003). In the current study, we examined the role of the superoxide radical ($\bullet\text{O}_2^-$) and nitric oxide (NO) in this action of AII in the RVLM.

We first evaluated the role of superoxide in the stress-induced neuronal excitation in the RVLM. We tested the cardiovascular response to airjet stress before and after injections of cell permeable superoxide dismutase (SOD) mimetics tempol, tiron or 3-carbamoyl proxyl (3-CP) into this region in conscious rabbits. Eight minute airjet stress evoked a sustained increase in BP ($+12\pm 2$ mmHg). Bilateral microinjections of equimolar doses (20 nmol; $n=7-9$) of tempol, tiron or 3-CP into the RVLM did not alter resting BP. Tempol and tiron attenuated the pressor response to airjet by $57\pm 12\%$ and $52\pm 8\%$, respectively. By contrast, 3-CP which is structurally similar to tempol but has a lower superoxide scavenging activity, did not alter the stress response. The SOD mimetics did not affect the renal sympathetic nerve activity (RSNA) baroreflex or the pressor response to local microinjection of glutamate.

In another series of experiments, we determined whether NO is important in mediating the circulatory stress reactions in the RVLM. Microinjections of NO donors, sodium nitroprusside or S-nitroso-N-acetylpenicillamine (1-20 nmol), dose-dependently increased BP, indicating that NO predominantly plays an excitatory role in the RVLM of the conscious rabbit. Microinjection of N(G)-nitro-L-arginine methyl ester (L-NAME), a NO synthase inhibitor (10 nmol), did not affect the pressor stress response, measured 10-20 min after injection. However, this response was diminished by $55\pm 13\%$ one hour later. Notably, L-NAME decreased the gain of the RSNA baroreflex by $38\pm 12\%$, suggesting that NO is involved in modulating baroreflexes.

In further experiments, we tested whether the inhibitory action of tempol in the RVLM depends on local NO levels. Co-injections of L-NAME and tempol ($n=4$) did not affect resting BP, but attenuated the pressor stress response by $31\pm 8\%$, indicating that the SOD mimetic acted, at least in part, via a NO-independent mechanism. Finally, we determined whether ROS in the RVLM mediate the pressor action of exogenously applied AII. Unilateral microinjections of AII (100 pmol) increased BP by 12 ± 3 mmHg. Tiron and tempol attenuated by the pressor response to AII by 59-64%. By contrast, L-NAME tended to increase the pressor response to AII.

It is plausible that stress-induced activation of the AII – superoxide signalling pathway is not confined to the RVLM. We have found, in a pilot study, that microinjections of either AT_1 -receptor antagonist candesartan (500 pmol) or the SOD mimetics into the dorsomedial hypothalamus also attenuated the pressor response to airjet by 30-46%.

Overall, these results suggest that the stress-induced neuronal excitation in the RVLM involves activating a redox sensitive signaling pathway in rabbits. Local superoxide, but not NO is critically important in mediating the acute pressor effects of emotional stress in rabbits. Together with our previous findings (Mayorov & Head, 2003), these results also indicate that superoxide is a key intracellular signaling molecule in the acute excitatory action of AII on the RVLM vasomotor neurons.

Mayorov & Head (2003). *Hypertension*, 41, 1168-1173.

Zimmerman, M.C., Lazartigues, C., Lang, J.A., Sinnayah, P., Ahmad, I.M., Spitz, D.R. & Davisson R.L. (2002). *Circulation Research*, 91, 1038-1045.

Modulation of neurohumoral effector gain as a novel mechanism for the long term regulation of blood pressure

G.A. Head and S.L. Burke, Baker Heart Research Institute, Commercial Road, Melbourne, Victoria 3004, Australia. .SP

There is increasing evidence for the importance of the sympathetic nervous system in a number of disease states such as hypertension, congestive heart failure and renal failure. While it is recognised that the sympathetic nervous system consists of differentially regulated outflow to a variety of organs, perhaps the most relevant to the long term regulation of blood pressure (BP) and also to hypertension is renal sympathetic nerve activity (RSNA). By regulating renal hemodynamics, tubular function, and renal renin release, RSNA has the potential to contribute to the initiation, development and maintenance of hypertension. DiBona and colleagues suggest that renal sympathetic activity at low frequencies affects renin release, moderate frequencies inhibits sodium excretion and only at high stimulation frequencies reduces renal blood flow (RBF) (DiBona & Kopp, 1997). They suggest that in conscious animals resting RSNA is too low to affect RBF. We developed a combined nerve electrode and flowprobe for conscious rabbits and examined the relationship between RSNA and RBF. Initial studies showed that RSNA can influence RBF especially when activated by physiological stimuli (Janssen *et al.*, 1997). In further studies we examined the effect of acute sympathetic inhibition with rilmenidine, and acute angiotensin converting enzyme inhibition with captopril. Rilmenidine produced hypotension but no change in renal vascular conductance in normal rabbits, renal vasodilatation in barodenervated rabbits and some renal vasoconstriction in renal denervated rabbits. By contrast captopril produced similar renal vasodilatation whether the RSNA increased or was absent. These results suggest that while RSNA can influence short term fluctuations in RBF, the renin angiotensin system is the major influence on RBF and can override the influence of RSNA. From these studies we might expect there to be little role for RSNA in conditions where there is elevated plasma renin such as in renovascular hypertension. However, there is a large body of evidence to suggest an important role of the sympathetic nervous system and the central nervous system in this form of hypertension (Fink, 1997). We assessed the contribution of the sympathetic nervous system using acute and chronic sympathetic inhibition with rilmenidine in 2K1C hypertensive rabbits. After establishing a stable level of hypertension, rilmenidine or vehicle (saline) was infused by osmotic minipump. After a further 2 weeks, an electrode for recording renal sympathetic nerve activity (RSNA) and a RBF probe was implanted under halothane anaesthesia. Five weeks after renal artery clipping, mean arterial pressure (MAP) was 34% higher and renin was elevated 5 fold, but rabbits treated with rilmenidine were normotensive with less elevated renin. RSNA, heart rate and blood flow to the unclipped left kidney were similar in both groups of rabbits. The acute response to rilmenidine was greater in the hypertensive group with a lesser fall in RSNA such that the change in BP per change in RSNA was 5 fold greater than in normotensive rabbits. Also the relative renin release in response to increased RSNA was increased 3 fold in 2K1C rabbits. By contrast the pressor response to airjet stress was similar in hypertensive and chronic rilmenidine treated (normotensive) rabbits indicating that vasoconstrictor neuroeffector mechanisms were not altered by high renin states. These studies suggest that in the long term the RSNA may make an increasing contribution to the maintenance of BP in renovascular hypertension, possibly though an amplification of the neural release of renin. The long term modulation of the renin neuroeffector mechanism which in our case took at least 4 weeks may be an important way in which the sympathetic nervous system contributes to the long term setting of BP.

DiBona, G.F. & Kopp, U.C. (1997) *Physiological Reviews*, 77(1): 75-197.

Fink, G.D. (1997) *Clinical and Experimental Pharmacology and Physiology*, 24(1):91-95.

Janssen, B.J.A., Malpas, S.C., Burke, S.L. & Head G.A. (1997) *American Journal of Physiology*, 273(2 Pt 2):R597-R608.

Role of angiotensin II in regulating long term levels of sympathetic activity

S.C. Malpas, C.J. Barrett, S.J. Guild, R. Ramchandra and D. Budgett, Department of Physiology and Bioengineering Institute, University of Auckland, Auckland, New Zealand. .SP

Angiotensin II is recognised to play a critical role in the regulation of arterial pressure. In addition to its direct vasoconstrictive actions there is strong evidence to indicate that angiotensin II maintains arterial pressure through an excitatory action on the sympathetic nervous system. This action may be via a direct action on central nervous system pathways involved in generating and regulating sympathetic nerve activity (SNA) or via an action on a pathway such as the arterial baroreflex, that plays an important role in regulating short term SNA. One concern is that the data used to base such hypotheses are generally taken from short-term recordings of SNA (generally less than 3 hours). Thus the mechanisms that regulate SNA under such conditions may not necessarily reflect those seen under more chronic conditions and thus be reflective of the human condition.

To address the question of how angiotensin II regulates SNA chronically we developed technology which enables us to record SNA for up to 50 days via telemetry in rabbits. We made continuous recordings of renal SNA before, during and after one week of angiotensin II based hypertension in rabbits living in their home cages. Angiotensin II infusion ($50 \text{ ng.kg}^{-1}.\text{min}^{-1}$) caused a sustained increase in arterial pressure ($18 \pm 3 \text{ mmHg}$). There was a sustained decrease in SNA, from 18 ± 2 normalised units (n.u.) before angiotensin II to 8 ± 2 n.u. on day 2 and 9 ± 2 n.u. on day 7 of the angiotensin II infusion ($P < 0.01$) before recovering to 17 ± 2 n.u. after ceasing angiotensin II. Analysis of the baroreflex response showed that while angiotensin II induced hypertension led to resetting of the MAP-HR relationship, there was no evidence of resetting of the MAP-SNA relationship. We propose that the lack of resetting of the MAP-SNA curve, with the resting point lying near the lower plateau suggests the sustained decrease in SNA during angiotensin II is baroreflex mediated.

Subsequently, to address whether the action of angiotensin II was solely via a sustained non-resetting of arterial baroreflexes or via a central action, we followed the same protocol as above but in sino-aortically denervated animals. Under these conditions the increase in arterial pressure was the same as previously observed in intact animals however there was no evidence of a reduction in SNA. Indeed mean SNA was unchanged after 7 days for angiotensin II infusion. These results suggest that the action of peripheral angiotensin II on SNA appear to be determined primarily via an arterial pressure dependent action through non-resetting of arterial baroreflexes. While a central action of angiotensin II on SNA may exist, we suggest that the lack of alteration in SNA levels in baroreceptor denervated animals indicates that this effect may be relatively minor.

Overall these results suggest two surprising findings; firstly that angiotensin II is sympathoinhibitory and not sympathoexcitatory as previously indicated, and that baroreflex control of renal SNA and thus renal function is likely to play a significant role in the control of arterial pressure in the long-term (Barrett *et al.*, 2003; Lohmeier, 2003).

Barrett C.J, Ramchandra R., Guild S.J., Lala A., Budgett D.M. & Malpas S.C. (2003). *Circulation Research*, 92, 1330-1336.

Lohmeier, T.E. (2003). *Circulation Research*, 92, 1282-1284.

Regulation of the epithelial sodium channels

A. Dinudom, Department of Physiology, University of Sydney, NSW 2006, Australia. .SP

The epithelial Na⁺ channel (ENaC) plays an important role in the regulation of extracellular fluid volume and blood pressure and in the regulation of the volume of the fluid bathing the apical surfaces of epithelia such as the respiratory and reproductive epithelia (Voilley *et al.*, 2002). Given that ENaC represents a passive pathway for Na⁺ to diffuse from the external environment into the cells, it also represents a significant mechanism by which changes in the sodium composition of the external environment, such as in the lumen of the kidney distal collecting tubule or in the lumen of salivary ducts, influences the cytosolic composition and volume of epithelial cells.

ENaC is subject to a wide range of regulatory mechanisms. These regulatory systems include the mineralocorticoid hormone aldosterone, growth factors such as insulin and IGF-I and cytokines such as TNF- α as well as the feedback mechanisms that regulate the activity of the channels in response to changes in intracellular Na⁺ and intracellular Cl⁻ (Dinudom *et al.*, 2002). In addition to these systems, the activity of ENaC is also known to be modulated by the Cl⁻ channel, cystic fibrosis transmembrane conductance regulator (Stutts *et al.*, 2002). Some of the systems that modulate the activity of ENaC have intracellular pathways in common. A good example of this is the relationship between aldosterone regulation and the feedback regulation of ENaC. It has been suggested that the early effects of aldosterone, on the activity of ENaC are mediated by suppression of the Na⁺ feedback regulatory system. This is proposed to operate by aldosterone increasing the expression of the serum and glucocorticoid-dependent protein kinase, Sgk, which phosphorylates the ubiquitin protein-ligase Nedd4-2, a principal mediator of the Na⁺ feedback system, so as to render it unable to interact with ENaC (Snyder *et al.*, 2002). Although the effect of Sgk on ENaC activity has been demonstrated for ENaC expressed in *Xenopus* oocytes, this phenomenon has not been observed in either isolated mouse mandibular duct cells or M1 mouse collecting duct epithelia. Interestingly, we have found that the activity of cytosolic kinases other than Sgk is essential for the maintenance of the basal activity of ENaC and that when activated, these kinases inhibit the Na⁺ feedback regulatory system. It is conceivable that these protein kinases may also be involved in the mechanism by which aldosterone upregulates ENaC activity.

Dinudom, A., Komwatana, P., Young, J.A. & Cook, D.I. (1995) *Journal of Physiology*, 487, 549-555.

Snyder, P.M., Olson, D.R. & Thomas, B.C. (2002) *Journal of Biological Chemistry*, 277, 5-8.

Stutts, M.J., Canessa, C.M., Olsen, J.C., Hamrick, M., Cohn, J.A., Rossier, B.C. & Boucher, R.C. (1995) *Science*, 269, 847-850.

Voilley, N., Galibert, A., Bassilana, F., Renard, S., Lingueglia, E., Coscoy, S., Champigny, G., Hofman, P., Lazdunski, M. & Barbry, P. (1997) *Comparative Biochemistry and Physiology*, 11, 193-200.

Links between cell proliferation and K channel activity

M.L. Day, Department of Physiology, University of Sydney, NSW 2006, Australia. .SP

Changes in the activity of potassium channels are required for proliferation of a wide variety of cell types. Pharmacological inhibition of K⁺ channel activity can cause cell cycle arrest. Our studies on the regulation of ion channels during pre-implantation development of the mouse embryo have provided some insight into the mechanisms linking channel activity to the cell cycle. Using the patch-clamp technique, we have shown that the activity of a large-conductance K⁺ channel in the early mouse embryo is regulated by the cell cycle (Day *et al.*, 1993). This K⁺ channel is active during M and G1 phases and inactive during S and G2 phases. In parallel with the changes in K⁺ channel activity there are changes in cell membrane potential such that the membrane potential is hyperpolarised when the channel is active.

The activation of this K⁺ channel at the G2/M transition of early embryonic cell cycles does not depend on the activation of the mitotic kinase, Cdk1, and does not require the presence of the nucleus (Day *et al.*, 1998a). Thus it appears that a cytoplasmic cell cycle is functional in the early mouse embryo to regulate K⁺ channel activity. This cytoplasmic clock is, however, not completely uninfluenced by the nuclear cell cycle clock since inactivation of the channel as the cell cycle exits M phase is affected by Cyclin B/Cdk1 activity, and inhibition of DNA synthesis prevents the decrease in channel activity that normally occurs at the G1-S transition. Thus, the K⁺ channel in the early mouse embryo is controlled both by nuclear and cytoplasmic clocks.

Several roles for K⁺ channels in cell proliferation have been proposed. For example, a change in K⁺ channel activity can cause a change in cell membrane potential that can then alter the activity of other voltage-gated ion channels, such as Ca²⁺ channels. In the case of the K⁺ channel in the embryo, this role is possible since we have observed not only parallel variations in membrane potential but also cell cycle-dependent changes in the amplitude of a T-type Ca²⁺ current (Day *et al.*, 1998b). A second, possible role for the K⁺ channel in the embryo is in cell volume homeostasis. There is some evidence for this possibility since a cell swelling-induced Cl current is regulated by the cell cycle in mouse embryos being inactive during metaphase of mitosis in the 2-cell embryo at a time when the K⁺ channel is also active (Kolajova *et al.*, 2001).

Day, M.L., Pickering, S.J., Johnson, M.H. & Cook, D.I. (1993) *Nature*, **365**: 560-562.

Day, M.L., Johnson, M.H. & Cook D.I. (1998a) *EMBO Journal*, **17**: 1952-1960.

Day, M.L., Johnson, M.H. & Cook D.I. (1998b) *Pflügers Archiv European Journal of Physiology*, **436**: 834-842.

Kolajova, M., Hammer, M., Collins, J. & Baltz, J. (2001) *Development*, **128**: 3427-3434.

Regulation of the glutamine transporter SN1 (SNAT3)

S. Bröer, School of Biochemistry & Molecular Biology, Australian National University, Linnaeus way 41, Canberra, ACT 0200, Australia. (Introduced by David Cook) .SP

The glutamine transporter SN1 is mainly expressed in hepatocytes and in brain astrocytes. It is involved in both uptake and efflux of glutamine and its activity is tightly regulated. Transport of glutamine via SN1 is coupled to the cotransport of 1 Na⁺ and the antiport 1H⁺ (Chaudhry *et al.*, 1999). As a result glutamine transport is electroneutral and its preferred direction is governed by extracellular pH and intracellular Na⁺ concentration. In addition, SN1 is allosterically regulated, becoming inactive at acidic pH (Broer *et al.*, 2002).

In the brain SN1 mediates the release of glutamine from astrocytes, which is used as a precursor for neurotransmitter glutamate biosynthesis in neurons. Increased extracellular glutamate concentrations induced a rapid increase of SN1 activity in astrocytes. The upregulation was not caused by activation of ionotropic or metabotropic glutamate receptors but required uptake of glutamate into astrocytes. Experiments in *Xenopus* oocytes* suggest that glutamate may act as a direct regulator of SN1 activity.

Severalfold evidence suggests that protein trafficking is a major mechanism by which SN1 activity is regulated. In *Xenopus* oocytes SN1 activity rapidly decreased after treatment of oocytes with phorbol ester. Confocal microscopy of oocytes expressing a GFP-SN1 construct revealed that loss of activity was accompanied by a retrieval of the transporter from the plasma membrane. Retrieval of SN1 was specific but did not involve phosphorylation of the transporter. A similar downregulation by incubation with phorbol ester was observed in cultured HepG2 cells but not in primary cultures of brain astrocytes.

A possible mechanism for the retrieval of transporter may involve ubiquitination followed by degradation of the transport protein. Coexpression of SN1 with the ubiquitin ligase Nedd4-2 reduced the transport activity of SN1, a downregulation that was abrogated by coexpression of protein kinase sgk1 or protein kinase B (PKB) (Boehmer *et al.*, 2003). Coexpression of sgk1 or PKB together with SN1 resulted in an increase of the transport activity.

Taken together these data provide evidence for a regulation of SN1 by plasma membrane trafficking. The actual components of the signal transduction pathways, however, are likely to differ between cell types.

Boehmer, C., Okur, F., Setiawan, I., Broer, S. & Lang, F. (2003) *Biochemical Biophysical Research Communication*, 306, 156-162.

Broer, A., Albers, A., Setiawan, I., Edwards, R. H., Chaudhry, F. A., Lang, F., Wagner, C. A. & Broer, S. (2002) *Journal of Physiology*, 539, 3-14.

Chaudhry, F. A., Reimer, R. J., Krizaj, D., Barber, D., Storm-Mathisen, J., Copenhagen, D. R. & Edwards, R. H. (1999) *Cell*, 99, 769-780.

*Animal experimentation protocols were approved by the Australian National University.

The familial intrahepatic cholestasis type 1 protein: a P-type ATPase influencing bile acid transporters

M.J. Harris^{1,2} and I.M. Arias², ¹ANZAC Research Institute, University of Sydney, Concord RG Hospital, Concord, NSW 2139 and ²Tufts University School of Medicine, Boston MA, USA.

(Introduced by David Cook) .SP

Progressive familial intrahepatic cholestasis type 1 (PFIC1) and benign recurrent intrahepatic cholestasis (BRIC) result from mutations in the familial intrahepatic cholestasis gene (FIC1). FIC1 is a member of the type IV P-type ATPase subfamily, which function as aminophospholipid translocases. Since the phenotype of these diseases manifests as impaired bile flow and considering that FIC1 is localised to the canalicular membrane in hepatocytes, we investigated whether FIC1 could transport bile acids and/or influence the apical bile acid transporters, either the bile salt export pump (BSEP) or the intestinal apical sodium dependent bile acid transporter (ASBT).

Method: Apical efflux assay: MDCK II cells which stably express Na⁺/taurocholate co-transporting polypeptide (NTCP) formed polarised monolayers when grown on Transwell filters and were transfected with FIC1 and/or BSEP. Two days after transfection, the basal medium was replaced with uptake buffer containing ³H-taurocholate (TC) and the cells were incubated at 37°C for 1 hour. TC efflux was determined by measurement of radioactivity in the apical medium. Apical uptake assays: MDCK II cells were transfected with FIC1, FIC1 mutants and/or ASBT. Two days after transfection, the apical media was replaced with uptake buffer containing ³H-TC and incubated at 37°C for 1 hour. Uptake of ³H-TC by ASBT was determined by measurement of intracellular radioactivity. In all studies, transfection with β-gal was used as a control and western blotting of membrane preparations confirmed expression of each relevant protein.

Results: Apical efflux: ³H-TC apical efflux in BSEP transfected cells was 2 fold higher than in non-transfected MDCKII-NTCP cells (p<0.05) and was unaffected by co-transfection of FIC1. In addition, FIC1 expression had no effect on ³H-TC efflux in cells which were not transfected with BSEP. Apical uptake: ³H-TC uptake in ASBT expressing cells was 10 fold higher than in β-gal or FIC1 transfected cells, and was unaffected by transfection of cells with both ASBT and FIC1, or ASBT and FIC1 mutants.

Summary: FIC1 did not transport taurocholate across the apical membrane of MDCK II cells. Expression of FIC1 or FIC1 mutants did not affect BSEP or ASBT function. These results suggest that FIC1 affects hepatic bile secretion and/or intestinal bile acid absorption by indirect mechanisms that are currently unknown. An alternative hypothesis is that FIC1 effects the trafficking of bile acid transporters to the apical membrane via its aminophospholipid translocase activity. This “flippase” function is required for the budding of vesicles from organelles such as the golgi, endosomes and the plasma membrane. These mechanisms are being investigated by siRNA knockout experiments.

Variations in myosin expression along the length of orbital fibres in the rabbit extraocular muscle

C.A. Lucas and J.F.Y. Hoh, Department of Physiology and Institute for Biomedical Research, School of Medical Sciences, Faculty of Medicine, The University of Sydney, NSW 2006, Australia. .SP

Extraocular muscles (EOM) have two layers of muscle fibres with different functions: orbital fibres that control the position of the recently discovered soft tissue pulleys (Demer *et al.*, 2000), and global fibres that rotate the globe. Pulleys make the axes of action of EOMs depend on eye orientation, and this is thought to provide a simple mechanism for implementing Listing's law governing eye rotations. Both layers have SIFs (singly innervated fibres) and MIFs (multiply innervated fibres), with ultrastructural features resembling amphibian fast twitch and slow-tonic fibres, respectively. EOM fibres express 9 myosin heavy chain (MyHC) isoforms, comprising those in developing and adult limb and cardiac muscles, and 2 EOM-specific isoforms, EO-MyHC and slow-tonic MyHC. Orbital fibres display a systematic variation of MyHCs along their length, correlated with ultrastructural features, but earlier studies were unable to specify the precise MyHC isoforms involved. We use here a battery of monoclonal antibodies capable of unambiguously identifying each of the 9 MyHCs to study MyHC changes in serial sections of rabbit superior rectus muscle by immunohistochemistry.

According to ultrastructural criteria (Davidowitz *et al.*, 1977), there are three major orbital fibre types: the oSIF, the coMIFs (orbital MIF of constant diameter); and the voMIFs, which vary in diameter from 5µm along the middle portion of their length to around 15 µm in their ends. The oSIFs and coMIFs are short, whilst the voMIFs are the longest. Orbital MIFs have an 'en plaque' neuromuscular junction in addition to distributed 'en grappe' endplates in global MIFs.

We show that variations in MyHC expression in orbital fibres closely parallel structural variation along the length. These changes occur at three sites: (1) At the EPZ, the oSIFs express EO-MyHC, the fastest MyHC, associated with high sarcoplasmic reticulum (SR) and mitochondrial volume. On either side of the EPZ, these fibres express the slower 2A and/or embryonic MyHCs, with decreased SR and mitochondrial volume. (2) The coMIFs and voMIFs at the EPZ express α -cardiac MyHC, the fastest of the slow MyHCs, where the ultrastructure is fast twitch. They continue to show twitch ultrastructure on either side of the EPZ, where they coexpress α -cardiac and embryonic MyHC. (3) In the distal quarter of the orbital layer, the oSIFs and coMIFs end, presumably by inserting onto the pulley, the orbital layer is entirely made up of voMIFs. Here the fibres mainly co-express slow-tonic and embryonic MyHC and show ultrastructural features of amphibian slow-tonic fibres. In the far proximal end of the muscle, oMIF mainly express embryonic MyHC with a small proportion of fibres co-expressing slow-tonic MyHC.

We propose that only the oSIFs and coMIFs insert into the pulleys and actively translocate them during saccades. Forward translocation of pulleys is achieved by passive stretching due to contraction of the antagonist, the presence of the very fast EPZ region permitting sudden collapse of tension necessary for rapid repositioning of the pulleys. The voMIFs insert onto the globe. The slow-tonic MyHC may provide ripple-free tension to hold the eyeball steady during a gaze, and the faster narrow segment may be a specialisation to allow for rapid relaxation and fibre lengthening during a change of gaze involving contraction of an antagonist.

Davidowitz, J., Philips, G. & Breinin, G. M. (1977) *Investigative Ophthalmology Visual Science*, 16, 711-729.

Demer, J.L., Oh, S.Y. & Poukens, V. (2000) *Investigative Ophthalmology Visual Science*, 41, 1280-1290.

Fibre types in rat laryngeal muscles and their transformations following denervation and reinnervation

H.S. Rhee, C.A. Lucas and J.F.Y. Hoh, Department of Physiology and Institute for Biomedical Research, School of Medical Sciences, Faculty of Medicine, The University of Sydney, NSW 2006, Australia. .SP

Intrinsic laryngeal muscles cricothyroid (CT) and thyroarythenoid (TA) differ in myosin expression. CT expresses limb myosin heavy chains (MyHCs) while TA expresses a MyHC found in extraocular (EO) muscles (Lucas *et al.*, 1995), in addition to limb isoforms. A definitive classification system for laryngeal muscle fibre types does not exist at present. Earlier studies on the effects of denervation (Shiotani & Flint, 1998) and reinnervation (Shiotani *et al.*, 2001) on the MyHC profiles of whole laryngeal muscles are suggestive of neural influence on MyHC expression, but fibre type transformation at the cellular level has not been shown.

Immunohistochemical analyses with highly specific monoclonal antibodies (mAbs) against various MyHCs were used to study muscle fibre types in rat CT and TA, and to investigate whether nerves to laryngeal muscles control MyHC expression. CT was found to have the full complement of limb fibre types. TA had three major fibre types based on MyHC composition: 2b/eo, coexpressing 2B and EO MyHCs, 2x/2b, coexpressing 2X and 2B MyHCs, and 2x, expressing 2X MyHC. Type 2a and slow fibres were absent. TA consisted of two divisions: the external division (TA-X), which is homogeneously 2b/eo, and the vocalis division (TA-V), composed principally of 2x and 2b/eo fibres, with a minority of 2x/2b fibres. The use of these mAbs has established the feasibility of classifying laryngeal muscle fibre types by their MyHC composition in spite of the extensive occurrence of hybrid fibres containing multiple isoforms.

The recurrent laryngeal nerve (RLN) which innervates both divisions of the TA as well as other laryngeal muscles except the CT were cut and allowed to reinnervate these muscles in 16 rats. The left RLN transection was performed on sixteen 10-week old Sprague Dawley rats. The animals were anaesthetised by intraperitoneal injection of ketamine hydrochloride (35mg/kg) and xylazine hydrochloride (5mg/kg). The TA from 4 animals were examined immunohistochemically at 2, 4, 6 and 12 weeks postoperatively. Commencing four weeks after cutting and re-uniting the RLN, numerous 2b/eo fibres in TA-X began to express 2X MyHC, while EO and 2B MyHC expression in these fibres progressively declined. By 12 weeks, 16.5 ± 2.5 (SE)% of fibres in the TA-X were of type 2x. These findings suggest that nerve fibres originally innervating 2x fibres in TA-V and other muscles had randomly cross-innervated 2b/eo fibres in the TA-X and converted them into 2x fibres. We conclude that MyHCs in laryngeal muscle fibres are subject to neural regulation, in common with limb and jaw muscles.

Lucas, C.A., Rughani, A. & Hoh, J.F.Y. (1995) *Journal of Muscle Research and Cell Motility*, 16:368-378.

Shiotani A. & Flint P.W. (1998) *The Laryngoscope*, 108:1225-1229.

Shiotani A., Nakagawa H. & Flint P.W. (2001) *The Laryngoscope*, 111:472-477.

There is no difference in the net efficiency of fast- and slow-twitch mouse muscles

C.J. Barclay and C.L. Weber, School of Physiotherapy & Exercise Science, Griffith University Gold Coast, PMB 50 Gold Coast Mail Centre, Gold Coast, Queensland 9726, Australia. .SP

It is commonly accepted that slow-twitch muscles are more efficient than fast-twitch muscles; that is, slow twitch muscles convert a greater fraction of the energy they use into mechanical work. Evidence supporting this idea comes from two types of experiment. First, humans with a greater fraction of slow-twitch fibres are more efficient when cycling on an ergometer (Coyle *et al.*, 1992) and, second, isolated preparations of slow-twitch muscle use less high energy phosphate per unit work performed than fast-twitch preparations (Barclay, 1996). The human experiments have the drawback that it is difficult to make inferences about muscle efficiency from measurements of whole body O₂ consumption. The isolated muscle experiments are difficult to relate to *in vivo* efficiency because: (1) efficiency was measured only during shortening, rather than over complete cycles of shortening and lengthening; and (2) because the indices of energy cost used did not encompass oxidative recovery processes. In the only study comparing efficiency of fast and slow muscles that used cyclic contractions and in which O₂ consumption was used as the index of energy use, slow-twitch rat muscles were found to be less efficient than fast-twitch muscles (Heglund & Cavagna, 1987). However, that study used a temperature of 20°C rather than physiological temperature.

The aim of this study was to measure efficiency of isolated fast- and slow-twitch muscles using a pattern of activity similar to that occurring *in vivo*, using the energetic equivalent of O₂ consumption as the index of energy cost and performing the experiments at a temperature of 35°C.

Experiments were performed *in vitro* using bundles of muscle fibres from the slow-twitch soleus and fast-twitch EDL muscles of mice. Muscles were dissected from mice that had been killed by inhalation of CO₂. Efficiency was calculated from measurements of work output and total heat production during and after a series of 20 contractions. The contraction protocol consisted of a realistic, cyclic pattern of muscle length changes with a brief contraction in each length cycle. Twenty contractions were performed at a frequency of 3.4 Hz. Net mechanical efficiency was defined as the ratio of work output to the total, suprabasal enthalpy output and enthalpy output was the sum of the heat and work output.

There was no difference in the maximal net efficiency of fast- and slow-twitch mouse muscles. Maximum efficiency of soleus muscles was 13.9 ± 0.8 % (n = 6) and of EDL muscles was 13.5 ± 0.5 % (n = 6).

This result suggests that any relationship between human efficiency and fraction of slow-twitch fibres is not a reflection of an intrinsic difference in efficiency of fast and slow muscle fibres.

Coyle, E.F., Sidossis, L.S., Horowitz J.F. & J.D. Beltz, J.D. (1992) *Medicine and Science in Sports and Exercise*, 24, 782-788.

Barclay, C.J. (1996) *Journal of Physiology*, 497, 781-794.

Heglund, N.C. & Cavagna, G.A. (1987) *American Journal of Physiology*, 223, C22-C29.

Treatment with the β_2 -agonists formoterol or salmeterol produce greater muscle hypertrophy in rats than fenoterol

J.G. Ryall, D.R. Plant and G.S. Lynch, Muscle Mechanics Laboratory, Department of Physiology, The University of Melbourne, Victoria 3010, Australia. .SP

Although traditionally administered at low doses for treating asthma, at higher doses, β_2 -adrenoceptor agonists (β_2 -agonists) have potent muscle anabolic effects. As such, β_2 -agonists may have therapeutic potential for pathologies where muscle wasting is indicated, such as cancer cachexia, muscular dystrophy and age-related muscle wasting (sarcopenia). Before these drugs can be considered as legitimate therapies, some safety concerns, especially their effects on the heart, need to be considered. The β_2 -agonists, formoterol and salmeterol were originally developed to increase the duration of bronchodilation. Previous studies have shown formoterol and salmeterol to have a duration of action of four and eight times greater, respectively, than the most widely used asthma drugs (Anderson, 1993). We have previously shown that the (short-acting) β_2 -agonist fenoterol has greater anabolic effects on skeletal muscle than the most widely described, in relation to skeletal muscle, β_2 -agonist, clenbuterol (Ryall *et al.*, 2002). In the present study, we tested the hypothesis that due to their long duration of action, chronic administration of salmeterol and formoterol would produce greater skeletal muscle hypertrophy than fenoterol. One of our research goals is to optimise the safe and effective use of β_2 -agonists to ameliorate muscle wasting in a number of pathologies.

Fenoterol, formoterol and salmeterol (kindly supplied by Astra-Zeneca) were administered to male Fischer 344 rats (12 weeks/age, body mass, 265g) at one of five different doses (0.025 - 2 mg/kg/day) for four weeks. Fenoterol and formoterol were administered by daily i.p. injection in saline, and compared to a control group receiving an equivolume of saline. Due to its highly lipophilic nature, salmeterol was administered via a daily i.p. injection in a lipid vehicle, and compared to a control group receiving an equivolume of lipid vehicle. The rats were deeply anaesthetised (sodium brieal, 60 mg/kg), and the heart, and the EDL and soleus hindlimb muscles were surgically excised, weighed, and then stored for histological analyses.

The rank order of efficacy (E_{\max}), based on skeletal muscle hypertrophy (β_2 -agonist induced increase in mass above control), was salmeterol = formoterol \gg fenoterol. Salmeterol had an E_{\max} at a dose of 1 mg/kg/day, increasing EDL, soleus and heart mass, 39, 28 and 25% above values for lipid vehicle control. Formoterol had an E_{\max} at a dose of 0.5 mg/kg/day, increasing EDL, soleus and heart mass, 36, 26 and 26% above values for saline control. Fenoterol had an E_{\max} at a dose of 2 mg/kg/day, increasing EDL, soleus and heart mass, 25, 14 and 23% above values for saline control. At the lowest dose examined (0.025 mg/kg/day) formoterol exhibited the greatest hypertrophy of both skeletal and cardiac muscle compared to values for saline control, (19, 13 and 12% greater for EDL, soleus and heart, respectively).

Our findings indicate that the β_2 -agonists, formoterol and salmeterol, have anabolic effects on muscle and produce greater muscle hypertrophy than fenoterol. Further research is needed to examine the effect of these drugs on skeletal and cardiac muscle function before their full therapeutic potential can be realised.

Anderson, G.P. (1993) *Life Sciences*, 52, 2145-2160.

Ryall, J.G., Gregorevic, P., Plant, D.R., Sillence, M.N. & Lynch, G.S. (2002) *American Journal of Physiology - Regulatory Integrative & Comparative Physiology*, 283, R1386-1394.

Supported by the Muscular Dystrophy Association (USA), the Rebecca L. Cooper Medical Research Foundation, and The University of Melbourne.

JGR is supported by a Postgraduate Scholarship from the National Heart Foundation of Australia

Ca²⁺ handling properties of mechanically skinned fibres from fast and slow muscles of adult and old rats following chronic fenoterol treatment

D.R. Plant, J.G. Ryall, P. Gregorevic and G.S. Lynch, Muscle Mechanics Laboratory, Department of Physiology, The University of Melbourne, Victoria 3010, Australia. .SP

Aging is associated with a progressive loss of motor function, a slowing of muscle movements, and a decline in muscle strength. These age-related changes in skeletal muscle contribute to the increased incidence of fall-related injuries in the elderly, resulting in a loss of functional independence. β_2 -agonists (such as fenoterol) have potent muscle anabolic effects and we have recently demonstrated that four weeks treatment with fenoterol is sufficient to ameliorate the age-related muscle weakness and slowing of contraction in rats (Ryall *et al.*, 2002). In another study we demonstrated that aging deleteriously affects aspects of excitation-contraction coupling and sarcoplasmic reticulum (SR) function in mechanically skinned fast muscle fibres from aged compared with adult mice (Plant & Lynch 2002). It is not known whether fenoterol treatment would affect these properties in mechanically skinned fast and slow muscle fibres from aged rats.

We tested the hypothesis that four weeks fenoterol treatment would alter SR Ca²⁺ handling properties of mechanically skinned skeletal muscle fibres differently in adult and old F344 rats. Adult (16 months/age) and old (28 months/age) rats were treated daily with either fenoterol (1.4 mg.kg⁻¹day⁻¹, i.p.) or saline vehicle, for four weeks. Following treatment, rats were anaesthetised with sodium pentobarbitone (60 mg.kg⁻¹, i.p.) and the fast-twitch extensor digitorum longus (EDL) and predominantly slow-twitch soleus muscles excised carefully to prepare mechanically skinned fibres. Fibres were tested according to the methods we have described in detail previously (Plant & Lynch, 2002).

Preliminary findings indicate no age-related changes in normalised SR Ca²⁺ reloading or leak of Ca²⁺ from the SR. Fenoterol increased leak of Ca²⁺ from the SR in EDL but not soleus muscle fibres from adult and old rats. Rate of Ca²⁺ reloading was decreased with fenoterol treatment in EDL muscle fibres from both adult and old rats, but soleus muscle fibres from adult and old rats were not affected. These findings suggest that fenoterol's effects are similar in mechanically skinned fibres from adult and old rats. The effects of fenoterol on depolarisation-induced force responses in mechanically skinned fibres has yet to be examined.

Plant, D.R. & Lynch, G.S. (2002) *Journal of Physiology*, 543, 169-176.

Ryall, J.G., Plant, D.R., Gregorevic, P., Sillence, M.N. & Lynch, G.S. (2002) *Proceedings of the Australian Health and Medical Research Congress*, A1120.

Supported by grants from the Muscular Dystrophy Association (USA)

Involvement of a voltage-dependent calcium channel in signal transduction in the 2-cell embryo

Y. Li¹, M.L. Day² and C. O'Neill¹, ¹Human Reproduction Unit, Royal North Shore Hospital, Department of Physiology, University of Sydney, NSW 2006 and ²Department of Physiology, University of Sydney, NSW 2006, Australia. .SP

Platelet-activating factor (PAF) is an autocrine trophic factor for the preimplantation embryo that induces a transient increase in $[Ca^{2+}]_i$ in the 2-cell embryo. The $[Ca^{2+}]_i$ transient had an absolute requirement for influx of external calcium and was inhibited by blockers of L-type calcium channel blockers but not by a variety of non-L-type channel blockers. This study used whole cell patch clamp methodology to assess whether the early mouse embryo expressed a functional calcium channel with the properties of an L-type channel.

Pre-implantation mouse embryos were recovered after superovulation of female QS mice by intraperitoneal injections of equine chorionic gonadotrophin (10 i.u.) followed 48 hours later by human chorionic gonadotrophin (10 i.u.) and mating. Mice were killed by cervical dislocation and 2-cell embryos were flushed from the reproductive tract into Hepes-modified HTF medium containing 3 mg/ml BSA. The zona pellucida was removed by brief treatment with 0.5% pronase. Standard whole-cell patch-clamp techniques were used to study Ca^{2+} currents in two-cell embryos. The membrane potential was held at -60mV and depolarising voltage pulses of 1s duration were applied between -20 and +80 mV at intervals of 5 s. Currents were low-pass filtered, sampled and digitised at 0.2 kHz. Ba^{2+} was used as the charge carrier. The currents at each voltage-step were recorded before and after treatment of embryos with different kinds of L-type Ca^{2+} channel blockers: diltiazem (75 μ M), nifedipine (80 μ M) and verapamil (80 μ M). Inward currents were measured as the difference between the whole cell currents before and after the addition of a drug or control to the bath solution, consisting of NaCl 55mM, KCl 4.69mM, $MgCl_2$ 0.2mM, Na_2EDTA 0.11mM, glucose 5mM, $CaCl_2$ 2.04mM (1.94 mM free Ca^{2+}), Hepes 20.4mM, $BaCl_2$ 50mM (49.99 mM free Ba^{2+}), adjusted to pH 7.4, 300 mosM/kg.

Using diltiazem, a current of 0.23 ± 0.03 nA (mean \pm SEM) was detected and was maximal at a voltage of 36.94 ± 2.59 mV. A similar current was evident when either nifedipine or verapamil were used. Prior treatment of embryos with exogenous PAF resulted in a significant ($P < 0.05$) reduction in the proportion of embryos expressing the current and the size of the current compared with those pre-treated with rPAF acetylhydrolase. The results show that 2-cell embryos possess a depolarisation-activated membrane channel, with the properties of an L-type calcium channel. The desensitisation of channel activity by prior PAF challenge suggests that the current was activated during PAF-induced calcium signalling.

Negative feedback inhibition of Ca²⁺ influx during P_{2Y2} receptor activation

H. Hu¹, M.M. Cummins¹, Y. Hosoda¹, P. Poronnik², M.L. Day¹ and D.I. Cook¹, ¹Department of Physiology, University of Sydney, NSW 2006 and ²School of Biomedical Sciences, University of Queensland, QLD 4072, Australia. .SP

G protein-coupled receptors transduce extracellular stimuli via G proteins to intracellular effectors resulting in the activation of second messenger signalling cascades mediated by Ca²⁺ or cAMP. In HT29 human colonic epithelial carcinoma cells, the activation of the M₃ muscarinic receptor by carbachol (CCh) results in a Ca²⁺ response with a characteristic prolonged plateau phase that occurs due to Ca²⁺ influx following activation of store-release sensitive channels in the plasma membrane. In contrast, the Ca²⁺ response following the activation of the P_{2Y2} purinergic receptor shows no plateau phase (Cummins *et al.*, 2000). Both of these responses are pertussis toxin insensitive and mediated by G proteins of the G_q family. These data suggest that during P_{2Y2} activation, the lack of a plateau phase may result from the inhibition of Ca²⁺ influx. The small G proteins Rac and Cdc42 are known to be involved in Ca²⁺ signalling pathways (Peppelenbosch *et al.*, 1996; Djouder *et al.*, 2000) and protein kinase C (PKC), a known target of Cdc42 (Slater *et al.*, 2001), has also been reported to regulate the Ca²⁺ signalling pathway (Petersen & Berridge, 1994; Lee *et al.*, 1997). The aim of this present study was to investigate the roles of Rac, Cdc42 and PKC in the inhibition of Ca²⁺ influx during P_{2Y2} receptor activation.

Standard Fura-2 imaging techniques were used to monitor changes in intracellular Ca²⁺ concentration in HT29 cells. Ca²⁺ influx was monitored using the rate of quenching of the Fura-2 signal by exogenous Mn²⁺. Replication-deficient adenoviruses expressing the cDNA encoding either wild type (wt), dominant negative (dn) or constitutively active (ca) mutants of Rac, Cdc42 and PKC α were created using standard techniques (Cummins *et al.*, 2000).

In HT29 cells exposed to UTP, the rate of Mn²⁺ influx as measured by Fura-2 quenching was 66% of the influx rate in response to CCh, indicating that the lack of a plateau phase during UTP exposure was due to reduced influx. When HT29 cells were infected with adenoviruses expressing dnRac or dnCdc42, the rates of Mn²⁺ influx increased to those observed with CCh stimulation. Furthermore, when the cells were infected with caRac, Mn²⁺ influx induced by CCh was reduced to below control levels. These indicate the involvement of both Rac and Cdc42 in the negative feedback inhibition of UTP mediated Ca²⁺ influx. Co-infection of dnCdc42 and caRac returned Mn²⁺ influx to the levels observed in control cells with UTP stimulation, indicating that Rac is upstream of Cdc42.

In HT29 cells infected with an adenovirus expressing wtPKC α , there was no change in the rates of Mn²⁺ influx in the presence of UTP. In contrast, when the cells were infected with a dnPKC α adenovirus, the rate of Mn²⁺ influx was increased to the levels observed with CCh, indicating a role for PKC α in the control of Ca²⁺ influx in these cells. To determine whether PKC α was acting via the same signalling pathway as Rac/Cdc42, HT29 cells were treated with Toxin B, an inhibitor of Rac/Cdc42, and dioleoylglycerol, an activator of PKC. This resulted in an inhibition of Mn²⁺ influx to levels similar to that observed with UTP, indicating that the effect of blocking Rac/Cdc42 could be overcome by activating PKC, demonstrating that PKC α is downstream of Rac/Cdc42. This study shows that the main difference in the muscarinic and purinergic Ca²⁺ responses in HT29 cells, is due to a Ca²⁺ influx negative feedback pathway that is activated by P_{2Y2} receptors.

Cummins, M.M., O'Mullane, L.M., Barden, J.A., Cook, D.I. & Poronnik, P. (2000) *Cell Calcium*, 27, 247-255.

Djouder, N., Prepens, U., Aktories, K. & Cavalie, A. (2000) *Journal of Biological Chemistry*, 275, 18732-18738.

Lee, H., Suh, B.C., & Kim, K.T. (1997) *Journal of Biological Chemistry*, 272, 21831-21838.

Petersen, C.C. & Berridge, M.J. (1994) *Journal of Biological Chemistry*, 269, 32246-32253.

Peppelenbosch, M.P., Tertoolen, L.G.J., Devriessmits, A.M.M., Qiu, R.G., Mrabet, L., Symons, M.H.,

Delaat, S.W. & Bos, J.L. (1996) *Journal of Biological Chemistry*, 271, 7883-7886.
Slater, S.J., Seiz, J.L., Stagliano, B.A. & Stubbs, C.D. (2001) *Biochemistry Journal*, 40, 4437-4445.

Calcium release-activated calcium current in rat hepatocytes

G.Y. Rychkov¹, T. Litjens¹, M.L. Roberts¹ and G.J. Barritt², ¹School of Molecular and Biomedical Sciences, University of Adelaide, SA 5005 and ²Flinders Medical Centre, Flinders University of South Australia, SA 5001 Australia.

Store-operated Ca²⁺ (SOC) channels play a central role in regulating intracellular Ca²⁺ concentration in hepatocytes and other nonexcitable animal cells (Gregory & Barritt, 2003). A major function of SOC channels appears to be to replenish intracellular Ca²⁺ stores when intracellular Ca²⁺ is lost from the cell during agonist-induced increases in the cytoplasmic Ca²⁺ concentration. One of the best-known store operated channels, Ca²⁺-release-activated Ca²⁺ (CRAC) channel has been extensively characterised in a number of immortalised cell lines. There is little evidence, however, that I_{CRAC} is activated in the physiological conditions in cells in primary culture. It has been speculated that the highly Ca²⁺-specific CRAC channels are only expressed in blood cells and in transformed cells.

The aim of the present experiments was to elucidate the properties of the SOC channels in rat hepatocytes. Hepatocytes were isolated by collagenase digestion and plated on glass coverslips. Patch-clamp recording was conducted in the whole-cell mode using standard procedures after 24-48 hours.

Depletion of intracellular Ca²⁺ stores in rat hepatocytes activated a Ca²⁺-selective inward current. Properties of this current, including high selectivity for Ca²⁺, strong inward rectification, fast Ca²⁺ dependent inactivation at negative potentials and block by La³⁺ and 2-APB, were similar or identical to those of I_{CRAC} found in mast cells, RBL cells, Jurkat T lymphocytes (Zweifach & Lewis, 1993; Hoth & Penner, 1992; Bakowski & Parekh, 2002) and H4-IIIE liver cells (Rychkov *et al.* 2001). The amplitude of I_{CRAC} in rat hepatocytes varied between -30 and -120 pA at -100 mV with an average density of about -1 pA/pF. Extracellular application of vasopressin or ATP activated a current with the same properties and the same size as that observed by InsP₃ induced depletion of the stores. I_{CRAC} developed more slowly with vasopressin than with ATP as agonist. Increasing the concentration of ATP shortened the delay in the development of I_{CRAC}, but did not change the amplitude of the current or the rate of its development. Concentrations of ATP (5-10 μM) that cause waves of increased cytoplasmic Ca²⁺ concentration also activated I_{CRAC}. So far, no other type of current activated by Ca²⁺ store depletion has been detected in these cells. It is concluded that CRAC channels are the major, and possibly the only, type of SOC channel in rat hepatocytes.

Bakowski, D. & Parekh, A.B. (2002) *Cell Calcium* **32**, 379-391.

Gregory, R.B. & Barritt, G.J. (2003) *Biochemical Journal* **369**, 1-7.

Hoth, M. & Penner, R. (1992) *Nature* **355**, 353-356.

Rychkov, G., Brereton, H.M., Harland, M.L. & Barritt, G.J. (2001) *Hepatology* **33**, 938-947.

Zweifach, A. & Lewis, R.S. (1993) *Proceedings of the National Academy of Sciences of the United States of America* **90**, 6295-6299.

Characterisation of chloride currents in the mouse pre-implantation embryo

I. Pons-Meneghetti¹, M.L. Day¹, D.I. Cook¹ and M.H. Johnson², ¹Laboratory of Developmental Physiology, Department of Physiology, Anderson Stuart Building (F13), University of Sydney, NSW 2006, Australia and ²Department of Anatomy, Dowlin St, Cambridge CB2 3DY, UK. .SP

Pre-implantation embryonic development describes the process by which the embryo grows from the zygote (one-cell) to the blastocyst (64-254 cells) after which it implants into the placenta. Blastocysts are composed of two different cell types, the inner cell mass (ICM) and trophoblast cells (TE). Chloride currents throughout these stages of embryonic development are not well characterised. A swelling activated Cl⁻ current was shown to be cell cycle dependent as well as developmentally regulated however this current was not examined in isotonic solutions (Kolajova *et al.*, 2001). In the blastocyst it is believed that Cl⁻ is transported by both paracellular (Manejwala *et al.*, 1998) and transcellular mechanisms (Brison & Leese, 1993) and that the expansion of the blastocoel cavity is largely reliant on Cl⁻ channels and a Cl⁻/HCO₃⁻ exchanger (Zhao *et al.*, 1997). The cystic fibrosis transmembrane conductance regulator (CFTR) was recently shown to be present in human blastocysts and it may play a role in the process described above (Ben-Chetrit *et al.*, 2002). This study aimed to characterise Cl⁻ currents observed in isotonic conditions in the pre-implantation embryo by looking at the eight distinct members of the voltage gated chloride channel family (CIC) (1-7 and K) as well as CFTR.

The mRNA expression pattern of CFTR and CIC channels in the early mouse embryo was determined by RT-PCR. The channels observed in the pre-implantation embryo were CIC-2 to CIC-7, CIC-K and CFTR. Furthermore, ICM and TE cells were separated and RT-PCR of CFTR was carried out for each cell type. The results showed that CFTR mRNA is only present in TE cells. These data suggest that Cl⁻ channels may play an important roles in the pre-implantation embryo.

The whole-cell patch-clamp technique was used in order to characterise Cl⁻ currents in the mouse pre-implantation embryo. In the late four-cell stage two major currents were identified through the use of various Cl⁻ channel antagonists. These included a DIDS-sensitive (non-specific Cl⁻ channel blocker) and glibenclamide-sensitive (CFTR blocker) current. DIDS inhibited approximately 46% and glibenclamide 38% of the Cl⁻ current. When both drugs were added simultaneously, the Cl⁻ current was reduced by approximately 74% indicating that the DIDS and glibenclamide sensitive currents are individual currents. In the ICM glibenclamide had no effect on the Cl⁻ current whereas in a 3.5 day trophoblast cell line preliminary results indicate that there is a large glibenclamide sensitive current. These electrophysiological results are consistent with the CFTR mRNA expression pattern observed.

The exact role that Cl⁻ channels play in the pre-implantation embryo still remains to be identified. The results described above show that CFTR along with other CIC channels are present in the pre-implantation embryo at the mRNA level and that they are most likely to be responsible for the currents observed.

Ben-Chetrit, A., Antenos, M., Jurisicova, A., Pasyk, E.A. Chitayat, D., Foskett, J.K., & Casper, R.F. (2002) *Molecular Human Reproduction*, 8:758-764.

Brison, D.R., & Leese, H.J. (1993) *Biology of Reproduction*, 48:692-702.

Kolajova, M., Hammer, M.A., Collins, J.L. & Baltz, J.M. (2001) *Development*, 128:3427-3434.

Manejwala, F.M., Cragoe, E.J., & Schultz, R.M. (1998) *Developmental Biology*, 133:210-220.

Zhao, Y., Doroshenco, P.A., Alper, S.L., & Baltz, J.M. (1997) *Developmental Biology* 189:148-160.

Clustering of recombinant GABA_A receptors alters channel properties

A.B. Everitt, M.L. Tierney and P.W. Gage, Division of Molecular Bioscience, John Curtin School of Medical Research, Australian National University, Canberra, ACT 2601, Australia. .SP

'Native' GABA_A receptors display distinct electrophysiological properties not always seen in recombinant receptors irrespective of subunit composition. Native channels can have conductances over 40pS (Gray & Johnson, 1985; Smith *et al.*, 1989; Curmi *et al.*, 1993). Moreover, the conductance of some channels can be increased by modulating drugs such as diazepam, pentobarbitone and propofol (Eghbali *et al.*, 1997; Guyon *et al.*, 1999; Eghbali *et al.*, 2003). By contrast, conductances of recombinant channels have never exceeded about 30pS and, although their open probability can be increased by modulating drugs, conductance is not enhanced by drugs.

It has been suggested that high channel conductances may represent cooperative openings of clustered channels resulting in an apparent high single channel conductance. We tested this hypothesis in an expression system by co-expressing two proteins known to cluster GABA_A receptors. Rapsyn is a membrane associated protein that plays a crucial role in clustering ACh receptors at the neuromuscular junction, but has also been shown to cluster expressed GABA_A receptors. GABARAP interacts with the GABA_A γ subunit and promotes receptor clustering (Wang *et al.*, 1999).

We co-transfected (lipofectin) GABA_A α 5 and β 1 subunit cDNAs with or without rapsyn into mouse fibroblast L929 cells. We measured single channel conductance in the cell-attached (c/a) or inside-out (i/o) configurations 24-72 hours later. In the control groups (i.e. GABA_A subunits alone), single channel conductances were within the range 10-35pS. When rapsyn was co-expressed with GABA_A subunits, 4 out of 8 patches showed single channel conductances greater than 40pS. Control patches expressing GABA_A α 1, β 1 and γ 2s subunits alone had a mean conductance of 22.3 ± 1.2 pS (n=15). In 16 out of 25 patches recorded from cells co-transfected with GABA_A α 1, β 1 and γ 2s subunits and GABARAP, single channel conductances were above 40pS (γ = 60.7 ± 4.3 pS, n=16). These 'high' conductance channels were never seen in control patches. High and low conductance channel activity was blocked by 100 μ M bicuculline. The current-voltage relationship of high conducting channels showed outward rectification of the current, similar to that seen in native receptors.

Diazepam can increase both open probability and conductance of GABA_A channels containing the γ subunit. In 5 patches from cells co-transfected with GABA_A α 1, β 1 and γ 2s subunits and GABARAP, both of these effects were seen irrespective of initial channel conductance. In control patches where GABARAP was not expressed, diazepam did not increase channel conductance.

Immunofluorescent studies revealed that coexpression of rapsyn or GABARAP with GABA_A subunits, showed a punctate pattern of staining of surface receptors compared to a diffuse pattern in control cells.

Our results show that co-expression with "clustering" proteins can change the properties of recombinant GABA_A channels. It is possible that clustered receptors may be able to couple and open cooperatively by virtue of their close physical proximity.

Curmi, J.P., Premkumar, L.S., Birnir, B & Gage, P.W. (1993) *Journal of Membrane Biology*, 136, 273-280.

Eghbali, M., Curmi, J.P., Birnir, B & Gage, P.W. (1997) *Nature*, 388, 71-75.

Eghbali, M., Gage, P.W. & Birnir, B. (2003) *European Journal of Pharmacology*, 468 (2): 75-82.

Gray, R. & Johnston, D. (1985) *Journal of Neurophysiology*, 54: 134-142.

Guyon, A., Laurent, S., Paupardin-Tritsch, D., Rossier, J. & Eugen, D. (1999) *Journal of Physiology*, 516, 719-737.

Smith, S.M., Zorec, R & McBurney, R.N. (1989) *Journal of Membrane Biology*, 108, 45-52.

Wang, H., Bedford, F.K., Brandon, N.J., Moss, S.J. & Olsen, R.W. (1999) *Nature*, 397, 69-72.

Signalling across the blood brain barrier: Implications for blood pressure control

J.F.R. Paton, School of Medical Sciences, Department of Physiology, University of Bristol, Bristol BS8 1TD, UK. .SP

Our long-term goal is to understand cellular signalling mechanisms involved in the etiology of essential hypertension. Our hypothesis is that this disease may arise, in part, from changes within brainstem circuits controlling arterial pressure, and in particular to occlusion of arterial baroreceptor afferent information at the level of the primary afferent relay within the brainstem. Although it is established that baroreceptors regulate arterial pressure on a moment-to-moment basis, they may also control it long term (Thrasher, 2002). It follows then that desensitisation of this reflex circuit could contribute to high levels of blood pressure. I will discuss the central actions of angiotensin II on neuronal circuitry dedicated to controlling the baroreceptor reflex. Based on *in vivo* somatic gene transfer studies to identify intracellular signalling pathways, and dynamic confocal calcium imaging from cells within the nucleus of the solitary tract (NTS), we hypothesise a novel form of inter-cellular communication, one of *vascular-neuronal signalling*. Our model includes a process whereby angiotensin II stimulates nitric oxide release from the endothelium, which crosses the blood brain barrier to modulate adjacent inhibitory synaptic processes and shunts out incoming afferent information from arterial baroreceptors. Such a signalling process is consistent with that described for the control of GnRH within the median eminence (Prevot *et al.*, 2000). Moreover, using focal genetic approaches to chronically block endothelial cell derived nitric oxide results in an augmentation of baroreceptor reflex function and a fall in arterial pressure towards control levels in a rat model of hypertension. I will demonstrate that the specificity of action of nitric oxide on inhibitory (GABA) transmission in the NTS likely relates to the low concentration of the gas and/or proximity of the nitric oxide synthase isoform to its target (Paton *et al.*, 2002). In conclusion, activation of endothelial nitric oxide synthase within the NTS, which can be induced by physiological levels of angiotensin II, plays a major role in regulating cardiovascular function. Hyperactivity of angiotensin II and/or endothelial nitric oxide synthase within this nucleus may contribute to the persistent elevation of arterial pressure as observed in essential hypertension.

Paton, J.F.R., Kasparov, S. & Paterson, D.J. (2002) *Trends in Neuroscience*, **25**, 626-631.

Prevot, V., Bouret, S., Stefano, G. B., & Beauvillain, J.-C. (2000) *Brain Research Reviews*, **34**, 27-41.

Thrasher, T. N. (2002) *American Journal of Physiology* **282**, R1044-R1053.

Research funded by the British Heart Foundation

Effect of oscillating airway smooth muscle length on bronchoconstriction – the role of the airway wall

P.B. Noble, P.K. McFawn and H.W. Mitchell, School of Biomedical and Chemical Sciences, University of Western Australia, Crawley, WA 6009, Australia. .SP

A period of deep inspiration in man is known to modulate subsequent bronchoconstriction (Crimi *et al.*, 2002; Kapsali *et al.*, 2000), an effect which may be elicited through direct stretch of airway smooth muscle (ASM). We investigated the response of porcine ASM to a period of length oscillation in three different preparations: whole bronchial segments; bronchial segments which had cartilage removed; and isolated ASM strips. ASM response to electrical field stimulation (EFS) was assessed before and at different time points after ASM length oscillation. In bronchial segments oscillation of ASM length was achieved by cycling intraluminal pressure from 5 to 25cmH₂O, while in isolated ASM length changes were directly imposed. In each of the three preparations the amplitude of length oscillation was 20-25% of resting ASM length cycled at 0.5Hz for a period of 10 minutes. ASM length and cartilage area were morphometrically determined in airways fixed at 5 and 25cmH₂O. In whole bronchial segments response to EFS was increased immediately after ASM length oscillation ($P<0.05$). In contrast to whole airways, 5 out of 7 cartilage-denuded airways had reduced response to EFS following length oscillation ($P<0.05$). ASM lengths were not significantly different between control and cartilage-denuded airways at either 5 or 25cmH₂O. Post oscillation response to EFS was positively correlated to airway wall cartilage ($P<0.05$). In isolated ASM, response to EFS was reduced immediately after length oscillation ($P<0.01$). In each preparation the effect of length oscillation was absent 10 minutes after oscillation had concluded. Our results show that the response of ASM to length oscillation is strongly influenced by the airway wall. Length oscillation enhanced ASM contraction *in situ*, but depressed contraction in isolated ASM. Following cartilage removal, the response of ASM to length oscillation mimicked the depression in contraction observed in isolated ASM, suggesting airway wall structure plays a substantial role in the effect observed with oscillation.

Crimi, E., Pellegrino, R., Milanese, M. & Brusasco, V. (2002) *Journal of Applied Physiology*, 93, 1384-1390.

Kapsali, T., Permutt, S., Laube, B., Scichilone, N. & Togias, A. (2000) *Journal of Applied Physiology*, 89, 711-720.

Bronchial response to protease-activated receptor stimulation of airway luminal and adventitial surfaces

H.W. Mitchell, H.L. Goh, N. Asokanathan, R.S. Lan, G.A. Stewart and A. Sharma, School of Biomedical and Chemical Sciences, University of Western Australia, Nedlands, WA, Australia. .SP

A recently characterised family of G protein coupled receptors, protease-activated receptors (PARs), modulate inflammatory and regulatory signals in the airway. There are currently four PARs (PAR1, PAR2, PAR3 and PAR4) that have been cloned and characterised. Trypsin is an endogenous activator of PAR2 and PAR4. Activating these PARs has been shown to release PGE₂ from airway epithelial cells and modulate smooth muscle tone in isolated airway preparations (Cocks *et al.*, 1999; Lan *et al.*, 2001). It is uncertain how these different actions of PARs expressed on the various cell types in the airway may modulate airway function where luminal and adventitial surfaces can be separately accessed by PAR activators. The present study investigates the actions of trypsin (300 µg/ml) and PAR agonist peptides (100-400 nM) on isolated whole airways in which the epithelial and adventitial surfaces can be separately exposed to PAR agonists. Bronchial airways were dissected from the lungs of pigs. Side branches were ligated and segments were placed in a bath at 37°C so that luminal and adventitial surfaces were bathed in Krebs solution. A pressure transducer measured airway luminal pressure, from which airway responses were assessed. Luminal Krebs solution was assayed for PGE₂ by ELISA. Trypsin added to the adventitia produced a short latency (<5 min) inhibition of carbachol-induced tone. However, trypsin added to the airway lumen produced a delayed (>45 min) suppression of acetylcholine dose-contraction curve. Moreover, both trypsin and the PAR2 agonist increased PGE₂ production. Indomethacin pre-treatment blocked production of PGE₂, but had no effect on trypsin-induced relaxation by either route. The PAR1, 2 and 3 agonists had no effect on airway tone, but the PAR4 agonist produced short latency relaxation that was blocked by indomethacin. The study confirms that trypsin relaxes airways and releases PGE₂. Moreover, the effects of trypsin are highly dependent on its route of delivery, suggesting the contribution of different cell types by each route of exposure. However, the results observed with trypsin and the PAR2 agonist appear to dissociate the possible link between PGE₂ release by PAR activation and subsequent airway relaxation in this whole airway preparation. These findings suggest that the functional responses to trypsin are likely to be mediated by a receptor other than the established PAR1, PAR2, PAR3 or PAR4.

Cocks, T.M., Fong, B., Chow, J.M., Anderson, G.P., Frauman, A.G., Goldie, R.G., Henry, P.J., Carr, M.J., Hamilton, J.R. & Moffatt, J.D. (1999) *Nature*, 398, 156-160.

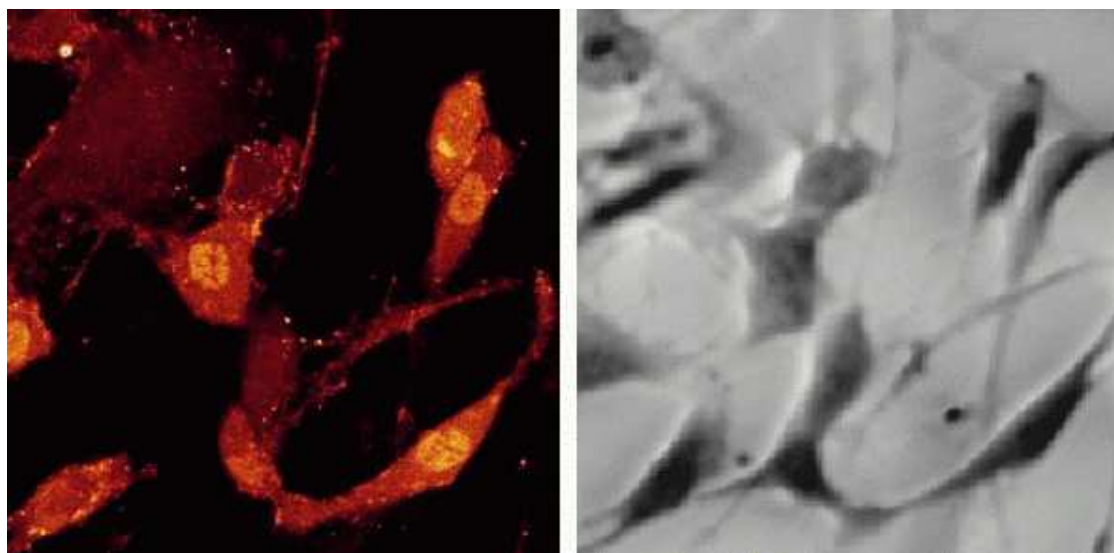
Lan, R.S., Knight, D.A., Stewart, G.A. & Henry, P.J. (2001) *British Journal of Pharmacology*, 132, 93-100.

Measurement of culture confluency and volume of human airway smooth muscle cells using quantitative phase microscopy

C.L. Curl¹, C.J. Bellair², T. Harris³, B.E. Allman⁴, A. Roberts², K.A. Nugent², P.J. Harris¹, A.G. Stewart³ and L.M.D. Delbridge¹, ¹Department of Physiology, ²Department of Physics, and ³Department of Pharmacology, University of Melbourne, Parkville, Victoria 3010 and ⁴IATIA Ltd., Rutland Rd, Box Hill, Victoria 3128, Australia.

Quantitative Phase Microscopy (QPM) is a recently developed computational approach that provides quantitative phase measurements of images captured using a bright-field microscope. Phase measurement is particularly useful in the evaluation of translucent objects, such as unstained viable cell specimens. QPM works via an algorithm which is applied to a standard bright-field and equidistant positive and negative de-focus images. From these images a phase map is generated which contains information about cell thickness and refractive index and can allow quantitation of cellular structure. QPM was used in conjunction with laser scanning confocal microscopy (LSCM) to measure volume and area in cultured human airway smooth muscle (HASM) cells.

HASM cells were obtained by collagenase and elastase digestion of smooth muscle from lung transplant resection patients. The resulting cell suspension was washed in phosphate buffered saline and seeded onto glass coverslips which were placed in the base of a plastic culture dish at 37°C in Dulbecco's Modified Eagles Media. The cells were imaged using both LSCM (optical slicing) and QPM techniques. For LSCM visualisation, cells were fluorescently labelled (fluo-3/AM, Molecular Probes, Eugene, OR, USA) and a series of images in the vertical (z) axis were recorded at intervals of 1µm using a Leica TCS 4D (x63, PL APO 1.40 NA oil immersion objective). From these images a calculation of cell depth was performed. Phase images of the same field of cells were then obtained using an inverted Zeiss Axiovert 100M microscope (×10, LD-Achroplan 0.3 NA objective) and a Coolsnap fx CCD camera (Photometrics, USA). Phase calculations were performed using QPM software (v2.0 IATIA Ltd, Australia).



On the basis of the cell depth determined by LSCM (left panel of Figure) and the phase measurements calculated by QPM (right panel of Figure) a mean refractive index (RI) for HASM was determined to be 1.4275 ± 0.009 . This RI was then used computationally by the QPM algorithm to determine cellular volume. The relationship between cell confluency and volume in HASM cultures passaged for variable periods was evaluated. The confluency of cells (% field area), calculated over a 92 hour growth period from phase maps and cell volume (μm^3) were highly correlated (i.e. r^2 values of 0.986 and 0.996 obtained for two different cell culture lines). Thus, in these HASM cells under the conditions specified, there is a well defined relationship between extent of confluence and total cell

volume in culture. QPM provides a convenient procedure for estimating cell volume, where prior determination of RI is required. We have demonstrated that this may be achieved by parallel specimen imaging using both LSCM and QPM.

Increases in renal angiotensinogen mRNA levels following a mixed amino acid infusion in late gestation fetal sheep

A.C. Boyce, K.J. Gibson, J. Wu and E.R. Lumbers, Dept of Physiology & Pharmacology, School of Medical Sciences, University of New South Wales, Sydney 2052, Australia. .SP

We have previously reported that prolonged infusions of amino acids to fetal sheep in late gestation stimulated renal growth, had profound, sustained effects on fetal renal function (including increases in glomerular filtration rate, renal blood flow, a diuresis, natriuresis and increased osmolar excretion), and induced changes indicative of extracellular volume expansion (Marsh *et al.*, 1999, Marsh *et al.*, 2002). This study aimed to determine whether the fetal renin-angiotensin system was also affected when plasma amino acid levels were increased long term.

Fetal sheep were chronically catheterised under general anaesthesia induced with 1 g sodium thiopentone i.v. and maintained with 2-3% halothane in oxygen. At least 5 days after surgery, 5 fetuses aged 122 ± 1 days gestation (term ~150 days) were infused i.v. for 7 days with a mixture of alanine, glycine, proline and serine (1:1:0.6:0.6) at $0.22 \text{ mmol min}^{-1}$ and 5 mL h^{-1} . Six control fetuses were infused with 0.15 M saline. Plasma and renal renin levels were measured as the rate of formation of angiotensin I (Ang I) when plasma or homogenates of renal cortex were incubated at 37°C and pH 7.4 with an excess of angiotensinogen (nephrectomised sheep plasma). Levels of mRNA for renin, angiotensinogen and the angiotensin receptor subtypes I and II (AT_1R and AT_2R) were measured in renal cortical homogenates by real time PCR, and expressed relative to a calibrator sample.

After 7 days of amino acid infusion, plasma concentrations of the infused amino acids had increased by between 8- and 36-fold ($P < 0.05$), and kidney weights were ~28% greater than those of control fetuses ($P < 0.05$). Circulating renin levels fell during the first 4 h, from 9.3 ± 2.1 (mean \pm SE) $\text{ng Ang I mL}^{-1} \text{ h}^{-1}$ in control to 4.7 ± 1.5 ($P < 0.05$), and remained low throughout the infusion (Day 4: 4.2 ± 2.5 , n.s.; Day 7: $2.2 \pm 1.1 \text{ ng mL}^{-1} \text{ h}^{-1}$, $P < 0.05$). Plasma renin levels did not change during saline infusion (baseline: $5.9 \pm 1.6 \text{ ng Ang I mL}^{-1} \text{ h}^{-1}$). Renal renin levels tended to be lower following amino acid infusion compared to control fetuses (1.1 ± 0.4 vs $2.1 \pm 0.4 \mu\text{g Ang I mg protein}^{-1} \text{ h}^{-1}$, n.s.). Renal renin mRNA levels were also lower (Amino acids: 3.6 ± 2.2 ; Saline: 10.5 ± 2.7 , $P = 0.075$). There was marked increase in renal angiotensinogen mRNA levels (3.6 ± 0.5 vs 1.4 ± 0.2 , $P < 0.005$). Renal AT_1R and AT_2R mRNA levels were not different between groups.

Prolonged increases in fetal plasma amino acid levels were therefore associated with a suppression of circulating renin levels, and tended to suppress the gene expression and levels of renin in the developing kidney. These changes were probably secondary to volume expansion. However, the stimulation of renal angiotensinogen gene expression by amino acids suggests that the renal renin-angiotensin system may have played a role in the stimulation of renal function and growth that occurred with amino acid infusion.

Marsh, A.C., Gibson, K.J. & Lumbers, E.R. (1999) *Proceedings of the Australian Society for Medical Research*, Oral 8-1.

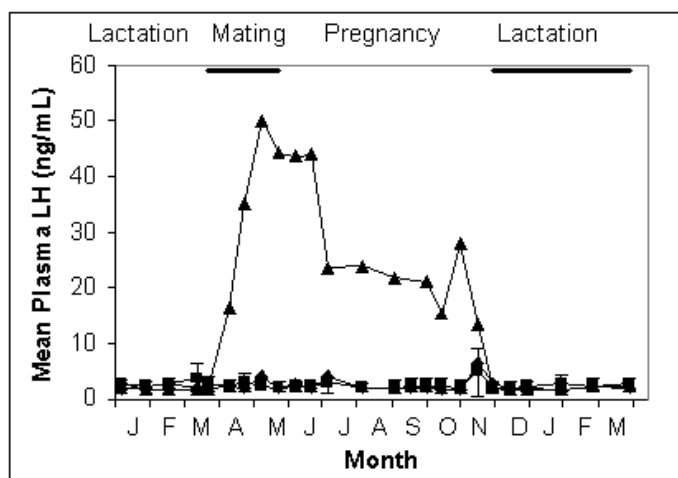
Marsh, A.C., Gibson, K.J. & Lumbers, E.R. (2002) *Journal of Physiology* **540**, 717.

Central program and ovarian feedback both influence LH secretion in flying-foxes

G.M. O'Brien and K.-A. Gray, School of Biological, Biomedical and Molecular Sciences, University of New England, NSW 2351, Australia.

Very large changes in plasma progesterone and oestradiol are observed during late pregnancy, in Australia's greyheaded flying-fox, *Pteropus poliocephalus*, but changes associated with ovulation are enigmatic. Attempts to identify the time of ovulation by monitoring peripheral hormones have been so unsuccessful that a question has arisen as to the nature of feedback between the ovary and the hypothalamus-pituitary axis in these animals. *P. poliocephalus* mate during April-May and deliver a single young in October-November. In captivity they can live for 20-30 years but wild populations are listed as 'threatened' under the Environment Protection and Biodiversity Conservation Act. Understanding their reproductive physiology is essential for recovery of the species. Important stages of reproduction, including ovulation, are regulated by luteinising hormone (LH) but plasma LH has not previously been measured in the Order Megachiroptera. Recent development of an assay for flying-fox LH (O'Brien *et al.*, in press) has made it possible to test for the effects of reproductive stage (copulation, pregnancy etc.) and ovarian feedback on mean plasma LH levels in female flying-foxes through an entire annual cycle of reproduction.

Methods. Blood samples were collected by venipuncture (O'Brien *et al.*, 1996), at intervals of 1 to 4 weeks. LH was measured by ^{125}I -RIA using monoclonal antibody 518B7, and ovine LH (oLH-G3-330-Br) as radioligand and standard (O'Brien *et al.*, in press). Animals were housed in a single-sex group (segregated \blacklozenge $n=4$) or in a large mixed-sex group (breeding \blacksquare sub-set $n=5$); each group had a long-term ovariectomised female with them (ovariectomised \blacktriangle data are average of 2).



Results shown in the Figure clearly demonstrate three phases of LH secretion during the year in the absence of ovarian steroid feedback (ovariectomised \blacktriangle): very high levels Apr-May; elevated levels Jun-Oct; baseline levels Nov-Mar. Mean plasma LH remained at baseline all year in intact animals (\blacklozenge , \blacksquare : Figure shows means and SD).

Discussion. The pituitary appears to be programmed to stimulate the ovaries from mid-autumn (April) until mid-spring (October) (see the Figure). Pituitary content of LH is high during April-May (O'Brien *et al.*, in press). However strong negative feedback from the ovaries reduced the frequency and/or

amplitude of LH pulses so dramatically that no elevation of mean plasma levels was observed in intact animals. There was no indication of the timing of ovulation. During pregnancy, placental steroids probably also contributed to the feedback.

The phase of the central program revealed during June-October probably provides a safety net in the event of early pregnancy loss and if so, would explain the occasional late births that are recorded. It may also provide the physiological substrate for the observed geographic variation in breeding times of a congeneric species, *P. alecto* (Vardon & Tidemann 1998).

The November-March phase reveals a centrally programmed anoestrus not previously known. This may explain why variations in the timecourse of lactation do not influence timing of the subsequent pregnancy (unpub. obs.).

O'Brien, G.M., Curlewis, J.D. & Martin, L. (1996) *General & Comparative Endocrinology* 104, 304-311.

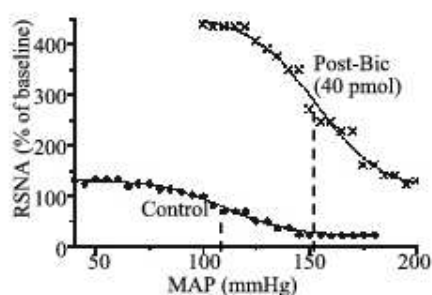
O'Brien, G.M., McFarlane, J.R. & Kearney, P.J. (in press) *Reproduction, Fertility and Development*.
Vardon, M.J. & Tidemann, C.R.. (1998) *Australian Journal of Zoology*, 46, 329-344.

The dorsomedial hypothalamic nucleus modulates the baroreceptor reflex

L.M. McDowall, S. Killinger and R.A.L. Dampney, Department of Physiology F13, University of Sydney, NSW 2006 Australia.

The dorsomedial hypothalamic nucleus (DMH) plays a critical role in mediating the increase in arterial pressure and heart rate evoked by an acute stress (Stotz-Potter, *et al.*, 1996). The cardiovascular changes evoked by acute stress are also associated with modulation of the baroreceptor reflex (Spyer, 1994). The aim of this study was to determine if the DMH is capable of modifying the baroreceptor reflex control of heart rate and sympathetic vasomotor activity.

Experiments were performed on rats anaesthetised with urethane (1.35g/kg i.p.). Arterial pressure, heart rate (HR) and renal sympathetic nerve activity (RSNA) were measured. The baroreceptor reflex function was determined by measuring the changes evoked in HR and RSNA by alterations in mean arterial pressure (MAP) over a wide range (50-200 mmHg), induced by intravenous infusions of a vasodilator (sodium nitroprusside) or vasoconstrictor (phenylephrine). In each experiment, baroreceptor reflex function curves were determined before and after microinjection of the GABA receptor antagonist bicuculline (4 or 40 pmol) or the vehicle solution of artificial cerebrospinal fluid (ACSF) into the DMH. A logistic function curve of best fit was calculated in each case.



As illustrated in the Figure, disinhibition of DMH neurons by bicuculline microinjection resulted in a shift in the baroreceptor reflex function curve. The baroreceptor reflex operating point (OP, dashed line) for the baroreflex control of both HR and RSNA was significantly increased (* $P < 0.05$) in a dose-dependent fashion by bicuculline microinjection, but not ACSF microinjection into the DMH (see the Table below). There was no reduction, however, in the gain of the renal sympathetic or cardiac component of the baroreceptor reflex.

		Δ OP (mm Hg)	
Bic (pmol)	n	HR	RSNA
0 (ACSF)	6	0 \pm 2.6	3 \pm 1.9
4	6	15 \pm 4.1*	9 \pm 2.4*
40	6	26 \pm 4.1*	18 \pm 5.7*

We conclude that activation of the DMH alters the operating point of the baroreceptor reflex, but that the reflex remains operational over a wide range of arterial pressures.

Spyer, K.M. (1994) *Journal of Physiology*, 474, 1-19.

Stotz-Potter, E.H., Willis, L.R. & DiMicco, J.A. (1996) *Journal of Neuroscience*, 16, 1173-1179.

Renal sympathoexcitatory response evoked from the dorsomedial hypothalamic nucleus is mediated by presympathetic vasomotor neurons in the rostral ventrolateral medulla

J. Horiuchi¹, S. Killinger¹, R.M. McAllen², A.M. Allen² and R.A.L. Dampney¹, ¹Department of Physiology, The University of Sydney, NSW 2006, Australia and ²Neurobiology Group, The Howard Florey Institute, The University of Melbourne, VIC 3010, Australia. .SP

The dorsomedial hypothalamic nucleus (DMH) plays a critical role in mediating the cardiovascular response to an acute stress (Stotz-Potter, *et al.*, 1996). Activation of neurons in the DMH causes an increase in arterial pressure, heart rate and renal sympathetic nerve activity (Fontes *et al.*, 2001). We have previously shown that the sympathoexcitatory vasomotor, but not cardiac, component of the DMH-evoked response is dependent upon a synapse in the rostral ventrolateral medulla (Fontes *et al.*, 2001). On the other hand, Samuels *et al.* (2002) showed that the cardiac component of the response is mediated by neurons in the midline raphe pallidus (RP) in the medulla, but did not examine the sympathoexcitatory vasomotor component. The aims of this study were (1) to determine if inhibition of RP neurons affects the sympathoexcitatory component of the DMH-evoked response, and (2) to determine the extent to which, at the single neuron level, RVLM presympathetic neurons are influenced by inputs from the DMH.

Experiments were performed on rats anaesthetised with urethane (1.4 g/kg i.p). Mean arterial pressure (MAP), heart rate (HR) and either renal sympathetic nerve activity (RSNA) or the extracellular activity of barosensitive and spinally-projecting RVLM neuron were recorded. Unilateral microinjections of the GABA receptor antagonist bicuculline (0.1-40pmol in 20nl) into the DMH resulted in dose-dependent increases in MAP, HR and rSNA. Inhibition of the RP by injections of muscimol (80pmol in 100nl) did not alter the increase in rSNA evoked by bicuculline (40pmol) in the DMH, whereas increases in MAP and HR were significantly attenuated, as Samuels *et al.* (2002) previously reported. In addition, the extracellular activity of 5 out of 6 barosensitive and spinally-projecting neurons in the RVLM were strongly excited (increase in firing rate of $417 \pm 125\%$) by unilateral injection of bicuculline (40pmol) into the DMH. The results demonstrate that the cardiac and sympathoexcitatory vasomotor components of the cardiovascular response elicited by disinhibition of the DMH are mediated via at least two different descending pathways in the medulla.

Fontes, M.A., Tagawa, T., Polson, J.W., Cavanagh, S.J. & Dampney, R.A.L. (2001) *American Journal of Physiology*, 280, H2891-H2901.

Samuels, B.C., Zaretsky, D.V. & DiMicco, J.A. (2002) *Journal of Physiology*, 538, 941-946.

Stotz-Potter, E.H., Willis, L.R. & DiMicco, J.A. (1996) *Journal of Neuroscience*, 16, 1173-1179.

Blockade of angiotensin type 1 (AT1) receptors in the rostral ventrolateral medulla increases renal sympathetic activity and arterial pressure under hypoxic conditions

J. Sheriff, M.A.P. Fontes, S. Killinger and R.A.L. Dampney, Department of Physiology F13, University of Sydney, NSW 2006, Australia. .SP

Administration of exogenous angiotensin II (AngII) into the rostral ventrolateral medulla (RVLM) increases sympathetic activity and blood pressure, indicating that it has an excitatory effect on presympathetic neurons in this region. Blockade of angiotensin type 1 (AT1) receptors in the RVLM under normal conditions results in little change in sympathetic activity, suggesting that under these conditions endogenous AngII has little tonic effect in the RVLM. Recently, however, it has been suggested that endogenous Ang II has a tonic action on both excitatory and inhibitory mechanisms in the RVLM, so that the ultimate effect on sympathetic activity depends upon the balance between the excitatory and inhibitory effects of endogenous AngII on presympathetic neurons (Hu *et al.*, 2002). If that is the case, then this balance could be altered under conditions in which the level of activity of excitatory or inhibitory synaptic inputs to RVLM neurons is altered. In this study we have tested this hypothesis by determining the effects of blockade of AT1 receptors in the RVLM under hypoxic conditions, which is known to enhance the excitatory glutamatergic inputs to RVLM presympathetic neurons. Rats were anaesthetised with urethane (I.P. 1.35g/kg) and arterial pressure, heart rate and renal sympathetic nerve activity were recorded. Unilateral microinjections of an AT1 receptor antagonist, candesartan (100pmol), into the RVLM during moderate hypoxia (PO₂ 10%) resulted in an increase in arterial pressure and renal sympathetic nerve activity, whereas microinjections of the vehicle solution had little effect. The results indicate that, under hypoxic conditions, endogenous AngII has a net tonic sympathoinhibitory effect. Taken together with other recent findings, the results are consistent with the hypothesis that AT1 receptors can mediate both tonic excitatory and inhibitory effects on RVLM sympathoexcitatory neurons, and the balance of these effects is altered under different physiological conditions.

Hu, L., Zhu, D., Yu, Z., Wang, J.Q., Sun, Z. & Yao, T. (2002) *Journal of Applied Physiology*, 92, 2153-2161.

Angiotensin II microinjections in the nucleus tractus solitarius has an inhibitory effect on the cardiac but not the non-cardiac sympathetic component of the baroreceptor reflex

P. Tan and R.A.L. Dampney, Department of Physiology F13, University of Sydney, NSW 2006, Australia. .fp 10 S

The nucleus tractus solitarius (NTS) is a major nucleus located in the dorsal medulla and is critical in the mediation of the baroreceptor reflex. It is also a site which contains a high density of high affinity binding sites for angiotensin II (AngII). Previous studies have shown that microinjections of AngII cause significant inhibition of the cardiac component of the baroreceptor reflex. However there is very little information on its effects on the non-cardiac sympathetic component, which is of critical importance in the regulation of blood pressure. Experiments were carried out in adult male Sprague-Dawley rats that were initially anaesthetised with pentobarbital sodium (60mg/kg, I.P.) and maintained by I.V. infusion of pentobarbital sodium (6mg/ml at 1-1.3ml/hr). The arterial pressure, heart rate (HR) and renal sympathetic nerve activity (RSN) were measured. The baroreceptors were stimulated by increases in mean arterial pressure (MAP) of 40-50 mmHg induced by a single bolus injection of phenylephrine, and the reflex decrease in HR and RSN measured.

Following bilateral microinjections of 40pmol AngII (50nl) into the NTS, the gain of the cardiac component of the reflex (measured as $\Delta\text{HR}/\Delta\text{MAP}$) was greatly reduced by $70 \pm 8.7\%$ compared with that before Ang II microinjections. In contrast, bilateral microinjections of AngII into the NTS had no significant effect (change of $1.4 \pm 5.5\%$) on the gain of the renal sympathetic component of the reflex (measured as $\Delta\text{RSNA}/\Delta\text{MAP}$). In control experiments, bilateral microinjections of the vehicle solution into the NTS had no effect on the gain of either the cardiac or renal sympathetic component of the reflex.

We conclude from these experiments that the inhibitory influence of AngII microinjections may be restricted to the cardiac component of the baroreflex. It is possible that in conditions where endogenous AngII activity is increased (e.g. hypertension or heart failure) the cardiac reflex response to changes in blood pressure may be inhibited, whereas the baroreceptor mediated vasomotor response is largely unaffected.

Angiotensin II via AT₁ receptors may mediate apoptosis in the cardiac conduction system of rats

U. Vongvatcharanon¹, S. Vongvatcharanon², N. Radenahmad¹, P. Kirirat¹, P. Intasaro¹, P. Sobhon³ and T. Parker⁴, ¹Department of Anatomy, Faculty of Science, Prince of Songkla University, Hat-Yai 90112, Thailand, ²Department of Oral Surgery, Faculty of Dentistry, Prince of Songkla University, Hat-Yai 90112, Thailand, ³Department of Anatomy, Faculty of Science, Mahidol University, Bangkok 10400, Thailand and ⁴School of Biomedical Science, Nottingham University, Nottingham NG7 2UH, UK. .SP

Apoptosis has been suggested as a possible cause of gradual development of complete heart block and fatal arrhythmias associated with absence of the AV node, sinus, and internodal pathways (James *et al*, 1996). Studies about apoptosis in the heart by means of cardiomyocyte cell culture have demonstrated that angiotensin II (Ang II) mediates cardiomyocyte apoptosis via angiotensin II type I receptors (AT₁) (Cigola *et al*, 1997). The transgenic *m(Ren-2)27* (TG) rat carries the additional *Ren-2* gene, the expression of which results in an increase of heart Ang II (Campbell *et al*, 1995), thus potentially affecting the cell growth/death equilibrium. This study addresses the question of role of Ang II/AT₁ receptors mediated apoptosis in the sinoatrial (SA) and atrioventricular nodes (AV).

Six, male 2 week TG and Hannover Sprague Dawley (SD) rats were anaesthetised by pentobarbitone sodium i.p. injection (100 mg/kg). The hearts were removed and fixed in 10% formaldehyde. Following dehydration and embedding in paraffin, 5 µm serial sections were cut then stained with Masson Trichrome to localize SA and AV nodes. The sections containing SA or AV node were processed for either: (a) calculation of apoptotic nuclei following terminal deoxynucleotidyl transferase nick end labelling of 3'-OH ends using Fluorescein-FragEL™; or (b) immunohistochemical labelling with antibodies to the AT₁ receptors prior to confocal scanning laser microscopical analysis. Quantification of AT₁ receptors was performed by using Microimage analysis software (Olympus).

Group	Apoptotic cells/mm ²		AT ₁ receptors (×10 ³)/mm ²	
	SA	AV	SA	AV
SD	0.040±0.07	0.164±0.12	1.14±0.17	7.63±1.91
TG	0.140±0.37*	0.433±0.11*	1.67±0.26*	12.50±3.97*

Data expressed as mean ± SD (n=6)

* = significant compared with control (P<0.05) (Independent-Sample T-test)

The table shows that the number of apoptotic cell in both the SA and AV node is significantly greater in the TG compared with the SD (p<0.05). Quantification of AT₁ receptors within SA and AV node shows that there were significantly more AT₁ receptors in the TG compared with the SD (p<0.05). These data suggest that an elevated level of apoptosis in the TG rat heart compared with the controls could be accounted for by *Ren-2* derived Ang II active via AT₁ receptors.

Campbell, D.J., Rong, P., Kladis, A., Rees, B., Ganten, D. and Skinner, S.L. (1995) Angiotensin and Bradykinin peptides in the TGR (*mRen-2*)27 rat. *Hypertension*, 25, 1014-1020.

Cigola, E., Kajstura, L.B., Meggs, L.G. and Anversa, P. (1997) Angiotensin II activates programmed myocyte cell death *in vitro*. *Experimental Cell Research*, 231, 363-371.

James, T.N., Martin, E., Willis, P.W. and Lohr, T.O. (1996) Apoptosis as a possible cause of gradual development of complete heart block and fatal arrhythmias associated with absence of the AV node, sinus, and internodal pathways. *Circulation*, 93, 1424-1432.

Effect of sinoaortic denervation on baroreflex sensitivity assessed with complex demodulation in the anaesthetised rat

Y.C. Tzeng, P.D. Larsen and D.C. Galletly, Department of Surgery and Anaesthesia, Wellington School of Medicine, PO Box 7343, Wellington, New Zealand. .SP

The relevance of baroreflex dysfunction in the clinical setting has stimulated a rapidly expanding area of research into the assessment of baroreflex sensitivity (BRS). Recent efforts have concentrated on developing non-invasive techniques that allow BRS to be determined from spontaneous heart rate and blood pressure recordings, such as the sequence method and the α -index. However, these techniques are limited as they provide average estimates over the entire period of recorded data. More recently, Kim & Euler (1997) introduced an alternative method of estimating BRS from spontaneous heart rate and blood pressure fluctuations based on complex demodulation (CMD) that is capable of assessing the dynamic changes in cardiovascular variability and baroreflex sensitivity as a function of time (Hayano *et al.* 1993). Using an anaesthetised rat model, the current study was conducted to validate the use of CMD analysis in sinoaortic denervated rats, and compare its performance to the Oxford method, sequence technique and α -index.

In 12 anaesthetised rats breathing isoflurane (1.5-2%) through a tracheal cannula, we recorded the ECG and continuous arterial blood pressure before and after sinoaortic denervation (SAD). Arterial baroreflex testing using the Oxford method was performed before and after SAD using similar doses of phenylephrine ($1.5 \mu\text{g kg}^{-1}$) and sodium nitroprusside ($2.5 \mu\text{g kg}^{-1}$) in 0.3 ml over 15 s administered intravenously. From spontaneous HR and SBP recordings we determined non-invasive BRS using CMD, sequence technique and the α -index.

Consistent with Kim & Euler's study, we found that BRS values obtained with CMD was strongly correlated to values derived from phenylephrine ($R=0.83$, $P<0.01$), nitroprusside ($R=0.77$, $P<0.01$), sequence technique ($R=0.85$, $P<0.01$) and α -index ($R=0.78$, $P<0.01$). The absolute values of BRS estimates obtained with CMD was similar to sequence technique and α -index, but were significantly greater than values obtained with the Oxford method. Following SAD, Oxford measures of BRS decreased to almost 0, while CMD and sequence techniques showed 50% reductions. The α -index method showed no significant decrease following SAD.

We conclude that the CMD approach to measuring BRS is at least as accurate as the sequence technique and is superior to the α -index. All three non-invasive measures differ markedly from the Oxford measure. The fine temporal resolution offered by CMD, and the high correlation with the Oxford method mean that this technique would be very useful as an index of BRS under conditions in which BRS is changing rapidly, and invasive measures are not possible.

Kim S.Y. & Euler D.E. (1997) *Hypertension*, 29, 1119-1125.

Hayano, J., Taylor, J.A., Yamada, A., Mukai, S., Hori, R., Asakawa, T., Yokoyama K., Watanabe. Y., Takata. K. & Fujinami. T. (1993) *American Journal of Physiology*, 264, H1229-H1238.

Change in baroreflex sensitivity during induction of anaesthesia with propofol

P.D. Larsen, Y.C. Tzeng and D.C. Galletly, Department of Surgery & Anesthesia, Wellington School of Medicine, PO Box 7343, Wellington, New Zealand. .SP

A number of studies have demonstrated that general anaesthesia with propofol results in a decrease in baroreflex sensitivity (BRS), and suggested that this is due to inhibition of sympathetic nervous activity (Ebert *et al.*, 1992, Sellgren *et al.*, 1994). These studies have compared pre-anaesthetic measures with measurements taken following induction, once a steady state of anaesthesia has been achieved. It has not been possible with existing techniques to examine the changes in BRS that occur during induction of anaesthesia, as measurements of BRS require stationarity for spectral measures, long time segments for sequence methods or a steady state at which interventions such as drug infusions can be performed. Kim & Euler (1997) have introduced an alternative method of estimating BRS from spontaneous heart rate and blood pressure fluctuations based on complex demodulation (CMD) that is capable of assessing the dynamic changes in cardiovascular variability and baroreflex sensitivity as a function of time, and does not assume stationarity of the signal.

In the current study we investigated the changes in baroreflex sensitivity that occur during induction of anaesthesia using CMD in 12 healthy male patients undergoing elective surgery. The injection of propofol (10mg/ml) 0.2ml kg^{-1} , followed by an infusion of $1\text{ml kg}^{-1}\text{ hr}^{-1}$, was associated with a transient tachycardia which commenced on average 25 s after the start of propofol injection. The HR reached a mean peak of 95 bpm at 47 s following the start of the injection of propofol and returned towards pre-anaesthetic rates, plateauing by approximately 84 s. The tachycardia occurred approximately 5 s prior to the onset of hypotension. Approximately 30 s following the start of injection of propofol, systolic and diastolic blood pressure fell, followed by a fall in pulse pressure at 34 s. Systolic pressure fell from a mean of 135 mmHg to 97 mmHg by 60 s after the start of the injection of propofol. BRS decreased to a minima at 35-40 seconds after the start of injection of propofol. On average BRS decreased 38% relative to preinduction levels. Following the initial minima, BRS increased, but in 8 of 12 subjects remained below preanaesthetic levels, while in 4 of 12 subjects BRS was elevated.

We conclude that CMD is a useful tool for examining dynamic changes in BRS, such as those occurring at induction of anaesthesia. The hypotension associated with the initial induction of anaesthesia with propofol cannot be accounted for by the brief initial decrease in BRS but may be caused either by intrathoracic pooling of blood, direct myocardial depression or vasodilatation.

Ebert, T.J., Muzi, M., Berens, R., Goff, D. & Kampine, J.P. (1992) *Anesthesiology*, 76(5):725-33.

Kim S.Y. & Euler D.E. (1997) *Hypertension*, 29, 1119-1125.

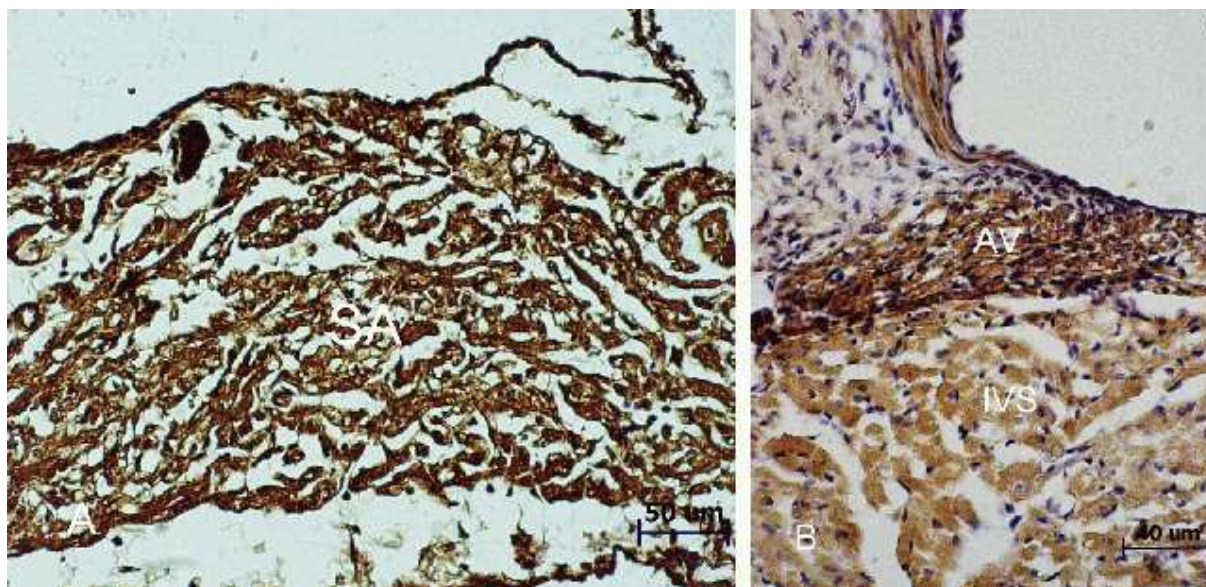
Sellgren, J., Ejnell, H., Elam, M., Ponten, J. & Wallin, B.G. (1994) *Anesthesiology*, 80(3):534-44,.

Calbindin D-28K and parvalbumin calcium-binding proteins in SA and AV nodes of rat heart

S. Vongvatcharanon¹ and U. Vongvatcharanon², ¹Department of Oral and Maxillofacial Surgery (Anesthesiology section), Faculty of Dentistry, and ²Department of Anatomy, Faculty of Science, Prince of Songkla University, Hat-Yai 90112, Thailand.

The role of Ca²⁺-release from the sarcoplasmic reticulum in influencing the pacemaker rate appears to be a common mechanism in sinoatrial node (SA) (Hata *et al.*, 1996) and atrioventricular node (AV) (Hancox *et al.*, 1994). An increased level of intracellular Ca²⁺ or Ca²⁺ overload has been suggested to be a major cause of arrhythmia (Blaustein & Lederer, 1999). Calbindin D-28K and parvalbumin calcium-binding proteins have been found in neurons, and function as intracellular Ca²⁺ buffering transport protein to maintain a constant intracellular Ca²⁺ level (Chard *et al.*, 1993). However, there have been no previous reports of calcium-binding protein in the SA and AV nodes. This study aimed to investigate whether the SA and AV nodes contain calbindin D-28K and parvalbumin.

Adult Wistar rats age 4 weeks were anaesthetised by ether inhalation. The hearts were removed and fixed in 10% formaldehyde. Following dehydration and embedding in paraffin, 5µm serial sections were cut in both the horizontal and coronal planes and then stained with Masson Trichrome to localise the SA and AV nodes. The sections containing SA or AV node were processed for immunohistochemical labeling with antibodies to calbindin D-28K and parvalbumin.



(A) Cross section of the heart at the junction of superior vena cava and right atrium, stained with calbindin D-28K antibody at a dilution of 1:400, showing immunoreactivity (brown color) in the cytoplasm of nodal fibers of SA node. (B) Coronal section of the heart, stained with parvalbumin antibody at a dilution of 1:2000, showing immunoreactivity (brown color) in the cytoplasm of nodal fibers of AV node.

The calbindin D-28K and the parvalbumin are found in both the SA and AV nodes, suggesting these two binding proteins may be involved in the generation and conduction of electrical impulses by maintaining a constant level of the intracellular calcium ions. It is hoped that the study of these calcium binding proteins will open new avenues for therapeutic interventions, especially for the treatment of Ca²⁺ overload and arrhythmia.

Blaustein, M.P. & Lederer, W.J. (1999) *Physiological Review*, 79, 763-854.

Chard, P.S., Bleakman, D., Christakos, S., Fullmer, C.S. & Miller, R.J. (1993) *Journal of Physiology*,

472, 341-357.

Hancox, H., Lederer, W.J. & Cannell, M.B. (1993) *Proceedings of the Royal Society B*, 255, 99-105.

Hata, T., Noda, T., Nishimura, M. & Watanabe, Y. (1996) *Heart and Vessels*, 11, 234-241.

Cardiac remodelling contributes to altered ventricular mechanics in hypertensive cardiomyopathy

A.P. Pope, B.H. Smaill and I.J. LeGrice, Department of Physiology/Bioengineering Institute, University of Auckland, Private Bag 92019 Auckland, New Zealand .SP

The complex organisation of cells and extracellular matrix (ECM) contributes to the diastolic properties of the heart. Remodelling of these structures is a significant feature of cardiovascular diseases such as hypertension and heart failure. The change in the content and organisation of ECM collagen is an important aspect of this remodelling because of the role collagen plays in interconnecting cells and limiting cellular movement during passive filling. The objective of this study was to characterise the differences in 3D collagen organisation in normal and diseased hearts and to link these differences to changes in diastolic function.

Ventricular structure and function measurements were made in Spontaneously Hypertensive rats (SHR) and Wistar-Kyoto (WKY) controls at 12 months. Geometry measurements were made using M-mode echocardiography and systolic blood pressure was measured prior to removal of the hearts. The passive left ventricular (LV) pressure-volume (PV) relationship was characterised for each heart by inflating an LV balloon to a pressure of 30 mmHg. Two hearts from each group were perfused with picosirius red dye via the coronary circulation to stain collagen. Samples from these hearts were resin embedded and imaged using a novel high throughput confocal microscope facility. Imaged blocks were typically 2mm × 0.5mm × 0.3mm with 1µm voxel dimension.

In vivo measurements confirmed that the SHRs were both hypertensive (SHR 152.4mmHg ± 7.7mmHg (n=8), WKY 117.6mmHg±3.8mmHg (n=9), $P=0.001$) and their hearts were hypertrophic (Posterior LV wall thickness: SHR 3.24mm ± 0.24mm (n=6), WKY 2.47mm±0.23mm (n=7), $P=0.042$). Active ventricular function was reduced in the SHR group with fractional shortening at 74.7%± 4.6% (n=6) compared to 61.1%±4.7 % (n=7) in the WKY group ($P=0.07$). The mean LV PV curve for the SHR group was shifted leftward with respect to control. LV stiffness ($\Delta P/\Delta V$) was greater in SHR than in WKY at pressures throughout the range 4 to 28mmHg ($P<0.05$; SHR n=8, WKY n=9).

In WKY blocks, perimysial collagen fibres grouped cells into layers and branched across spaces between the layers whereas the layers in SHR blocks were tightly approximated and there were dense planes of collagen separating them. Furthermore, the epimysial collagen mesh was more obvious in the SHR blocks and both pericellular and perivascular collagen were substantially greater with some regions of cellular necrosis evident.

We believe that these differences in myocardial organisation are responsible for differences in both local and global passive mechanical function. The increased ECM around cells and layers will change cell-to-cell mechanical coupling and limit the ability of myocardial layers to shear relative to each other, likewise increased epimysial collagen will limit ventricular expansion. Additionally, dense collagen around both vessels and individual cells may impair diffusion of oxygen and metabolites and lead to tissue necrosis and scar formation. These changes in local mechanical properties are very likely to be the cause of the reduced ventricular compliance in SHR hearts as compared to WKY and will subsequently result in impaired diastolic function in the diseased hearts.

Autoperfused hindlimb as a physiologically relevant model to study skeletal muscle function and metabolism

A.J. Hoy, G.E. Peoples and P.L. McLennan, Smart Foods Centre, Department of Biomedical Science, University of Wollongong, NSW 2522, Australia. .SP

The aim of this project, was to establish a small animal model that could provide adequate oxygen delivery at physiological vascular resistance to support studies of metabolism and blood flow in both resting and contracting muscle.

Male Hooded Wistar rats were anaesthetised with sodium pentobarbital (6mg/100g body weight i.p.). Polyethylene tubing filled with 0.9% heparinised saline containing 6% w/v dissolved dextran 70 was used as cannulae at all times. The left carotid artery was cannulated to record mean systemic blood pressure. The right femoral artery (non-perfused) was cannulated to supply arterial blood to the left hindlimb femoral artery (perfused) and allow arterial sampling. This loop was passed through a pump for constant flow with perfused hindlimb pressure recorded via a side arm pressure transducer distal to the pump. Passive venous return occurred via a cannula from the left femoral vein to the right external jugular vein, allowing for venous sampling. The left sciatic nerve was stimulated via a bipolar electrode with force produced recorded. Blood was sampled from the venous and arterial loops and oxygen uptake ($\dot{V}O_2$) determined using the Fick equation. Rats were kept normothermic and were ventilated during experiments to control arterial O_2 content. Extracorporeal blood volume was ≤ 2 ml.

At $1 \text{ ml}\cdot\text{min}^{-1}$ mean systemic pressure was $99.32 \pm 4.06 \text{ mmHg}$ ($n = 44$, mean \pm SEM), mean hindlimb perfusion pressure was $92.31 \pm 3.08 \text{ mmHg}$. $\dot{V}O_2$ was $0.328 \pm 0.022 \mu\text{mol}^{-1}\cdot\text{min}^{-1}\cdot\text{gww}^{-1}$ and $(a-\bar{v})O_2$ diff of $5.03 \pm 0.35 \text{ ml}\cdot 100\text{ml}^{-1}$. At $2 \text{ ml}\cdot\text{min}^{-1}$ with muscle stimulation mean hindlimb pressure was $166.41 \pm 5.16 \text{ mmHg}$ ($n = 8$) with a $\dot{V}O_2$ of $0.570 \pm 0.084 \mu\text{mol}^{-1}\cdot\text{min}^{-1}\cdot\text{gww}^{-1}$ and $(a-\bar{v})O_2$ diff of $4.44 \pm 0.69 \text{ ml}\cdot 100\text{ml}^{-1}$. $\dot{V}O_2$ is decreased at higher flow rates without stimulation ($0.190 \pm 0.02 \mu\text{mol}^{-1}\cdot\text{min}^{-1}\cdot\text{gww}^{-1}$) but with muscle contraction was increased. The Table summarises the blood profile during both flow rates.

Arterial		Venous	1ml/min	2ml/min + stim
pH	7.37 ± 0.01	pH	7.27 ± 0.01	7.29 ± 0.01
pCO ₂ (mmHg)	34.77 ± 0.72	pCO ₂ (mmHg)	51.44 ± 1.11	50.60 ± 1.45
pO ₂ (mmHg)	101.47 ± 1.31	pO ₂ (mmHg)	46.33 ± 1.49	45.40 ± 2.52
Hct (%)	45.41 ± 0.42	Hct (%)	47.11 ± 0.42	49.75 ± 0.92
K ⁺ (mmol/l)	3.65 ± 0.04	K ⁺ (mmol/l)	3.33 ± 0.05	3.70 ± 0.05
Hb (g/dL)	14.80 ± 0.14	Hb (g/dL)	15.37 ± 0.14	16.26 ± 0.31
SO ₂ (%)	97.57 ± 0.10	SO ₂ (%)	71.22 ± 1.77	71.69 ± 3.71

The development of an autoperfused rat hindlimb by this laboratory gives rise to a physiologically relevant model to study skeletal muscle function and metabolism.

Vascular remodeling and changes in cellular coupling during vascular disease

N.M. Rummery, S.L. Sandow, T.D. Brackenbury and C.E. Hill, Division of Neuroscience, John Curtin School of Medical Research, Australian National University Canberra, ACT 0200, Australia. .sp -0.25c

Changes in blood vessel morphology and function, including vascular remodeling and endothelial dysfunction, accompany the increase in peripheral vascular resistance and blood pressure, characteristic of hypertension. Altered gap junction expression has also been described during hypertension (Severs, 1999; Rummery *et al.*, 2002). This study examined the nature of vascular remodeling in two functionally different blood vessels, and correlated this with changes in the distribution of Cxs during the development of hypertension.

The development of hypertension in the spontaneously hypertensive rat (SHR) begins at approximately 4 weeks of age, animals becoming hypertensive compared to age matched control Wistar-Kyoto rats (WKY) at 9 weeks of age (Rummery *et al.*, 2002). In all experiments, rats were anaesthetised with ketamine/rompun (44/8 mg/kg respectively, i.p.) and tissue was prepared for electron microscopy, RNA extraction or immunohistochemistry.

Electron microscopy was used to determine structural characteristics of thoracic aorta (ThA) and caudal artery (CA) obtained from 12 week SHR and WKY. In the CA, but not the ThA, luminal diameter was decreased, while the number of smooth muscle cell layers and the medial cross-sectional area was increased in SHR compared to the WKY. Remodeling of the endothelium was examined in the ThA and CA using immunohistochemistry (IHC). In the 3-week old CA, there was no difference in endothelial cell (EC) morphology between strains, while at 12 weeks, area, length and perimeter of ECs was reduced in SHR. Between 3 and 12 weeks, there was an increase in area and a decrease in length of ECs in WKY, while the area, length and perimeter of ECs in SHR decreased. EC morphology was not different in the ThA of SHR compared to WKY at 12 weeks.

Expression of mRNA and protein for Cxs 37, 40, 43 and 45 was quantified in the ThA and CA of the WKY and SHR using real-time PCR and IHC. At 12 weeks, Cx43 predominated in the ThA, punctate labeling being found in the media. Cx45 was detected in the media of the ThA and CA. Expression of both Cxs was significantly reduced in the SHR. Cx37 was abundantly expressed in the media of the CA, and sparsely in the ThA. This expression did not differ in either artery during hypertension. In the endothelium, Cxs 37, 40, and 43 were detected in both vessels. The density of Cx37 expression was significantly reduced in the endothelium of the ThA in SHR compared to WKY, while Cx40 was decreased in the CA. Between 3 and 12 weeks, the density of Cx40 was reduced in the SHR at 12 weeks compared to 3 weeks of age.

At 3 weeks, mRNA for Cxs 37 and 43 was equally expressed in the ThA of both WKY and SHR, while Cxs 40 and 45 were sparse. In the ThA, expression of protein for Cx43 was similar in both strains, while Cxs 37, 40 and 45 were not detected. In the CA, mRNA for Cx37 was abundantly expressed in both WKY and SHR however expression was significantly less in the WKY. Similarly, mRNA for Cx45 was decreased in the WKY. In the CA, there were no differences in Cx protein expression between strains. Between 3 and 12 weeks, there was no difference in mRNA expression in the ThA. In the CA, mRNA for Cxs 37 and 40 was greater at 3 week compared to 12 weeks in both strains, while Cx45 was greater in the CA of the WKY at 3 weeks. Expression for Cxs 37 and 43 in the ThA was greater in the WKY at 12 compared to 3 weeks. In the CA of both WKY and SHR, protein for Cx45 was greater at 12 compared to 3 weeks, however in the SHR, this was not significant. Expression for Cxs 37, 40 and 43 was not altered in the media of the CA during development.

Results indicate that vascular remodeling occurs in the media and endothelium of muscular but not elastic arteries during hypertension. In the endothelium this remodeling develops coincident with the increasing blood pressure. Changes in Cx expression during hypertension differed depending on the vessel studied, with significant changes occurring with the development of hypertension. The

changes described here may have significant consequences for blood vessel function during the development of hypertension.

Severs, N.J. (1999) *Novartis Foundation Symposium*, 219:188-211.

Rummery, N.M., McKenzie, K.U.S., Whitworth, J.A. & Hill, C.E. (2002) *Journal of Hypertension*, 20:247-253.

Initiation and coordination of vasomotion in rat cerebral arteries

R.E. Haddock, T.D. Brackenbury and C.E. Hill, Division of Neuroscience, John Curtin School of Medical Research, Australian National University, Canberra, ACT 2601, Australia. .SP

In cerebral blood vessels, rhythmical contractions in vessel diameter, or vasomotion, play an important role in determining blood flow and vascular resistance. In mesenteric arteries, the endothelium and cGMP have been shown to be essential for initiating vasomotion, presumably through the release of nitric oxide (NO) (Peng *et al.*, 2001), while cell coupling is suggested to coordinate calcium oscillations (Sell *et al.*, 2002). Vasomotion in the basilar artery is dependent on intracellular calcium stores and an interplay between voltage activated calcium and potassium channels (Haddock & Hill, 2002), while the role of the endothelium and cell coupling is unknown. We have therefore investigated the role and distribution of vascular connexins (Cx) and the role of the endothelium in the initiation and coordination of vasomotion in the juvenile rat basilar artery.

Wistar rats (14-17 days) were anaesthetised with ether and decapitated (Animal Experimentation Ethics Committee, ANU). The basilar artery and its branches were isolated and pinned in a recording chamber which was perfused with physiological saline. Changes in membrane potential were measured with sharp microelectrodes (140-220 M Ω), which were filled with propidium iodide to identify the impaled cells. Changes in arterial wall or individual smooth muscle cell (SMC) intracellular calcium ($[Ca^{2+}]_i$) were assessed using Fura 2-AM, and either photometry or an intensified CCD camera respectively. Contractions of the same vessels were simultaneously recorded using videomicroscopy. Immunohistochemistry was performed on intact vessels following perfusion fixation (2% paraformaldehyde in phosphate buffer) and imaged using confocal microscopy. Serial section electron microscopy was used to investigate the presence of myoendothelial gap junctions (MEJGs).

Under control conditions, rhythmical depolarisations and $[Ca^{2+}]_i$ oscillations in both the arterial wall and in individual SMCs preceded rhythmical contractions. Membrane potential recordings from either SMCs or ECs were not significantly different and serial section electron microscopy confirmed that MEJGs connected the endothelium to the SMCs. The NOS inhibitor L-NAME (10 μ M) and the selective guanylate cyclase inhibitor ODQ (10 μ M) increased the frequency and amplitude of rhythmical activity and constricted the vessel. ODQ, but not L-NAME, hyperpolarised the vessel. Removal of the endothelium resulted in irregular contractions, asynchronous $[Ca^{2+}]_i$ oscillations in adjacent SMCs and a small depolarisation of the vessel. Addition of ODQ to endothelial denuded preparations prevented the constriction and augmentation of residual rhythmical activity induced by cGMP inhibition, but had no effect on the hyperpolarisation. Cx37, 40 and 43, but not Cx45, were found in the endothelium, while Cx 37, 43 and 45 were expressed to a lesser extent in SMCs. The gap junction uncoupler ^{37,43}Gap 27 (100 μ M) abolished rhythmical activity and hyperpolarised the SMCs, while ⁴⁰Gap 27 resulted in irregular contractions and asynchronous $[Ca^{2+}]_i$ oscillations in SMCs, but had no effect on membrane potential.

We conclude that the endothelium is essential for the coordination but not initiation of $[Ca^{2+}]_i$ oscillations and vasomotion in the basilar artery. This does not occur through the release of NO and activation of a depolarising current, but may instead be due to electrical coupling through MEJGs containing Cx40. The hyperpolarisation caused by ODQ suggests effects on ion channels of additional cGMP within SMCs. The persistence of vasomotion in the presence of ODQ confirms that cGMP was also not responsible for the initiation of vasomotion. Together the data indicate that the mechanism responsible for the initiation of vasomotion in cerebral arteries differs from that in systemic vessels.

Haddock R.E. & Hill C.E. (2002) *Journal of Physiology*, 545, 615-627.

Peng H., Matchkov V., Ivarsen A., Aalkjaer C. & Nilsson H. (2001) *Circulation Research*, 88, 810-815.

Sell M., Boldt W. & Markwardt F. (2002) *Cell Calcium*, 3, 105-120.

Functional remodeling in response to prolonged agonist exposure or elevated pressure delays arteriolar relaxation

S.J. Potocnik¹, M.A. Hill¹, L.A. Martinez-Lemus² and G.A. Meininger², ¹Microvascular Biology Group, School of Medical Sciences, RMIT University, Melbourne, Vic. 3081 Australia and

²Department of Medical Physiology, College of Medicine, Texas A&M University, College Station, Texas 77843, USA.

While arteriolar contraction is dependent on Ca²⁺- induced myosin phosphorylation, other mechanisms including Ca²⁺ sensitisation and time-dependent phenomena such as cytoskeletal and cellular reorganisation may contribute to contractile events. We have hypothesised that if arteriolar smooth muscle exhibits time-dependent behavior that this may be manifested in differences in relaxation following short and long-term exposure to contractile agonists. Consistent with this, isolated skeletal muscle arterioles showed a significantly delayed return to pre-agonist exposure diameter following washout of noradrenaline (5µM) which had been applied for 4 hours as compared to 5 minutes. A similar phenomenon was not observed when contraction was induced by KCl (75 mM) suggesting a possible requirement for receptor activation. As removal of extracellular Ca²⁺ caused a rapid return to passive diameter, the delayed relaxation following 4 h norepinephrine exposure was viewed as being functional in character. The enhanced constrictor response following prolonged norepinephrine exposure was prevented by several tyrosine kinase inhibitors (genistein, PP1 and PD9859; Hill *et al.*, 2003). Arterioles were cannulated onto glass micropipettes and studied *in vitro* using video microscopy, following dissection (4°C) from the cremaster muscle, sampled from anaesthetised rats. Further studies presented here showed that the impaired relaxation is not inhibited in the presence of the Rho kinase inhibitor Y27632. This observation suggests the mechanism is not due to Rho kinase-induced Ca²⁺ sensitisation events contributing to an enhanced constrictor response, while the former implicates events involving a cSrc/p42/44 MAP kinase pathway. In these spontaneously myogenic arterioles, the constrictor stimulus of elevated intraluminal pressure, from 50 to 120 mmHg for 4 hours also results in delayed myogenic vasodilation when the luminal pressure is returned to 50 mmHg. Confocal microscopy studies (using a fluorescein dye exclusion imaging method) aimed at examining smooth muscle cell position within the intact vessel wall suggested that cellular realignment occurs during the 4 hour agonist exposure, consistent with the proposition that early remodelling events are occurring during this 4 hour time course. In particular, an increase in the extent of overlap between neighbouring vascular smooth muscle cells was observed after the prolonged agonist exposure period. Collectively, these data are consistent with the action of prolonged constrictor stimuli, either noradrenaline exposure or elevated luminal pressure, resulting in an early functional remodelling process that involves tyrosine kinase-dependent processes and results in impaired relaxation on removal of the stimulus.

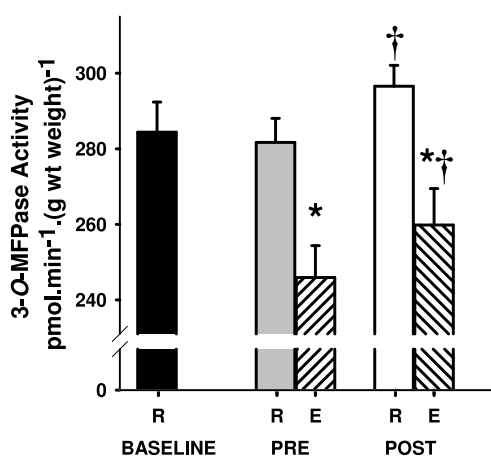
Hill, M.A., Potocnik, S.J., Martinez, L.A. & Meininger, G.A. (2003) *American Journal of Physiology*, 285:H849-H856.

Opposing effects of acute and chronic high intensity exercise on Na⁺K⁺ATPase activity in skeletal muscle

R.J. Aughey¹, K.T. Murphy¹, S.A. Clark², J. Christie², A.G. Hahn³, C.J. Gore³, A.P. Garnham⁴, C.M. Chow⁵, J.A. Hawley² and M.J. McKenna¹, ¹Centre for Rehabilitation, Exercise and Sports Science, Victoria University of Technology, Melbourne, ²RMIT University, Melbourne, ³Australian Institute of Sport, Canberra, ⁴Deakin University, Melbourne and ⁵University of Sydney, NSW, Australia.

The Na⁺K⁺ATPase enzyme is critical in maintaining muscle trans-sarcolemmal [Na⁺] and [K⁺] gradients and membrane excitability. However, repeated maximal muscle contractions reduce maximal Na⁺K⁺ATPase activity (Fraser *et al.*, 2002). High-intensity interval training is commonly used by endurance athletes to improve endurance performance, but the effects of acute high-intensity interval exercise on muscle Na⁺K⁺ATPase activity are not known. Furthermore, although sprint training increases muscle Na⁺K⁺ATPase content (McKenna *et al.*, 1993), the effects of high-intensity interval training on muscle Na⁺K⁺ATPase activity are unknown. We therefore examined the possible contradictory effects of acute and chronic high-intensity interval exercise on the muscle Na⁺K⁺ATPase activity in seven male endurance-trained athletes.

A vastus lateralis muscle biopsy was taken at rest, 3-wks prior to (Base), at rest and immediately after exercise prior to (Pre) and after (Post) 3-wks of training. Muscle samples were analysed for maximal *in vitro* Na⁺K⁺ATPase (K⁺ stimulated 3-O-MFPase) activity. Performance was characterised by incremental $\dot{V}O_2$ and peak power output (PPO); and during a simulated 40km time-trial, by mean power output (MPO). A t-test was used for resting 3-O-MFPase activity to determine reproducibility (Base – Pre) and to compare change scores (Base-Pre, & Pre-Post) to identify a change with training. A two-way ANOVA with repeated measures was applied to test for main effects of exercise (Rest, Ex) and training (Pre, Post).



Resting muscle 3-O-MFPase activity did not differ between Base and Pre. Acute high-intensity interval exercise depressed muscle 3-O-MFPase activity by $12.7 \pm 1.2\%$ (mean \pm SEM, Exercise main effect, $P < 0.05$, *, see figure). In contrast, training increased 3-O-MFPase activity by $4.9 \pm 0.7\%$ (training main effect, $p < 0.05$, †, see figure). Resting 3-O-MFPase activity was increased after training by $5.4 \pm 1.0\%$ (Pre – Post change score, $P < 0.05$). Neither $\dot{V}O_2$ (Base 64.4 ± 1.6 ; Pre 64.3 ± 1.5 ; Post 65.8 ± 1.9), PPO (Base 368 ± 12 ; Pre 374 ± 13 ; Post 379 ± 14), or MPO in the 40km time-trial (Base 279 ± 12 ; Pre 303 ± 15 ; Post 303 ± 13) differed significantly after training.

In conclusion, Na⁺K⁺ATPase measures were reproducible in resting muscle. Acute and chronic high-intensity interval exercise had converse effects on Na⁺K⁺ATPase activity. The small rise in Na⁺K⁺ATPase activity with training was insufficient to improve exercise performance.

Fraser, S. F., Li, J. L., Carey, M. F., Wang, X. N., Sangkabutra, T., Sostaric, S., Selig, S.E., Kjeldsen, K. & McKenna, M. J. (2002) *Journal of Applied Physiology*, **93**, 1650-1659.

McKenna, M.J., Schmidt, T.A., Hargreaves, M., Cameron, L., Skinner, S.L. & Kjeldsen, K. (1993) *Journal of Applied Physiology*, **75**, 173-180.

This study was partially funded by an Australian Research Council SPIRT grant (C00002552).

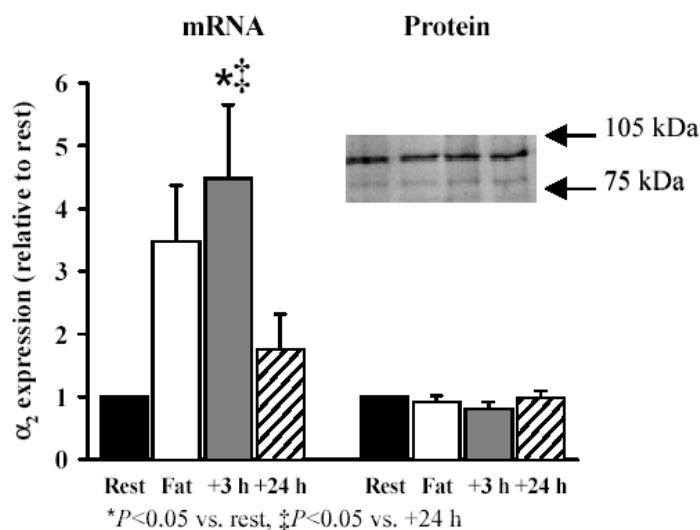
Acute intense exercise upregulates Na⁺,K⁺-ATPase isoform mRNA, but not protein expression in human skeletal muscle

K.T. Murphy¹, R.J. Snow², A.C. Petersen¹, R.M. Murphy², J. Mollica², J.S. Lee¹, A.P. Garnham², R.J. Aughey¹, J.A. Leppik¹, I. Medved¹, D. Cameron-Smith² and M.J. McKenna¹, ¹Muscle, Ions and Exercise Group, School of Human Movement, Recreation and Performance, Centre for Rehabilitation, Exercise and Sports Science, Victoria University of Technology, PO Box 14428, MCMC Melbourne, Victoria 8001 and ²Exercise, Muscle and Metabolism Unit, School of Health Sciences, Deakin University, Burwood, Victoria 3125, Australia.

The Na⁺,K⁺-ATPase comprises a catalytic α subunit (~100-112kDa) and a glycosylated β subunit (~40-60kDa), and belongs to a multi-gene family, with different genes encoding for four α (α_1 , α_2 , α_3 , α_4) and three β isoforms (β_1 , β_2 , β_3). Characterisation of the Na⁺,K⁺-ATPase isoforms expressed in healthy human skeletal muscle, and consequently also the acute exercise effects on these isoforms remains incomplete. We therefore investigated Na⁺,K⁺-ATPase isoform expression in human skeletal muscle, and the effects of a single bout of intense exercise on the mRNA and protein expression of these isoforms.

Fifteen healthy subjects (eight males, seven females) performed a single bout of isokinetic one-legged knee extensor exercise, continued until fatigue (time to fatigue 352 ± 69 s; mean \pm SD). A vastus lateralis muscle biopsy was taken from each subject at rest, fatigue (Fat), 3 h (+3 h) and 24 h (+24 h) post-exercise and analysed for mRNA and protein expression using Real-Time RT-PCR and immunoblotting, respectively. The Na⁺,K⁺-ATPase isoforms probed were α_1 , α_2 , α_3 , β_1 , β_2 and β_3 . To ensure maximal recovery of Na⁺,K⁺-ATPase enzymes, all immunoblots were conducted on crude muscle homogenates.

Muscle from each individual expressed gene transcripts and protein bands for each of the Na⁺,K⁺-ATPase α_1 , α_2 , α_3 , β_1 , β_2 and β_3 isoforms. These were also expressed in a skeletal muscle cell culture. Exercise immediately increased α_3 and β_2 mRNA expression ($P < 0.05$), whereas upregulation of α_1 and α_2 (see the Figure) isoform mRNA ($P < 0.05$) occurred at 24 h and 3 h post-exercise, respectively. Although significant differences between times were not found for β_1 and β_3 mRNA due to variable time-dependent responses, the peak post-exercise mRNA expression of these isoforms was elevated ($P < 0.05$). In contrast to the dramatic mRNA upregulation, exercise had no significant effect on the crude muscle homogenate protein expression of any of the α_1 - α_3 and β_1 - β_3 isoforms.



In conclusion, the vastus lateralis muscle from healthy humans expresses each of the Na⁺,K⁺-ATPase α_1 - α_3 and β_1 - β_3 isoforms at both the transcription and protein levels. Further, only 6 min of exercise was sufficient to dramatically increase the mRNA expression of each of these six isoforms. In contrast, this exercise bout had no effect on isoform protein expression, suggesting this

was an insufficient stimulus for Na⁺,K⁺-ATPase upregulation in muscle. These findings indicate different transcriptional and post-transcriptional Na⁺,K⁺-ATPase regulation with exercise in human skeletal muscle.

Increased Na⁺K⁺ATPase content is associated with improved potassium regulation during maximal exercise after sprint training in non-diabetics, but not in type 1 diabetes mellitus

A.R. Harmer^{*1}, P.A. Ruell¹, M.J. McKenna², D.J. Chisholm³, J.M. Thom¹, S.K. Hunter¹ and J.R. Sutton^{†1}, ¹School of Exercise & Sports Science, The University of Sydney, New South Wales, ²School of Human Movement, Recreation, and Performance, Centre for Rehabilitation, Exercise and Sports Science, Victoria University of Technology, Victoria, and ³Garvan Institute of Medical Research, Darlinghurst, New South Wales, Australia.

Sprint training attenuates the rise in plasma [K⁺] (Δ [K⁺]) during intense exercise (Harmer *et al.*, 2000) and increases Na⁺K⁺adenosine triphosphatase (Na⁺K⁺ATPase) content (McKenna *et al.*, 1993) in non-diabetics. In type 1 diabetes mellitus (T1D), Na⁺K⁺ATPase content has been reported to be higher than normal (Schmidt *et al.*, 1994). However, plasma [K⁺] may also be higher if subjects with T1D are hyperglycaemic (Shalwitz *et al.*, 1991). The effects of intense exercise and training on plasma [K⁺] regulation and Na⁺K⁺ATPase content in T1D have never been examined.

Eight subjects with T1D and seven non-diabetics (CON) undertook 7 weeks of sprint cycling training. Before training, subjects cycled to exhaustion at 130% $\dot{V}O_{2\text{ peak}}$. After training subjects cycled at the same workrate for the same duration. Subjects with T1D delayed insulin administration until after testing, which was conducted in the fasted state. Vastus lateralis biopsies obtained at rest were assayed for Na⁺K⁺ATPase content (³H]ouabain binding). Arterialised venous blood drawn during rest, exercise and recovery was analysed for plasma glucose, [K⁺], [Na⁺], catecholamines, insulin (IRI), and glucagon (IRG).

Na⁺K⁺ATPase content (T1D, 328±24; CON, 313±29 pmol•(g ww)⁻¹) and Δ [K⁺] with a single bout of maximal exercise did not differ between groups (T1D 1.3±0.1; CON, 1.6±0.3 mmol•l⁻¹). Noradrenaline and the rise in plasma glucose were higher in T1D during exercise ($P<0.05$). In late recovery in T1D, plasma glucose ($P<0.001$), [K⁺], and IRG/IRI were higher, and plasma [Na⁺] lower than in CON ($P<0.05$). Training increased Na⁺K⁺ATPase content by 8.2±2.2% and reduced Δ [K⁺] by 21±7% ($P<0.05$), with no difference between groups. These variables were correlated in CON ($r = -0.65$, $P<0.05$), but not T1D.

These findings demonstrate that acute regulation of plasma [K⁺] during a single bout of maximal exercise is similar in subjects with T1D who are relatively hypoinsulinaemic versus non-diabetics, however in late recovery, hyperglycaemia-induced hyperkalaemia may be anticipated. Sprint training enhanced plasma [K⁺] regulation, associated with increased Na⁺K⁺ATPase content in CON. Although K⁺ regulation was also improved in T1D, the lack of correlation with Na⁺K⁺ATPase content suggests that other factors, e.g. altered hormonal conditions (higher noradrenaline), may play a significant role during intense exercise.

Harmer, A. R., McKenna, M. J., Sutton, J. R., Snow, R. J., Ruell, P. A., Booth, J., Thompson, M. W., Mackay, N. A., Stathis, C. G., Cramer, R. M., Carey, M. F. & Eager, D. M. (2000) Skeletal muscle metabolic and ionic adaptations during intense exercise following sprint training in humans. *Journal of Applied Physiology*, 89: 1793-1803.

McKenna, M. J., Schmidt, T. A., Hargreaves, M., Cameron, L., Skinner, S. L. & Kjeldsen, K. (1993) Sprint training increases human skeletal muscle Na⁺-K⁺-ATPase concentration and improves K⁺ regulation. *Journal of Applied Physiology*, 75: 173-180.

Schmidt, T. A., Hasselbalch, S., Farrell, P. A., Vestergaard, H. & Kjeldsen, K. (1994) Human and rodent muscle Na⁺-K⁺-ATPase in diabetes related to insulin, starvation and training. *Journal of Applied Physiology*, 76: 2140-2146.

Shalwitz, R. A., Gingerich, R. L., McGill, J. B. & McDonald, J. M. (1991) Effect of hyperglycemia on plasma sodium and potassium concentration revisited. *Clinical Chemistry*, 37: 293-294.

* Current address: Physiotherapy Department, Sydney Adventist Hospital, Wahroonga, 2076

† Deceased 1996

Effect of exercise on intracellular insulin signalling in human skeletal muscle

K.F. Howlett¹, K. Sakamoto², H. Yu², L.J. Goodyear² and M. Hargreaves¹, ¹School of Health Sciences, Deakin University, Burwood, 3125, Australia and ²Joslin Diabetes Center, Harvard Medical School, Boston, 02215, USA. .SP

Exercise enhances skeletal muscle insulin action, and subsequently affects a number of insulin sensitive processes such as glucose uptake and glycogen synthesis. The effects of exercise on insulin action and glucose homeostasis have important implications for the maintenance of good health and in the treatment and prevention of type 2 diabetes. However, the underlying mechanism/s mediating the increase in skeletal muscle insulin action following exercise are equivocal. One hypothesis is that exercise or muscle contraction enhances intracellular insulin signalling events downstream of the insulin receptor. Recently we have demonstrated in mouse skeletal muscle, that prior exercise enhances insulin-stimulated insulin receptor substrate-2 (IRS-2) phosphorylation and associated phosphatidylinositol (PI) 3-kinase activity (Howlett *et al.*, 2002). However, no study has examined whether this exercise-mediated effect on IRS-2 signalling also occurs in human skeletal muscle. In light of this, the aim was to examine insulin signalling in human skeletal muscle in response to a hyperinsulinaemic euglycaemic clamp following an acute bout of exercise. Seven untrained males (24 ± 2 yr, 73 ± 3 kg, $\dot{V}O_{2\text{ peak}} = 3.63 \pm 0.22$ l.min⁻¹) were studied at rest and after 60 min of strenuous exercise ($75 \pm 4\%$ $\dot{V}O_{2\text{ peak}}$). Immediately following rest or exercise, a 120 min hyperinsulinaemic (40 mU.m⁻²) euglycaemic (5 mM) clamp was performed. Muscle biopsies were obtained at rest, post exercise, and 30 and 120 min of hyperinsulinaemia. Plasma insulin levels were similar during hyperinsulinaemia (Rest, 704 ± 34 ; Exercise, 691 ± 40 pmol.l⁻¹). Insulin-mediated glucose disposal rates were similar during the final 30 min of the clamp (Rest, 9.1 ± 1.1 ; Exercise, 8.3 ± 1.0 mg.kg⁻¹.min⁻¹). Insulin had no significant effects on IRS-1 and IRS-2 associated PI 3-kinase activity. Exercise, per se, tended to decrease IRS-1 (0.70 ± 0.13 fold) and IRS-2 (0.71 ± 0.10 fold) associated PI 3-kinase activity. Following exercise, insulin-stimulated IRS-2 associated PI 3-kinase activity tended to increase at 30 min (1.29 ± 0.11 fold) and was further enhanced at 120 min (2.83 ± 0.81 fold, $p < 0.05$). In contrast, following exercise insulin-stimulated IRS-1 associated PI 3-kinase activity increased to a peak at 30 min (1.88 ± 0.40 fold, $p < 0.05$), although remained elevated above basal at 120 min (1.67 ± 0.18 fold, $p < 0.05$). Despite the effect of exercise on these proximal insulin signalling proteins, there was no significant effect of exercise on insulin-stimulated activation of downstream insulin signalling proteins, including phosphorylation of Akt (Ser473) and GSK3- β (Ser9). However, exercise did result in an increase in insulin stimulated phosphorylation of GSK3- α (Ser21). In conclusion, prior exercise increases insulin-stimulated IRS-2 signalling in human skeletal muscle. It appears that insulin-stimulated IRS-1 and IRS-2 signalling in human skeletal muscle may be differentially regulated by exercise.

Howlett, K.F., K. Sakamoto, M.F. Hirshman, W.G. Aschenbach, M. Dow, M.F. White and L.J.

Goodyear. (2002). Insulin signaling after exercise in insulin receptor substrate-2 deficient mice. *Diabetes* 51: 479-483.

Exercise and myocyte enhancer factor 2 regulation in human skeletal muscle

M. Hargreaves and S.L. McGee, School of Health Sciences, Deakin University, Burwood, VIC 3125, Australia. .SP

We have previously shown that a single bout of endurance exercise increases GLUT-4 mRNA in human skeletal muscle (Kraniou *et al.*, 2000), implying an increased rate of transcription. It has also been demonstrated that myocyte enhancer factor 2 (MEF-2) binding activity is necessary for regulation of the GLUT-4 gene in skeletal muscle (Thai *et al.*, 1998). In the basal state, MEF-2 is believed to be inhibited by the class II histone deacetylases (HDACs), an association that is broken by phosphorylation of HDACs and their subsequent nuclear export. Association of MEF-2 with co-activators possessing histone acetylase (HAT) activity is thought to be mediated by the calcineurin/nuclear factor of activated T-cells (NFAT) pathway. Calcineurin dephosphorylates NFAT, resulting in its nuclear translocation where it recruits co-activators possessing HAT activity to MEF-2 allowing maximal MEF-2 DNA binding. While this is sufficient to initiate transcription, the rate of MEF-2 mediated transcription is increased by MEF-2 phosphorylation, with one putative kinase being p38 MAPK. In the present study, we sought to examine whether these various mechanisms may be involved in human skeletal muscle responses to exercise.

Seven healthy, untrained men (27 ± 3 yrs, 83 ± 4 kg, $\dot{V}O_{2\text{peak}} = 47 \pm 2$ ml•kg⁻¹•min⁻¹, mean \pm SD) performed cycle ergometer exercise for 60 min at a power output eliciting $74 \pm 2\%$ $\dot{V}O_{2\text{peak}}$. Muscle samples were obtained from vastus lateralis immediately before and after exercise and quickly (~15 s) frozen in liquid nitrogen for later analysis. Total and nuclear proteins were isolated as described previously (McGee *et al.*, 2003) and quantified by immunoblotting and co-immunoprecipitation. Nuclear HDAC5 content was decreased 54% ($P < 0.05$) following exercise, while there was no change in whole cell HDAC5 content. The association of HDAC5 with MEF-2 was reduced by 26% ($P < 0.05$). Nuclear NFAT content was similar before and after exercise. Total p38 MAPK phosphorylation increased 4.8 fold ($P < 0.05$), while nuclear p38 MAPK phosphorylation increased 1.8 fold ($P < 0.05$), with no change in the abundance of either total or nuclear p38 MAPK proteins. Association of p38 MAPK protein with MEF-2 increased 2.7 fold ($P < 0.05$) following exercise, while association of phosphorylated p38 MAPK with MEF-2 increased 1.75 fold ($P < 0.05$). These results suggest that HDAC5 and p38 MAPK are involved in the regulation of MEF-2 in response to exercise in human skeletal muscle, while the calcineurin/NFAT pathway may be less important under these conditions.

Kraniou, Y., Cameron-Smith, D., Misso, M., Collier, G. & Hargreaves, M. (2000) *Journal of Applied Physiology*, 88, 794-796.

McGee, S.L., Howlett, K.F., Starkie, R.L., Cameron-Smith, D., Kemp, B.E. & Hargreaves, M. (2003) *Diabetes*, 52, 926-928.

Thai, M.V., Guruswamy, S., Cao, K.T., Pessin, J.E. & Olson, A.L. (1998) *Journal of Biological Chemistry*, 273, 14285-14292.

Effect of exercise on Ca²⁺-sensitive protein kinases in human skeletal muscle

A.J. Rose¹, B. Mitchell², B.E. Kemp² and M. Hargreaves¹, ¹Exercise, Muscle & Metabolism Unit, School of Health Sciences, Deakin University, Vic., 3125 and ²St. Vincent's Institute of Medical Research, Fitzroy, Vic., 3065, Australia. .fp 10 S

There is evidence in rodents that PKC (Richter *et al.*, 1989; Chen *et al.*, 2002) and CaMKII (Tavi *et al.*, 2003) activities are higher in contracting skeletal muscle, and that these kinases may regulate skeletal muscle function, including metabolism, during exercise. To investigate this in humans, healthy men ($n=8$, 24 ± 5 yr, 23 ± 2 kg•m⁻², $\dot{V}O_{2\text{ peak}} = 51 \pm 6$ ml•kg⁻¹•min⁻¹) performed cycle ergometer exercise for 40 min at 76 ± 1 % $\dot{V}O_{2\text{ peak}}$ with skeletal muscle samples taken at rest and after 5 and 40 min of exercise. PKC and CaMKII expression and activities were examined by immunoblotting and *in vitro* kinase assays. There were no differences in maximal (+Ca²⁺/CaM) CaMKII activity during exercise compared with basal. Autonomous (-Ca²⁺/CaM) CaMKII activity was 9 ± 1 % of maximal at rest, unchanged at 5 min, and increased to 17 ± 1 % ($P < 0.01$) at 40 min. There were no differences in CaMKII expression ($P > 0.1$). There were no changes in cPKC or PKC θ activities ($P > 0.1$), however aPKC activity was ~70% higher ($P < 0.05$) at 5 and 40 min and total PKC activity was slightly higher at 40 min in an enriched membrane fraction ($P < 0.05$).

The activities of these kinases were also examined in response to maximal aerobic exercise. Healthy men ($n=9$, 25 ± 5 yr, 24 ± 2 kg•m⁻², 52 ± 9 ml•kg⁻¹•min⁻¹) performed cycle ergometer exercise for 10 min at 50 % $\dot{V}O_{2\text{ peak}}$, after which the workload was increased to elicit 100 % $\dot{V}O_{2\text{ peak}}$ with muscle samples taken at rest and at volitional fatigue. Autonomous CaMKII activity was increased by 74 ± 17 % ($P < 0.001$) with no change in maximal CaMKII activity. There were no changes in total PKC, PKC δ , PKC θ , or aPKC activities.

These data demonstrate that CaMKII and aPKC are activated in contracting skeletal muscle, and thus may represent key signalling proteins potentially regulating skeletal muscle function and metabolism during exercise in humans.

Chen, H.C., Bandyopadhyay, G., Sajan, M.P., Kanoh, Y., Standaert, M., Farese, R.V. Jr. & Farese, R.V.

(2002) *Journal of Biological Chemistry*, 277, 23554-23562.

Richter, E.A., Cleland, P.J., Rattigan, S., Clark, M.G. (1989) *FEBS Letters*, 217, 232-236.

Tavi, P., Allen, D.G., Niemela, P., Vuolteenaho, O., Weckstrom, M. & Westerblad, H. (2003) *Journal of Physiology*, in press.

The effect of repeated bouts of level and downhill treadmill walking on plasma interleukin-6

N.C. Bevan¹, P.M. Bergin¹, T.J. Connor^{1,2} and S.A. Warmington¹, ¹*Department of Physiology and*
²*Institute of Neuroscience, The University of Dublin, Trinity College, Dublin 2, Ireland. .SP*

The increase in plasma interleukin-6 (IL-6) appears dependent on factors such as exercise intensity, duration, muscle mass recruited, and mode (concentric vs eccentric) (for review see Febbraio & Pederson, 2002). Particularly during the later stages of prolonged endurance exercise the increase in plasma IL-6 is most pronounced. The late appearance in the plasma following prolonged exercise suggests that a component of the rise in plasma IL-6 may be via damage to skeletal muscle. A single bout of eccentric exercise produces significant muscle damage. However, the same eccentric exercise bout performed some weeks afterward shows minimal damage to the active muscle (McHugh *et al.* 1999). Therefore, the aim of this experiment was to investigate the plasma IL-6 response with a single eccentric exercise bout, and 5 weeks later, with another identical “repeated” bout of eccentric exercise, to assess the contribution of skeletal muscle damage to the IL-6 response.

Fifteen inactive males volunteered for this study. Following ethical approval subjects were randomly assigned to a concentric exercise group (CON; n=7) or an eccentric exercise group (ECC; n=8). Subjects performed two bouts of walking exercise separated by 5 weeks (B1 & B2) on a motor driven treadmill at a constant speed (5 km.hr⁻¹) for 90 min. CON walked on the flat (0° decline) while ECC walked downhill (14° decline). Forearm venous samples were collected at regular intervals Pre-, during and post-exercise for determination of plasma IL-6 (R&D systems ELISA kit). Maximal voluntary isometric contraction (MVC) of the quadriceps muscle group, and delayed onset muscle soreness (DOMS) were determined at the same time points, except during exercise. A 2-way ANOVA for repeated measures and Student-Newman-Keuls *post hoc* test was used to assess significance with p<0.05.

MVC and DOMS showed no muscle damage in either B1 or B2 in CON. However, there was significant muscle damage in ECC post B1 only (not B2). Similarly, plasma IL-6 was elevated in ECC only (towards the end of B1), and peaked immediately post-exercise. All changes returned to baseline levels within 7 days.

In this study exercise intensity was not different between B1 & B2 for both CON and ECC. With no muscle damage or change in plasma IL-6 in B2, yet elevated plasma IL-6 in ECC in B1, it appears that exercise-induced muscle damage contributes almost exclusively to the increase in IL-6 reported following under these low intensity walking exercise conditions.

Febbraio, M.A. & Pedersen, B.K. (2002) *FASEB Journal* 16, 1335-1347.

McHugh M.P., Connolly, D.A.J., Eston, E.J. & Gleim, G.W. (1999) *Sports Medicine* 18, 157-170.

Determinants of muscle buffer capacity

D. Bishop and J. Edge, School of Human Movement and Exercise Science, The University of Western Australia, 35 Stirling Highway, Crawley, WA 6009, Australia. .SP

Little is known about the stimulus required to increase muscle buffer capacity ($\beta_{in-vitro}$). It has been hypothesised that it is important that training is: (1) of high intensity; and (2) is performed under conditions of high skeletal muscle hydrogen ion (H^+) accumulation (Weston et al., 1996). We tested this first hypothesis by investigating the effects on $\beta_{in-vitro}$ of two training protocols of different intensity, but matched for total work. It has previously been shown that increasing the extracellular buffer concentration can reduce the skeletal muscle H^+ accumulation during high-intensity exercise (Costill et al., 1984). We therefore tested the second hypothesis by experimentally manipulating the extracellular buffer concentration during training.

For the first study, 18 untrained females (mean \pm SD: age 19 ± 1 y, mass 59.8 ± 5.8 kg) were randomly assigned to high-intensity interval training (INT-5) or moderate intensity continuous (CON-5) training. Training was matched for total work and consisted of 6 - 10 \times 2 min intervals (1 min rest) at 130 - 160% of lactate threshold (LT) (INT-5) or 20 - 35 min of continuous cycling at 85 - 95% of LT (CON-5), 3 \times per week for 5 weeks. For the second study, 10 untrained females (mean \pm SD: age 20 ± 3 y, mass 62.3 ± 10.0 kg) were also randomly assigned to one of two training groups, matched for total work. One group (BIC-8) ingested sodium bicarbonate ($NaHCO_3$, 0.4 g \cdot kg $^{-1}$) while the control group (INT-8) ingested a placebo ($NaCl$, 0.2 g \cdot kg $^{-1}$) prior to each training session. Training consisted of 6 - 12 \times 2 min intervals (1 min rest) at 130 - 180% of LT, 3 \times per week for eight weeks. Muscle biopsies (vastus lateralis) were taken at rest to determine muscle lactate ($[La^-]_m$), pH_m and $\beta_{in-vitro}$.

Training responses are summarised in the table. All training programs resulted in a significant improvement in $O_{2\ peak}$ and LT with no significant difference between groups. However, relative to CON-5, INT-5, INT-8 and BIC-8 had a significantly greater improvement in $\beta_{in-vitro}$. The pooled data revealed a significant negative correlation between initial $\beta_{in-vitro}$ and percent change with training ($r=0.58$; $P<0.05$).

Training	Peak O_2		LT		$\beta_{in-vitro}$	
	Pre	Post	Pre	Post	Pre	Post
CON-5	41.3 \pm 7.3	45.6 \pm 5.7*	137 \pm 33	152 \pm 29*	123 \pm 32	125 \pm 19
INT-5	42.8 \pm 6.6	48.1 \pm 7.4*	141 \pm 27	149 \pm 27*	126 \pm 15	150 \pm 19*
INT-8	40.7 \pm 5.6	47.7 \pm 6.1*	113 \pm 18	130 \pm 21*	140 \pm 32	161 \pm 19*
BIC-8	35.2 \pm 7.1	43.0 \pm 6.4*	109 \pm 21	137 \pm 20*	129 \pm 32	156 \pm 19*

* significantly different to pre-training ($p<0.05$)

Despite similar changes in aerobic fitness, INT-5 had a significantly greater increase in $\beta_{in-vitro}$ than CON-5. This suggests that it is the intensity of training, not the total work performed, that is the stimulus for change in $\beta_{in-vitro}$. We have also shown that ingesting $NaHCO_3$ and therefore altering the likely accumulation of H^+ during training, did not affect these adaptations.

Costill, D.L., Verstappen, F., Kuipers, H., Janssen, E. and Fink, W. (1984) *International Journal of Sports medicine* 5, 228-231.

Weston, A.R., Wilson, G.R., Noakes, T.D. and Myburgh, K.H. (1996) *Acta Physiologica Scandinavica* 157, 211-216.

Activation of renal calcium and water excretion by novel activators of the calcium-sensing receptor

A.D. Conigrave and H. Lok, School of Molecular and Microbial Biosciences (G08), University of Sydney, NSW 2006, Australia. (Introduced by M. Day) SP

Recently, two new classes of calcium-sensing receptor (CaR) activators have been identified. The type-II calcimimetics (e.g. NPS R-467) were developed from a lead phenylalkylamine compound identified in a large-scale drug screen (Nemeth *et al.*, 1998). Type-II calcimimetics sensitise the CaR to calcium ions by binding to a site in the receptor's transmembrane region (Hauache *et al.*, 2000). Several sub-classes of L-amino acids (including aromatic, polar, and aliphatic amino acids) have been shown to act as allosteric activators of the CaR (Conigrave *et al.*, 2000). The amino acid binding site is likely to lie in the conserved N-terminal, Venus FlyTrap domain. In the kidney, the CaR is expressed in multiple sites. These include the proximal tubule, the cortical thick ascending limb (CTAL) and the medullary collecting ducts (Ward & Riccardi, 2002). Expression of the CaR in the CTAL has been linked to the control of urinary calcium excretion. Expression of the CaR in the collecting tubule, on the other hand, has been linked to the control of urinary water excretion and osmolality. In particular, CaR activation may suppress vasopressin-induced water reabsorption facilitating the excretion of solutes such as calcium, phosphate and oxalate that might otherwise contribute to the formation of renal calculi (Brown & Hebert, 1996). This pattern of expression implies roles for CaR activators in the regulation of multiple renal functions including proximal tubular transport, calcium excretion and urinary concentration. In particular, CaR-active amino acids (e.g., L-Phe and L-Ala) and type-II calcimimetics are predicted to promote calcium excretion, raise urine flow and suppress urinary osmolality.

We have examined the impact of intravenously administered L-amino acids or the type-II calcimimetic, NPS R-467 on renal calcium and water excretion. In female Wistar rats (200-300 g), anaesthetised with halothane, both jugular veins were cannulated and the animals were infused (2-4 mL/h) with isotonic physiological saline solution (140 mM NaCl, 4.0 mM KCl, 15 mM NaHCO₃, 2.5 mM CaCl₂, 1 mM MgCl₂). After a 60 min equilibration, L-amino acids were infused for 60 min prior to return to the control solution. Blood samples (0.25 mL) were collected at regular intervals for analysis of creatinine, osmolality, total calcium and various amino acids. Urine samples were collected at 15 min intervals to assess flow rate, osmolality and creatinine, calcium and amino acids. In some experiments, bolus injections were administered to test for acute effects of R-467 and amino acids. The type-II calcimimetic R-467 enhanced urinary calcium excretion (~3 fold) and urinary flow rate. In addition, R-467 suppressed urinary osmolality consistent with an inhibitory action of the CaR on vasopressin-induced water reabsorption in the collecting ducts. R-467 also lowered serum total calcium levels as previously reported (Fox *et al.*, 1999). The inactive isomer, S-467 was much less effective than R-467 on all three parameters tested. Infusions of the CaR-active L-amino acid, L-Phe sufficient to raise the serum level from 0.05 mM to about 2 mM, also elevated calcium excretion (~2-fold) and urinary flow rate, and suppressed urinary osmolality. Bolus injections of L-Phe and L-Ala also acutely elevated urinary calcium excretion and flow rate and lowered osmolality.

Taken together the data are consistent with the idea that novel activators of the CaR including L-amino acids and type-II calcimimetics such as R-467 mimic the effects of elevated plasma Ca²⁺ concentration on urinary calcium excretion, flow rate and osmolality.

Brown, E. & Hebert, S.C. (1996) *Kidney International*, 49, 1042-1046.

Conigrave, A.D., Quinn, S.J. & Brown, E.M. (2000) *Proceedings of the National Academy of Sciences of the USA*, 97, 4814-4819.

Fox, J., Lowe, S.H., Petty, B.A. & Nemeth, E.F. (1999) *Journal of Pharmacology & Experimental Therapeutics*, 290, 473-479.

Hauache, O.M., Hu, J., Ray, K., Xie, R., Jacobson, K.A. & Spiegel, A.M. (2000) *Endocrinology*, 141, 4156-4163.

Nemeth, E.F., Steffey, M.E., Hammerland, L.G., Hung, B.C.P., van Wagenen, B.C., Delmar, E.G. & Balandrin, M.F. (1998) *Proceedings of the National Academy of Sciences of the USA*, 95,

4040-4045.

Ward, D.T. & Riccardi, D. (2002) *Pflügers Archiv European Journal of Physiology*, 445, 169-176.

Molecular changes in proximal tubule function in diabetes mellitus

P. Poronnik¹ and C.A. Pollock², ¹School of Biomedical Sciences, University of Queensland, St Lucia, QLD 4072 and ²Department of Medicine, University of Sydney, Royal North Shore Hospital, St Leonards, NSW 2065, Australia. (Introduced by David J Adams) .SP

Our studies focus on the changes in the tubulointerstitium (proximal tubule, cortical fibroblast and endothelial cells) that occur when exposed to a 'diabetic environment', i.e. high glucose, low density lipoproteins and cytokines implicated in the pathogenesis of diabetic nephropathy. The current discussion focuses on the specific changes in proximal tubule function that occur following exposure to high glucose. In the normal kidney, the proximal tubule plays a crucial role in the reabsorption of 50-70% of the filtered Na^+ and the receptor mediated uptake of the protein that crosses into the filtrate from the glomerulus. Diabetic nephropathy is frequently associated with increased Na^+ retention, proteinuria and thickening of the tubular basement membrane is the earliest histological abnormality.

Using experimental models, which include both primary cultures of human proximal tubule (hPTC) cells as well as immortalised cell lines, we found initially that high glucose increases the activity of Na^+ - H^+ exchanger 3 (NHE3), the key transporter that mediates Na^+ uptake in the proximal tubule. This increase is paralleled by an increase in the mRNA for NHE3. There is also a similar increase in the activity and protein levels of the V-H^+ -ATPase, which plays a role in HCO_3^- reabsorption. In a recent study we have shown that the activity of NHE3 is upregulated by exposure to albumin. NHE3 and V-H^+ -ATPase are also known to be critical in the endocytosis of albumin, and indeed further studies confirmed that tubular exposure to high glucose increased albumin uptake. These data suggest a possible mechanism linking defective Na^+ reabsorption and protein handling in the kidney in diabetes mellitus.

One of the key regulators of proximal tubule function implicated in the pathogenesis of diabetic nephropathy is angiotensin II (AngII). We have shown that tubular production of AngII is increased significantly following exposure to high glucose. As AngII is also known to increase the activity of both NHE3 and V-H^+ -ATPase this may underlie the abnormalities in transport and tubular protein reabsorption in diabetic nephropathy. The profibrotic cytokine transforming growth factor beta ($\text{TGF}\beta$) has been shown to be upregulated in animal models of diabetic nephropathy and normalised by blockade of the renin-angiotensin system. We have demonstrated that high glucose induces $\text{TGF}\beta$ mRNA within 30 minutes of exposure. $\text{TGF}\beta$ in turn induces both collagen and non-collagen matrix production in the proximal tubule, an effect that is facilitated by the autocrine production of CTGF.

Thus our data provide further insights into the mechanisms by which high glucose induces tubular pathology in the human kidney and are consistent with the deleterious effects of high glucose being mediated at least in part by elevated intrarenal AngII and downstream cytokine production.

Differential neural control of glomerular ultrafiltration

K.M. Denton, S.E. Luff, A. Shweta and W.P. Anderson, *Department of Physiology, Monash University, Victoria 3180, Australia*

SE described the renal nerves in his landmark book *The Physiology of the Kidney* (1937). Following the first kidney transplantations, the apparent lack of long-term effects on body fluid balance were taken as confirmation of the independence from nervous system control of renal vascular and tubular function. It is now appreciated that transplanted kidneys rapidly re-innervate and that changes in renal nerve activity are implicated in many clinical conditions (DiBona & Kopp, 1997).

The resurgence of interest in the neural control of renal function followed the first comprehensive anatomic study of the renal innervation (Barajas, 1978), demonstrating that all the major structural elements of the kidney were innervated. Although the glomerular afferent and efferent arterioles are densely innervated, the prevailing view today is that tubular innervation is of greater importance for body fluid homeostasis. Reviewing the literature, DiBona & Kopp (1997) argued that the evidence supports the hypothesis that changes in renal nerve activity around resting levels affect renin secretion and tubular function but not blood vessel tone. However, the majority of studies utilised electrical stimulation of the renal nerves, which does not resemble the normal nerve discharge pattern. Our studies suggest a very different situation.

Performing a detailed analysis of the renal innervation, we demonstrated that there are two distinct nerve types, that are differentially distributed to afferent and efferent arterioles (Luff *et al.*, 1992). Type I nerves almost exclusively innervate the afferent arteriole (Luff *et al.*, 1992). Type II nerves, are NPY positive (Anderson *et al.*, 2001) and evenly distributed on both arterioles (Luff *et al.*, 1992). We hypothesised that the different patterns of sympathetic outflow to the kidney may evoke selective changes in glomerular ultrafiltration.

We examined the effects of physiologically induced increases in renal sympathetic nerve activity (RSNA) in response to graded hypoxia on renal pre and postglomerular vascular resistances in anaesthetised rabbits (pentobarbitone, 90-150 mg plus 30-50 mg/h) (Denton *et al.*, 2002b). We demonstrated that 10% oxygen (O₂) caused neurally mediated increases in both pre and postglomerular resistance as reflected by the decrease in both renal blood flow (RBF) and glomerular filtration rate (GFR). However, 14% O₂ which induced a lesser increase in RSNA caused a predominant increase in postglomerular resistance and maintenance of GFR at a time when renal blood flow fell. These results provide evidence that different levels of reflexly induced increases in RSNA may differentially control pre- and post- glomerular vascular resistances, compatible with selective activation of Type I and II renal sympathetic nerves. A caveat to this conclusion was that, though in response to 14% O₂ plasma renin activity was not increased, intrarenal actions of neurally stimulated ANG II may have been responsible for the increase in postglomerular resistance in response to 14% O₂.

This question was investigated in rabbits receiving an ANG II clamp infusion (Denton *et al.*, 2002a). Measurements were made before (room air) and after 14% O₂. As seen in the previous study RSNA increased in response to 14% O₂ and decreased RBF without effecting GFR or arterial pressure. However, glomerular capillary pressure increased in both the vehicle and ANG II clamp groups during 14% O₂ indicating that ANG II was not responsible for the increase in glomerular pressure following RSNA. These results are compatible with our hypothesis that different populations of renal nerves selectively control pre and postglomerular resistance and hence glomerular pressure and ultrafiltration.

Anderson, W.P., Denton, K.M., Luff S.E. & Young, S.B. (2001) <http://iups.org/2001/iups/abstracts/pdfs/a1037.pdf>, IUPS Congress Abstract 1037.

Barajas, L. (1978) *Federation Proceedings*, 37:1192-1201.

Denton, K.M., Flower, R.L. & Anderson, W.P. (2002a) *Hypertension*, 40:408 (P77).

Denton, K.M., Shweta, A. & Anderson, W.P. (2002b) *Journal of the American Society of Nephrology*, 13:27-34.

DiBona, G.F. & Kopp, U.C. (1997) *Physiological Reviews*, 77:75-197.

Luff, S.E., Hengstberger, S.G., Mclachlan, E.M. & Anderson, W.P. (1992) *Journal of the Autonomic Nervous System*, 40:239-254.

Smith, H.W. *The physiology of the kidney*. Oxford University Press, New York, USA, 1937.

Neural control of renal medullary perfusion

R.G. Evans¹, G.A. Eppel¹, S.C. Malpas² and K.M. Denton¹, ¹Department of Physiology, PO Box 13F, Monash University, Victoria 3800, Australia and ²Department of Physiology, University of Auckland Medical School, Private Bag 92019, Auckland, New Zealand. .SP

Over the last decade, evidence has accumulated that the renal medullary circulation plays a key role in regulating arterial pressure in the long-term (Mattson, 2003). A favoured hypothesis rests on the notion of relatively poor autoregulation of medullary blood flow (MBF), allowing changes in MBF in response to changes in arterial pressure to initiate compensatory alterations in tubular sodium reabsorption. Indeed, alterations in MBF have been proposed as the chief mediator of pressure diuresis/natriuresis (Mattson, 2003). We have set out to elucidate the mechanisms that regulate MBF under physiological conditions. A key finding from our studies using laser Doppler flowmetry in anaesthetized (pentobarbitone, 90-150 mg plus 30-50 mg/h) and conscious rabbits, has been that vasoactive hormones can differentially affect MBF and cortical blood flow (CBF) (Evans *et al.*, 2000). This likely represents an important mechanism underlying hormonal control of blood pressure.

Until recently, our understanding of the impact of the renal sympathetic nerves on MBF has been rudimentary. Our recent findings show that MBF is less sensitive than CBF, to electrical stimulation of the renal nerves, particularly at low frequencies of stimulation (Leonard *et al.*, 2000). The responses of MBF to renal nerve stimulation appear to be similar in the outer and inner medulla (Guild *et al.*, 2002). We have also obtained evidence that the medullary circulation is normally insensitive to increases in endogenous renal sympathetic nerve activity within the physiological range, in that increases in renal sympathetic nerve activity of ~80% induced by hypoxia reduce CBF (by ~14%) but not MBF (Leonard *et al.*, 2001).

Our attention has now turned to elucidating the mechanisms underlying the relative insensitivity of MBF to renal nerve activation. Failure of these mechanisms would promote reductions in MBF in response to physiological activation of renal sympathetic nerve activity, which could in turn lead to salt and water retention and hypertension. We have preliminary evidence for a paradoxical role of angiotensin II in selectively blunting responses of MBF to activation of the renal sympathetic nerves. The renal medulla is unique in that, under certain conditions, angiotensin II can induce vasodilatation through release of nitric oxide and/or prostaglandins (Duke *et al.*, 2003). In anaesthetised rabbits, renal arterial infusion of angiotensin II at a dose that reduced basal CBF but not MBF, abolished reductions in MBF induced by renal nerve stimulation (Guild *et al.*, 2003). Ongoing studies are also investigating the roles of nitric oxide, prostaglandins, adrenoceptor subtypes, and sympathetic co-transmitters in the neural regulation of MBF.

Duke, L.M., Eppel, G.A., Widdop, R.E. & Evans, R.G. (2003) *Hypertension*, 42, in press.

Evans, R.G., Madden A.C. & Denton K.M. (2000) *Acta Physiologica Scandinavica*, 169, 297-308.

Guild, S.-J., Barrett, C.J., Evans, R.G. & Malpas, S.C. (2003) *Experimental Physiology*, 88, 229-241.

Guild, S.-J., Eppel, G.A., Malpas, S.C., Rajapakse, N.W., Stewart, A. & Evans, R.G. (2002) *American Journal of Physiology*, 283, R1177-R1186.

Leonard, B.L., Evans, R.G., Navakatikyan, M.A. & Malpas S.C. (2000) *American Journal of Physiology*, 279, R907-R916.

Leonard, B.L., Malpas, S.C., Denton, K.M., Madden, A.C. & Evans, R.G. (2001) *American Journal of Physiology*, 280, R62-R68.

Mattson, D.L. (2003) *American Journal of Physiology*, 284, R13-R27.

Gaining new insights into physiological function from biophotonics

M.B. Cannell, Department of Physiology, University of Auckland, PB92019, New Zealand. .SP

Compared to conventional electronic based instrumentation, photonic methods are exquisitely sensitive. As an example, it is quite easy to measure photon fluxes of a few per second while equivalent electron flows are far below that realised even with sensitive patch-clamp amplifiers. However, the sensitivity of biophotonic methods extends to well below the level of the single cell by providing methods to detect and manipulate even single molecules.

Two decades ago, physiologists struggled to make measurements of intracellular calcium with ion-sensitive electrodes and bio-luminescent probes but the development of new fluorescent molecules for calcium measurement has made calcium measurement quite straightforward – if not always precise and easy. Cell calcium measurements with imaging systems have revealed new levels of complexity in signaling and as a result of the advances in instrumentation and methods it is now clear that the cell does not achieve function like a well stirred bucket of constituents. For example, the discovery of calcium sparks a decade ago clearly reinforced this idea – but we still don't understand how excitation-contraction coupling really works. This problem will be highlighted by some recent results from our laboratory where we have tried to develop and test ways of measuring the minute calcium fluxes underlying calcium sparks.

The microanatomy of the cell must be important for helping turn the cell from a large number of lipid and water soluble chemicals into life. Here new light imaging techniques are playing an important role and combination of computer image processing with high resolution imaging techniques reveals new levels of complexity in cell structure. Furthermore, with biophotonic methods, we can look inside the living working cell (an obvious advantage for those who are interested in how the living cell works). This has always been the classical province of the physiologist.

Promising new directions for physiological research include manipulation of proteins with molecular techniques and again, biophotonics provides powerful methodologies to study the results of such experiments. In this symposium we will look at new data and methods being applied to increased our understanding of physiology. We will see how new biophotonic methods offer ways to probe cell function with unprecedented fidelity and sensitivity. When one considers what may now be achieved with these methods, it would seem that the future of molecular-based physiology is very bright indeed.

Biosensors for investigating neuronal Ca²⁺ signalling

D.A. Williams, M.L. Smart and C.A. Reid, Department of Physiology, University of Melbourne, Victoria 3010, Australia. .SP

Biosensors are genetically engineered protein sensors of a selected intracellular target (e.g. ions, metabolites) that can be directed to intracellular locations by targeting sequences that are encoded within the sequence of a protein. This presentation will focus on studies on designing and making new sensor molecules and addressing the utility of biosensors for making measurements, of Ca²⁺ (and ATP), in functionally important cell locations, such as pre-synaptic terminals. In particular, the coupling of these biosensors with fast imaging procedures will be highlighted by example studies.

New views of lens structure and function

P.J. Donaldson, A.C. Grey, B.R. Merriman-Smith, A.M.G. Sisley, C. Soeller, M.B. Cannell and M.D. Jacobs, Department of Physiology, School of Medical Sciences, University of Auckland, Auckland 006, New Zealand. .SP

The ability of the ocular lens to focus light on the retina is the result of a unique cellular physiology and tissue architecture, which eliminates light scattering and improves the optical properties of the lens. The lens is a relatively simple avascular tissue. A single layer of cuboidal epithelial cells covers its anterior surface. At the lens equator these epithelial cells divide, elongate and differentiate into fibre cells, which form the bulk of the lens. Fibre cells adopt a flattened hexagonal profile that facilitates packing into an ordered cellular array, which minimises light scattering. During differentiation, the fibre cells lose their organelles, and undergo significant changes in the expression of cytoplasmic and membrane proteins. Since lens growth continues throughout life, younger fibre cells are laid down on top of existing fibre cells, internalising these older cells and thereby creating an inherent gradient of fibre cell age.

Maintenance of this lens tissue architecture requires special mechanisms, not only to supply the older anucleate fibre cells with nutrients, but also to control the volume of these cells. It has been proposed that the lens operates an active micro-circulation system that delivers nutrients to, and removes wastes, from the lens, thereby maintaining ionic homeostasis and the volume of the inner fibre cells (Donaldson *et al.*, 2001). It is believed that the ionic currents that drive this internal circulation are generated by spatial differences in the distributions of ion channels and transporters between the younger nucleated fibre cells in the periphery, and the older anucleate cells in the interior of the lens.

To systematically study this circulation system we have developed a series of imaging protocols that have allowed us to quantitatively assess how the distribution and function of key transport proteins vary during the course of fibre cell differentiation. These protocols allow us to map protein distribution over large distances with subcellular resolution (Jacobs *et al.*, 2001). Studies conducted on gap junctions (Jacobs *et al.*, 2001), glucose transporters (Merriman-Smith *et al.*, 2003) and an adhesion molecule, MP20 (Grey *et al.*, 2003), will be reviewed to illustrate how the adoption of our imaging protocols can yield new insights into the relationship between lens structure and function.

Donaldson, P., Kistler, J. & Mathias, R.T. (2001) *News in Physiological Sciences*, 16, 118-123.

Grey, A. C., Jacobs, M.D., Gonen, T., Kistler, J. & Donaldson, P.J. (2003) *Experimental Eye Research*, in press.

Jacobs, M.D., Soeller, C., Cannell, M.B. & Donaldson, P.J. (2001) *Cell Communication & Adhesion*, 8, 349-353.

Merriman-Smith, B.R., Krushinsky, A., Kistler, J. & Donaldson, P.J. (2003) *Investigative Ophthalmology & Visual Sciences*, in press.

Support: New Zealand Health Research Council, Lottery Health Board, Marsden Fund, University of Auckland Research Committee.

Quantitative phase microscopy - a new way to interrogate the structure and function of unstained viable cells

C.L. Curl and L.M.D. Delbridge, Department of Physiology, University of Melbourne, Victoria 3010, Australia. .SP

The optical transparency of unstained viable cell specimens limits the extent to which information can be recovered from bright field microscopic view as these specimens generally lack visible, amplitude modulating components. However, if the phase-shift component of the cellular material is utilised, an information-rich image can be obtained. Optical phase microscopy, and derivatives of this technique such as Differential Interference Contrast (DIC) and Hoffman Modulation Contrast (HMC) have been widely applied in the visualisation of cellular specimens to enhance contrast. Whilst providing significantly enhanced contrast, useful in viewing specimens, the capacity to extract quantitative information from the phase content available in these optical techniques has not previously been explored.

Quantitative Phase Microscopy (QPM) is a new method for visualising transparent objects. This recently developed computational approach extracts quantitative phase measurements from images captured using a bright-field microscope without phase or interference contrast optics. QPM works via an algorithm which is applied to an in-focus image and a pair of equidistant de-focus images (one positive and one negative de-focus). From these images a phase map is generated which can be used to quantitatively emulate other contrast image modes such as DIC, dark field or HMC. The generation of these analogue images using phase mapping obviates the inherent problems associated with optical phase imaging, including cell edge distortion and edge halo effects. As it is implemented on an optically simple bright field microscope, the QPM methodology is also an economical alternative for cellular imaging applications.

Of particular importance is the capacity to quantitatively analyse the recovered phase images using QPM. The phase map generated from the bright field images contains information about cell thickness and refractive index and can allow quantitation of cellular morphology under 'real-time' conditions. For instance, the proliferative properties of human airway smooth muscle cells have been evaluated using QPM techniques to track cell culture confluency and growth (Curl *et al.*, 2002). In addition, cell volume measurement techniques have been applied to investigate the responses of erythrocytes to different osmotic challenges using QPM (Curl *et al.*, 2003).

QPM is a valuable new imaging tool which extends the capacity to interrogate viable cells to obtain structural and functional information in a rapid and non-destructive manner.

Curl C.L., Harris T., Kabbara A.A., Allman B.E., Roberts A., Nugent K.A., Harris P.J., Stewart A.G. & Delbridge L.M.D. (2002) *Proceedings of Australian Health and Medical Research Congress*, 1: 1126.

Curl C.L., Bellair C.J., Allman B.E., Roberts A., Nugent K.A., Harris P.J. & Delbridge L.M.D. (2003) *Proceedings of Experimental Biology 2003*: LB65.

High throughput imaging of extended tissue volumes

I.J. LeGrice, G. Sands, D. Hooks, D. Gerneke and B.H. Smaill, Bioengineering Institute & Physiology Department, University of Auckland, Auckland, New Zealand. .SP

In many fields, three-dimensional (3D) information is necessary to understand the organisation and spatial relationships within biological samples. Our group has previously used a confocal microscope and microtome to assemble large, high-resolution volume images from resin-embedded heart tissue (Young *et al.*, 1998). Digital reslicing, segmentation and volume rendering methods can be applied to the resulting volumes to provide quantitative structural data about the 3D organisation of myocytes, extracellular collagen matrix and blood vessel network of the heart not previously available. Information such as this is necessary to quantify the heart wall remodelling associated with various types of cardiac disease. It is also required for computer models, which are necessary to examine the effects of myocardial structure on the function of the heart. For example, we have used structural data extracted from an extended volume image of rat left ventricular myocardium (3.8mm × 0.8mm × 0.8mm at 1.5µm pixel size, 0.72×10⁹ voxels) to model the influence of structural discontinuities on the propagation of electrical activation in the heart (Hooks *et al.*, 2002). However, acquisition of volume images of this scale requires weeks of painstaking work using conventional techniques.

We have developed a novel high throughput imaging system that enables extended volume images to be collected flexibly and efficiently. The system consists of a confocal microscope (Leica TCS 4D) with a Kr/Ar laser, a variable speed Ultramill (Leica) which cuts to 1µm over a 75mm path using diamond or tungsten carbide tips, and a three-axis translation stage (Aerotech) with XYZ movement of 1000, 200 and 75mm, respectively at 100nm step size. This stage controls the positioning of specimens for imaging and milling. The microscope and mill are supported above the translation stage using rigid mounting systems designed to facilitate alignment of imaging and cutting planes. The system is mounted on an anti-vibration table. Z-stack volume images are acquired for overlapping x-y areas that cover the region of interest. The imaged volume is then milled off and the process is repeated. The images acquired may then be combined to reconstruct the volume in 3D. A major advantage of this method is that alignment of the sample elements is maintained throughout the imaging and milling operations, thereby preserving spatial registration and making reconstruction of the complete volume image easier and faster.

The system is controlled using a dedicated computer (Dell P4, 1.8GHz, 1GB RAM, Windows 2000) using custom software written using the LabVIEW™ programming language. A single user interface has been developed that enables image acquisition and milling to be controlled interactively or automatically and allows the operator to process, reconstruct and visualise the image volumes. The flexible user interface provides the ability to image chosen sub-volumes at high resolution, but placing them within the context of a large volume imaged at lower resolution.

Preliminary studies carried out with cardiac tissue specimens demonstrates that the system has the capacity to acquire a 62.5 million voxels per hour, each averaged over 8 scans. This translates to acquisition of a fully registered image volume 1mm³ at 1µm pixel size (10⁹ voxels), with 8× averaging, in 16 hours, representing greater than an order of magnitude speedup from the manual technique. The volumes imaged to date have been limited to heart tissue perfusion stained with picrosirius red. We are currently working on techniques to extend the range of tissues and fluorescent markers suitable for imaging with the system.

Hooks, D.A., Tomlinson, K.A., Marsden, S.G., LeGrice, I.J., Smaill, B.H., Pullan, A.J. & Hunter, P.J. (2002) Cardiac microstructure: implications for electrical propagation and defibrillation. *Circulation Research*, 91: 331-338.

Young, A.A., LeGrice, I.J., Young, M.A. & Smaill, B.H. (1998) Extended confocal microscopy of myocardial laminae and collagen network. *Journal of Microscopy*, 192, 139-150.

Active learning: If it works, why aren't we all doing it?

J.A. Michael, Department of Molecular Biophysics and Physiology, Rush Medical College, 1750 W. Harrison St., Chicago, IL 60612, USA. (Introduced by M. Roberts) .SP

What is active learning? We are all familiar with passive learning (rote memorisation). When students are engaged in active learning, on the other hand, they are overtly testing and refining their mental model of the new information being acquired. Active learning is usually interactive, and it is much more student-centered than passive learning. When students learn actively they are more likely to achieve meaningful learning (learning with understanding).

What does it mean to say that active learning “works?” When we ask whether active learning “works” we need to be clear about what criteria are being applied. Does more learning occur? Is more knowledge accumulated? Is less time required for learning? Is the learning “deeper” (greater understanding)? Is retention of new knowledge better . . . short-term or long-term? Or are we asking whether students, or even faculty, “like” it better than something else?

How would we attempt to find out if active learning “works?” Obviously we need to define some measure(s) of the outcomes to be assessed. We would want to try active learning in a wide variety of disciplines and courses, and with a wide variety of students. Unfortunately, the wider our sampling, the greater number of known and unknown variables that might be present to influence the outcomes we measure. Finally, we are clearly most interested in long-term outcomes (does active learning affect performance or behaviour one month, one year, 10 years later). But even if we can do the required studies, the longer we wait to look, the more intervening influences will be present (other than the exposure to active learning) that can potentially affect the results.

Does active learning, in fact, work? The available evidence, whether obtained in the cognitive science laboratory or the classroom, overwhelmingly supports the efficacy of active learning. That is to say, active learning has been shown to result in more learning with understanding, acquisition of more knowledge, and better retention of what is being learned, at least in the short term. There have been few, if any, studies carried out about the long-term effects.

If active learning “works,” why aren't we all doing it? It is clear that we do not all teach in a way that encourages and facilitates student active learning. There are many reasons for this. First, change is always difficult and many teachers perceive that a change to an active learning mode of teaching would require too much additional work. Second, teaching in an active learning environment can be scary for many teachers, even quite experienced ones. The teacher has less “control” than in a more passive learning environment and students are more likely to ask questions for which the teacher doesn't have ready answers. Third, many teachers fear that active learning will take so much time that they will not be able to “cover” all the material they think they need to cover. Finally, many teachers are discouraged from pursuing more active learning approaches by clear opposition from students who do want to have to learn in a new way.

What does it take to get started doing active learning? The two necessary, if not sufficient, steps are: (1) recognition that learning is done by the learner and only the learner, and (2) recognition that your job as a teacher, really the only thing that you can do, is to help the learner to learn! Once you have redefined your job in this way you will find that creating an active learning environment in your classroom is a natural step. Then, of course, you have to actually do it.

Promoting active learning with a Generic Skills Guide

M.I. Frommer, Department of Physiology, University of Sydney, NSW 2006, Australia. (Introduced by Ann Sefton) .SP

A “No Frills Generic Skills” guide for physiology students was compiled in 2000 to bring together various learning resources and exercises which had been produced over the previous decade, and presented to students in a series of learning tutorials. It was initially provided in paper form, but with the advent of WebCT as a means of managing resources for our units of study, it was incorporated into this platform for 2003.

The guide consists of nine sections, each headed by fairly simple questions which a student might ask in relation to a particular topic, and for which the answer is then provided. Anecdotal accounts of experience with earlier student cohorts are included in order to illustrate the development of our ideas over time. Additional documents include Exercises, a Skills Development Table, and five Appendices on different aspects of learning.

Use of the guide to foster active learning is encouraged by various links:

1. from Course Resources, the complete hyper-linked text
2. from Learning Tutorials, a summary table showing relevant connections
3. from notes for Writing Essays and Practical Reports
4. from Challenge Questions for practical self-assessment

The questions relate to three broad topic areas:

skills for science graduates -

- What are generic skills?
- Which generic skills are most relevant to science graduates?

skills for designing experiments, analysing and reporting data -

- What is meant by scientific method?
- What are the main ingredients of a successful experiment?
- How should I record my data? How should I analyse my results?
- How should I report my findings? How should I write scientific material?

skills for effective learning and exam performance -

- What are the characteristics of a successful learning style?
- What is the best way to study for exams?
- What new ways of learning can I try?

The additional documents include exercises on data handling, common confusions, logical thinking and concepts, excerpts from “The Making of Memory” (Rose, 1993), extended matching exercises and problem-based learning examples.

The question on a successful learning style is the most relevant to our symposium on Active Learning. The answer begins with three definitions of learning, lists four essential attributes of successful learning, then uses the analogy of building a wall, first developed by Mike Prosser (personal communication), to expand on eight key characteristics. It concludes with seven tips for taking responsibility for personal active learning, which are also included in our course guide.

How effective this learning resource for active learning has proven to be will be discussed with reference to various outcomes.

Rose, S. (1993) *The Making of Memory*. Bantam Books: London.

Where should we focus, teaching or learning?

M.L. Roberts, Discipline of Physiology, School of Molecular and Biomedical Science, University of Adelaide, Adelaide, South Australia 5005, Australia. .SP

If we were to list what we believe to be the generic characteristics of a good scientist and to compare that with what can be achieved by students in most undergraduate courses, we would find a great difference. The list for the scientist would contain attributes that would be described by the more complex categories in Bloom's (1956) taxonomy for all three domains of learning, cognitive, affective and psychomotor. The achievements of undergraduate students, particularly as reflected in assessment tasks, are best described by the simplest categories in the taxonomy, and are largely confined to the cognitive domain. Given that the more complex categories of learning cannot be achieved by passive processes, there is a need to develop strategies which allow active learning and which can be applied efficiently to classes with large numbers of students within the financial and human resources available. Ideally, one would achieve this with a planned development of the student's skills over the three years of the degree.

A number of approaches to the theory, tutorial and practical activities that are more active than the traditional physiology courses will be outlined. These have been planned to provide a sequential and graded development of skills. Evaluation of the impact of these learning activities has allowed an informed, progressive refinement in the quest of that elusive perfect course.

Bloom, B.S. (1956) *Taxonomy of educational objectives: the classification of educational goals*. London: Longman Group.

Role of the calcineurin signal transduction pathway in muscle regeneration in dystrophic *mdx* mice

N. Stupka, D.R. Plant and G.S. Lynch, Muscle Mechanics Laboratory, Department of Physiology, The University of Melbourne, Vic. 3010, Australia. .SP

Whilst sharing the same genotype as in Duchene muscular dystrophy (DMD), *mdx* mice exhibit a more benign dystrophic phenotype. Only the diaphragm muscle of *mdx* mice shows a severe and progressive pathology. Limb muscles of *mdx* mice undergo a bout of severe muscle degeneration at 2 to 4 weeks of age, but a high regenerative capacity ensures almost complete functional and structural recovery (Lynch *et al.*, 2001). The cellular mechanisms responsible for the enhanced regenerative capacity of *mdx* hindlimb muscles are not well understood. Calcineurin, a phosphatase enzyme that regulates transcription by sensing changes in intracellular calcium, has been shown to regulate skeletal muscle regeneration (Sakuma *et al.*, 2003). We have recently shown that inhibiting the calcineurin signal transduction pathway interferes with successful muscle regeneration in young *mdx* mice (Stupka *et al.*, 2002).

When 18 day old *mdx* mice were treated for 16 days with cyclosporine A (CsA; 30 mg•kg⁻¹•day⁻¹), an inhibitor of calcineurin, muscle regeneration was severely impaired. EDL and soleus muscle mass was ~25% lower and maximum force producing capacity was 30-35% lower in CsA treated *mdx* mice compared with vehicle treated littermates (Stupka, *et al.*, 2002). In the present study, we performed histological and immunohistochemical analyses to confirm the inhibitory effects of CsA treatment on muscle regeneration in young *mdx* mice.

Muscle sections were stained with haematoxylin and eosin for analysis of general muscle architecture, Van Gieson's stain for collagen deposition, and reacted with antibodies against myogenin (marker of satellite cell differentiation), and macrophages, as markers of regeneration. In CsA treated *mdx* mice, EDL and soleus muscle fibre cross-sectional area was ~25-30% smaller, had fewer centrally nucleated fibres, and more collagen, connective tissue, and mononuclear cell infiltration, than vehicle treated littermates. CsA administration did not affect macrophage infiltration in EDL or soleus muscles from *mdx* mice. Despite having significantly fewer centrally nucleated fibres, EDL and soleus muscles from CsA treated *mdx* mice had two to four times more myogenin positive nuclei than control *mdx* mice. Even though satellite cells from CsA treated *mdx* mice expressed myogenin they did not undergo normal differentiation and myoblast fusion.

Given that the calcineurin signal transduction pathway is essential for successful regeneration of hindlimb muscles in young *mdx* mice, we hypothesise that the pathology of the diaphragm muscle in *mdx* mice may be due to impairment of the calcineurin signal transduction pathway. To test this hypothesis, both upstream and downstream markers of the calcineurin signal transduction pathway in soleus, tibialis anterior, and diaphragm muscles from adult *mdx* and wild type (C57BL/10) mice were examined using a variety of biochemical and immunohistochemical techniques. Preliminary data suggests that there are differences in phosphorylated (inactivated) and dephosphorylated (activated) NFATc1 protein content and calcineurin-A protein content. Understanding the cellular mechanisms responsible for the difference in pathology between *mdx* diaphragm and hind limb muscles may provide insights into the regenerative process of dystrophic muscle and potential novel treatment strategies for DMD.

Lynch, G.S., Hinkle, R.T., Chamberlain, J.S., Brooks, S.V. & Faulkner, J.A. (2001) *Journal of Physiology*, 535, 591-600.

Stupka, N., Gregorevic, P., Plant, D.R. & Lynch, G.S. (2002) *Proceedings of the Australian Health and Medical Research Congress*, A2404.

Sakuma, K., Nishikawa, J., Nakao, R., Watanabe, K., Totsuka, T., Nakano, H., Sano, M. and Yasuhara, M. (2003) *Acta Neuropathologica* 105, 271-280.

Supported by grants from the Muscular Dystrophy Association (USA).

Muscle damage in *mdx* mice is reduced after treatment with streptomycin

N.P. Whitehead and D.G. Allen, *Department of Physiology, University of Sydney (F13), NSW 2006, Australia.*

Extensive research has been carried out on the cellular mechanisms underlying Duchenne Muscular Dystrophy (DMD) and a number of therapeutic options have been proposed for the treatment of this muscle disease. However, while much progress has been made, there are currently no effective therapies that significantly slow the progression of the disease. It has been hypothesised that dystrophin may be important in maintaining the normal function of certain membrane channels, in particular stretch-activated channels (SAC), and that calcium entry through these channels could initiate degradative pathways that leads to muscle fibre degeneration (Franco & Lansman, 1990). Recent research in our laboratory has focused on the role of SAC in muscle damage using *mdx* mice, an animal model of DMD. In single muscle fibres from *mdx* mice, it has been found that a component of the damage induced by a series of eccentric contractions can be prevented by two known SAC blockers, gadolinium and streptomycin (Yeung, Head & Allen, 2003; personal communication).

The current study aimed to investigate the role of SAC in muscle damage *in vivo* by using *mdx* mice that were given either normal drinking water (control) or water containing streptomycin (3mM). A previous study by McBride *et al.*, (2000) showed that this concentration of streptomycin prevents the muscle fibre depolarisation caused by eccentric contractions, which has also been attributed to the entry of Na⁺ through SAC. It is known that muscle damage in *mdx* mice begins at about 21 days after birth (McGeachie *et al.*, 1993), and that the first signs of regenerating fibres, evident by the presence of centrally located nuclei, occurs at 24 days. Thus, the mice used in the current study began the streptomycin treatment at 18 days, that is, three days before the onset of any muscle damage. At various times after the onset of the treatment, mice were killed by cervical dislocation and the EDL muscles were dissected out and placed in a normal physiological solution. Each muscle was attached to steel frame on a cork pad and immersed in embedding medium (Tissue-Tek) before being frozen in liquid nitrogen. Muscle cross-sections (10µm thick) were stained with haematoxylin and eosin, and viewed under a light microscope, with digital images taken for analysis of the location (central or peripheral) of muscle fibre nuclei.

At 24 days, the number of fibres with nuclei that were centrally located was 25% for control *mdx* mice compared to 4% for the streptomycin treated *mdx* mice. Over the next three days, the number of fibres with central nuclei for the control mice remained fairly similar with a peak of 30%. Values for the streptomycin treated mice also increased, peaking at 20%, but always remained lower than those of their age-matched control mice. This difference was statistically significant ($P < 0.05$; two-factor ANOVA). Other indicators of muscle damage, such as plasma creatine kinase levels and serum albumin localisation within muscle fibres, are currently being used in order to further investigate and quantify the effect of streptomycin in preventing damage in *mdx* muscle.

Franco, A. & Lansman, J.B. (1990) *Nature*, 344, 670-673.

McBride T.A., Stockert, B.W., Gorin, F.A. & Carlsen, R.C. (2000) *Journal of Applied Physiology*, 88, 91-101.

T.A. & Morgan, J.E. (1993) *Journal of the Neurological Sciences*, 119, 169-179.

Supported by the ARC

Influence of lowered $[Na^+]_o$ on single and trains of action potentials in soleus muscle fibres of the mouse

S.P. Cairns¹ and J.M. Renaud², ¹Division of Sport and Recreation, Faculty of Health, Auckland University of Technology, Private Bag 92006, Auckland 1020, New Zealand and ²Department of Cellular and Molecular Medicine, University of Ottawa, Ottawa, Canada. .SP

A reduction of extracellular $[Na^+]_o$ ($[Na^+]_o$), diminishes peak force and exacerbates fatigue during continuous tetanic stimulation of isolated skeletal muscle (Bezanilla *et al.*, 1972; Bouclin *et al.*, 1995; Cairns & Dulhunty, 1995). The mechanism for this effect is not fully understood. The aim of this study was to determine whether changes to the action potential could explain the reduced force at lowered $[Na^+]_o$ in mammalian skeletal muscle.

Isometric contractions and action potentials were elicited by supramaximal electric field stimulation via wire electrodes (10 V, 0.3 ms pulses) in isolated soleus muscles from mice. Muscles were bathed in control Krebs solution containing 147 mM Na^+ , and then at lowered $[Na^+]_o$ (100, 60, 40 or 30 mM; NaCl was replaced by N-methyl-D-glucamine) at 25°C. Intracellular recordings of action potentials were made using conventional glass microelectrodes. Trains of action potentials (50 or 125 Hz, for 2 s) were recorded in deep fibres after stretching the muscle, in order to prevent movement artifacts.

Single action potentials: Lowered $[Na^+]_o$ had no effect on the resting membrane potential but caused action potentials to become progressively smaller and broader. The overshoot fell from +32 mV at 147 mM Na^+ , to -20 mV at 30 mM Na^+ . All fibres were excitable at 147-60 mM Na^+ , but 19% and 40% of the fibres were inexcitable at 40 and 30 mM Na^+ , respectively.

Trains of action potentials: At 147 mM Na^+ , the 2-s trains of stimuli triggered action potentials on every occasion (100 or 250 action potentials), in association with a decrease in resting potential (between action potentials) and overshoot during the trains. At 40 mM Na^+ , complete trains of small action potentials were produced at 50 Hz, as observed in frog muscle fibres (2). However, at 125 Hz there was considerable skipping leading to a complete failure to generate action potentials, usually within 500 ms.

Action potentials and force: The peak twitch force - overshoot relationship (determined by combining twitch and single action potential responses) showed that force was well maintained until the overshoot disappeared. Trains of action potentials evoked at 125 Hz at 147 mM Na^+ , often had the peak of the action potential between 0 and -30 mV and this occurred without any fade (decline of peak force within a tetanus). At 40 mM Na^+ , the peak tetanic force fell to 53% of the control at 50 Hz, and to 19% of the control at 125 Hz; the difference was linked to the failure to generate action potentials during a train.

In summary, the decline of peak tetanic force at lowered $[Na^+]_o$ can be explained by (i) the presence of inexcitable fibres, and (ii) a failure to generate action potentials during trains when evoked at high frequency. There is a considerable safety margin for a decline of the overshoot before peak twitch force is impaired. Our data also suggests that (iii) smaller action potentials during a train may make a moderate contribution to the decline of peak tetanic force.

Bezanilla, F, Caputo, C, Gonzalez-Serratos, H. & Venosa, R.A. (1972) *Journal of Physiology*, 223: 507-523.

Bouclin, R, Charbonneau, E. & Renaud, J.M. (1995) *American Journal of Physiology*, 268: C1528-C1536.

Cairns, S.P. & Dulhunty, A.F. (1995) *Muscle and Nerve*, 18: 890-898.

This work was supported by grants from the New Zealand Lottery Grants Board, and the National Science and Engineering Research Council of Canada.

The effect of reactive oxygen species on muscle fatigue at room temperature compared to body temperature

T.R. Moopanar and D.G. Allen, Department of Physiology and Institute for Biomedical Research, University of Sydney (F13), NSW 2006, Australia. .SP

The production of reactive oxygen species (ROS), in particular superoxide anion radicals, plays a significant role in the modulation of muscle function (Clarkson & Urso, 2003). During intense exercise, there is an increased production of ROS, which leads to oxidative stress on muscle. Such stresses are thought to lead to the loss of contractile function, reduction in Ca^{2+} handling and contribution to fatigue (Reid, 2001). Also, it has been shown that increased temperature results in muscle dysfunction due to oxidative stress (van der Poel & Stephenson, 2002).

The present study is concerned with muscle performance during several bouts of fatigue at room temperature compared to body temperature. In particular, the influence of ROS at these temperatures is assessed in terms of onset of fatigue and maximum force.

Small muscle bundles (5 - 10 fibres per bundle) were dissected from the flexor brevis muscle of mice and were subjected to a fatigue protocol at room temperature (25°C) and at body temperature (37°C). Muscles were fatigued until force reached 50 % of the initial force. For each preparation, bundles were subjected to three fatigue runs (R1, R2, R3) allowing adequate time for muscles to recover between each run (45 minutes).

It was observed that there was no significant difference in the time taken for muscles to fatigue to 50% of the maximum force ($T_{1/2}$) at 25°C for R1, R2 and R3. Tiron (20mM), a free radical scavenger, was applied for 30 minutes between R1 and R2 and this treatment had no significant effect on the $T_{1/2}$ of R2 and R3 at 25°C. At 37°C however, $T_{1/2}$ was reduced to 65 ± 6 % for R2 and 26 ± 11 % for R3 compared to the $T_{1/2}$ for R1. When muscle preparations were treated with 20mM tiron, $T_{1/2}$ recovered to 106 ± 16 % for R2 and 103 ± 15 % for R3 compared to the value of R1. These results show that the ROS production has a profound effect on muscle fatigue at 37°C.

At 25°C there was no significant change in the fall of maximum force between each of the fatigue runs. At 37°C however, there was a significant decline in the maximum force when comparing R2 and R3 ($P < 0.05$); and R1 and R3 ($P < 0.01$). Treatment with tiron significantly reversed the decline of maximum force at 37°C. These results suggest that the production of free radicals at higher temperatures adversely affect the contractile properties, which are in some way responsible for the observed decline in maximum force.

The present study clearly shows that multiple bouts of fatigue at body temperature, in contrast to room temperature, progressively decreases muscle performance in terms of the onset of fatigue and maximum force development. Reduced muscle performance at 37°C appears to be partly caused by an increase in the production of ROS.

Reid, M.B. (2001) *Journal of Applied Physiology*, 90, 724-731

Urso, M.L. & Clarkson, P.M. (2003) *Toxicology*, 189, 41-54.

Van der Poel, C. & Stephenson, D.G. (2002) *Journal of Physiology*, 544.3, 765-776

Terence Rae Moopanar acknowledges receipt of an Australian Postgraduate Award - supported by the NHMRC

Nutritive and non-nutritive blood flow and oxygen consumption in active rat skeletal muscle

A.J. Hoy, G.E. Peoples and P.L. McLennan, Smart Foods Centre, Department of Biomedical Science, University of Wollongong, NSW, 2522. .SP

The objective of this study was to investigate the relationship between muscle metabolism and vascular distribution in the rat hindlimb. Clark *et al.*, (1995) categorised vasoconstrictors into two groups using a perfused sacrificed hindlimb model. All increase perfusion pressure, with Type A (low dose noradrenaline (NAd), vasopressin, angiotensin II) increasing oxygen uptake ($\dot{V}O_2$) redirecting blood into nutritive capillary beds associated with the muscle tissue) and Type B (serotonin (5-HT), high dose noradrenaline) decreasing hindlimb oxygen consumption, redirecting blood into non-nutritive capillary beds (associated connective tissue, adipose and septum). We used the in vivo autoperfused rat hindlimb with maintained vascular resistance to test the hypothesis that nutritive/ non-nutritive blood flow distribution can be observed in metabolically active (contracting) muscle and can be differentiated by vasodilators.

Male Wistar rats were anaesthetised with sodium pentobarbital (6mg/100g body weight i.p.). Polyethylene cannulae were filled with 0.9% heparinised saline containing 6% w/v dissolved dextran70. Mean systemic blood pressure was recorded from the left common carotid artery. The right femoral artery was cannulated to supply blood to the left femoral artery (perfused) passed through a pump for constant flow. Perfused hindlimb pressure was recorded via a side arm pressure transducer distal to the pump. Passive venous return occurred from the left femoral vein to the right external jugular vein. The left sciatic nerve was stimulated via a bipolar electrode and tension development recorded in the gastrocnemius muscle bundle. Vasoactive drugs (2 constrictor, 8 dilator) were prepared with saline and 0.01% ascorbic acid, and injected into the arterial loop. Blood was sampled from the venous and arterial loops and $\dot{V}O_2$ determined using the Fick equation.

During basal conditions, NAd (100nM – 256 μ M) increased mean perfusion pressure by up to $260 \pm 34\%$ ($P < 0.001$, $n = 6$, mean \pm SEM) and 5-HT (12.5 μ M – 100 μ M) by up to $225 \pm 30\%$ ($P < 0.005$, $n = 6$). The $\dot{V}O_2$ did not change during NAd infusion but decreased by up to $67 \pm 7\%$ during 5-HT infusion ($P < 0.005$). Mean perfusion pressure was decreased during the infusion of isoprenaline by $33 \pm 2\%$ ($P < 0.001$, $n = 6$) and histamine by $25 \pm 2\%$ ($P = 0.05$, $n = 6$) whilst $\dot{V}O_2$ did not change.

During muscle contraction, NAd increased mean hindlimb pressure by $96 \pm 3\%$ ($P < 0.001$) and 5-HT increased by $112 \pm 12\%$ ($P < 0.001$). $\dot{V}O_2$ by $46 \pm 10\%$ ($P < 0.05$). Isoprenaline and histamine decreased mean perfusion pressure by $24 \pm 3\%$ ($P < 0.005$) and $9 \pm 3\%$ respectively ($P < 0.01$). Both vasodilators increased $\dot{V}O_2$, isoprenaline by $175 \pm 40\%$ ($P < 0.01$) and histamine by $96 \pm 40\%$ ($P < 0.05$).

These results show that the vasoconstrictors NAd and 5-HT have opposing effects on $\dot{V}O_2$ during both basal and twitch conditions. However we were unable to find a vasodilator that could decrease $\dot{V}O_2$ in a similar fashion to 5-HT. The reduced effect of 5-HT on $\dot{V}O_2$ during twitch maybe due to local effects of the twitch (such as vasoactive metabolites) on oxygen demand, hence overriding the vasoconstriction of the nutritive pathway.

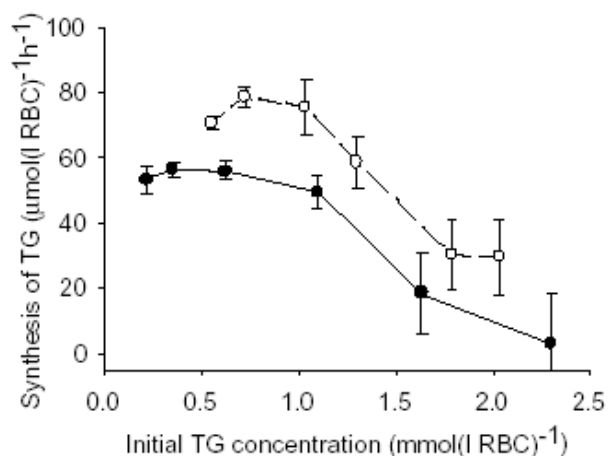
Clark, M.G., Colquhoun, E.Q., Rattigan, S., Dora, K.A., Eldershaw, T.P.D., Hall, J.L. & Ye, J. (1995) *American Journal of Physiology: Endocrinology and Metabolism*, 31, E797-E812.

Glutathione synthesis in whole human red blood cells

J.E. Raftos, Department of Biological Sciences, Macquarie University, NSW 2109, Australia.

The maintenance of adequate levels of the cell antioxidant glutathione (GSH) is essential for defence against oxidative disruption of membranes, proteins and DNA. These vital cell constituents are protected by the preferential oxidation of GSH to glutathione disulfide (GSSG) which is rapidly reduced back to GSH by NADPH and glutathione reductase. Recycling of GSSG to GSH allows for slow replacement of total glutathione (GSH & GSSG; TG) with a turnover time of six days in red blood cells (RBCs). However, oxidative stress can cause accumulation of GSSG and its export from the cell. Under such circumstances, the rate of TG synthesis is thought to be increased by reduced product inhibition by GSH on the rate limiting enzyme γ -glutamyl-cysteine synthase.

GSH synthesis has been studied using lysates and purified enzymes, but little is known of the control of GSH production within whole RBC. Although sensitive and specific spectrophotometric methods have long been available for measuring TG (Tietze, 1969), its synthesis in RBC is too slow to measure in this way particularly against the high concentrations ($2.3 \text{ mmol(l RBC)}^{-1}$) normally present.



GSH is also active in glutathione S-transferase catalysed conjugation with hydrophobic, electrophilic compounds including toxins and drugs. Glutathione S-conjugates are actively exported from RBCs. One such S-transferase substrate 1-chloro-2,4-dinitrobenzene (CDNB) has been used extensively for depleting cell TG content for experimental purposes. For RBCs suspended at a 10% haematocrit in buffer containing 2 mM dithiothreitol, I found that incubation for 40 minutes at 37°C with CDNB concentrations from 0.08 to 0.40 mM reduced the TG levels by 30 to 90%, respectively. When the TG depleted RBCs were washed free of the water soluble glutathione-CDNB conjugate and resuspended in a HEPES buffered solution containing 5 mM N-acetylcysteine and glucose, the TG levels in the RBC, measured by a modified version of Tietze's assay, increased in a linear fashion for several hours. The rate of TG production was dependent on the degree of depletion of TG with a maximum rate of synthesis of $72.6 \pm 15.0 \mu\text{mol(l RBC)}^{-1}\text{h}^{-1}$ (mean \pm SD) which is a five-fold increase on rates previously measured in RBCs with normal levels of GSH (Griffith, 1981). The results of 2 of 5 such experiments are presented in the Figure. The error bars are the SE of the rates of synthesis returned by linear regression. Buthionine sulfoximine a potent inhibitor of γ -glutamyl-cysteine synthase was shown to inhibit the rate of TG increase in RBC by 55% confirming that the accumulation of TG observed was due to synthesis. The controlling factors of TG synthesis within whole RBCs will be determined by measuring TG production under various experimental conditions. Once identified, manipulation of controlling factors may be used to prevent depletion or stimulate production of GSH in several disease states characterised by reduced cell TG.

Griffith, O.W. (1981) *Journal of Biological Chemistry* 256, 4900-4.
Tietze, F. (1969) *Analytical Biochemistry* 27, 502-22.

Circadian gene expression in mouse uterus and liver

A.A. Lim¹, M.H. Johnson² and M.L. Day¹, ¹*Department of Physiology and Institute for Biomedical Research, University of Sydney, N.S.W. 2006, Australia and* ²*Department of Anatomy, University of Cambridge, CB2 3DY, United Kingdom. .SP*

The circadian rhythm of the suprachiasmatic nucleus (SCN) of the brain is entrained by light. Upon input of light, the circadian rhythm is generated as follows: the transcription factors CLOCK and BMAL1 heterodimerise to upregulate transcription of the genes *Per1-3* and *Cry1-2*. PER and CRY proteins heterodimerise, then translocate to the nucleus where they down-regulate CLOCK/BMAL1 activity. This reduces *Per* and *Cry* transcription and PER and CRY decay, releasing the inhibition on BMAL1. Eventually BMAL1 levels increase, initiating the next 24 h cycle of transcription. The circadian clock in the SCN coordinates circadian clocks in peripheral tissues (Reppert & Weaver, 2002). In the female reproductive tract and embryo, timers control when developmental events occur (Johnson & Day, 2000). It is possible that the circadian clock acts as one such timer as we have shown that the circadian genes, *Per1-3*, *Cry1-2*, *Bmal1* and *Clock*, are expressed in the female reproductive tract (uteri and oviducts) and in preimplantation embryos of the mouse (Johnson *et al.*, 2002). To determine whether a circadian clock exists in the uterus, we have quantified mRNA using real-time PCR.

Female MF1 mice were housed on a 12/12 h light/dark cycle. Liver and uterine tissues were obtained from mice euthanised by cervical dislocation at circadian times 0, 4, 8, 12, 16 and 20 of the proestrous, oestrous and dioestrous periods of the oestrous cycle. Whole tissues were snap frozen in liquid nitrogen and total RNA was purified. The RNA concentration was determined by RiboGreen assay, then reverse transcribed to cDNA. Expression of the circadian genes *Per2*, *Cry1*, *Bmal1* in the cDNA was then quantified by real-time PCR using SYBR Green I. Standard curves were run for each gene (*β-actin*, *Per2*, *Cry1*, *Bmal1*) using cDNA. From each standard curve the amount of each gene expressed was calculated and then normalised to *β-actin*.

Timed liver cDNA samples showed changes in circadian gene expression similar to that in the literature (Lee *et al.*, 2001). This confirmed the use of the real time PCR protocol for use on uterine samples. In uterine cDNA, preliminary results suggest that *Per2* and *Bmal1* expression change with a circadian rhythm. Further research will determine whether a circadian clock exists in other periods of the oestrous cycle.

Johnson, M. H. & Day, M. L. (2000) *BioEssays*, **22**: 57-63.

Johnson, M. H., Lim, A., Fernando, D. & Day, M. L. (2002) *Reproductive BioMedicine Online*, **4**: 140-145.

Lee, C., Etchegaray, J.-P., Cagampang, F.R.A., Loudon, A.S.I. & Reppert, S M. (2001) *Cell*, **107**: 855-867.

Reppert, S.M. & Weaver, D.R. (2002) Coordination of circadian timing in mammals. *Nature*, **418**: 935-941.

Effects of vitamin D insufficiency in the fetus and in early life on vascular reactivity in young adult rats

H.C. Parkinson¹, S.J. Emmett¹, R. Morley², C. Skordilis¹, H.A. Coleman¹ and M. Tare¹, ¹Department of Physiology, Monash University, Victoria 3800 and ²University of Melbourne Department of Paediatrics, Royal Children's Hospital, Victoria 3052, Australia. .SP

Inappropriate nutrition in fetal and postnatal life can lead to increased cardiovascular risk in the offspring. Vitamin D (vit D) is an important factor little studied in the context of offspring health. The prevalence of vit D insufficiency is increasing in western societies including Australia, and of particular concern, low levels are seen in pregnant women (Grover & Morley, 2001). It has been suggested that maternal vit D insufficiency may increase the risk of autoimmune disease in the offspring, with increased incidence of type 1 diabetes, chronic inflammatory disorders, some cancers, heart disease, high blood pressure, insulin resistance, and elements of Syndrome X. Here we investigated whether vit D deficiency in fetal and early life results in vasodilator dysfunction, as observed in young adult rats.

Female Sprague Dawley rats were fed chow that was vit D deficient (free of added vit D) from 4 weeks of age, with controls fed normal chow (2000U/kg cholecalciferol, vit D). This feeding regime was continued until the end of the study. After 6 weeks, all rats were mated, the litter size reduced to 10 pups on day 4 post-natal, and the pups weaned at 3 weeks of age. Pups from vit D deficient and control dams were maintained on vit D deficient and normal chow, respectively. At 7 weeks of age, a catheter was inserted into the ventral tail artery under isoflurane anaesthesia. Following 2-3 h recovery, arterial pressure was recorded for 1 h. Blood was then obtained via the catheter for serum vit D and Ca²⁺ determinations. The rats were killed by decapitation. The stage of the estrus cycle was determined from a vaginal smear, uterine weight and ovarian inspection. A segment of mesenteric artery, immediately before it entered the wall of the intestine, was mounted on a pressure myograph fitted with an in-line pressure transducer, and pressure set at 57 mmHg without flow. The segment was continuously superfused externally with bicarbonate-buffered physiological saline solution (PSS) at 35°C and 14 ml/min. Segment diameter was recorded using DIAMTRAK[®] (Neild, 1989). Maximal constriction was determined using 100 mM K⁺ PSS and also in response to 10 µM phenylephrine. Endothelium-dependent vasodilation was tested using discrete 2 min applications of acetylcholine in the presence of 70% of maximal tone evoked with arginine vasopressin. Nitric oxide (NO) and prostanoid production was blocked as required using N[®]-nitro-L-arginine methyl ester (100 µM) and indomethacin (1µM), respectively.

Serum vit D levels were 8±1 ng/ml in rats fed vit D deficient chow compared with 126±10 ng/ml in controls, and serum Ca²⁺ was halved in deficient animals. Vit D deficient animals were some 20% lighter in weight than normal fed controls. Organ weights were appropriately smaller, except for the brain, in which weight was preserved in vit D deficiency. In vit D deficient rats, conscious blood pressure and heart rate were significantly greater compared with controls (by: 9±3 mmHg and 40±13 beats/min, n=11 in males; 16±4 mmHg and 24±9 beats/min, n=11 in females). Resting tone was doubled in vit D deficiency while the ability to maximally constrict was similar in all groups. Endothelium derived NO vasodilation was halved in vit D deficient males and diestrous females, while the dilation attributable to endothelium-derived hyperpolarising factor (EDHF) was preserved. Conversely, in segments from vit D deprived females in estrus, the dilation evoked by NO was preserved, while that attributed to EDHF was abolished.

These results demonstrate that vit D deprivation in fetal and early life leads to growth retardation and higher arterial pressure in young adult rats. The higher pressure was reflected in elevated resting tone in small mesenteric arteries and marked reductions in endothelium dependent vasodilation, with the vasodilators involved differing depending on the sex steroid status.

Grover, S., & Morley, R. (2001) *Medical Journal of Australia*, 175, 251-252.

Neild, T.O. (1989) *Blood Vessels*, 26, 48-52.

Possible role of the brain angiotensin system in programming and maintaining hypertension in sheep prenatally exposed to dexamethasone

A. McAlinden¹, A. Jefferies¹, M. Cock¹, E. Wintour¹, C. May² and M. Dodic¹, ¹Department of Physiology, Monash University, Clayton, Victoria 3800 and ²Howard Florey Institute of Experimental Physiology and Medicine, University of Melbourne, Parkville, Victoria 3010, Australia. (Introduced by R. Evans) .SP

Recent studies have generated the hypothesis that a suboptimal intrauterine environment, during a critical stage of development, 'programs' the development of fetal tissues, enabling fetal survival, but with adverse consequences in adult life (Dodic *et al.*, 2002a).

We have shown that elevated mean arterial pressure (MAP) in both male and female adult sheep can be 'programmed' by brief, prenatal exposure to an excess of the synthetic glucocorticoid (GC), dexamethasone (DEX), for only 48 hours, at day 26-28 of the 150 day gestational period (Dodic *et al.*, 1998). Late in gestation (130 days), no elevation in MAP was observed in DEX exposed fetuses, however real-time PCR studies revealed an increase in gene expression levels of angiotensinogen in the hypothalamus and angiotensin II (ANG II) type 1 (AT₁) receptors in the medulla oblongata (Dodic *et al.*, 2002b). When killed at 7 years of age, the sheep prenatally exposed to DEX were found to have increased expression of AT₁ receptors in the medulla oblongata (Dodic *et al.*, 2002b).

Our aim was two-fold: i) to determine if the brain angiotensin system (AS) contributes to the maintenance of elevated MAP; and ii) whether the sensitivity of the brain AS is altered in DEX exposed sheep. Studies were carried out on a cohort of adult male sheep prenatally exposed to either DEX (0.48mg/h) or saline (control) at 26-28 days of gestation. Sheep were instrumented with brain guide tubes (lateral ventricle) and allowed 2 weeks recovery. General anesthesia was induced with an intravenous injection of 5% Sodium Pentothal (0.4mg/kg), then the sheep was intubated and anesthesia maintained with Halothane in 100% oxygen. Cardiovascular function (MAP, cardiac output and heart rate) was measured for one hour (control period), followed by either a four hour intracerebroventricular (icv) infusion of the AT₁ receptor blocker losartan (1mg/h) or artificial cerebrospinal fluid (vehicle). In addition, brain AS sensitivity was tested by measuring cardiovascular function during icv infusions of ANG II (1 or 10µg/h), each dose running for one hour.

Our results show that the MAP response to losartan was similar between the two groups of animals. The MAP response to icv ANG II (1µg/h) was greater ($p < 0.05$) in DEX exposed animals compared with the control group. The maximal MAP response to icv ANG II (1µg/h) was higher ($\Delta\text{MAP} = 10 \pm 1.9 \text{ mmHg}$, $n = 7$) in the DEX group compared with the saline group ($\Delta\text{MAP} = 6 \pm 2.1 \text{ mmHg}$, $n = 7$, $P < 0.05$). There was no significant difference in MAP response to icv ANG II (10µg/h) between the two groups, however there was a trend towards higher maximal MAP response to ANG II (10µg/h) in the DEX group ($\Delta\text{MAP} = 19 \pm 1.8 \text{ mmHg}$, $n = 7$) compared with the saline group ($\Delta\text{MAP} = 14 \pm 2.1 \text{ mmHg}$, $n = 7$).

These results suggest that the basal brain AS activity does not contribute to the maintenance of elevated MAP in DEX exposed sheep. However, there might be a greater sensitivity of the brain AS to icv ANG II in the DEX exposed animals.

Dodic, M., May, C., Wintour, E. & Coghlan, J. (1998) *Clinical Science*, **94**, 149-155.

Dodic, M., Moritz, K., Koukoulas I., & Wintour, E. (2002a) *Trends in Endocrinology & Metabolism*, **13**, 403-408.

Dodic, M., Abou-Antoun, T., O'Connor, A., Wintour, E. & Moritz, K. (2002b) *Hypertension*, **40**, 729-734.

The effects of maternal renal dysfunction and a high salt diet on the renin angiotensin systems of the pregnant ewe and her fetus

K.J. Gibson, A.C. Boyce, B.M. Karime, C.L. Thomson, J. Wu, Y.P. Zhou and E.R. Lumbers, Department of Physiology and Pharmacology, School of Medical Sciences, University of New South Wales, NSW 2052, Australia. .SP

We previously reported that maternal renal dysfunction, caused by subtotal nephrectomy (STNx) prior to mating, resulted in fetuses with high urine flow rates, high urinary sodium excretions and low haematocrits (Gibson *et al.*, 2002). These changes were suggestive of exposure to an increased fluid and solute load from the mother. To determine whether the fetal renin angiotensin system was suppressed, we measured plasma renin levels in 17 STNx and 14 control ewes and their fetuses at 122-128 days gestation (term = 150 days). In addition, we examined the effects of a high salt diet.

At least two months prior to mating, STNx was carried out under general anaesthesia (1 g sodium thiopentone i.v. followed by 1-3% halothane in oxygen). The right kidney was removed and a branch of the left renal artery (supplying at least one third of the kidney) was ligated. At 112-122 days the fetuses and ewes were chronically catheterised under general anaesthesia. No measurements were taken until at least 5 days after surgery. Plasma renin levels were measured as the rate of generation of angiotensin I ($\text{ng ml}^{-1} \text{h}^{-1}$) in samples incubated with nephrectomised sheep plasma (a source of angiotensinogen).

Maternal renin levels were similar in the two groups (Control 1.4 ± 0.4 (SE), $n=14$; STNx $1.2 \pm 0.3 \text{ ng ml}^{-1} \text{h}^{-1}$, $n=17$). However, fetal plasma renin levels were lower in the STNx group (6.8 ± 3.0 , $n=17$) than in the control group ($15.1 \pm 7.9 \text{ ng ml}^{-1} \text{h}^{-1}$, $n=14$, $P=0.07$).

Six ewes in each group received a high salt diet for 4 days i.e. they had access to 8 l day⁻¹ of 0.17 mol l⁻¹ NaCl instead of their normal drinking water. When both groups were combined, maternal plasma renin levels fell from 1.9 ± 0.4 to $0.5 \pm 0.2 \text{ ng ml}^{-1} \text{h}^{-1}$ ($n=12$, $P<0.05$). Interestingly, in the STNx ewes on the high salt diet, the increase in urinary sodium output was greater than the increase in sodium intake, so their sodium balance became negative. Fetal plasma renin levels rose from 10 ± 7.7 ($n=6$) before salt, to $19.3 \pm 7.4 \text{ ng ml}^{-1} \text{h}^{-1}$ ($n=6$) after salt ($P=0.05$ after log transformation of the data). By contrast, in the control ewes on the high salt diet, maternal sodium balance remained positive, and there was no change in fetal plasma renin levels (before salt 11.0 ± 5.2 , $n=5$; after salt $12.8 \pm 8.8 \text{ ng ml}^{-1} \text{h}^{-1}$, $n=5$).

It is concluded that the fetal renin angiotensin system was suppressed in this model of maternal renal dysfunction. The renin angiotensin system is essential for normal renal development (Guron & Friberg, 2000). Therefore, by suppressing this system, maternal renal dysfunction may impair fetal renal development and predispose the offspring to hypertension. Furthermore, fetuses whose mothers have renal impairment may be exposed to greater fluctuations in salt and water balance than those whose mothers have normal renal function.

Gibson, K.J., Karime, B.M., Zhou, Y.P., Boyce, A.C. & Lumbers, E.R. (2000). *Proceedings of the Australian Health and Medical Research Congress*, 1210.

Guron, G. & Friberg, P. (2000). *Journal of Hypertension*, 18:123-127.

The role of renal sympathetic nerve activity in the hypertension induced by chronic nitric oxide blockade

R. Ramchandra, C.J. Barrett, S.J. Guild and S.C. Malpas, Circulatory Control Lab, Department of Physiology, University of Auckland, Private Bag 92019, Auckland, New Zealand. .SP

Chronic blockade of nitric oxide leads to an increase in blood pressure that is maintained over the period of the blockade in baroreceptor intact animals (Scrogin *et al.*, 1998). In addition to the vascular actions of endothelium-derived nitric oxide, indirect evidence supports a role for the sympathetic nervous system in maintaining the hypertension. The decrease in blood pressure with ganglionic blockade is exaggerated with blockade of nitric oxide suggesting an increase in sympathetic tone (Liu *et al.*, 1998; Scrogin *et al.*, 1998). Guanethidine-induced sympathetomy also attenuates the hypertension induced by chronic nitric oxide blockade (Sander *et al.*, 1997).

In order to test this possible interaction between nitric oxide and sympathetic nerve activity directly, we measured arterial pressure and renal sympathetic nerve activity before, during and after nitric oxide blockade using L-NAME (50mg/kg/day *via* drinking water) over 7 days, in baroreceptor intact and sino-aortic denervated (SAD) conscious rabbits.

In the baroreceptor intact animals, blockade of nitric oxide led to a significant increase in mean arterial pressure (from 75 ± 2 to 84 ± 3 mmHg) and decrease in heart rate (from 233 ± 8 to 195 ± 8 bpm) that was sustained over the 7 days of nitric oxide blockade. In all SAD animals, an initial increase in arterial pressure (82 ± 3 mmHg on the second day) was seen but was not sustained and recovered back to pre L-NAME levels. Direct recordings of renal sympathetic nerve activity suggest the increase in blood pressure in the baroreceptor intact animals is not accompanied by a change in renal sympathetic tone (9 ± 3 normalised units during control *v/s* 10 ± 4 normalised units at day 7 of L-NAME treatment). There is evidence of resetting of the blood pressure- renal sympathetic nerve activity baroreflex curve such that blood pressure is maintained at a hypertensive level.

In summary, our results do not support a role for increased renal sympathetic nerve activity in maintaining the hypertension with nitric oxide blockade in baroreceptor intact animals. The lack of a sustained increase in pressure in the SAD animals suggests an important role for baroreflexes in the long-term control of arterial pressure.

Liu, Y., Tsuchihashi, T., Kagiya, S., Matsumura, K., Abe, I. & Fujishima, M. (1998) *Journal of Hypertension*, 16, 1165-1173.

Sander, M., Hansen, J. & Victor, R.G. (1997) *Hypertension*, 30, 64-70.

Scrogin, K.E., Hatton, D.C., Chi, Y. & Luft, F.C. (1998) *American Journal of Physiology*, 274, R367-R374.

Supported by the Auckland Medical Research Foundation, the Health Research Council, the Maurice and Phyllis Paykel Trust and the University of Auckland.

Baroreflexes play a major role in regulating the long-term level of sympathetic nerve activity

S.J. Guild, C.J. Barrett, R. Ramchandra and S.C. Malpas, Circulatory Control Laboratory, Department of Physiology, University of Auckland, Private Bag 921019, Auckland, New Zealand. .SP

It is accepted dogma that arterial baroreflexes play no role in the long-term regulation of arterial pressure because they exhibit resetting in response to sustained increases in arterial pressure. However, a recent study from our laboratory (Barrett *et al.*, 2003) challenges this view. We observed that chronic infusion of angiotensin II (7 days, 50ng/kg/min i.v.) caused an increase in mean arterial pressure (MAP) and a sustained decrease in renal sympathetic nerve activity (RSNA). Also, although the MAP-heart rate baroreflex curve showed resetting, the MAP-RSNA baroreflex curve did not. These results suggest that baroreflex control of RSNA is likely to play a significant role in the long-term control of arterial pressure. Full interpretation of these results is however made difficult by the direct and central nervous system effects of angiotensin II on RSNA. It is important therefore to investigate this result further using an alternative method of increasing arterial pressure. In this current study chronic infusion of phenylephrine was chosen.

In New Zealand white rabbits, living in their home cages, arterial pressure and RSNA were recorded continuously using telemetry devices before, during and after a 7-day infusion of phenylephrine (30mg/kg/hr i.v.) using an osmotic mini pump. The modest but sustained increase in MAP during phenylephrine infusion was accompanied by significant bradycardia and decreased RSNA (~30%) over the 7-day infusion period. Baroreflex responses were derived using rapid infusions of sodium nitroprusside and phenylephrine before, at day 2, and 7 of phenylephrine infusion and again after removal of the osmotic pump. The MAP-RSNA curves during phenylephrine infusion not only showed no evidence of the rightward shift suggesting resetting, but also showed a decrease in range and the resting points lie near the lower plateau of these curves suggesting that the decreased RSNA observed during phenylephrine infusion is due to the baroreflex. These results suggest that the similar changes to the baroreflex curves observed during angiotensin II infusion are independent of the central or direct effects of angiotensin II and are mediated by the inducement of hypertension. Overall these results support the notion that the baroreflexes **do** play an important role in regulating the long-term level of RSNA.

Barrett, C.J., Ramchandra, R., Guild, S.J., Lala, A., Budgett, D.M. & Malpas, S.C. (2003). *Circulation Research* **92**(12): 1330-6.

NO and α -adrenoceptor subtypes in regional renal vascular responses to renal nerve stimulation in rabbits

G.A. Eppel¹, L.L. Lee¹, K.M. Denton¹, S.C. Malpas² and R.G. Evans¹, ¹Department of Physiology, Building 13F, Monash University, VIC 3800, Australia and ²Department of Physiology, University of Auckland, Auckland, New Zealand.

Introduction. Renal medullary blood flow (MBF) plays a critical role in long-term control of arterial pressure. Therefore understanding the mechanisms controlling MBF is important. When renal sympathetic drive is increased reflexively (Leonard *et al.*, 2001), or by electrical stimulation (RNS, Leonard *et al.*, 2000), MBF is reduced much less than cortical or total renal blood flow (CBF, RBF). Zou and Cowley (2000) have shown that MBF responses to noradrenaline infusion are blunted by α_2 -adrenoceptor mediated NO release. We tested whether this mechanism blunts MBF responses to RNS in pentobarbitone anaesthetised rabbits (90-150mg + 30-50mg/h iv).

Methods. RBF was measured by transit-time ultrasound flowmetry, CBF and MBF were measured by laser-Doppler flowmetry. RNS was performed at a supramaximal voltage (2ms pulse duration) for 3min at each frequency (0.5,1,2,4 and 8Hz in random order). In Experiment 1, RNS was performed before and after prazosin (α_1 -adrenoceptor antagonist; 0.2mg/kg + 0.2mg/kg/h iv; n=6), rauwolscine (α_2 -adrenoceptor antagonist; 0.5mg/kg + 0.25mg/kg/h iv; n=6) or vehicle treatment (n=6). In Experiment 2, responses to RNS were measured under control conditions, after NO synthase blockade with N^G-nitro-L-arginine (L-NNA, 20mg/kg/min + 5mg/kg/h iv), and then during co-infusion of glyceryl trinitrate at a dose that restored arterial pressure and RBF to control levels (10-50 μ g/kg/min iv). A second group (n=6) served as a time control, receiving only vehicle treatment.

Results. In all groups RBF, CBF and to a lesser extent MBF, were reduced by RNS in a stimulus-dependent manner. In Experiment 1, prazosin decreased baseline arterial pressure by $-11\pm 4\%$ and CBF by $-18\pm 3\%$. Prazosin blunted RNS-induced responses of RBF and CBF but not MBF. For example at 4Hz, RBF, CBF and MBF were reduced by $-85\pm 3\%$, $-89\pm 2\%$ and $-20\pm 12\%$ respectively during the control period, and by $-39\pm 3\%$, $-42\pm 5\%$ and $-28\pm 7\%$ during prazosin treatment. Rauwolscine increased arterial pressure by $8\pm 2\%$ and decreased RBF by $-25\pm 2\%$ and CBF by $-14\pm 3\%$. Rauwolscine increased CBF and MBF responses to RNS but only at frequencies ≤ 2 Hz. For example RNS at 1Hz reduced CBF by $-21\pm 2\%$ but not MBF ($+9\pm 9\%$) during the control period. During rauwolscine treatment, RNS at 1Hz reduced CBF by $-30\pm 6\%$ and MBF by $-12\pm 8\%$. Baseline haemodynamic variables and responses to RNS were not significantly affected by vehicle treatment. In Experiment 2, L-NNA increased arterial pressure by $34\pm 4\%$ and decreased RBF and MBF by $-16\pm 2\%$ and $-52\pm 5\%$ respectively. L-NNA treatment enhanced responses to RNS, particularly MBF at the lower frequencies. For example, stimulation at 2Hz during the control period reduced RBF by $-48\pm 7\%$ and CBF by $-39\pm 6\%$ but not MBF ($+1\pm 18\%$). During L-NNA treatment the responses were $-58\pm 6\%$, $-43\pm 4\%$ and $-32\pm 11\%$ for RBF, CBF and MBF respectively. Glyceryl trinitrate infusion restored arterial pressure, RBF and MBF to control levels and also restored RBF, CBF and MBF responses to RNS to their control levels. Responses to RNS remained relatively stable in the time control group.

Conclusions. These data indicate that both α_2 -adrenoceptor activation and NO blunt MBF responses to RNS at low frequencies, but also blunt CBF responses to some extent. Whether the impact of α_2 -adrenoceptor activation is mediated by NO, remains to be determined. MBF remained less responsive to RNS than CBF during NO synthase and α_2 -adrenoceptor blockade, indicating that other mechanisms also contribute to the differential impact of RNS on CBF and MBF. α_1 -adrenoceptors make an important contribution to RNS-induced changes in CBF but seem to contribute less to RNS-induced changes in MBF.

Leonard, B.L., Evans, R.G., Navakatikyan, M.A. & Malpas, S.C.. (2000) *American Journal of Physiology*, 279, R907-916.

Leonard, B.L., Malpas, S.C., Denton, K.M., Madden, A.C. & Evans, R.G. (2001) *American Journal of Physiology*, 280, R62-68.
Zou A.P. & Cowley, A.W. (2000) *American Journal of Physiology*, 279, R769-77.

Do nitric oxide and prostaglandins protect the renal medullary circulation from ischaemia during renal nerve stimulation?

N.W. Rajapakse¹, G.A. Eppel¹, K.M. Denton¹, S.C. Malpas² and R.G. Evans¹, ¹Department of Physiology, Monash University, Melbourne, Australia and ²Department of Physiology, University of Auckland, Auckland, New Zealand. .SP

Renal medullary blood flow (MBF) is less sensitive than cortical blood flow (CBF) to sympathetic activation (Guild *et al.*, 2002), in part because of a counter regulatory vasodilator role of nitric oxide (NO) (Eppel *et al.*, in press). Thus, blockade of NO-synthase in anaesthetised rabbits enhances responses of total renal blood flow (RBF), CBF, and particularly MBF, to renal nerve stimulation (RNS) (Eppel *et al.*, in press). However, other mechanisms must also be involved, because even after NO-synthase blockade, RNS still reduces CBF more than MBF.

In the present study we tested whether prostaglandins contribute to the relative insensitivity of MBF to renal sympathetic drive in pentobarbitone (90-150 mg + 30-50 mg h⁻¹) anaesthetised rabbits. We also tested the effects of NO-synthase inhibition on regional kidney blood flow responses to RNS in rabbits pre-treated with a cyclooxygenase inhibitor.

A transonic flow probe was used to measure RBF and laser-Doppler flow probes were used to measure CBF and MBF. Responses to RNS were tested before and after intravenous ibuprofen (12.5 mg/kg plus 12.5 mg/kg/h; n = 18) or its vehicle (n = 6). In ibuprofen-treated rabbits, responses were then tested after N^G-nitro-L-arginine (L-NNA; 20 mg/kg + 5 mg/kg/h; n=6), L-NNA + glyceryl trinitrate (GTN; 8 - 22 µg/kg/min; n = 6) or vehicle (n = 6).

Ibuprofen but not its vehicle reduced basal RBF, CBF and MBF. Subsequent treatment with L-NNA, but not L-NNA + GTN or vehicle, increased mean arterial pressure and reduced RBF and MBF. RNS (0.75 – 6 Hz) caused stimulus-dependent reductions in RBF (85 ± 4% at 6 Hz) and CBF (87 ± 3% at 6 Hz) more than MBF (36 ± 14% at 6 Hz) in vehicle-treated rabbits. Ibuprofen did not significantly affect responses of RBF, CBF or MBF to RNS. L-NNA, but not vehicle or L-NNA + GTN, significantly enhanced RNS-induced reductions in RBF (P ≤ 0.001) and CBF (P = 0.02) but not MBF (P = 0.8).

We conclude that cyclooxygenase products have little net impact on regional kidney blood flow responses to RNS. Our finding that NOS blockade did not affect responses of MBF to RNS after cyclooxygenase blockade contrast with our previous findings in rabbits with intact cyclooxygenase activity (Eppel *et al.*, in press). This may reflect interactions between nitric oxide and vasoconstrictor prostaglandins in modulating responses of MBF to RNS. This notion is consistent with previous studies of isolated perfused kidneys, in which NO blockade enhances vasoconstrictor responses to noradrenaline under control conditions, but not after cyclooxygenase blockade (Zhang & Sassard, 1993).

Eppel, G.A., Denton, K.M., Malpas, S.C. & Evans, R.G. *Pflügers Archiv-European Journal of Physiology*, in press.

Guild, S.-J., Eppel, G.A., Malpas, S.C., Rajapakse, N.W., Stewart, A. & Evans, R.G. (2002) *American Journal of Physiology*, **283**, R1177-R1186.

Zhang, B.L. & Sassard, J. (1993) *British Journal of Pharmacology*, **110**, 235-238.

Ion channelopathies: What have they taught us about arrhythmias and anti-arrhythmic therapy?

J.I. Vandenberg and T.J. Campbell, Electrophysiology and Biophysics Program, Victor Chang Cardiac Research Institute, Level 9, 384 Victoria Street. Darlinghurst, NSW 2010 and Department of Medicine, St. Vincent's Hospital. University of NSW, NSW 2052, Australia .SP

The efficient pumping of blood by the heart requires the co-ordinated activity of the billions of cardiac myocytes that make up the heart. This is achieved by an electrical communication system the centrepiece of which consists of voltage-gated ion channels. Over the last decade the molecular identity of most (if not all) the voltage-gated ion channels in the heart has been elucidated. More importantly it has also been found that mutations in some of these channels (most notably the cardiac sodium channel, SCN5a, and the delayed rectifier potassium channels, KvLQT1 and HERG) result in a marked increase in the risk of lethal cardiac arrhythmias, the so-called "cardiac ion channelopathies". Determination of the mechanisms underlying the increased risk of arrhythmias in patients with these mutant channels has taught us a great deal about the molecular basis of arrhythmias. This is perhaps best illustrated in the case of loss-of-function mutations in the HERG K⁺ channel and the increased risk of arrhythmias initiated by premature beats (see e.g. Lu *et al.*, 2001). Understanding the cardiac ion channelopathies has also provided insights into why so many drugs developed to be anti-arrhythmic turned out to be "pro-arrhythmic". For example most Class III anti-arrhythmics inhibit the HERG K⁺ channel resulting in a "drug-induced long QT syndrome" (Vandenberg *et al.*, 2001). The big challenge now is to utilise the knowledge we have gained from understanding cardiac ion channelopathies to develop more effective anti-arrhythmic therapies.

One of the major issues that has yet to be fully addressed with respect to the role of ion channels in the genesis of cardiac arrhythmias is the heterogeneity of ion channel expression. This heterogeneity of electrical activity is most clearly illustrated by the differences in the shape and duration of cardiac action potentials recorded from cells in different regions of the heart. One consequence of this heterogeneity is that any drug that modulates ion channel activity will have different effects in different regions of the heart and by altering the delicate balance of inward and outward currents has the potential to be pro-arrhythmic. However, before we can understand the specifics of such postulated pro-arrhythmic mechanisms we need to know much more about the spatial patterns of ion channel expression in the heart and how they are affected by disease processes (see e.g. Wong *et al.*, 2000).

Lu, Y., Mahaut-Smith, M.P., Varghese, A., Kemp, P.R., Huang, C.L.H. & Vandenberg, J.I. (2001) *Journal of Physiology*, 537(3):843-51.

Vandenberg, J.I., Walker, B.D. & Campbell, T.J. (2001) *Trends in Pharmacological Sciences*, 22(5):240-6

Wong, K.R., Trezise, A.E.O. & Vandenberg, J.I. (2000) *Biochemical and Biophysical Research Communications*, 278(1):144-9.

Cardiac hypertrophy: comparing models and counting genes

L.M.D. Delbridge, Department of Physiology, University of Melbourne, Parkville, Victoria 3010, Australia. .SP

In the study of cardiac hypertrophy, much has been learned from polygenic models developed by conventional selective in-breeding techniques (*i.e.* the Spontaneously Hypertensive Rat, SHR). As many cardiovascular disease states comprise a complex multigenic-dependent phenotype, it is particularly valid to use these models for investigation of the natural history of disease development and progression. However a major difficulty with these models has been that hypertrophy and hypertension are frequently coincident and identification of the genetic factors which contribute to cardiac growth independently of blood pressure has been difficult. Furthermore, the failure to co-derive genetically homogenous control strains for some models has further confounded the interpretation of data obtained from these animals.

We have recently reported the development of a novel polygenic rat strain of primary cardiac hypertrophy derived from a cross of Fisher (F344) and SHR (Harrap *et al.*, 2002). Our new Hypertrophic Heart Rat (HHR) strain exhibits cardiac and cardiomyocyte hypertrophy in the absence of hypertension. In parallel we have co-developed a Normal Heart Rat (NHR) strain with small hearts and low blood pressure as a control strain. Exploration of the cardiac growth responses in the HHR and NHR provides an opportunity to characterise the processes underlying the development of load-independent hypertrophy.

A complementary genetic approach which can be of particular value in providing insight into the mechanisms of cardiac hypertrophy is the study of mono-genetically manipulated animal models. We have investigated transgenic and gene-knockout models to explore the role of trophic and metabolic factors in inducing cardiac hypertrophy. Our studies of a transgenic cardiac-specific angiotensinogen over-expressing mouse and a cardiac-specific glucose Glut4 transporter Cre-Lox KO mouse have revealed that similar functional adaptations can be linked with quite different alterations in myocyte calcium handling in hypertrophy.

In both multigenic and unigenic models of cardiac hypertrophy we have applied candidate gene and expression profiling techniques to undertake comparative genotype-phenotype analyses. In our candidate gene investigations we have focussed on expression shifts in transporters important in modulating excitation-contraction coupling. Our genome scale 'snapshot' studies have suggested that regardless of the instigating genetic stimulus, the hypertrophic phenotype is associated with a major remodelling of metabolic processes.

Thus, the value of both unigenic and polygenic animal models in the study of cardiac hypertrophy is particularly evident when candidate gene analysis and genome-scale expression profiling techniques are used as complementary approaches.

Harrap, S.B., Danes, V.R., Ellis, J.A., Griffiths, C.D., Jones, E.F. & Delbridge, L.M.D. (2002) *Physiological Genomics*, 9, 43-48.

Modelling and imaging cardiac function during excitation-contraction coupling

C. Soeller and M.B. Cannell, Department of Physiology, School of Medical Science, University of Auckland, Private Bag 92019, Auckland, New Zealand. .SP

Cardiac excitation-contraction (E-C) coupling takes place in the narrow diadic cleft between the transverse-tubular membrane and the closely apposed terminal cisternae of the sarcoplasmic reticulum (SR). Within the cleft (which is only ~15nm high and some 100nm wide) large clusters of SR Ca²⁺ release channels or ryanodine receptors (RyRs) are located. It is now generally accepted that the opening of these clusters of RyRs underlies the elementary events of muscle activation called “calcium sparks”, brief microscopic increases in intracellular Ca²⁺, which can be observed in heart cells loaded with fluorescent Ca²⁺ indicators such as fluo-3.

As a result of Ca²⁺ binding reactions and indicator diffusion Ca²⁺ spark records do not provide a direct measure of the time course of Ca²⁺ release. To robustly reconstruct the underlying Ca²⁺ release time course we developed novel algorithms in which a parametric Ca²⁺ spark model is fit to experimental records. Using this approach we calculated that the peak flux amplitude is ~7-12pA suggesting that at least 15 RyRs contribute to a Ca²⁺ spark. To obtain further insight into the gating of RyRs underlying Ca²⁺ sparks we constructed a detailed Monte Carlo model of RyR gating and associated Ca²⁺ movements within the diad. In this model the movement of individual Ca²⁺ ions was traced and diffusion was implemented as a random walk. RyR gating was described by a phenomenological 4-state scheme (Stern *et al.*, 1999) that included explicit inactivation. Our calculations suggest that the geometry of the diad and the RyR cluster can significantly affect the time course of release. In our spatially explicit model we observe waves of RyR openings originating at the initial site of activation. In elongated clusters of RyRs the time course of release therefore depends on the site of wave initiation while the total amount of Ca²⁺ that is released stays nearly constant.

We also explored the effect of allosteric coupling between RyRs on the gating of large RyR clusters in the model. Allosteric coupling was implemented as a nearest neighbour interaction where transition rates of receptors in the cluster were modified based on the state of adjacent RyRs. With moderate coupling our model generated a mean Ca²⁺ release time course that was similar to that reconstructed from experimental sparks. On the other hand, strong coupling resulted in increased variability and duration of the Ca²⁺ release time course.

It has been suggested that the protein FKBP12.6 may be the molecular basis of allosteric coupling between RyRs. To test this idea we recorded sparks in the presence of FK506, a drug which removes FKBP12.6 from RyRs. Analysis of our data suggests that, although the amplitude of Ca²⁺ sparks is reduced in FK506 (as compared to control sparks), the decay time and variability of Ca²⁺ sparks is only weakly changed by 50 μM FK506 which argues against a significant role of FKBP12.6 in coupling RyR gating.

We are currently extending the model to investigate other RyR gating schemes and the effect of local SR depletion on cluster gating. Our work suggests that the combination of mathematical modelling with high resolution Ca²⁺ imaging will provide valuable insight into cardiac E-C coupling.

Stern, M.D., Song, L.S., Cheng, H.P., Sham, J.S.K., Yang, H.T., Boheler, K.R. & Rios, E. (1999) *Journal of General Physiology*, 113:469-489.

Cardiac structure and electrical activation: models and measurement

B.H. Smaill, Bioengineering Institute and Department of Physiology, University of Auckland, Private Bag 92019 Auckland, New Zealand. .SP

Re-entrant arrhythmia and fibrillation are three-dimensional (3D) events that involve relatively large tissue volumes and are influenced by regional variation of the electrical properties of cardiac tissue and by the complex architecture of the heart. Within this context, computer models that incorporate realistic descriptions of cardiac anatomy and the electrical properties of myocardium provide a powerful tool with which to interpret and interpolate experimental observations.

Our group has systematically measured the 3D geometry of right and left ventricles in dog and pig hearts, and has characterised myocyte orientation throughout the ventricular wall in these species. These data have been incorporated into a detailed finite element model of cardiac anatomy which has been used by ourselves and others to study normal electrical activation and re-entrant arrhythmia.

We have developed a confocal imaging technique that enables us to reconstruct the 3D organisation of cardiac myocytes and extracellular collagen matrix in relatively large tissue volumes at up to 1µm voxel resolution. Morphometric studies employing this approach confirm that ventricular myocardium is a complex hierarchy in which myocytes are arranged in discrete layers separated by cleavage planes that are relatively extensive, particularly in the left ventricular (LV) midwall.

The effect of structural discontinuity on the propagation of electrical activation has been modelled using a finite element formulation in which the electrical properties of intracellular and extracellular domains are explicitly represented. Detailed information on 3D cleavage plane organisation and muscle fibre orientation, extracted from an extended volume image of a transmural segment of rat LV myocardium, was incorporated into the model. For an ectopic midwall stimulus, the predicted spread of electrical activation was initially non-uniform and markedly affected by the discontinuous 3D arrangement of muscle layers.

The model has been validated by recording extracellular potentials at up to 36 sites within the LV free wall in sinus rhythm and during intramural pacing. *In situ* measurements were made first in an anaesthetised (Zoletil, 10mg/kg im, initially and then 2-5% halothane in oxygen), ventilated open-chest pig preparation and comparable data were then recorded with the hearts isolated and mounted in a Langendorff apparatus. Intramural transmembrane potentials were recorded adjacent to extracellular measurement sites in the isolated hearts employing a multi-channel fluorescence imaging system and a novel fibre optic probe. The results obtained are consistent with model predictions and reinforce the hypothesis that structural discontinuity may give rise to non-uniform, anisotropic propagation of electrical activation.

The significance of these observations with respect to normal activation, re-entrant arrhythmia and defibrillation will be discussed. Finally, the need for, and progress toward, development of a new generation of computer models of re-entrant arrhythmia that are anatomically realistic and incorporate accurate representations of cellular electrophysiology and include data on the spatial distribution of key transmembrane ion channels will be reviewed.

Differential regulation of two modes of exocytosis by protein phosphatases

A.T.R. Sim, School of Biomedical Sciences, The University of Newcastle, and Hunter Medical Research Institute, Callaghan, NSW 2308, Australia. (Introduced by D. Adams) .SP

Phosphorylation and dephosphorylation of nerve terminal proteins are involved in the regulation of neurotransmitter release. However, it is now clear that there are multiple modes of exocytosis in neurons and the specific roles for different kinases and phosphatases remain unknown. The most well characterised mode of exocytosis involves docking and fusion of a synaptic vesicle with the plasma membrane followed by full incorporation of the vesicle into the plasma membrane, so called full fusion exocytosis. Vesicles are subsequently recovered by Clathrin-mediated endocytosis. However, an alternative mode, termed kiss-and-run, has now been demonstrated, where neurotransmitter is released without complete fusion of the vesicle with the plasma membrane, and the vesicle is rapidly retrieved and refilled with neurotransmitter. Kiss-and-run therefore accelerates the turnover of the limited pool of synaptic vesicles in neurons and may have both beneficial and pathological outcomes. In studies to identify the molecular events underlying these different modes, we have shown that serine/threonine and potentially tyrosine phosphatases have specific regulatory roles.

We used selective pharmacological inhibitors of different protein phosphatases to investigate their roles in the different modes of exocytosis in neurons and mast cells. Two chemical depolarising agents were used (KCl and 4-aminopyridine) that can selectively induce full fusion and kiss-and-run exocytosis, and exocytosis was measured by two complementary assays that can distinguish between these 2 modes of exocytosis. Measurement of endogenous, soluble, glutamate release detects both full fusion and kiss-and-run modes of exocytosis. In contrast, measuring the release of the lipophilic styryl dye FM 2-10, reflects the time dependent dissociation of the dye from vesicle membranes, and is therefore much less capable of detecting the rapid, transient exocytosis that occurs during kiss-and-run. Our results suggest that protein phosphatase 2A positively regulates the full fusion mode of exocytosis, whilst protein phosphatase 2B, in addition to its recognised role in regulating endocytosis, negatively regulates the kiss-and-run mechanism of exocytosis.

We have also studied the role of the Src family of tyrosine kinases in regulating these two modes of exocytosis. Inhibition of the Src family kinases, using the specific inhibitor, PP1 (10 μ M), significantly increased kiss-and-run release, but had no effect on full fusion release. The inactive analog, PP3, had no effect on either mode. Measurement of depolarisation induced changes in synaptosomal protein tyrosine phosphorylation did not show any association between Src kinase activity and kiss-and-run exocytosis. This indicates that the effect of Src kinase inhibition is either to remove a constitutive phosphorylation dependent restraint on exocytosis, perhaps mimicking an endogenous tyrosine dephosphorylation event that promotes the kiss-and-run mode, or to inhibit a depolarisation dependent activation of a member of the Src kinase family that is not Src.

Since the fundamental molecular machinery involved in full fusion exocytosis is highly conserved, we have also used a mast cell model to further investigate the molecular events underlying the control of full fusion exocytosis by PP2A. These studies indicate that translocation of PP2A from cytosolic to membrane-associated locations within the cell and the formation of transient complexes with myosin are critical for the regulation of exocytosis.

Coupling G protein-coupled receptors to exocytosis

P.D. Marley, Department of Pharmacology, University of Melbourne, Vic. 3010, Australia. (Introduced by D.J. Adams) .SP

The primary driving force for regulated exocytosis is the elevation of cytosolic Ca^{2+} . In excitable cells, this is normally achieved by extracellular Ca^{2+} entering the cell through Ca^{2+} -permeable channels in the plasma membrane. Ionotropic receptors evoke exocytosis either by being themselves permeable to Ca^{2+} or by being non-selective cation channels that depolarise the cell, so activating voltage-sensitive Ca^{2+} channels (VOCCs). In contrast, the mechanisms by which G protein-coupled receptors (GPCRs) cause extracellular Ca^{2+} entry are much less clear. Possible mechanisms have been exploring using the secretion of catecholamines evoked by histamine H1 receptors from adrenal chromaffin cells (Marley, 2003).

Adrenal chromaffin cells express one of the highest densities of H1 receptor of any tissue and these are of critical importance in protecting against anaphylactic shock. The chromaffin cell H1 receptors are coupled through *Pertussis* toxin-resistant G proteins to the hydrolysis of membrane phosphatidylinositol 4,5-bisphosphate and the generation of inositol 1,4,5-trisphosphate (IP3), which mobilises Ca^{2+} from intracellular stores. Of the GPCRs expressed by chromaffin cells, histamine H1 receptors are particularly effective at evoking exocytosis, having almost half the efficacy of powerful nicotinic receptor agonists. The great majority of this secretory response is inhibited by antagonists to L, N and P/Q-type VOCCs, indicating histamine recruits VOCCs, however histamine has complex effects on the membrane potential of these cells (Wallace *et al.*, 2002). Initially there is a transient hyperpolarisation that is abolished if intracellular Ca^{2+} stores are depleted and which is due to activation of small conductance Ca^{2+} -activated K^+ (SK) channels by store Ca^{2+} released by IP3. The hyperpolarisation is followed after 10-20 s by a slow depolarisation and an increase in frequency of spontaneous action potentials. The latter two effects persist after store depletion and after block of SK channels, and are accompanied by an increase in membrane resistance and by a small inward current. The latter are in part the result of the closure of a K^+ channel responsible for a novel M current that helps set the resting membrane potential. How the H1 receptors cause the closure of these channels is presently unknown, however the secretory response to histamine is not prevented by inhibitors of IP3 receptors or ryanodine receptors, by depletion of intracellular Ca^{2+} stores, or by protein kinase C inhibitors (Donald *et al.*, 2002). The identity of the cause of the rest of the depolarisation also remains unknown. H1 receptors regulate the activity of at least five classes of K^+ channels in chromaffin cells, however the secretory response is not prevented by blocking SK channels, intermediate- or large-conductance Ca^{2+} -activated K^+ (IK or BK) channels, K_{ATP} channels, delayed rectifier channels or A type channels, and inward rectifier K^+ channels are not expressed in these cells.

The results from such studies raise a number of important questions, including (i) what is the molecular mechanism by which GPCRs inhibit K^+ channels, (ii) through what other channels can GPCRs depolarise cells, and (iii) why do some GPCRs evoke large secretory responses, while others have very low efficacy, while apparently activating similar signaling pathways in the same cells?

Donald A.N., Wallace D.J., McKenzie S. & Marley P.D. (2002) *Journal of Neurochemistry*, **81**, 1116-1129.

Marley P.D. (2003) *Pharmacology & Therapeutics*, **98**, 1-34.

Wallace D.J., Chen C. & Marley P.D. (2002) *Journal of Physiology*, **540**, 921-929.

PI-3 kinase type II C2 α is essential for ATP-dependent priming of neurosecretory granules prior to exocytosis

F.A. Meunier¹, G. Hammond¹, P.J. Parker¹, G. Schiavo¹, F.T. Cooke² and J. Domin³, ¹Cancer Research UK, London Research Institute, Lincoln's Inn Fields Laboratories, 44 Lincoln's Inn Fields, London WC2A 3PX, UK, ²Biochemistry and Molecular Biology, University of College, London, Darwin Building, Gower Street, W1E 6BT, London, UK and ³Renal section, Faculty of Medicine, Imperial College School of Medicine, London W12 0NN, UK. (Introduced by D.J. Adams) .SP

Phosphatidylinositol 3-kinases (PI3K) are implicated in a variety of synaptic functions including axonal guidance and long-term depression and potentiation (reviewed in Osborne *et al.*, 2001). However, a direct involvement of this class of enzymes and their lipid products in neuroexocytosis has been questioned (Chasserot-Golaz *et al.*, 1998), based on the low sensitivity of exocytosis to PI3K inhibitors wortmannin and LY294002 (Martin *et al.*, 1997; Wiedemann *et al.*, 1996).

Neurotransmitter release from synaptosomes and hormonal secretion from chromaffin cells are only sensitive to high concentrations of the PI3K inhibitors wortmannin and LY294002, pointing to a possible role for the less sensitive PI3K-C2 α . In support of this, PI3K-C2 α was detected on a subpopulation of mature secretory granules abutting the plasma membrane in neurosecretory cells. Furthermore, both PI3K inhibitors and sequestration of PI3K-C2 α with specific antibodies selectively prevented ATP-dependent priming in permeabilised chromaffin cells.

Transient over-expression of PI3K-C2 α in PC12 cells potentiated evoked secretion, whereas its dominant negative mutant abolished exocytosis, suggesting PtdIns3P, the main catalytic product of this enzyme plays a role in neuroexocytosis. Consistent with this, treatment of PC12 cells transiently expressing PtdIns3P-sequestering FYVE domain with low concentrations of wortmannin selectively abolished early endosomal staining and revealed a full co-localisation of the FYVE domain with PI3K-C2 α on PC12 granules. Finally sequestration of PtdIns3P by the FYVE domain also abolished secretion from PC12 cells demonstrating that PtdIns3P production is needed in the process of acquisition of fusion competence secretory vesicles undergo, during or following docking to the plasma membrane.

Chasserot-Golaz, S., Hubert, P., Thierse, D., Dirrig, S., Vlahos, C. J., Aunis, D., & Bader, M.F. (1998)

Journal of Neurochemistry, 70, 2347-2356.

Martin, T.F., Loyet, K.M., Barry, V.A., & Kowalchuk, J.A. (1997) *Biochemical Society Transactions*, 25, 1137-1141.

Osborne, S.L., Meunier, F.A., & Schiavo, G. (2001) *Neuron*, 32, 9-12.

Wiedemann, C., Schafer, T., & Burger, M.M. (1996) *Embo Journal*, 15, 2094-2101.

Pre- and postsynaptic factors controlling synaptic efficacy at central synapses

M.C. Bellingham and M.L. Kerr, School of Biomedical Sciences, University of Queensland, St. Lucia, Queensland 4072, Australia. (Introduced by D.J. Adams) .SP

Synaptic efficacy is a measure of the strength of postsynaptic electrical signals arising from synaptic release of chemical neurotransmitters. Both pre- and postsynaptic factors can alter synaptic efficacy. Most synapses are located on dendrites, whose passive and active electrical properties can distort recorded signals arising from remote synapses. These distortions are avoided at certain central synapses, such as that between the endbulbs of Held and bushy cells in the cochlear nucleus, where the glutamate-releasing presynaptic terminals of cochlear nerve fibres direct contact the bushy cell soma. Whole cell patch clamp recordings of eEPSCs were made from bushy cells (n=113) in cochlear nucleus slices obtained from postnatal day (P) 4-21 rats anaesthetised with sodium pentobarbitone (20 mg/kg i.p.), in order to investigate pre- and postsynaptic factors contributing to developmental changes in synaptic efficacy.

Postsynaptic changes: At endbulb-bushy cell synapses, α -amino-3-hydroxy-5-methyl-4-isoxazolepropionic acid receptor (AMPA)-mediated single fibre evoked EPSCs (eEPSCs) increase in amplitude with age while N-methyl-D-aspartate receptor (NMDAR)-mediated eEPSCs decrease in amplitude and decay time constant. The functional characteristics of AMPARs and NMDARs depend on subunit composition. NMDARs with NR2B subunits have high Ca^{2+} permeability and long decay time constant are typically more common in neonatal brains and may play an important role in synapse development. We investigated developmental changes in subunit composition of postsynaptic receptors using subunit-specific antagonists. Ifenprodil (10 μM), an NR2B subunit-selective NMDAR antagonist, reduced NMDAR eEPSC amplitude to 24 \pm 3% (mean \pm SEM, n=13) of control in P4-8 rats, significantly greater than NMDAR EPSC reduction in P10-17 rats (40 \pm 4% of control, n=13) suggesting that NR2B subunits are exchanged during development to probably NR2A subunits. Pentobarbitone (100 μM), which selectively inhibits AMPARs containing GluR2 subunits, reduced AMPAR EPSC amplitude in P4-6 rats to 51 \pm 2% of control (n=4), to 73 \pm 5% (n=3) at P8-11 and to 40 \pm 14% (n=3) in P12-15 rats. The intracellular polyamine spermine blocks Ca^{2+} -permeable AMPARs lacking GluR2 subunits at positive voltages. After inclusion of spermine (100 μM) in the electrode solution, the mean rectification index (RI) of AMPAR EPSC I-Vs increased with age (P4-6, RI=1.2 \pm 0.5 (n=5), P7-11, RI= 4.5 \pm 0.5 (n=8), P12-15, RI= 5.6 \pm 0.8 (n=10). suggesting that AMPARs in older animals are likely to lack GluR2 subunits and be more Ca^{2+} permeable.

Presynaptic changes: Paired stimuli at 5-140 ms caused marked facilitation of 2nd eEPSC amplitude at P4-7 (mean ratio \pm SEM at 10 ms = 1.7 \pm 0.1, n=17), marked depression at >P11 (0.6 \pm 0.05, n=17), and a mixture of facilitation and depression at P8-10 (1.0 \pm 0.15, n=18). Depletion of the synaptic vesicle pool by 10 stimuli at 100 Hz caused eEPSC amplitude depression at all ages (P4-7, 0.03 \pm 0.04, n=7; P8-10, 0.02 \pm 0.03, n=6; >P11, 0.13 \pm 0.08, n = 13). Recovery from depletion was similar at short delays but slower at >P11 for longer delays. Varying external Ca^{2+} caused larger changes in eEPSC amplitude and paired pulse ratio at ages <P11, indicating that sensitivity of synaptic release to external Ca^{2+} altered with development.

Conclusions: These data suggest that presynaptic factors regulating Ca^{2+} -sensitive synaptic release and short term plasticity, and that subunit composition of postsynaptic AMPARs and NMDARs can be rapidly modified during synaptic development. It is proposed that Ca^{2+} influx through NMDA receptors may contribute to these developmental changes, so to increase synaptic efficacy with large and rapid AMPA responses at mature synapses.